รายงานวิจัยฉบับสมบูรณ์

โครงการ : การวิจัยสหสาขาเพื่อพัฒนาศักยภาพการวิจัยด้านแคลเซียมและกระดูก

Multidisciplinary approach to cultivate and strengthen research in calcium and bone metabolism

ทุนส่งเสริมกลุ่มวิจัย สัญญาเลขที่ RTA 5080008

ผู้วิจัย ศาสตราจารย์ ดร.นทีทิพย์ กฤษณามระ
สังกัด ภาควิชาสรีรวิทยา และเครือข่ายวิจัยด้านแคลเซียมและกระดูก
คณะวิทยาศาสตร์ มหาวิทยาลัยมหิดล

สนับสนุนโดย สำนักงานคณะกรรมการอุดมศึกษาและสำนักงานกองทุนสนับสนุนการวิจัย

พฤศจิกายน 2553

บทคัดย่อ

การที่เราจะป้องกันหรือลดอุบัติการณ์ของโรคกระดูกพรุนและ Metabolic bone disease อื่น ๆ ในผู้สูงอายุ ซึ่งเพิ่มขึ้นตามสัดส่วนของประชากรสูงอายุนั้น เราจะต้องมีความเข้าใจถึงปัจจัยที่มีผลต่อมวลกระดูก สาเหตุของพยาธิสรีรวิทยาตลอดจนปัจจัยที่จะช่วยชะลอการเสียมวลกระดูก เครือข่ายวิจัยด้านแคลเซียมและกระดูกจึงมีวัตถุประสงค์ที่จะใช้การวิจัยสหสาขาค้นคว้าให้ได้องค์ความรู้ที่เป็นองค์รวม ตั้งแต่กลไกการดูดซึมแคลเซียมที่ลำไส้ วัฏจักรการสร้าง-สลายกระดูก และปัจจัยควบคุมต่างๆ เพื่อให้ความรู้เหล่านี้สามารถใช้เป็นฐานต่อยอดสู่การพัฒนาวิธีป้องกัน การวินิจฉัยและการรักษาต่อไป

การวิจัยแบ่งเป็นสองส่วน คือ การวิจัยบทบาทของโพรแลคตินในฐานะฮอร์โมนควบคุมสมดุลแคลเซียมและกระดูก โดยเฉพาะในแม่ที่ตั้งท้องและให้นมลูก และการศึกษาวิจัยเกี่ยวกับการควบคุมวัฏจักรการสร้าง-สลายกระดูก (bone turnover) โดยระบบประสาท

การวิจัยของเราในสัตว์ทดลองและเซลล์เพาะเลี้ยงพบว่า โพรแลคตินเป็นฮอร์โมนที่ทำให้ร่ายกายของแม่มีแคลเซียมในเลือดเพียงพอสำหรับการเจริญเติบโตของลูกในท้อง และสำหรับการสังเคราะห์น้ำนมเลี้ยงลูกอ่อน โดยมีผลกระตุ้นการดูดซึมแคลเซียมที่ลำไส้ทั้งการดูดซึมแบบผ่านเซลล์โดยใช้พลังงาน ATP (transcellular active transport) และแบบขนส่งผ่านช่องระหว่างเซลล์แบบไม่ใช้ ATP โดยตรง (paracellular transport) การที่แม่หนูมีระดับของโพรแลคตินในเลือดสูงมากเป็นเวลานาน เช่น 75-100 นาโนกรัม/มิลลิลิตรในช่วงท้อง และ 200-300 นาโนกรัม/มิลลิลิตรในช่วงหลังคลอดจะมีผลระยะยาวทำให้เซลล์ดูดซึมสร้างโปรตีนขนส่งแคลเซียมแบบผ่านเซลล์มากขึ้น เช่น ช่องขนส่งแคลเซียมชนิด TRPV6 TRPV5 โปรตีนจับแคลเซียม Calbindin D9k และลดการสร้างโปรตีนควบคุม tight junction เช่น occludin และ ZO-1 ทำให้แคลเซียมผ่านช่องระหว่างเซลล์ได้ดีขึ้น การเพิ่มการขนส่งแคลเซียมถึง 2 เท่าจากภาวะปกตินี้ เราเรียกว่า เป็นขั้น -1 (Step -1) การดูดซึมแคมเซียมขั้น -1 นี้จะถูกกระตุ้นให้สูงมากขึ้นอีกเป็นขั้น -2 (Step-2) เมื่อระดับของโพรแลคตินในเลือดพุ่งขึ้นไปถึง 600-800 นาโนกรัม/มิลลิลิตร เช่น 15-90 นาทีหลังลูกดูดนม ขั้น - 2 นี้ ใช้กลไกการตอบสนองระดับเซลล์อย่างเฉียบพลันและไม่ใช้การแสดงออกของยีนขนส่งแคลเซียม ความรู้ที่ได้จากการวิจัยนี้สามารถนำไปใช้ให้เกิดประโยชน์ เช่น ให้คำแนะนำแก่แม่ที่ให้นมลูกว่าควรดื่มนมหรือรับประทานแคลเซียมเสริมประมาณ 30 นาทีก่อนให้ลูกดูดนม ทั้งนี้เพราะระดับโพรแลคตินที่พุ่งสูงขึ้นในขั้น -2 นี้จะทำให้แม่ดูดซึมแคลเซียมได้เพิ่มมากขึ้น เป็นผลให้มีแคลเซียมเพียงพอในการผลิตน้ำนม โดยร่างกายไม่จำเป็นต้องดึงแคลเซียมมาจากกระดูก ซึ่งจะเป็นประโยชน์ในระยะยาว นอกจากนั้นเรายังพบว่าโพรแลคตินมีผลกระตุ้นวัฏจักรการสร้าง-สลายกระดูก โดยมีส่วนทำให้มีการสะสมแคลเซียมในกระดูกของแม่ในช่วงตั้งท้อง และกระตุ้นการสลายกระดูกหลังคลอดเพื่อดึงแคลเซียมมาใช้ผลิตน้ำนม เราได้พิสูจน์ว่าโพรแลคตินสามารถออกฤทธิ์โดยตรงที่เซลล์กระดูกออสติโอบลาสท์โดยมีผลกระตุ้นการหลั่ง RANKL และลดการหลั่ง Osteoprotegerin เพื่อกระตุ้นการเจริญเติบโตของเซลล์สลายกระดูกออสติโอคลาสท์ องค์ความรู้ใหม่เกี่ยวกับโพรแลคตินนี้ได้ตีพิมพ์เป็นบทความปริทัศน์ใน Trends in Endocrinology & Metabolism 2010 Vol.21,pp. 395-456

ในการศึกษาส่วนที่สองเกี่ยวกับระบบประสาทและการควบคุมวัฏจักรการสร้าง-สลายกระดูก (Bone turnover) เราได้พบว่านอกจากการกระตุ้นของระบบซิมพาเตติกผ่านทางตัวรับอดริ

เนอจิกชนิด เบต้า-2 (β_2-AR) และ อัลฟ่า-1 (α_1-AR) ซึ่งเป็นที่ทราบกันแล้วนั้น เรายังพบว่าการควบคุมเกิดขึ้นผ่านตัวรับอดริเนอจิก เบต้า 3 (β_3-AR) ด้วย มีผลทำให้เซลล์ต้นแบบเจริญไปเป็นเซลล์ออสติโอบลาสท์เร็วขึ้น แต่ถ้าใช้ยายับยั้ง β_3-AR ในขนาดยาต่ำๆกลับมีผลกระตุ้นการสร้างกระดูก โดยปกติแล้วการป้องกันไม่ให้สูญเสียมวลกระดูกมักใช้ยาลดการสลายกระดูก ทั้งนี้เนื่องจากไม่ค่อยมีปัจจัยหรือยาที่สามารถกระตุ้นการสร้างกระดูกอย่างมีประสิทธิภาพ ดังนั้นผลการวิจัยนี้จึงมีประโยชน์มากและสามารถต่อยอดสู่การพัฒนายา β_3-AR เพื่อใช้เป็นตัวเร่งอัตราการสร้างกระดูกได้ อนึ่งวัฏจักรของการสร้าง-สลายกระดูกนี้เกี่ยวข้องโดยตรงกับการขนส่งสารอิเล็กโทรไลท์ระหว่างน้ำกระดูก (bone fluid) กับเลือด ซึ่งในปัจจุบันมีสมมติฐานว่าการขนส่งจะถูกควบคุมโดยเยื่อเมมเบรนที่ผิวกระดูก (bone membrane) ที่เกิดจากการเรียงตัวของเซลล์ออสติโอบลาสท์ที่ต่อกันเป็นแผ่น epithelium เราได้พิสูจน์คุณสมบัติของเยื่อเมมเบรนนี้โดยตรวจพบการแสดงออกของ mRNA ของโปรตีนที่เป็นตัวบ่งชี้ความเป็น epithelium tight junction ได้แก่ (ZO-1,-2,-3, cingulin, occludin, cingulin-1 ถึง -12, -14 ถึง -20, -22 และ -23 และโปรตีนคลอดินหลายตัวโดยเฉพาะคลอดิน -16 ซึ่งทำหน้าที่เป็นช่องผ่านของแคลเซียมใน tight junction จึงเป็นการพิสูจน์ว่าเยื่อเมมเบรนที่กระดูกมีจริงซึ่งจะเป็นประโยชน์ต่อการลดอุบัติการณ์ของโรคกระดูกพรุนและ metabolism bone disease อื่นๆ และน่าจะเป็นเป้าหมายใหม่สำหรับการวิจัยหาวิธีควบคุมอัตราการสลายกระดูก

Abstract

In order to prevent and reduce the incidence of osteoporosis and other metabolic bone diseases in the elderly, the proportion of which is on the rise, we need to understand what factors and how they that determine bone mass, etiology and pathophysiology and factors that can slow down changes in bone microarchitecture and bone loss. Our Consortium for Calcium and Bone Research (COCAB), thus aimed to use a multidisciplinary approach to obtain knowledge regarding the mechanisms of intestinal calcium absorption, bone remodeling and factors involved in their regulation so that these findings would provide solid foundation for future research for prevention, diagnoses, and treatment.

Our research was divided into two major projects. First was the study of the role of prolactin as a calcium regulating hormone, especially its significance in pregnancy and lactation. The second project was the study of regulation of bone turnover by the nervous system.

Study in experimental animals and cultured cells showed that prolactin, a pituitary hormone, enables maternal boby to provide adequate calcium for fetal development and milk production by stimulating the intestinal calcium absorption, both the transcellular active transport and paracellular transport. For example, in rats, long termed elevation of circulating prolactin to 75-100 ng/mL in pregnancy and 200-300 ng/mL in lactation increases the expression of proteins involved in the transcellular calcium transport, namely TRPV6, TRPV5, and calbindin D9k, and reduces the expressions of proteins that regulate tight junction, namely occludin and ZO-1 resulting in increased paracellular calcium transport, we call this approximately two-fold increase in intestinal calcium absorption Step-1, which is immediately increased to Step-2 when blood prolactin level shoots up to 600-800 ng/mL 15-90 minutes after the start of nursing. This Step-2 response is acute and does not involve expression of calcium transporter genes. Based on this information, lactating mothers should drink a glass of milk or take calcium supplement about 30 minutes before nursing the baby as the elevated prolactin level in Step-2 will further increase maternal calcium absorption. The absorbed calcium will thus be available for milk production and help reduce demand for resorbed calcium from bone, which will be benefitial to mother in the long run.

Prolactin also has a stimulating effect on bone remodeling. Together with other hormones, prolactin induces bone calcium accumulation during pregnancy and bone resorption during lactation. We have shown that prolactin can directly stimulate osteoblasts to secrete RANKL and to stop secreting osteoprotegerin, thus resulting in enhanced osteoclastogenesis and bone resorption. Our work on prolactin and its calcium regulating

roles has recently been published as a review in Trends in Endocrinology & Metabolism, 2010 Vol.21, and pp 395-456.

In part two of our project, we studied the neural control of bone turnover by identifying adrenergic receptors as the sympathetic nervous system has been known to regulate bone remodeling. Besides β_2-adrenergic receptor (β_2-AR) and α_1-adrenergic receptor (α_1-AR), we found that it was β_3-adrenergic receptor β_3-AR that mediates the stimulatory effect of the sympathetic neural control on differentiation of progenitor cells in to osteoblasts. In addition, we showed that low doses of β_3-AR blocker could induce bone formation. Decrease in bone loss is generally achieved by preventing bone resorption and not by increasing bone formation as anabolic agents are rare. However, our finding is of potential importance and can lead to development of β_3-adrenergic agonists that could be used to enhance bone formation.

It is well known that bone remodeling or bone turnover is directly associated with ion exchanges eg., calcium and phosphate between the extracellular fluid and bone fluid. However, very little is known about the barrier separating the two compartments or “bone membrane”, which is believed to be an epithelium–like layer of bone lining cells (also known as inactive osteoblasts). Another of our recent investigations has provided evidence of the existence of this bone membrane. We showed that osteoblasts expressed mRNA of epithelial tight junction–associated proteins, namely, ZO-1,-2,-3, cingulin, occludin, claudins-1 to -12, -14 to -20, -22 and -23. Many claudin proteins were expressed; of special interest is claudin -16, which is like a calcium channel in the tight junction. Therefore, we have provided evidence in support of the existence of bone membrane, which could be an important new target for research on drugs to modulate bone resorption.

สรุปโครงการ (EXECUTIVE SUMMARY)
ทุนส่งเสริมกลุ่มวิจัย
ประจำปี พ.ศ. 2550

Title: Multidisciplinary approach to cultivate and strengthen research in calcium and bone metabolism

ชื่อเรื่อง: การวิจัยสหสาขาเพื่อพัฒนาศักยภาพการวิจัยด้านแคลเซียมและกระดูก

Project Director: Professor Nateetip Krishnamra, Ph.D

Institution: Department of Physiology
Consortium for Calcium and Bone Research
Faculty of Science, Mahidol University, Bangkok, Thailand

Telephone: 0-2201-5629 **Fax simile:** 0-2354-7154

E-mail: scnks@mahidol.ac.th

Field of Research: Directed Biomedical Research

Background and Rationale:

At present, there is little basic biomedical research on calcium and bone metabolism in Thailand. One of the reasons for this lack of interest in this field is that metabolic bone diseases are mostly chronic, not easily diagnosed in the early stages, and are not life threatening compared to other diseases such as cardiovascular or infectious diseases. However, incidence of bone diseases has been known to increase dramatically in recent years with prolonged life expectancy and the increase in the elderly population in both developed countries and developing countries including Thailand. Undoubtedly, bone diseases will have a negative socioeconomic impact in Thailand in the very near future. It is thus necessary for Thailand to encourage basic research in the field of calcium and bone metabolism which will ultimately lead to better understanding of the etiology and mechanisms of bone diseases, effective treatment and prevention. Multidisciplinary research approach is the best way to tackle complex research problems because it provides alternative views as well as ways to solve the problem.

Our research group known as the Consortium for Calcium and Bone Research or COCAB was established in 2003 as a research unit in the Center of Excellence of the

Faculty of Science, Mahidol University. The present members also include academicians from the Faculty of Medicine, Ramathibodi Hospital, Mahidol University, as well as from other universities. We carry out research together in two major projects; Prolactin, its role in the regulation of calcium and bone metabolism and Regulation of bone remodeling in health and disease.

Research Projects

I. Prolactin
   1. Mechanism of prolactin in the regulation of intestinal calcium absorption.
   2. Mechanism of prolactin in the regulation of bone metabolism.
   3. Effect of estrogen on the regulation of transport-related functions of prolactin in the endometrium.

II. Regulation of Bone Remodelling
   1. Expression and physiological roles of claudins in bone : evidence supporting the existence of bone lining epithelium
   2. Modulation of nerve innervations and its neurotransmitter in bone related to osteoporosis.
   3. Anti-osteopenic actions of estrogen in chronic depressive female rats
   4. Application of atomic force microscopy (AFM) in characterization of bone surface structure and investigation of prolactin and estrogen actions

Output

1. International Publications (19 papers)

1.1 Seriwatanachai D, Thongchote K, Charoenphandhu N, Pandaranandaka J, Tudpor K. Teerapornpuntakit J. Suthiphongchai T, Krishnamra N. Prolactin directly enhances bone turnover by raising osteoblast-expressed receptor activator of nuclear factor kB ligand/osteoprotegerin ratio. **Bone 2008**; 42: 535-46.

1.2 Thongchote K, Charoenphandhu N, Krishnamra N. High physiological prolactin induced by pituitary transplantation decreased BMD and BMC in the femoral metaphysis, but not in the diaphysis of adult female rats. **J Physiol Sci 2008**; 58: 39-45.

1.3 Charoenphandhu N, Teerapornpuntakit J, Methawasin M, Wongdee K, Thongchote K, Krishnamra N. Prolactin decreases expression of Runx2,

osteoprotegerin, and RANK in primary osteoblasts derived from tibiae of adult female rats. **Can J Physiol Pharmacol 2008**; 86: 1-9.

1.4 Thongon N, Nakkrasae L, Thongbunchoo J, Krishnamra N, Charoenphandhu N. Prolactin stimulates transepithelial calcium transport and modulates paracellular permselectivity in Caco-2 monolayer: mediation by PKC and Rock pathways. **Am J Physiol Cell Physiol 2008**; 294: C1158-68.

1.5 Deachapunya C, Poonyachoti S, Krishnamra N. Regulation of electrolyte transport across cultured-endometrial epithelial cells by prolactin. **J Endocrinol 2008**; 197: 575-82.

1.6 Wongdee K, Pandaranandaka J, Teerapornpuntakit J, Tudpor K, Thongbunchoo J, Thongon N, Jantarajit W, Krishnamra N, Charoenphandhu N. Osteoblasts express claudins and tight junction-associated proteins. **Histochem Cell Biol 2008**; 130(1):79-90.

1.7 Seriwatanachai D, Charoenphandhu N, Suthiphongchai T, Krishnamra N. Prolactin decreases the expression ratio of receptor activator of nuclear factor kB-ligand/osteoprotegerin in human fetal osteoblast cells. **Cell Biol Inter 2008**; 32: 1126-35.

1.8 Charoenphandhu N, Wongdee K, Teerapornpuntakit J, Thongchote K, Krishnamra N. Transcriptome responses of duodenal epithelial cells to prolactin in pituitary-grafted rats. **Molec Cell Endocrinol 2008**; 296: 41-52.

1.9 Seriwatanachai D, Krishnamra N, van Leeuwen JPTM. Evidence for direct effects of prolactin on human osteoblasts: inhibition of cell growth and mineralization. **J Cell Biochem 2009**; 107: 677-85.

1.10 Thongon N, Nakkrasae L, Thongbunchoo J, Krishnamra N, Charoenphandhu N. Enhancement of calcium transport in Caco-2 monolayer through PKCζ-dependent $Ca_v1.3$-mediated transcellular and rectifying paracellular pathways by prolactin. **Am J Physiol Cell Physiol 2009**; 296(6): C1373-82.

1.11 Kraidith K, Jantarajit W, Teerapornpuntakit J, Nakkrasae L, Krishnamra N, Charoenphandhu N. Direct stimulation of the transcellular and paracellular calcium transport in the rat cecum by prolactin. **Pflügers Archiv - Eur J Physiol 2009**; 458(5): 993-1005.

1.12 Charoenphandhu N, Nakkrasae L, Kraidith K, Teerapornpuntakit J, Thongchote K, Thongon N, Krishnamra N. Two-step stimulation of intestinal Ca^{2+} absorption

during lactation by long-term prolactin exposure and suckling-induced prolactin surge. **Am J Physiol Endocrinol Metab 2009**; 297(3): E609-19.

1.13 Suntornsaratoon P, Wongdee K, Krishnamra N, Charoenphandhu N. Femoral bone mineral density and bone mineral content in bromocriptine-treated pregnant and lactating rats. **J Physiol Sci 2010**; 60(1): 1-8.

1.14 Nuntapornsak A, Wongdee K, Thongbunchoo J, Krishnamra N, Charoenphandhu N. Changes in the mRNA expression of osteoblast-related genes in response to β_3-adrenergic agonist in UMR106 cells. **Cell Biochem Func 2010**; 28(1): 45-51.

1.15 Nakkrasae L, Thongon N, Thongbunchoo J, Krishnamra N, Charoenphandhu N. Transepithelial calcium transport in prolactin-exposed intestine-like Caco-2 monolayer after combinatorial knockdown of TRPV5, TRPV6 and $Ca_v1.3$. **J Physiol Sci 2010**; 60(1): 9-17.

1.16 Wongdee K, Riengrojpitak S, Krishnamra N, Charoenphandhu N. Claudin expression in the bone-lining cells of female rats exposed to long-standing acidemia. **Explt Molec Pathol 2010**; 88(2): 305-10.

1.17 Charoenphandhu N, Wongdee K, Krishnamra N. Is prolactin the cardinal calciotropic hormone in mothers? **Trends Endocrinol Metab 2010**; 7: 395-401.

1.18 Suntornsaratoon P, Wongdee K, Goswami S, Krishnamra N, Charoenphandhu N. Bone modeling in bromocriptine-treated pregnant and lactating rats: possible osteoregulatory role of prolactin in lactation. **Am J Physiol Endocrinol Metab 2010** (in press).

1.19 Suntornsaratoon P, Wongdee K, Krishnamra N, Charoenphandhu N. Possible chondroregulatory role of prolactin as indicated by changes in tibial growth plate in bromocriptine treated pregnant and lactating rats. **Histochem Cell Biol 2010** (in press).

2. Manuscripts in Preparation

2.1 Wongdee K, Tulalamba W, Thongboonchu J, Krishnamra N, Charoenphandhu N. Prolactin alters the mRNA expression of osteoblast-derived osteoclastogenic factors in osteoblast-like UMR 106 cells. **Molec Cell Biochem** (submitted)

3. Academic Position Promotion

3.1 Assistant professor

Dr. Theeraporn Puntheeranurak	(Mahidol University)

3.2 Associate professor

Dr. Narattaphol Charoenphandhu	(Mahidol University)
Dr. Sutthasinee Poonyachoti	(Chulalongkorn University)

4. Graduate Students (Status at present)

M.Sc.

Miss Walailak Jantarajit	(Staff at Rangsit University)
Miss Jarinthorn Teerapornpuntakit	(now a Ph.D. student)
Miss Panan Suntornsaratoon	(now a Ph.D. student)
Miss Nitita Dorkkam	(now a Ph.D. student)
Miss Jenjira Assapun	(Staff at Hua Chiew University)
Miss Kamonchanok Kraidith	(Researcher at University of Regensberg, Germany)
Miss Norathee Buathong	(2^{nd} year at Srinakarinwirot University)
Miss Pimwipa Auasilamongkol	(Chulalongkorn University)

Ph.D

Miss Kannikar Wongdee	(Staff at Burapa University)
Mr. Narongrit Thongon	(Staff at Burapa University)
Mr. Suparerk Laohapitakworn	(Ph.D. M.D. program Mahidol University)
Mr. Yoswee Srisomboon	(2^{nd} year at Srinakarinwirot University)

5. Postdoctoral Fellow

Dr. Suchanda Goswami	(Researcher at Otto von Guericke University Germany)
Dr. La-iad Nakkrasae	(Staff at Khonkaen University)

6. Senior Research /Scholar Academic Meetings

6.1 December 22, 2006 at the Faculty of Science. Mahidol University. (Attendance: 70 academicians)

6.2 June 11, 2010 at the Faculty of Science. Mahidol University. (Attendance: 53 academicians)

7. Special Invited Speakers

7.1 October 12, 2010 “Research for healthy Bone” Interfaculty Seminar between the Consortium for Calcium and Bone Research and the Primate Research Unit, Faculty of Science, Chulalongkorn University.

7.2 “New insights into properties and physiological functions of two low–voltage activated calcium channels ($Ca_v1.3$ and Ca_v 3.2) in heart and neurons.” Dr. Jöel Nargot, Director of Department of Physiology, Institute de Génomique Functionnelle (IGF) INSERM U 661, Universites de Montpellier, France, March 29, 2010.

7.3 “Signature of serum glycopoteins level and fucosylation for the differential diagnosis of liver diseases.” Prof. B.P Chatterjee. West Bengal University of Technology, Kolkata, India, May 6, 2009.

7.4 “Silk-new material in biomedical application.” Dr. Bavornlak Oonkhanond Faculty of Engineering, Mahidol University, November 5, 2008

7.5 “Osteoblastic events: The quest for novel regulators and markers of bone metabolism to improve risk assessment and therapy” Prof. J PTM Hans Van Leeuwen, Bone and Calcium group, Erasmus Medical Center, Rotterdam, The Netherlands, August 25, 2008

7.6 “Bestrophin: an ion channel that is important for epithelial to mesenchymal transition and proliferation.” Prof Karl Kunzelmann, University of Regensburg, Germany, March 18, 2008.

8. Conferences, Scientific Meetings, Lectures

	Date	Topic	Presenter/Speaker	Conference/Meeting
1.	26/04/10	Soybean phytoestrogens modulate ion transport in porcine endometrial epithelial cell (poster)	Chatsri Dechapunya	Experimental Biology 2010, Anaheim, California, USA
2.	27/04/10	Prolactin Stimulates K^+ secretion in isolated rat distal colon (poster)	Chatsri Dechapunya	Experimental Biology 2010, Anaheim, California, USA

	Date	Topic	Presenter/Speaker	Conference/Meeting
3.	27/04/10	Neurochemical alterations of sensory nerve in bone of osteoporosis-induced female rats. (poster)	Suthasinee Poonyachoti	Experimental Biology 2010, Anaheim, California, USA
4.	28/06/10	Prolactin-enhanced calcium absorption in the duodenum of lactating rats is mediated by the phosphoinositide 3-kinase (Pi3K) pathway (poster)	Narattaphol Charoenphandhu	36th International Congress of Physiological Science (IUPS 2009), Kyoto, Japan
5.	28/06/09	Prolactin stimulates transepithelial calcium transport in the cecum of female rats (poster)	Kamonchanok Kraidith	36th International Congress of Physiological Science (IUPS 2009), Kyoto, Japan
6.	28/09/09	Estrogen (E_2) dependent effect of the selective serotonin reuptake inhibitor fluoxetine on anxiety-like behaviours in female rats (poster)	Jantarima Charoenphandhu	36th International Congress of Physiological Science (IUPS 2009), Kyoto, Japan
7.	07/05/09	Healthy and non healthy bone: insight from atomic force microscopy and scanning electron microscopy (poster)	Theeraporn Puntheeranurak	2nd Thailand International Conference on Oral Biology, Bangkok, Thailand

	Date	Topic	Presenter/Speaker	Conference/Meeting
8.	07/05/09	Osteoblast structure and biomineral formation investigated by atomic force microscopy (poster)	Theeraporn Puntheeranurak	2nd Thailand International Conference on Oral Biology, Bangkok, Thailand
9.	29/01/09	Characterization of osteoblasts and biomineral formation by atomic force microscopy study (poster)	Theeraporn Puntheeranurak	26th Annual Conference of the Microscopy Society of Thailand Chiangmai, Thailand
10.	10/10/08	Osteoblasts express claudins and tight junction-associated proteins (poster)	Narattaphol Charoenphandhu	Roche Genetics Day, Bangkok, Thailand
11.	06/08/08	Osteoblasts express claudins and tight junction-associated proteins	Narattaphol Charoenphandhu	CHE-USDC Congress I, Chonburi, Thailand
12.	23/06/08	Healthy and Non-healthy bone: Insight from atomic force microscopy and scanning electron microscopy	Theeraporn Puntheeranurak	10th International Scanning Probe Microscopy Conference, Seattle, USA.
13.	18/01/08	Potential of atomic force microscopy to investigate biological material	Theeraporn Puntheeranurak	2nd Progress in Advanced Materials: Micro/Nano material and Applications Khonkaen, Thailand
14.	10/01/08	Characterization of biological materials by using atomic force microscopy	Theeraporn Puntheeranurak	Pisanulok, Thailand

9. Awards

9.1 Narongrit Thongon

- Graduate Student Publication Awards 2008 Mahidol University
- Outstanding Oral Presentation Award in the RJG Meeting April 4-6, 2008 Chonburi, Thailand
- Outstanding Oral Presentation Award in the 37th Physiological Society of Thailand Annual Conference

9.2 Prof. Nateetip Krishnamra

- Outstanding Female Scientist for Sustainable Development Award in the occasion of 100th anniversary of L'Oreal, France, 2009.

9.3 Assoc Narattaphol Charoenphandh

- Young Scientist Award 2008
- Outstanding Young Scientist Award 2008 (TRF-CHE)

รายงานวิจัย
ทุนส่งเสริมกลุ่มวิจัย (เมธีวิจัยอาวุโส สกว.)
พ.ศ. 2550-0553

การวิจัยสหสาขาเพื่อพัฒนาศักยภาพการวิจัยด้านแคลเซียมและกระดูก
Multidisciplinary approach to cultivate and strengthen research in calcium and bone metabolism

หัวหน้าโครงการวิจัย: ศาสตราจารย์ ดร.นทีทิพย์ กฤษณามระ
ภาควิชาสรีรวิทยา
เครือข่ายวิจัยด้านแคลเซียมและกระดูก (COCAB)
คณะวิทยาศาสตร์ มหาวิทยาลัยมหิดล

งบประมาณ: 6,000,000 บาท

ระยะเวลา: 3 ปี (พ.ศ. 2550–2553)

1. โครงการวิจัย

1.1 โพรแลคติน : บทบาทในฐานะฮอร์โมนควบคุมเมตาบอลิซึมของแคลเซียมและกระดูก

1.2 การควบคุมวัฏจักรการสร้าง – สลายกระดูก (Bone Remodeling)

2. คณะผู้ดำเนินการวิจัย

2.1 ชื่อ ดร. นทีทิพย์ กฤษณามระ
คุณวุฒิ ปริญญาเอก **ตำแหน่ง** ศาสตราจารย์
สถานที่ทำงาน ภาควิชาสรีรวิทยา คณะวิทยาศาสตร์ มหาวิทยาลัยมหิดล
โทรศัพท์ 02-2015629 **โทรสาร** 02-354-7154
E-mail scnks@mahidol.ac.th
หน้าที่ความรับผิดชอบ หัวหน้าโครงการ

2.2 ชื่อ นพ. ดร. นรัตถพล เจริญพันธุ์
คุณวุฒิ ปริญญาเอก **ตำแหน่ง** รองศาสตราจารย์
สถานที่ทำงาน ภาควิชาสรีรวิทยา คณะวิทยาศาสตร์ มหาวิทยาลัยมหิดล
โทรศัพท์ 02-201-5629 **โทรสาร** 02-354-7154
E-mail naratt@narattsys.com
หน้าที่ความรับผิดชอบ ผู้ร่วมวิจัยหลัก

2.3 ชื่อ ดร. ธีราพร พันธุ์ธีรานุรักษ์
คุณวุฒิ ปริญญาเอก **ตำแหน่ง** ผู้ช่วยศาสตราจารย์
สถานที่ทำงาน ภาควิชาชีววิทยา คณะวิทยาศาสตร์ มหาวิทยาลัยมหิดล
โทรศัพท์ 02-201-5275 **โทรสาร** 02-354-7161
E-mail sctpt@mahidol.ac.th
หน้าที่ความรับผิดชอบ ผู้ร่วมวิจัย

2.4 ชื่อ ดร. ฉัตรศรี เดชะปัญญา
คุณวุฒิ ปริญญาเอก **ตำแหน่ง** รองศาสตราจารย์
สถานที่ทำงาน ภาควิชาสรีรวิทยา คณะแพทยศาสตร์ มหาวิทยาลัยศรีนครินทรวิโรฒ
โทรศัพท์ 02-649-5374 **โทรสาร** 02-260-1533
E-mail chatsri@swu.ac.th
หน้าที่ความรับผิดชอบ ผู้ร่วมวิจัย
2.5 ชื่อ ดร. สพญ. สุทธาสินี ปุญญโชติ
คุณวุฒิ ปริญญาเอก **ตำแหน่ง** รองศาสตราจารย์
สถานที่ทำงาน ภาควิชาสรีรวิทยา คณะสัตวแพทยศาสตร์ จุฬาลงกรณ์มหาวิทยาลัย
โทรศัพท์ 081-901-6916 **โทรสาร** 02-613-6967
E-mail sutthasinee@gmail.com
หน้าที่ความรับผิดชอบ ผู้ร่วมวิจัย
2.6 ชื่อ ดร. จันทริมา เจริญพันธุ์
คุณวุฒิ ปริญญาเอก **ตำแหน่ง** อาจารย์
สถานที่ทำงาน ภาควิชาสหเวชศาสตร์ คณะแพทยศาสตร์ มหาวิทยาลัยธรรมศาสตร์
โทรศัพท์ 02-926-5725 **โทรสาร** 02-926-9711
E-mail jantarima@naratt.com
หน้าที่ความรับผิดชอบ ผู้ร่วมวิจัย
2.7 ชื่อ นางวาสนา แสงอำนาจ
คุณวุฒิ ปริญญาตรี **ตำแหน่ง** นักวิทยาศาสตร์
สถานที่ทำงาน ภาควิชาสรีรวิทยา คณะวิทยาศาสตร์ มหาวิทยาลัยมหิดล
โทรศัพท์ 02-201-5629 **โทรสาร** 02-354-7154
E-mail scwsg@mahidol.ac.th
หน้าที่ความรับผิดชอบ ผู้ช่วยวิจัย/เลขานุการโครงการ
2.8 ชื่อ นางสาวจีรวรรณ ทองบุญชู
คุณวุฒิ ปริญญาตรี **ตำแหน่ง** ผู้ช่วยวิจัย
สถานที่ทำงาน เครือข่ายวิจัยด้านแคลเซียมและกระดูก คณะวิทยาศาสตร์ มหาวิทยาลัยมหิดล
โทรศัพท์ 02-201-5629 **โทรสาร** 02-354-7154
E-mail jirawan-thong@yahoo.com
2.9 ชื่อ นางสาวสุดาทิพย์ พรหมอารักษ์
คุณวุฒิ ปริญญาตรี **ตำแหน่ง** ผู้ช่วยวิจัย
สถานที่ทำงาน เครือข่ายวิจัยด้านแคลเซียมและกระดูก คณะวิทยาศาสตร์ มหาวิทยาลัยมหิดล
โทรศัพท์ 02-201-5629 **โทรสาร** 02-354-7154
E-mail aeyly_73@yahoo.com

3. Background and Rationale :

At present, there is little basic biomedical research on calcium and bone metabolism in Thailand. One of the reasons for this lack of interest in this field is that metabolic bone diseases are mostly chronic, not easily diagnosed in the early stages, and are not life threatening compared to other diseases such as cardiovascular or infectious diseases. However, incidence of bone diseases has been known to increase dramatically in recent years with prolonged life expectancy and the increase in the elderly population in both developed countries and developing countries including Thailand. Undoubtedly, bone diseases will have a negative socioeconomic impact in Thailand in the very near future. It is thus necessary for Thailand to encourage basic research in the field of calcium and bone metabolism which will ultimately lead to better understanding of the etiology and mechanisms of bone diseases, effective treatment and prevention. Multidisciplinary research approach is the best way to tackle complex research problems because it provides alternative views as well as ways to solve the problem.

Our research group known as the Consortium for Calcium and Bone Research or COCAB was established in 2003 as a research unit in the Center of Excellence of the Faculty of Science, Mahidol University. The present members also include academicians from the Faculty of Medicine, Ramathibodi Hospital, Mahidol University, as well as from other universities. We carry out research together in two major projects; Prolactin, its role in the regulation of calcium and bone metabolism and Regulation of bone remodeling in health and disease.

4. Objectives :

Our aim is to understand the basic mechanisms of hormonal and neural control of the target cells. More emphasis is put on bone metabolism and the mechanism underlying metabolic bone disorders. Our strategy is to continue with our basic research in calcium and bone metabolism in experimental animals (in vivo system), organ and cell culture (in vitro system) using physiological, histological, biochemical, biophysical and molecular approaches.

โครงการวิจัยแบ่งเป็นโครงการย่อย ดังต่อไปนี้

1. Mechanism of prolactin in the regulation of intestinal calcium absorption and bone metabolism
2. Effect of estrogen on the regulation of transport-related functions of prolactin in the endometrium

3. Expression and physiological roles of claudins in bones: evidence that bone-lining epithelium exists.
4. Modulation of nerve innervation and its neurotransmitter in bone related to osteoporosis
5. Anti-osteopenic actions of estrogen in chronic depressive female rats
6. Application of atomic force microscopy (AFM) in characterization of bone surface, structure and investigation of prolactin and estrogen actions.

5. Summary of the Research Finding

5.1 Prolactin: its novel role as calcium regulating hormone

Since female mammals including women lose a large amount of calcium for fetal bone development during pregnancy and for milk production in lactation, it was not surprising that their intestinal calcium absorption shows a marked increase which is seen as an adaptive change to accommodate the high demand for calcium. Although $1,25(OH)_2D_3$, an active vitamin D hormone, has been known to be a major regulator of intestinal calcium absorption, its circulating levels are not elevated during these reproductive periods. Moreover, vitamin D-deficient pregnant and lactating rats still exhibit markedly increased intestinal calcium absorption. Thus, it seems that $1,25(OH)_2D_3$ is not crucial for calcium absorption in pregnant and lactating periods. In addition, vitamin D receptor knockout mice show upregulation of the transient receptor potential channel subfamily V, member 6 (TRPV6), an apical calcium channel required for transcellular calcium absorption. Therefore, maternal calcium metabolism appears to be regulated by some other hormones.

Considering prolactin with its elevated level during the reproductive periods and being associated with electrolyte transport in many types of epithelia, **we proposed that prolactin is a calcium regulating hormone in pregnancy and lactation.**

Our present projects are a continuation of the decade-long investigations on the physiological role of prolactin in the regulation of calcium metabolism with special focus on two major target organs, namely, intestine and bone. We are the first to demonstrate this novel role of prolactin and **the summary of our findings has been presented in a recent review "Is prolactin the cardinal calciotropic maternal hormone? "In Trends in Endocrinology and Metabolism 2010; 21: 395-401.**

Prolactin and Intestinal Calcium Absorption

The mechanistic action of prolactin on the intestinal calcium absorption depends on its circulating level. This has been observed in non-mated as well as in pregnant and lactating animals. Briefly, prolactin stimulates the transepithelial calcium transport in a two-step manner. Sustained hyperprolactinemia such as in pregnancy and lactation, induces a long-lasting adaptation in the absorptive cells to elevate the baseline calcium transport by approximately 2-fold (we call this "Step-1"), that is further increased ("Step-2") by transient prolactin surge such as in suckling or nursing. Step-1 changes involve transcription of genes encoded for protein required for calcium absorption, e.g. TRPV6 and calbindin-D9k. Step-2 appears to correlate with milk production, and through the orchestrating actions of prolaction on other target tissues, involves mobilization of calcium from sites in the body such as bone.

Calcium traverses across the intestinal epithelium via two routes, transcellular and paracellular, with the latter being predominant. We have shown that prolactin stimulates both pathways. For the transcellular pathway, prolactin upregulates transporter genes encoded for TRPV 5, TRPV 6, voltage-dependent L-type calcium channel (Ca_v) 1.3, and parvalbumin, as well as increasing the activity of Ca-ATPase-1b ($PMCA_{1b}$) basolateral membrane.

Regarding the paracellular route, prolactin lowers the transepithelial resistance and increases calcium permeability by downregulating the tight junction-associated proteins occludin and ZO-1, resulting in Step-1 paracellular calcium transport. Step-2 paracellular transport is increased by prolactin-induced serine phosphorylation of claudin-15. Prolactin signaling pathway appears to involve phosphoinositide-3-kinase (PI3K) and Rho-associated kinase (ROCK) and not the classical Janus kinase-2 pathway.

We have also shown that the acute effect of prolactin is through activation of prolactin receptor long form (PRLR-L) and its down stream mediators, PI3K and protein kinase C, leading to Step-2 transcellular calcium transport.

Prolactin and Bone Turnover

Mammalian skeletal system shows remarkable adaptation during the reproductive cycles with bone calcium accumulation in early and mid pregnancy, slight bone loss in the third trimester and as high as 10-30 % reduction in bone mineral density in lactation. This bone loss caused by milk production can lead to pregnancy and lactation–associated osteoporosis (PLO) with symptoms like back pain, vertebral fracture and height loss.

To prove a direct action of prolactin on bone, we were able to demonstrate the presence of PRLR in osteoblasts. Moreover, we showed that prolactin by downregulating osteoprotegerin (a decoy receptor for RANKL) and upregulating RANKL, results in

increased bone resorption. Since prolactin downregulates Runx2 (a transcription factor for osteoblast differentiation), it can also decrease the number of differentiated osteoblasts. Prolactin appears to have more effect on trabecular bone than cortical bone. But it is not known what factors determine the site and magnitude of action. PRLR distribution is possibly one of the factors.

We have recently focused our investigation on changes in the microstructure of maternal bone to cope with calcium demand for fetal development in pregnancy and milk production in lactation. We found bone accretion in both cortical and trabecular parts of the long bone in pregnant rat, suggesting the building up of calcium reserved pool. As expected lactation induces progressive trabecular bone loss. Studies in pregnant and lactating rats also showed a marked increase in the length of long bone, leading us to look at changes in the growth plate. We found that chondrocytes in every growth plate zone express PRLR. We are the first to provide evidence on the chondroregulatory action of prolactin in the tibial growth plate of lactating rats. Growth plate changes observed in pregnancy, in contrast, are not dependent on prolactin. The chondroregulatory actions of prolactin is apparent only in mammals with persistent growth plate cartilage. However, in other mammals, including humans, prolactin increases bone resorption and can induce bone loss if intestinal calcium absorption is inadequate.

Although we have already provided evidence showing the remarkable actions of prolactin in orchestrating calcium transport in the intestine and bone with an aim to provide adequate calcium supply for developing fetuses and postnatal milk production, we still have to answer many remaining questions regarding the relative contribution of absorbed calcium versus resorbed calcium from bone to meet calcium demand under different physiological conditions, the cellular and molecular mechanism of action of prolactin in bone cells, and how different PRLR isoforms determine the outcome of prolactin action.

Polactin and Electrolyte Transport in the Endometrium

As we know, blastocyst implantation and embryo development require optimal intrauterine environment which unquestionably depends on the transport activities of the endometrial epithelial cells. Among a number of hormones, growth factors and cytokines, prolactin as a hormone with markedly elevated levels during pregunancy and lactation, is found to have a regulatory role.

In the present investigation, we used primary cell culture of porcine glandular endometrial epithelial cells to study the action of prolactin. We found that prolactin acutely stimulated anion secretion across the epithelial cells. The action is mediated by activation of the PRLR-short isoform (PRLR-S), which are present on both apical and

basolateral membranes, and the JAK2 signaling pathway. The prolactin-stimulated anion secretion is mostly a result of the activation of DPC- and NPPB- sensitive Cl^- channel, and bumetanide sensitive Na^+-K^+-$2Cl^-$ cotransport. Although the exact role of prolactin in the human endometrium is not known, the pattern of prolactin secretion and expression supports its role in implantation and placentation. Based on the present data and other reports, it is likely that prolactin helps regulate the volume and composition of the fluid within the uterine cavity.

5.2 Regulation of Bone Remodeling

Bone Lining Epithelium

Besides providing support for the body, bone also acts as a huge ion exchange system that is a part of the pH buffering system as well as regulation of ionic composition of the extracellular fluid. Bone extracellular fluid (BECF) itself is probably under regulation since its composition is not the same as the extracellular fluid (ECF), for example it has a higher K^+ concentration than that of the ECF. It has been proposed that osteoblasts and bone – lining cells (formerly thought to be inactive osteoblasts) form bone membrane that actively controls the paracellular ion exchange between BECF and ECF similar to an epithelium. However, there has been no direct evidence to support the existence of this epithelium like bone membrane.

In 2008, we were able to provide evidence in support of this hypothesis. Since one of the most important properties of and epithelium is the formation of tight junctions to hold epithelial cell together as a sheet of cells, we set out to investigate the presence of tight junctions. We found that primary rat osteoblasts and bone tissues express the tight junction associated proteins, namely ZO-1,-2,-3, cingulin, occludin, claudin-1 to -12, -14 to -20, -22 and -23. By using western blot analyses, we showed expression of claudin-5,-11,-14 and -15. Claudin -16 was shown by immunofluorescent study in decalcified tibia section, specifically on the trabecular surface. In addition, expression of claudin -5,-11,-14, -15 and -16 were found in bone lining cells. We also demonstrate that primary osteoblasts cultured in permeable Snapwell formed a monolayer with transepithelial resistance of ~110-180 Ω cm^2, conferring the presence of barrier functions of the tight junction. We conclude that osteoblasts express several tight junction-associated proteins which are likely to have regulatory role on ion transport across bone membrane.

Nerve Innervations of Bone and Osteoporosis

It is known that bone is regulated by humoral and neural control, the latter via autonomic catecholamine secreting function. The sympathetic nervous system has been shown to suppress osteoblast-induced bone formation and to stimulate osteoclast

differentiation and bone resorption. Many studies further showed β_2- adrenergic receptor in osteoblast as being responsible for sympathetic nervous system-induced up regulation of RANKL and subsequent bone loss. Moreover, previous investigation showed that osteoblast response may depend on adrenergic receptor (AR) subtypes, eg. α_1 -AR, β_1-AR, β_2-AR and β_3-AR. β_3-AR transcripts are primarily expressed in adipocytes, heart, skeletal muscle, smooth muscle of the gastrointestinal tract and the urogenital system. Since activation of β_3-AR could accelerate the differentiation process in several cell types and regulate expression of many transcription factor genes, we investigated β_3-AR expression in rat osteoblast–like UMR 106 cells.

Our investigation showed that activation of β_3-AR could modulate expression of several genes related to osteoblast functions and bone remodelling in primary osteoblasts and the osteoblast-like UMR 106 cells. β_3-AR activation is likely to direct proliferation of pre-osteoblasts toward differentiation process since β_3-AR agonist induced down regulation of Runx 2, important for proliferation of osteoblast progenitors and upregulations of several osteoblast differentiation markers ie., osterix. osteocalcin, and osteopontin. Furthermore, the low-dose β_3-AR agonist may provide a protective effect against bone resorption as indicated by a decrease in the ratio of RANKL/OPG expression ratio. Thus, our investigation indicates the significance of β_3-AR system in the regulation of osteoblast function and bone remodeling. However, further study is required to demonstrate the molecular mechanisms of β_3-AR and its significance in the in vivo control of bone metabolism.

7. ภาคผนวก

8. บทความสำหรับเผยแพร่

ความรู้ทางด้านวิทยาศาสตร์และเทคโนโลยีในปัจจุบันทำให้มีความก้าวหน้าทางการแพทย์และการสาธารณสุขอย่างรวดเร็ว มีผลให้ประเทศพัฒนาและกำลังพัฒนา เช่น ประเทศไทยมีประชากรสูงอายุเพิ่มขึ้นอย่างรวดเร็วเช่นกัน ประชากรสูงอายุของประเทศไทยมีอัตราเพิ่มขึ้นปีละประมาณ 4.5 % เปรียบเทียบกับอัตราการเพิ่มของประชากรทั่วไปไม่ถึง 1 % คาดการณ์ได้ว่าโรคของผู้สูงอายุเช่น โรคกระดูกจะมีอุบัติการณ์เพิ่มขึ้นและจะเป็นปัญหาด้านสาธารณสุขเศรษฐกิจและสังคมอย่างแน่นอน การป้องกันและลดอุบัติการณ์ของโรคกระดูกในผู้สูงอายุจะต้องดำเนินการตั้งแต่ในเด็ก เราต้องหาวิธีการที่จะทำให้เด็กมีการเจริญเติบโตของกระดูกที่ดีจนมีค่ามวลกระดูกสูงที่สุดเท่าที่จะเป็นไปได้ในช่วงอายุ 25-30 ปี และหาวิธีชะลอการสูญเสียกระดูกในสตรีวัยหมดประจำเดือน และการสูญเสียมวลกระดูกในวัยผู้สูงอายุ ดังนั้นกลุ่มวิจัยของเราจึงมีวัตถุประสงค์ที่จะศึกษาวิจัยเพื่อให้ได้องค์ความรู้ที่เป็นองค์รวมเกี่ยวกับกลไกการดูดซึมแคลเซียมและวัฏจักรสร้าง-สลายกระดูก (Bone turnover) และปัจจัยควบคุมต่างๆ ตลอดจนสาเหตุของพยาธิสภาพ ความรู้เหล่านี้สามารถใช้เป็นฐานต่อยอดความรู้ทางการแพทย์เพื่อพัฒนาไปสู่วิธีการป้องกัน การวินิจฉัยความผิดปกติ และการรักษาได้

กลุ่มวิจัยของเรา คือ **เครือข่ายวิจัยด้านแคลเซียมและกระดูก (Consortium for Calcium and Bone Research หรือ COCAB)** ได้ใช้สัตว์ทดลองศึกษาวิจัยกลไกการดูดซึมแคลเซียมและวัฏจักรการสร้าง-สลายกระดูกทั้งในแนวราบหรือในสภาวะต่างๆ เช่น วัยเจริญเติบโต วัยเจริญพันธุ์ ภาวะท้องและให้นมลูก และในพยาธิสภาพ เช่น ภาวะเลือดเป็นกรดและภาวะขาดฮอร์โมนเพศ และศึกษาในแนวลึกคือ กลไกในระดับร่างกาย อวัยวะ เนื้อเยื่อ เซลล์ โปรตีนไปจนถึงระดับโมเลกุล การศึกษาโดยใช้เทคนิควิจัยหลากหลายสาขา (Multidisciplinary) เช่น สรีรวิทยา ชีวเคมี จุลกายวิภาค ชีวโมเลกุล และพยาธิชีววิทยาทำให้เราสามารถตอบโจทย์วิจัยได้เป็นภาพรวมและสามารถอธิบายการเปลี่ยนแปลงที่เกิดขึ้นในระดับต่างๆของร่างกาย

การวิจัยในส่วนแรกเกี่ยวกับ**บทบาทใหม่ของโพรแลคตินในฐานะฮอร์โมนควบคุมสมดุลแคลเซียมและกระดูก**โดยเฉพาะในภาวะท้องและให้นมบุตร โพรแลคตินเป็นฮอร์โมนที่หลั่งจากต่อมใต้สมอง ปกติจะมีในระดับเลือดต่ำมาก แต่มีระดับสูงขึ้นหลายเท่าตัวในช่วงท้องและให้นม โดยมีหน้าที่หลักคือ กระตุ้นการสังเคราะห์น้ำนมในเต้านม งานวิจัยในหลายๆ ปีที่ผ่านมาของเราได้นำไปสู่องค์ความรู้ใหม่เกี่ยวกับโพรแลคติน เราพบว่าโพรแลคตินมีหน้าที่จัดการให้ร่างกายของแม่มีแคลเซียมในเลือดในระดับที่เพียงพอสำหรับส่งผ่านรกเพื่อใช้ในการเจริญเติบโตของลูกในท้อง และเพียงพอสำหรับเซลล์เต้านมใช้ในการผลิตน้ำนมเลี้ยงลูกหลังคลอด โดยโพรแลคตินออกฤทธิ์กระตุ้นลำไส้ส่วนต้นทำให้ดูดซึมแคลเซียมได้มากขึ้น และยังกระตุ้นการสลายแคลเซียมจากกระดูกอีกด้วย ขณะเดียวกันก็ลดการขับถ่ายแคลเซียมทิ้งทางปัสสาวะ เป็นที่น่าสนใจมากว่าผลของโพรแลคตินต่อการดูดซึมแคลเซียมเกิดขึ้นเป็น 2 ขั้นตอน ทั้งนี้ขึ้นอยู่กับระดับฮอร์โมนในเลือด กล่าวคือโพรแลตตินที่มีระดับในเลือดสูงเป็นระยะเวลานาน เช่น 75 -100

นาโนกรัม/มิลลิลิตรระหว่างตั้งท้องและ 200-300 นาโนกรัม/มิลลิลิตร ในช่วงให้นมหลังคลอดมีผลกระตุ้นการแสดงออกของยีนส์ที่เกี่ยวข้องกับการขนส่งแคลเซียมในโพรงลำไส้มีผลให้การดูดซึมแคลเซียมเพิ่มจากภาวะไม่ท้องถึง 2 เท่า เราเรียกการเปลี่ยนแปลงนี้ว่า ขั้นที่ 1 ในช่วงหลังคลอดเมื่อลูกดูดนมโพรแลคตินของแม่จะพุ่งสูงขึ้นอีกถึง 600-800 นาโนกรัม/มิลลิลิตร การดูดซึมแคลเซียมก็พุ่งสูงตามเป็นขั้น -2 การดูดซึมแคลเซียมในขั้น 2 นี้มีความสัมพันธ์กับปริมาณน้ำนมที่หลั่งและเป็นการตอบสนองอย่างเฉียบพลันโดยใช้กลไกกระตุ้นให้โปรตีนขนส่งแคลเซียมทำงานดีขึ้น งานวิจัยนี้แสดงว่าแม่จะได้ประโยชน์จากการดูดซึมแคลเซียมมากขึ้น ถ้าดื่มนมหรือรับประทานแคลเซียมเสริมประมาณครึ่งชั่วโมงก่อนให้นมลูก ระดับโพรแลคตินในเลือดที่พุ่งสูงขึ้นตอนลูกดูดนมและช่วยกระตุ้นการดูดซึมแคลเซียมของแม่ ทำให้แม่มีแคลเซียมเพียงพอในการผลิตน้ำนม โดยไม่ต้องดึงแคลเซียมออกมาจากกระดูก ซึ่งจะเป็นประโยชน์ต่อสุขภาพของแม่ในระยะยาว

ผลของโพรแลคตินที่กระดูกก็น่าสนใจมาก เราพบว่าโพรแลคตินร่วมกับฮอร์โมนอีกบางชนิดกระตุ้นให้แม่สะสมแคลเซียมในกระดูกในช่วงตั้งท้อง แต่พอหลังคลอดโพรแลคตินก็จะมีผลให้มีการสลายกระดูกปล่อยแคลเซียมมาเพื่อใช้ผลิตน้ำนม บางครั้งแม่อาจมีความหนาแน่นของกระดูกลดลงถึง 30 % แต่ก่อนเชื่อว่าโพรแลคตินมีผลสลายกระดูกผ่านทางการยับยั้งการหลั่งฮอร์โมนเพศหญิงเอสโตรเจนเท่านั้น แต่เราได้พิสูจน์แล้วว่าโพรแลคตินสามารถออกฤทธิ์โดยตรงที่เซลล์กระดูกออสติโอบลาสท์ ซึ่งจะหลั่งสารเช่น RANKL เพิ่มขึ้นและหลั่ง osteoprotegerin ลดลง ทำให้เกิดการสลายกระดูกโดยเซลล์ออสติโอคลาสท์มากขึ้น จึงจะเห็นได้ว่าโพรแลคตินเป็นฮอร์โมนสำคัญที่มีบทบาทควบคุมการเคลื่อนย้ายหรือขนส่งแคลเซียมระหว่างอวัยวะต่าง ๆ ทั้งนี้เพื่อให้แม่มีแคลเซียมเพียงพอเพื่อการเจริญเติบโตของลูกในท้อง และการผลิตน้ำนมเพื่อลูกอ่อน

การวิจัยอีกส่วนหนึ่งเกี่ยวกับ**กลไกการควบคุมวัฏจักรการสร้าง-สลายกระดูกโดยระบบประสาท** ระบบประสาทเป็นระบบควบคุมหลักของร่างกาย แต่ความรู้เกี่ยวกับการควบคุมกระดูกโดยระบบประสาทมีน้อยมาก มีรายงานว่าระบบประสาทซิมพาเตติกสามารถควบคุมเซลล์กระดูกออสติโอบลาสท์ผ่านตัวรับ β_2-AR ทำให้มีการหลั่งRANKL มากขึ้นและหลั่ง osteoprotegerin ลดลง ซึ่งมีผลเพิ่มจำนวนเซลล์ออสติโอคลาสท์ให้ไปสลายกระดูกมากขึ้น จากงานวิจัยเราได้พบตัวรับอีกชนิดหนึ่งที่เซลล์ออสติโอบลาสท์ ได้แก่ β_3-AR ซึ่งเราพบว่ามีหน้าที่ป้องกันการสลายกระดูกและยังช่วยให้มีการสร้างกระดูกมากขึ้น ในปัจจุบันมียาหลายชนิดที่ใช้ลดการสลายกระดูกเพื่อป้องกันการสูญเสียมวลกระดูก โดยเฉพาะในสตรีวัยหมดประจำเดือนหรือผู้ป่วยโรคกระดูกพรุน แต่ยาที่ใช้กระตุ้นการสร้างกระดูกมีเพียงฮอร์โมนพาราไทรอยด์ที่ใช้ฉีดให้ผู้ป่วย ดังนั้นองค์ความรู้ใหม่นี้น่าจะนำไปสู่การวิจัยต่อยอดเพื่อพัฒนายากระตุ้น β_3-AR เพื่อเพิ่มการสร้างกระดูกและลดการสูญเสียมวลกระดูก

ดังนั้นงานวิจัยองค์ความรู้ใหม่ของเรา ไม่ว่าจะเป็นเรื่องบทบาทใหม่ของโพรแลคตินในฐานะฮอร์โมนควบคุมสมดุลแคลเซียมและวัฏจักรการสลายกระดูก หรือเกี่ยวกับบทบาทของระบบประสาทซิมพาเตติกในการควบคุมกระบวนการสร้าง/สลายกระดูก ทำให้เราเข้าใจว่าการดูด

ซึมแคลเซียมที่ลำไส้ และกระบวนการสร้าง-สลายกระดูกที่เกิดขึ้นตลอดเวลานี้มีกลไกอย่างไร มีการควบคุมอย่างไร และสามารถใช้ข้อมูลเหล่านี้เป็นฐานให้ค้นคว้าวิธีการที่จะทำให้จะใช้บทบาทของฮอร์โมนในร่างกายเองให้เกิดประโยชน์สูงสุด และเป็นฐานให้พัฒนาวิธีการให้คนไทยมีกระดูกที่แข็งแรงและสุขภาพดีจนวัยสูงอายุ

Histochem Cell Biol (2010) 134:483–491
DOI 10.1007/s00418-010-0745-3

ORIGINAL PAPER

Possible chondroregulatory role of prolactin on the tibial growth plate of lactating rats

Panan Suntornsaratoon · Kannikar Wongdee · Nateetip Krishnamra · Narattaphol Charoenphandhu

Accepted: 16 September 2010 / Published online: 2 October 2010

Abstract Besides calcium accretion in the cortical envelope, a marked increase in the length of long bone was observed in pregnant and lactating rats, and thus the growth plate change was anticipated. Since several bone changes, such as massive trabecular bone resorption in late lactation, were found to be prolactin (PRL)-dependent, PRL may also be responsible for the maternal bone elongation. Herein, we investigated the growth plate change and possible chondroregulatory roles of PRL in the tibiae of rats at mid-pregnancy until 15 days postweaning. We found that the tibial length of lactating rats was increased and was inversely correlated with the total growth plate height, as well as the heights of proliferating zone (PZ) and hypertrophic zone (HZ), but not the resting zone (RZ). Chondrocytes in all zones expressed PRL receptors as visualized by immunohistochemistry, suggesting that the growth plate cartilage was a target of PRL action. Further investigations in lactating rats treated with an inhibitor of pituitary PRL release, bromocriptine, with or without PRL supplement, revealed the PRL-induced decreases in total growth plate height and HZ height from early to late lactation. However, decreases in RZ and PZ heights were observed only in late and mid-lactation, respectively. Thus, this was the first report on the chondroregulatory action of PRL on the growth plate of long bone in lactating rats. The results provided better understanding of the maternal bone adaptation during lactation.

Keywords Cartilage · Chondrocytes · Goldner's trichrome · Hyperprolactinemia · Immunohistochemistry · Prolactin receptor

P. Suntornsaratoon · K. Wongdee · N. Krishnamra · N. Charoenphandhu
Consortium for Calcium and Bone Research (COCAB), Faculty of Science, Mahidol University, Rama VI Road, Bangkok 10400, Thailand

P. Suntornsaratoon · N. Krishnamra · N. Charoenphandhu (✉)
Department of Physiology, Faculty of Science, Mahidol University, Rama VI Road, Bangkok 10400, Thailand
e-mail: naratt@narattsys.com

K. Wongdee
Faculty of Allied Health Sciences, Burapha University, Chonburi 20131, Thailand

Introduction

During pregnancy and lactation, the microstructure of maternal bone is markedly changed to meet mineral demand for fetal skeletal development and milk production (Bowman and Miller 2001; Charoenphandhu et al. 2010). Specifically, pregnancy induces bone calcium accretion in the cortical and trabecular parts of the long bone as a reserved pool for later use, whereas lactation induces progressive trabecular bone loss (Charoenphandhu et al. 2010; Suntornsaratoon et al. 2010a, b). Although maternal osteopenia in humans is usually asymptomatic and reversible, some individuals may experience severe pathological bone loss, known as pregnancy/lactation-induced osteoporosis with low-back pain, loss of height, fragility fracture, and non-traumatic vertebral compression (Ofluoglu and Ofluoglu 2008). Besides cortical and trabecular bone changes, femoral bone length in rats was also increased during pregnancy and appeared to continue through late lactation, presumably to further expand the calcium reserve pool, and to maintain bone strength (Suntornsaratoon et al. 2010a, b). Such increased bone

length probably results from the pregnancy- and/or lactation-induced endochondral bone growth, which is the principal mechanism for elongation of long bones, especially femora, tibiae, and humeri (Bowman and Miller 2001; Rauch 2005). This process might also help replenish the metaphyseal spongiosa that is markedly resorbed during lactation (Rauch 2005; Suntornsaratoon et al. 2010a).

Generally, endochondral bone growth initiates at the growth plate cartilage with a sequence of chondrocyte proliferation, differentiation, hypertrophy, and apoptosis, thereby permitting vascular invasion and entrance of osteoprogenitor cells to replace degenerated chondrocytes with calcified bone matrix (Gartner and Hiatt 2001; Olsen 2006; Rauch 2005). In tibiae and femora, the growth plate cartilage is organized into three zones, namely resting zone (RZ), proliferating zone (PZ) and hypertrophic zone (HZ) (Rauch 2005). Van Buul-Offers and colleagues (1984) reported that longitudinal bone growth in rodents was closely associated with the heights of the growth plate zones, and an increase in tibial length showed negative correlations with the heights of RZ and PZ. Therefore, changes in the growth plate zones were anticipated in pregnant and lactating rats with the increased bone length.

Complex maternal bone changes are tightly regulated by a number of humoral factors, such as osteoprotegerin, insulin-like growth factor (IGF)-1, and parathyroid hormone-related peptide (PTHrP) (Hong et al. 2005; Kovacs 2005; O'Brien et al. 2006). Moreover, a recent investigation in rats revealed that prolactin (PRL) released from the pituitary gland during pregnancy (plasma levels ~100–200 ng/mL) and lactation (up to ~650 ng/mL; normal levels ~7–10 ng/mL) was also an important regulator of bone metabolism during these reproductive periods (Seriwatanachai et al. 2008; Suntornsaratoon et al. 2010a). After binding to PRL receptors (PRLR) on osteoblasts, PRL induced trabecular bone resorption and calcium release through the synthesis of an osteoblast-derived osteoclastogenic factor, namely receptor activator of nuclear factor-κB ligand (Seriwatanachai et al. 2008). Besides the osteoblasts, chondrocytes isolated from the rat articular cartilage were also found to express functional PRLR, which could prevent apoptosis of this cell type in vitro (Zermeño et al. 2006). Nevertheless, whether the growth plate changes during pregnancy and lactation were also PRL-dependent remained unknown.

Therefore, the objectives of the present study were (1) to demonstrate that growth plate chondrocytes expressed PRLR proteins, (2) to investigate changes in the growth plate zones during pregnancy and lactation, and (3) to provide evidence that growth plate changes in these reproductive periods were dependent on PRL.

Materials and methods

Animals

Non-mated (nulliparous) and pregnant Sprague-Dawley rats were obtained from the National Laboratory Animal Centre, Salaya, Nakhon Pathom, Thailand. They were housed in standard stainless steel cages under 12-h light/dark cycle for at least 7 days prior to the experiments and were fed standard chow and distilled water ad libitum. The room temperature was 25 ± 2°C with average illuminance of 200 lux and relative humidity of ~50–60%. This study has been approved by the Animal Care and Use Committee of the Faculty of Science, Mahidol University, Thailand.

Experimental design

The present experimental design was based on the previous experiment by Suntornsaratoon et al. (2010a, b) and used a new collection of bone specimens. In brief, the tibial growth plate changes were investigated in different reproductive phases, i.e., mid-pregnancy (day 14 of pregnancy; P14), late pregnancy (day 21; P21), early lactation (day 8 of lactation; L8), mid-lactation (day 14; L14), late lactation (day 21; L21) and day 15 postweaning (PW), as well as in the age-matched nulliparous controls. The ages of P14, P21, L8, L14, L21, and PW rats were 10, 11, 12, 13, 14, and 16 weeks, respectively. After delivery, the litter size was adjusted to 8 pups/dam for all lactating groups. In some experiments, dams were daily injected for 7 days prior to the experiment with 4 mg/kg bromocriptine s.c. (Bromo) (Sigma, St. Louis, MO, USA), or Bromo + PRL s.c. (purified from ovine pituitary gland; catalog no. L6520; Sigma). PRL doses for pregnant and lactating rats were 0.4 and 0.6 mg/kg/day, respectively, as reported previously (Charoenphandhu et al. 2009). This regimen of Bromo administration was found to successfully abolish hyperprolactinemia in maternal rats (Charoenphandhu et al. 2009). Finally, maternal rats were killed on the aforementioned designated time. Their tibiae and femora were removed and measured for total length.

Histomorphometric measurement of growth plate height

After being removed from maternal rats, tibiae were cleaned off adhering connective tissue and bone marrow. Tibial length was measured by a vernier caliper. Each specimen was then dehydrated serially in 70, 95, and 100% *v*/*v* ethanol for 3, 3, and 2 days, respectively, as described previously (Assapun et al. 2009). Dehydrated bone was embedded in methyl methacrylate resin at 42°C for 48 h. The resin-embedded bone was cut longitudinally into 7-μm sections by

a microtome equipped with a tungsten carbide blade (model RM2255; Leica, Nussloch, Germany). Bone sections were then mounted on microscope slides, deplastinated, dehydrated, and processed for the Goldner's trichrome staining (van't Hof et al. 2003). Growth plate height was measured under a light microscope (model BX51TRF; Olympus, Tokyo, Japan) with the computer-assisted Motic Images Plus 2.0 (Motic Instruments Inc., Richmond, Canada).

Histomorphometric measurement of growth plate zones (i.e., RZ, PZ and HZ) was previously described by Yakar and colleagues (2002). In brief, all measurements were performed within the central two-thirds of growth plate section. The height of each zone was determined by using the following criteria: (1) PZ contains three or more cells aligned with the long axis of the bone and each cell was not greater than 10 μm in height, (2) HZ is measured from the end of PZ to the border of primary spongiosa (i.e., at the site of vascular invasion), and (3) RZ is the subtraction of PZ and HZ heights from the total growth plate height.

Immunohistochemical localization of PRLR

Tibiae were dissected from lactating (L8) rats. After removal of adhering tissue and bone marrow, they were fixed overnight at 4°C in 0.1 M phosphate-buffered saline (PBS) containing 4% *w/v* paraformaldehyde. Decalcification was performed by immersing bone specimens in 15% *w/v* ethylenediaminetetraacetic acid (EDTA; Sigma) for 3 weeks (Wongdee et al. 2010). Decalcifying solution was changed every 3 days. After being embedded in paraffin, the specimens were cut longitudinally into 7-μm sections which were later incubated at 37°C for 30 min in antigen retrieval solution (0.01 mg/mL proteinase K, 50 mM Tris–HCl pH 8.0 and 5 mM EDTA). Thereafter, the sections were incubated for 1 h with 3% H_2O_2 to inhibit endogenous peroxidase activity. Non-specific bindings were blocked by 2-h incubation with 4% bovine serum albumin, 10% normal goat serum, and 0.7% Tween-20 in PBS. The sections were then incubated at 4°C overnight with 1:50 rabbit polyclonal primary antibody against PRLR (catalog no. sc-30225; Santa Cruz Biotechnology, CA, USA). After being washed with 0.7% Tween-20 in PBS, the sections were incubated for 1 h at room temperature with 1:500 biotinylated goat anti-rabbit IgG (catalog no. 656140; Zymed, South San Francisco, CA, USA), followed by 1-h incubation with streptavidin-conjugated horseradish peroxidase solution (Zymed) and 3,3′-diaminobenzidine chromogen (Pierce, Rockford, IL, USA). As for the negative control, the sections were incubated with 0.7% Tween-20 in PBS in the absence of PRLR primary antibody. Finally, the sections were counterstained with hematoxylin (Sigma), and examined under a light microscope and Image Pro Plus 5 (Media Cybernetics, Bethesda, MD, USA).

Statistical analysis

Unless otherwise specified, the results are expressed as means ± SE. Two sets of data were compared by the unpaired Student's *t*-test. One-way analysis of variance (ANOVA) with Newman–Keuls multiple comparison test was used for multiple sets of data. The level of significance for all statistical tests was $P < 0.05$. Data were analyzed by GraphPad Prism 4.0 for Mac OS X (GraphPad Software Inc., San Diego, CA, USA).

Results

Correlations between the heights of growth plate zones and tibial length

Consistent with the previous report (Suntornsaratoon et al. 2010a), the tibial and femoral lengths of maternal rats were significantly increased by ~2 and ~3%, respectively, at late lactation (L21) when compared with the age-matched controls (Fig. 1). Correlation plots indicated that the tibial length of L21 rats was negatively correlated with the total growth plate height, as well as PZ and HZ heights (Fig. 2). However, there was no correlation between the tibial length and RZ height (Fig. 2b).

Expression of PRLR in growth plate

Prior to investigation of possible PRL effect on growth plate, PRLR protein expression in the growth plate was first demonstrated by immunohistochemistry in decalcified tibial sections. As shown in Fig. 3, positive brownish signals of PRLR were localized in chondrocytes in all three zones of tibial growth plate cartilage from L21 lactating rats.

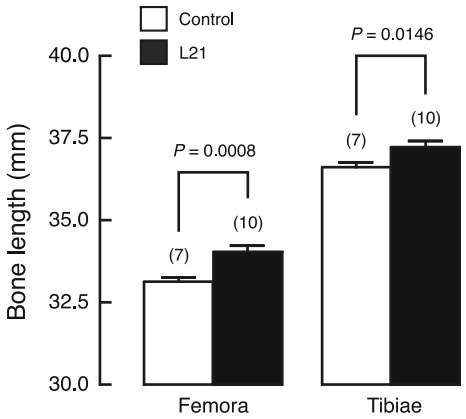

Fig. 1 Femoral and tibial lengths of L21 and age-matched control rats. *Numbers* in parentheses represent the numbers of experimental animals. *P*-values (unpaired Student's *t*-test) are presented above the corresponding *bars*

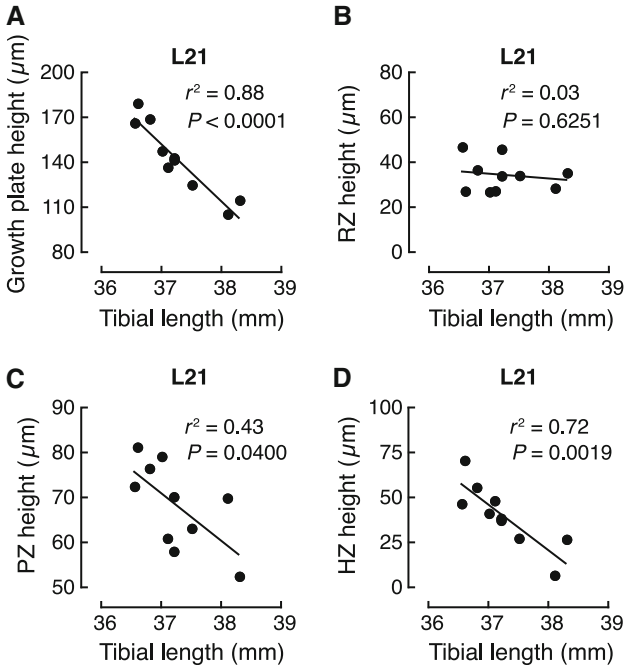

Fig. 2 Graphs of the lengths versus the heights of **a** growth plate, **b** resting zone (RZ), **c** proliferating zone (PZ), and **d** hypertrophic zone (HZ) in tibiae obtained from L21 rats. *P*-values, coefficients of determination (r^2), and regression lines are presented. The tibial length of L21 rats showed negative correlations with the heights of growth plate, PZ and HZ ($P < 0.05$), but showed no correlation with RZ height ($P > 0.05$)

However, in RZ, PZ and upper 2/3 of HZ, PRLR proteins were abundant in the cytoplasm, whereas they were localized at the cell periphery, presumably on the plasma membrane, in hypertrophic chondrocytes near primary spongiosa (lower 1/3 of HZ; Fig. 3f). PRLR proteins were also expressed in osteoblasts covering bone trabeculae (visualized at 1,000×; data not shown), but not in the embedded osteocytes. Similar pattern of PRLR protein expression was observed in the tibial growth plate cartilage of non-pregnant rats (Fig. 4).

Changes in growth plate height during pregnancy and lactation

Microscopic examination of tibial growth plate in different reproductive phases was performed in Goldner's trichrome-stained undecalcified sections. The total growth plate height of proximal tibia was initially decreased at late pregnancy (P21) by ~22%, when compared with the corresponding age-matched controls (Fig. 5). Thereafter, it was progressively decreased to the lowest point (~70% of the control value) in late lactation (L21), and was partially restored postweaning. Representative photomicrographs of the growth plate in L21 rats are also presented (Fig. 6). Inhibition of pituitary PRL secretion by Bromo completely prevented the reduction in growth plate heights in L14 and L21 rats (Figs. 5, 6). Bromo also partially restored the decreased growth plate height in L8 rats, but did not alter that in P21 rats (Fig. 5). Moreover, exogenous PRL supplement to Bromo-treated lactating rats reduced the growth plate heights to the values observed in lactation (Figs. 5, 6). The results suggested that the growth plate change during lactation was dependent on PRL.

Changes in the heights of growth plate zones during pregnancy and lactation

Histomorphometric analysis of Goldner's trichrome-stained tibial sections further revealed that the heights of all growth plate zones were markedly changed during pregnancy and lactation but within different timeframe. Although the RZ height (Fig. 7a) was significantly decreased only at late lactation (L21), the heights of PZ (Fig. 7b) and HZ (Fig. 7c) were dramatically reduced, especially from late pregnancy (P21) to mid-lactation (L14). A decrease in HZ height persisted until late lactation (L21). Fifteen days after weaning, PZ and HZ heights were still significantly lower than those of the controls.

Further investigations in Bromo- and Bromo + PRL-treated rats revealed that the pregnancy-induced changes in growth plate zones were independent of pituitary PRL (Fig. 7). On the other hand, the lactation-induced decreases in RZ and PZ heights in late and mid-lactation, respectively, were found to be PRL-dependent (Fig. 7a–b). Moreover, PRL was responsible for the reduction in HZ height throughout the lactating period (Fig. 7c). Our results therefore suggested the chondroregulatory action of PRL in maternal long bone during lactation.

Discussion

Whether PRL plays a role in the regulation of growth plate cartilage during pregnancy and lactation has not been known. Here, we provided, for the first time, suggestive evidence on the chondroregulatory action of PRL in the tibial growth plate, especially in lactating rats. Normally, PRL is one of the maternal calciotropic hormones, which helps supply sufficient calcium for the developing fetuses and milk production, in part, by increasing intestinal calcium absorption and enhancing bone resorption (Ajibade et al. 2010; Charoenphandhu et al. 2010). In order to supply adequate calcium from maternal bone for milk production, calcium accumulation in cortical envelope and continuing trabecular formation are requisite throughout the reproductive periods, particularly in pregnancy and early lactation (Bowman and Miller 2001; Miller et al. 1986; Suntornsaratoon et al. 2010a, b). Thereafter, in late

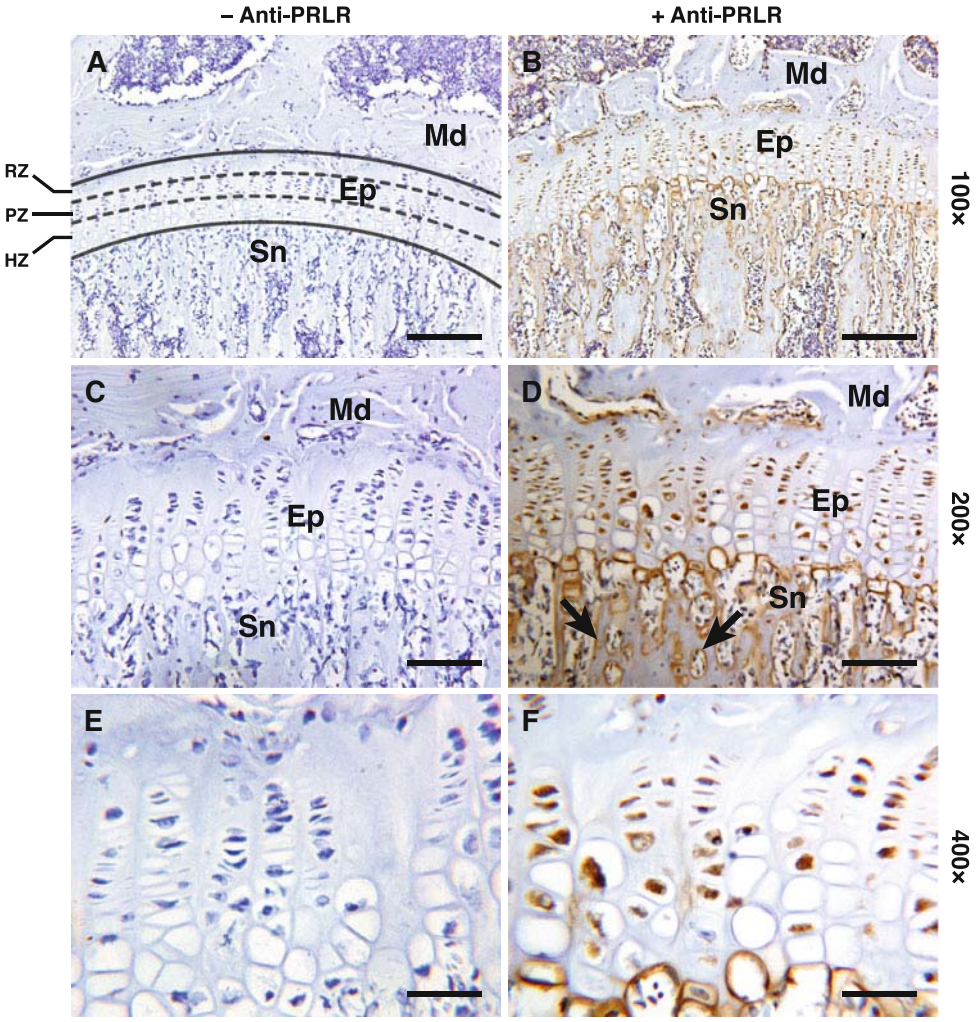

Fig. 3 **a–f** Immunohistochemical localization of PRLR proteins in paraffin-embedded decalcified tibial sections from lactating rats (L8; $n = 4$) at 100× (*bars*, 200 μm), 200× (*bars*, 100 μm), and 400× (*bars*, 50 μm) magnifications. The immuno-stained (+Anti-PRLR) and corresponding negative control (−Anti-PRLR) sections were incubated in the presence and absence of anti-PRLR antibody, respectively. Images of negative control do not show immunoreactive signal. The positive *brownish* signals are observed in chondrocytes in all three zones of the epiphyseal plate (*Ep*), i.e., resting zone (*RZ*), proliferating zone (*PZ*) and hypertrophic zone (*HZ*). Positive signals are also localized in osteoblasts in the primary spongiosa (*Sn*), but not in osteocytes embedded in mineralized matrix (*Md*) of bone trabeculae (*arrows*)

lactation, both cortical envelope and metaphyseal trabeculae are resorbed to release the stockpiled calcium under a concerted regulation of several hormones, such as PRL and PTHrP (Charoenphandhu et al. 2010; Kovacs 2005). Since bone resorption usually exceeds bone formation during lactation, osteopenia does occur in nursing mothers; however, bone loss is gradually reversed postweaning (Charoenphandhu et al. 2010; Kovacs 2005).

Elongation of the maternal bone during the reproductive periods is not uncommon in rodents (Dengler-Crish and Catania 2009). In primiparous mole rats, the lumbar vertebral length was markedly increased during pregnancy, and this lengthening was dampened after delivery (Dengler-Crish and Catania 2009). Our previous study in rats also demonstrated that, in addition to the increased bone length, the cortical envelope of long bone was also thickened during pregnancy, presumably to help maintain bone strength and/or prevent fracture during the lactation-induced massive trabecular bone loss (Suntornsaratoon et al. 2010a). This increase in bone length in lactating rats was previously shown to be dependent on PRL (Suntornsaratoon et al. 2010a). Moreover, as shown in the present study, the tibial length was negatively correlated with the total growth plate height, PZ height, and HZ heights, similar to that reported previously in mice (van Buul-Offers et al. 1984), thereby supporting the hypothesis that the increased length of maternal long bone resulted from the adaptive changes in the growth plate cartilage, and particularly from the accelerated endochondral ossification.

Data from the Bromo-treated P21 rats (Fig. 7b–c) indicated that the pregnancy-induced changes in growth plate zones were independent of pituitary PRL because PRL supplement was unable to restore the zone heights. It is currently not known why Bromo, a dopaminergic agonist, slightly but significantly diminished the change in HZ height in P21 rats (Fig. 7c). However, the direct Bromo effect on growth plate cartilage could not be excluded despite lack of reports on dopaminergic D2 receptor expression in growth plate cartilage of pregnant rats. A previous report using radioligand binding assays in human articular cartilage suggested that, under certain conditions

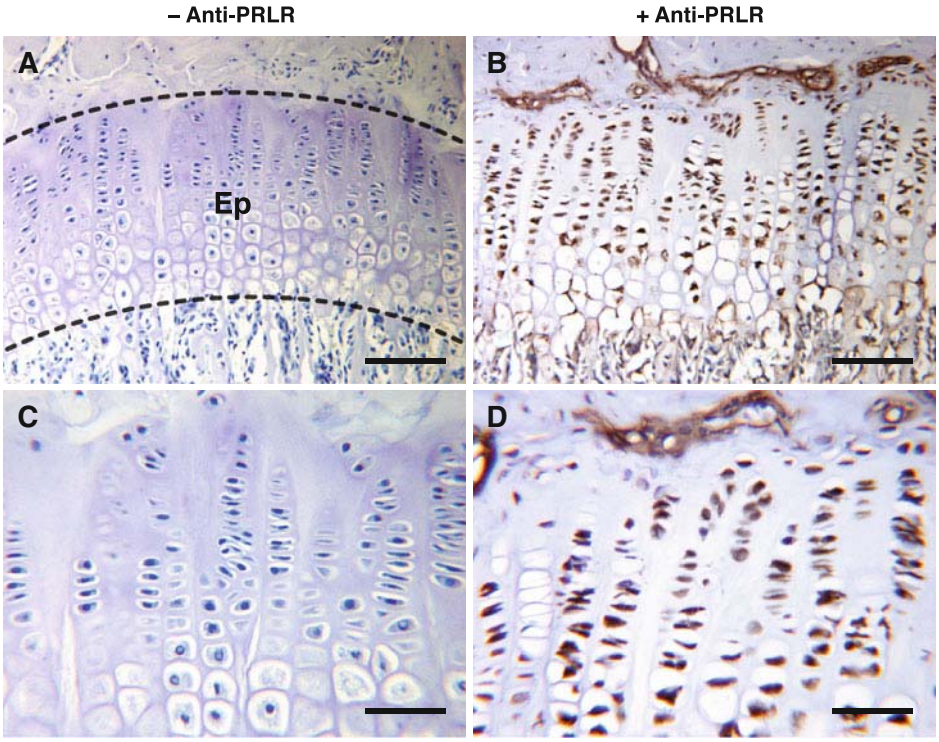

Fig. 4 **a–d** Immunohistochemical localization of PRLR proteins in paraffin-embedded decalcified tibial sections from non-pregnant rats (normal rats; $n = 5$) at 200× (*bars*, 100 μm) and 400× (*bars*, 50 μm) magnifications. The immuno-stained (+Anti-PRLR) and corresponding negative control (−Anti-PRLR) sections were incubated in the presence and absence of anti-PRLR antibody, respectively. Images of negative control sections do not show immunoreactive signal. The positive *brownish* signals are observed in chondrocytes in all three zones of the epiphyseal plate (*Ep*)

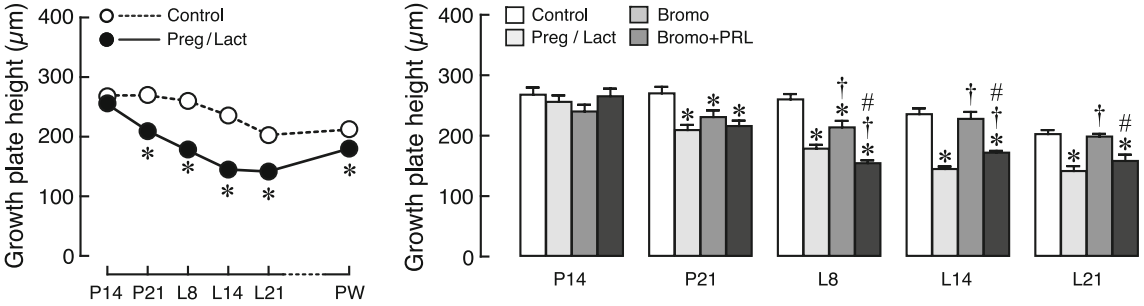

Fig. 5 Growth plate height of tibiae obtained from pregnant (P14 and P21), lactating (L8, L14 and L21), 15-day postweaning (PW), and aged-matched control rats. Some pregnant and lactating rats were administered for 7 days with 4 mg/kg/day bromocriptine s.c. (Bromo), or Bromo and PRL s.c. (Bromo + PRL). The PRL doses for pregnant and lactating rats were 0.4 and 0.6 mg/kg/day, respectively. All values in line graphs and bar graphs are presented as means ± SE ($n = 6$–10 rats per condition). $^{*}P < 0.05$ compared with age-matched control group. $^{\dagger}P < 0.05$ compared with the corresponding lactating group. $^{\#}P < 0.05$ compared with Bromo group

(e.g., osteoarthritis), chondrocytes might be responsive to dopamine agonist (Vignon et al. 1990).

On the other hand, the lactation-induced decreases in the total growth plate height as well as RZ, PZ, and HZ heights in different phases of lactation were found to be PRL-dependent (Fig. 7). Although decreases in the total height and HZ height observed throughout the entire lactating period were induced by PRL, the responses of the chondrocytes in RZ and PZ to PRL were less consistent (Fig. 7). Localization of PRLR proteins on the plasma membrane of hypertrophic chondrocytes (Fig. 3f) could partially explain why the PRL effects were clearly observed in HZ. It was also possible that PRL acted specifically on fully differentiated chondrocytes in HZ rather than on young proliferating and progenitor cells in PZ and RZ, respectively. The differential responsiveness to PRL was previously reported in human undifferentiated mesenchymal stem cells and their chondrocyte-like progeny expressing intermediate and long isoforms of PRLR, respectively (Ogueta et al. 2002), the latter of which was the functional PRLR isoform in several cell types, including mammary and intestinal epithelial cells (Binart et al. 2010; Thongon et al. 2008).

Although the underlying mechanism of PRL action on the growth plate is not known, the strong expression of

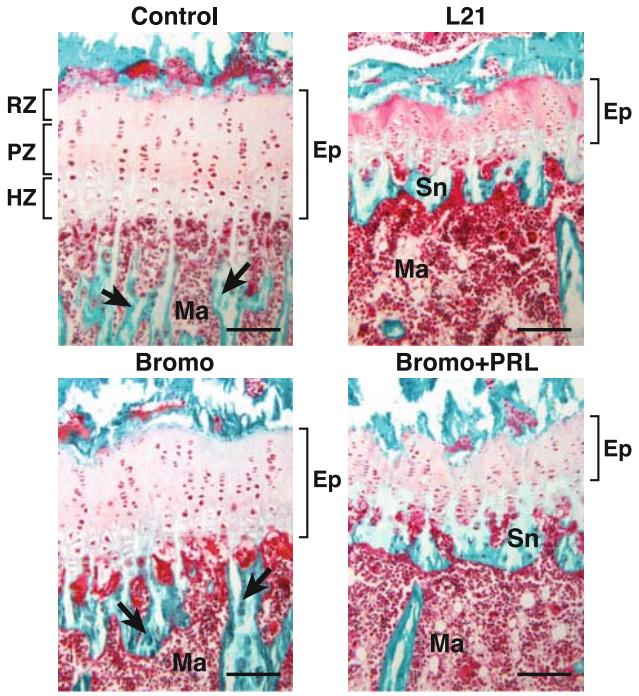

Fig. 6 Representative photomicrographs of Goldner's trichrome-stained tibial growth plates dissected from L21, Bromo-treated L21, Bromo + PRL-treated L21, and age-matched control rats. Primary spongiosa (*Sn*) and all three zones of epiphyseal plate (*Ep*), i.e., resting zone (*RZ*), proliferating zone (*PZ*) and hypertrophic zone (*HZ*) were identified. Mineralized trabeculae (*arrows*) and marrow cells (*Ma*) were stained *green* and *red*, respectively. *Bars*, 100 μm

PRLR in the growth plate chondrocytes of lactating rats suggested a direct action of PRL. Coss and co-workers (2000) also showed that PRLR was widely expressed in the growth plate chondrocytes in the digits of neonatal rats. Besides the growth plate chondrocytes, PRLR expression has been reported in articular chondrocytes from both humans and rats (Ogueta et al. 2002; Zermeño et al. 2006). In the articular chondrocytes in vitro, PRL has been found to inhibit apoptosis induced by serum starvation (Zermeño et al. 2006) and to increase type II collagen expression (Ogueta et al. 2002). Moreover, PRL could directly induce proliferation and chondrogenic differentiation of the human marrow-derived mesenchymal stem cells to mature chondrocytes (Ogueta et al. 2002). Although the chondrocytes in articular cartilages may have different functions from those in the growth plate since the articular chondrocytes do not proceed to hypertrophic differentiation, the aforementioned findings corroborated that PRL is a regulator of the growth of cartilage.

In addition to possible stimulatory effects of PRL on chondrogenesis (Ogueta et al. 2002; Zermeño et al. 2006), a previous study that showed the delay of calvarial ossification and a decrease in femoral mineral apposition rate in PRLR knockout mice also suggested a stimulatory action of PRL on osteogenesis (Clément-Lacroix et al. 1999). Since the growth plate height is normally maintained by keeping a precise balance between chondrogenesis and osteogenesis, the PRL-induced growth plate narrowing might be due to the enhanced turnover of chondrocyte replication and growth plate ossification, the latter of which probably occurred at the faster rate. Nevertheless, once bone trabeculae which serve as calcium storage pools are formed, later on, by as yet unknown mechanism, PRL appears to enhance bone resorption at the rate that matches the maternal requirement (Charoenphandhu et al. 2010).

In addition to PRL, other hormones, such as IGF-1, placental lactogen (PL) and PTHrP, released during pregnancy and lactation might participate in the present growth plate changes. Plasma levels of IGF-1 and PL were elevated in pregnant humans and rats (Freeman et al. 2000; O'Brien et al. 2006). Both systemic and local IGF-1 productions were known to be essential for chondrogenesis and endochondral ossification (Wang et al. 2006; Yakar et al. 2002). PL can bind to PRLR (Cohick et al. 1996), and thus can mimic the PRL effect on cartilage. In addition, growth plate changes during certain phases of lactation might be due to the circulating PTHrP from the mammary glands and its downstream Indian hedgehog signaling pathways (Goltzman 2010; Maeda et al. 2007; Olsen 2006). Nevertheless, further experiments are required to elucidate the interplay between these maternal hormones and their influence on the growth plate function.

However, the chondroregulatory actions of PRL should be apparent only in mammals with persistent growth plate cartilage. In adolescent humans, the accelerated endochondral ossification might be a compensatory mechanism which helped to maintain bone growth during lactation, despite having lactation-induced bone loss. We also further speculated that, in lactating mammals without growth plates, the PRL-induced bone loss became more pronounced, especially when the intestinal calcium absorption was restricted by inadequate calcium intake.

In conclusion, there was a decrease in the tibial growth plate height from late pregnancy to 15 days postweaning. Such a decrease in the total height in lactation showed a negative correlation with the tibial length, and was mainly due to a decrease in HZ height in a PRL-dependent manner. The presence of PRLR protein expression in growth plate chondrocytes further suggested that PRL exerted a direct action on the tibial growth plate cartilage. Although additional investigations are needed to demonstrate the underlying mechanism, the present results are helpful in understanding better the maternal bone adaptation during

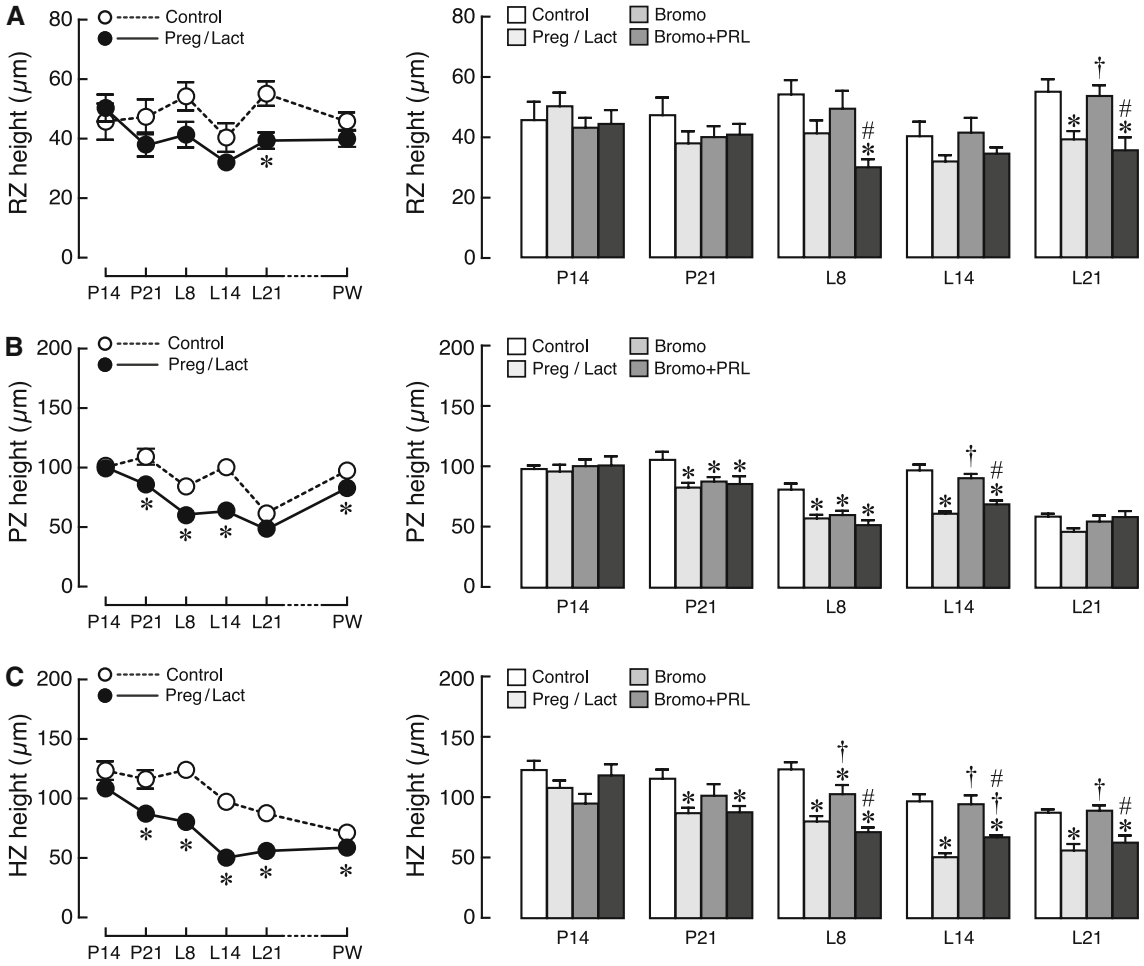

Fig. 7 The heights of **a** resting zone (RZ), **b** proliferating zone (PZ), and **c** hypertrophic zone (HZ) of tibial growth plate obtained from pregnant (P14 and P21), lactating (L8, L14 and L21), 15-day postweaning (PW), and age-matched control rats. Some pregnant and lactating rats were administered for 7 days with 4 mg/kg/day bromocriptine s.c. (Bromo), or Bromo and PRL s.c. (Bromo + PRL). The PRL doses for pregnant and lactating rats were 0.4 and 0.6 mg/kg/day, respectively. All values in *line graphs* and *bar graphs* are presented as means ± SE (n = 6–10 rats per condition). $^{*}P < 0.05$ compared with age-matched control group. $^{\dagger}P < 0.05$ compared with the corresponding lactating group. $^{\#}P < 0.05$ compared with Bromo group

lactation, and substantiate the chondroregulatory role of PRL in lactating rats.

Acknowledgments This research was supported by grants from the King Prajadhipok and Queen Rambhai Barni Memorial Foundation (to P. Suntornsaratoon), the Faculty of Graduate Studies, Mahidol University (to P. Suntornsaratoon), and the Thailand Research Fund (RSA5180001 to N. Charoenphandhu).

Conflict of interest The authors declare no conflicts of interest.

References

Ajibade DV, Dhawan P, Fechner AJ, Meyer MB, Pike JW, Christakos S (2010) Evidence for a role of prolactin in calcium homeostasis: regulation of intestinal transient receptor potential vanilloid type 6, intestinal calcium absorption, and the 25-hydroxyvitamin D_3 1α hydroxylase gene by prolactin. Endocrinology 151:2974–2984

Assapun J, Charoenphandhu N, Krishnamra N (2009) Early acceleration phase and late stationary phase of remodeling imbalance in long bones of male rats exposed to long-standing acidemia: a 10-month longitudinal study using bone histomorphometry. Calcif Tissue Int 85:1–9

Binart N, Bachelot A, Bouilly J (2010) Impact of prolactin receptor isoforms on reproduction. Trends Endocrinol Metab 21:362–368

Bowman BM, Miller SC (2001) Skeletal adaptations during mammalian reproduction. J Musculoskelet Neuronal Interact 1:347–355

Charoenphandhu N, Nakkrasae LI, Kraidith K, Teerapornpuntakit J, Thongchote K, Thongon N, Krishnamra N (2009) Two-step stimulation of intestinal Ca^{2+} absorption during lactation by long-term prolactin exposure and suckling-induced prolactin surge. Am J Physiol Endocrinol Metab 297:E609–E619

Charoenphandhu N, Wongdee K, Krishnamra N (2010) Is prolactin the cardinal calciotropic maternal hormone? Trends Endocrinol Metab 21:395–401

Clément-Lacroix P, Ormandy C, Lepescheux L, Ammann P, Damotte D, Goffin V, Bouchard B, Amling M, Gaillard-Kelly M, Binart

N, Baron R, Kelly PA (1999) Osteoblasts are a new target for prolactin: analysis of bone formation in prolactin receptor knockout mice. Endocrinology 140:96–105

Cohick CB, Dai G, Xu L, Deb S, Kamei T, Levan G, Szpirer C, Szpirer J, Kwok SC, Soares MJ (1996) Placental lactogen-I variant utilizes the prolactin receptor signaling pathway. Mol Cell Endocrinol 116:49–58

Coss D, Yang L, Kuo CB, Xu X, Luben RA, Walker AM (2000) Effects of prolactin on osteoblast alkaline phosphatase and bone formation in the developing rat. Am J Physiol Endocrinol Metab 279:E1216–E1225

Dengler-Crish CM, Catania KC (2009) Cessation of reproduction-related spine elongation after multiple breeding cycles in female naked mole-rats. Anat Rec (Hoboken) 292:131–137

Freeman ME, Kanyicska B, Lerant A, Nagy G (2000) Prolactin: structure, function, and regulation of secretion. Physiol Rev 80:1523–1631

Gartner LP, Hiatt JL (2001) Cartilage and bone. In: Gartner LP, Hiatt JL (eds) Color textbook of histology. Saunders, Philadelphia, pp 94–101

Goltzman D (2010) Emerging roles for calcium-regulating hormones beyond osteolysis. Trends Endocrinol Metab 21:512–518

Hong JS, Santolaya-Forgas J, Romero R, Espinoza J, Goncalves LF, Kim YM, Edwin S, Yoon BH, Nien JK, Hassan S, Mazor M (2005) Maternal plasma osteoprotegerin concentration in normal pregnancy. Am J Obstet Gynecol 193:1011–1015

Kovacs CS (2005) Calcium and bone metabolism during pregnancy and lactation. J Mammary Gland Biol Neoplasia 10:105–118

Maeda Y, Nakamura E, Nguyen MT, Suva LJ, Swain FL, Razzaque MS, Mackem S, Lanske B (2007) Indian hedgehog produced by postnatal chondrocytes is essential for maintaining a growth plate and trabecular bone. Proc Natl Acad Sci USA 104:6382–6387

Miller SC, Shupe JG, Redd EH, Miller MA, Omura TH (1986) Changes in bone mineral and bone formation rates during pregnancy and lactation in rats. Bone 7:283–287

O'Brien KO, Donangelo CM, Zapata CL, Abrams SA, Spencer EM, King JC (2006) Bone calcium turnover during pregnancy and lactation in women with low calcium diets is associated with calcium intake and circulating insulin-like growth factor 1 concentrations. Am J Clin Nutr 83:317–323

Ofluoglu O, Ofluoglu D (2008) A case report: pregnancy-induced severe osteoporosis with eight vertebral fractures. Rheumatol Int 29:197–201

Ogueta S, Muñoz J, Obregon E, Delgado-Baeza E, García-Ruiz JP (2002) Prolactin is a component of the human synovial liquid and modulates the growth and chondrogenic differentiation of bone marrow-derived mesenchymal stem cells. Mol Cell Endocrinol 190:51–63

Olsen BR (2006) Bone embryology. In: Favus MJ (ed) Primer on the metabolic bone diseases and disorders of mineral metabolism. American Society for Bone and Mineral Research, Washington, DC, pp 2–6

Rauch F (2005) Bone growth in length and width: the Yin and Yang of bone stability. J Musculoskelet Neuronal Interact 5:194–201

Seriwatanachai D, Thongchote K, Charoenphandhu N, Pandaranandaka J, Tudpor K, Teerapornpuntakit J, Suthiphongchai T, Krishnamra N (2008) Prolactin directly enhances bone turnover by raising osteoblast-expressed receptor activator of nuclear factor κB ligand/osteoprotegerin ratio. Bone 42:535–546

Suntornsaratoon P, Wongdee K, Goswami S, Krishnamra N, Charoenphandhu N (2010a) Bone modeling in bromocriptine-treated pregnant and lactating rats: possible osteoregulatory role of prolactin in lactation. Am J Physiol Endocrinol Metab 299:E426–E436

Suntornsaratoon P, Wongdee K, Krishnamra N, Charoenphandhu N (2010b) Femoral bone mineral density and bone mineral content in bromocriptine-treated pregnant and lactating rats. J Physiol Sci 60:1–8

Thongon N, Nakkrasae LI, Thongbunchoo J, Krishnamra N, Charoenphandhu N (2008) Prolactin stimulates transepithelial calcium transport and modulates paracellular permselectivity in Caco-2 monolayer: mediation by PKC and ROCK pathways. Am J Physiol Cell Physiol 294:C1158–C1168

van Buul-Offers S, Smeets T, Van den Brande JL (1984) Effects of growth hormone and thyroxine on the relation between tibial length and the histological appearance of the proximal tibial epiphysis in Snell dwarf mice. Growth 48:166–175

van't RJ, Clarkin CE, Armour KJ (2003) Studies of local bone remodeling: the calvarial injection assay. In: Helfrich MH, Ralston SH (eds) Bone research protocols. Humana Press, New Jersey, pp 345–351

Vignon E, Broquet P, Mathieu P, Louisot P, Richard M (1990) Histaminergic H1, serotoninergic, β-adrenergic and dopaminergic receptors in human osteoarthritic cartilage. Biochem Int 20:251–255

Wang Y, Nishida S, Sakata T, Elalieh HZ, Chang W, Halloran BP, Doty SB, Bikle DD (2006) Insulin-like growth factor-I is essential for embryonic bone development. Endocrinology 147:4753–4761

Wongdee K, Riengrojpitak S, Krishnamra N, Charoenphandhu N (2010) Claudin expression in the bone-lining cells of female rats exposed to long-standing acidemia. Exp Mol Pathol 88:305–310

Yakar S, Rosen CJ, Beamer WG, Ackert-Bicknell CL, Wu Y, Liu JL, Ooi GT, Setser J, Frystyk J, Boisclair YR, LeRoith D (2002) Circulating levels of IGF-1 directly regulate bone growth and density. J Clin Invest 110:771–781

Zermeño C, Guzmán-Morales J, Macotela Y, Nava G, López-Barrera F, Kouri JB, Lavalle C, de la Escalera GM, Clapp C (2006) Prolactin inhibits the apoptosis of chondrocytes induced by serum starvation. J Endocrinol 189:R1–R8

Bone modeling in bromocriptine-treated pregnant and lactating rats: possible osteoregulatory role of prolactin in lactation

Panan Suntornsaratoon, Kannikar Wongdee, Suchandra Goswami, Nateetip Krishnamra and Narattaphol Charoenphandhu

Am J Physiol Endocrinol Metab 299:E426-E436, 2010. First published 15 June 2010; doi:10.1152/ajpendo.00134.2010

Am J Physiol Endocrinol Metab 299: E426–E436, 2010.
First published June 15, 2010; doi:10.1152/ajpendo.00134.2010.

Bone modeling in bromocriptine-treated pregnant and lactating rats: possible osteoregulatory role of prolactin in lactation

Panan Suntornsaratoon,[1,2] Kannikar Wongdee,[1,3] Suchandra Goswami,[1] Nateetip Krishnamra,[1,2] and Narattaphol Charoenphandhu[1,2]

[1]*Consortium for Calcium and Bone Research (COCAB),* [2]*Department of Physiology, Faculty of Science, Mahidol University, Bangkok; and* [3]*Faculty of Allied Health Sciences, Burapha University, Chonburi, Thailand*

Submitted 1 March 2010; accepted in final form 8 June 2010

Suntornsaratoon P, Wongdee K, Goswami S, Krishnamra N, Charoenphandhu N. Bone modeling in bromocriptine-treated pregnant and lactating rats: possible osteoregulatory role of prolactin in lactation. *Am J Physiol Endocrinol Metab* 299: E426–E436, 2010. First published June 15, 2010; doi:10.1152/ajpendo.00134.2010.—The lactogenic hormone prolactin (PRL) directly regulates osteoblast functions in vitro and modulates bone remodeling in nulliparous rats, but its osteoregulatory roles in pregnant and lactating rats with physiological hyperprolactinemia remained unclear. Herein, bone changes were investigated in rats treated with bromocriptine (Bromo), an inhibitor of pituitary PRL release, or Bromo+PRL at different reproductive phases, from mid-pregnancy to late lactation. PRL receptors were strongly expressed in osteoblasts lining bone trabeculae, indicating bone as a target of PRL actions. By using dual energy X-ray absorptiometry, we found a significant increase in bone mineral density in the femora and vertebrae of pregnant rats. Such pregnancy-induced bone gain was, however, PRL independent and may have resulted from the increased cortical thickness. Bone trabeculae were modestly changed during pregnancy as evaluated by bone histomorphometry. On the other hand, lactating rats, especially in late lactation, showed massive bone loss in bone trabeculae but not in cortical shells. Further study in Bromo- and Bromo+PRL-treated rats suggested that PRL contributed to decreases in trabecular bone volume and number and increases in trabecular separation and eroded surface, as well as a paradoxical increase in bone formation rate in late lactation. Uncoupling of trabecular bone formation and resorption was evident in lactating rats, with the latter being predominant. In conclusion, pregnancy mainly induced cortical bone gain, whereas lactation led to trabecular bone loss in both long bones and vertebrae. Although PRL was not responsible for the pregnancy-induced bone gain, it was an important regulator of bone modeling during lactation.

bone histomorphometry; hyperprolactinemia; ion chromatography; osteopenia; uncoupling

IN PREGNANT AND BREASTFEEDING WOMEN, massive calcium loss occurs for fetal development (~200–300 mg/day) and lactogenesis (~300–1,000 mg/day), respectively (4, 23, 36). A huge amount of calcium demand is accomplished, in part, by enhanced intestinal calcium absorption during these reproductive periods (9). Our recent studies in rats demonstrated that the lactogenic hormone prolactin (PRL), released from the anterior pituitary gland during pregnancy (~100–200 ng/ml) and lactation (~200–300 ng/ml), was the principal calciotropic maternal hormone, which was capable of stimulating calcium absorption in the small intestine and proximal large intestine (7, 21). Moreover, lactation-induced bone resorption provides additional calcium to match the increased calcium demand of the offspring, which in turn induces reversible osteopenia in mothers (20, 36).

In both humans and rodents, hormonal regulation of bone changes during pregnancy and lactation is not completely understood, but it is not directly regulated by the major calciotropic hormones, namely parathyroid hormone (PTH) and 1,25-dihydroxyvitamin D_3 [1,25$(OH)_2D_3$] (9, 30, 36). Other hormones with elevated plasma levels, such as PRL, PTH-related peptide (PTHrP), calcitonin, and insulin-like growth factor (IGF)-I, might contribute to the maternal bone changes, perhaps with each exerting action at different times and in a bone site-specific manner (4, 20). Among these hormones, PRL is of special interest, since its plasma levels are increased ~10-fold and ~20-fold in pregnant and lactating rats, respectively (6). In addition, primary osteoblasts cultured from rat bones were found to strongly express mRNAs and proteins of PRL receptors (PRLR), suggesting that bone could be another target tissue of PRL actions (40).

A recent investigation in nulliparous rats with hyperprolactinemia induced by pituitary transplantation showed that PRL could induce both bone formation and bone resorption, with the latter being predominant, thereby leading to net bone loss and osteopenia (40). $PRLR^{-/-}$ mice also manifested an impairment of bone growth and mineralization of bone matrix (11). Moreover, pathological hyperprolactinemia in nonpregnant patients with prolactinoma or chronic uses of antipsychotic drugs (i.e., dopaminergic antagonists) may lead to progressive osteopenia and osteoporosis (27, 42). Such bone loss in rodents was apparent mainly in the primarily trabecular site (e.g., vertebrae) or the trabecular parts of the long bone (e.g., metaphysis or secondary spongiosa) but was rarely observed in the cortex (8, 44). The PRL-related bone loss may result from direct actions of PRL on osteoblasts as well as indirectly from the PRL-induced hypoestrogenemia (8, 12, 27, 40).

Although pregnancy and lactation are considered a physiological hyperprolactinemic state (9), little is currently known regarding the effects of PRL on cortical and trabecular sites at different phases of the reproductive periods (e.g., early vs. late lactation). Generally, longitudinal studies of PRL actions on maternal bone metabolism are carried out in animals treated with bromocriptine (Bromo), an agonist of the PRL-inhibiting factor dopamine, which can inhibit pituitary PRL release by ~80–90% (3, 7, 35), in the presence or absence of exogenous PRL administration (43). The uses of $PRL^{-/-}$ or $PRLR^{-/-}$ mice are not possible due to infertility (2). Furthermore, disruption of PRL synthesis in the first week of pregnancy in rodents could lead to abortion (2). Thus, by using Bromo-treated lactating rats, the effect of PRL on the long bone could be demonstrated by densitometric analysis (43), but whether

Address for reprint requests and other correspondence: N. Charoenphandhu, Dept. of Physiology, Faculty of Science, Mahidol University, Rama VI Road, Bangkok 10400, Thailand (e-mail: naratt@narattsys.com).

microstructural changes in the cortices and trabeculae were different remained to be investigated. Nevertheless, the aforementioned findings in nulliparous rats (40, 44) suggested that PRL could have action on maternal bone, particularly in the trabeculae.

Therefore, the objectives of the present longitudinal study were *1*) to investigate macroscopic and microscopic bone changes by using dual energy X-ray absorptiometry (DEXA) and bone histomorphometry, respectively, in pregnant and lactating rats, from mid-pregnancy to day 15 postweaning, *2*) to reveal the possible roles of PRL in regulating maternal bone changes, and *3*) to demonstrate differential responses of maternal cortical and trabecular bones to PRL in different reproductive periods.

MATERIALS AND METHODS

Animals. Pregnant and age-matched nulliparous Sprague-Dawley rats (8 wk old) were obtained from the National Laboratory Animal Centre in Thailand. They were housed in the husbandry unit under a 12:12-h light-dark cycle (lights on at 0600) for at least 5 days prior to the experiments and were fed standard chow and distilled water ad libitum. The room had a temperature of 25 ± 2°C with average illuminance of 200 lux. This study was approved by the Animal Care and Use Committee of the Faculty of Science, Mahidol University. All animals were cared for in accordance with the principles and guidelines of the American Physiological Society's "Guiding Principles in the Care and Use of Animals."

Experimental design. Bone changes were investigated in different reproductive phases, i.e., mid-pregnancy (day 14, P14), late pregnancy (day 21, P21), early lactation (day 8, L8), mid-lactation (day 14, L14), late lactation (day 21, L21), and day 15 postweaning (PW). Since bone growth and calcium accretion are normally age dependent, we used age-matched nulliparous rats as a control group. Ages of P14, P21, L8, L14, L21, and PW rats were 10, 11, 12, 13, 14, and 16 wk old, respectively. Body weights of all rats were recorded weekly (Supplemental Fig. S1; supplemental materials are found in the online version of this paper at the Journal website). After delivery, litter size was adjusted to eight pups per dam for lactating groups, whereas in nonsuckling groups all pups were permanently separated from dams from birth. Such nonsuckling mothers were reported to have no hyperprolactinemia because the suckling-induced PRL surge was absent, and plasma PRL levels rapidly declined within 12 h after cessation of suckling (26, 34). In some experiments, dams were injected daily subcutaneously for 7 days with 4 mg/kg Bromo sc (Sigma, St. Louis, MO) or Bromo+PRL (purified from ovine pituitary gland; catalog no. L6520, Sigma) before being killed. PRL doses for pregnant and lactating rats were 0.4 and 0.6 mg/kg, respectively (7). These PRL regimens have been reported to completely restore the Bromo-induced decrease in the intestinal calcium absorption in pregnant and lactating rats (7). Finally, all rats in each pregnant (P14 and P21) or lactating (L8, L14, and L21) group were killed on the same day, between 0800 and 1000.

Preparation of bone samples. As previously described by Charoenphandhu et al. (8), femora (primarily cortical sites) and *L5* vertebrae (primarily trabecular sites) were cleaned and subjected to densitometric analysis. In some experiments, femoral length and dry and ash weights were recorded. Femora were dried in an oven at 80°C for 3 days and then ashed at 800°C overnight in a muffle furnace (model 48000; Thermolyne, Dubuque, IA). After bone ash was dissolved with 3.0 N HCl, the samples were diluted with a solution containing 0.38% wt/vol $SrCl_2$ and 0.9% vol/vol $HClO_4$ and were analyzed for total calcium and magnesium contents by atomic absorption spectrophotometry (for calcium only; model SpectrAA-300, Varian Techtron, Springvale, Australia) and ion chromatography (for calcium and magnesium).

Tibiae (primarily cortical sites) were also removed, cleaned, and fixed for PRLR expression study and histomorphometric analysis of their cortical and trabecular portions.

Immunohistochemical analysis of PRLR expression. Tibiae were dissected from P21 and L8 rats. After cleaning, they were fixed overnight in 0.1 M phosphate-buffered saline (PBS) containing 4% paraformaldehyde. Decalcification was later performed by immersing bone specimens in 15% wt/vol ethylenediaminetetraacetic acid (EDTA; Sigma) at 25°C for 3 wk. Decalcifying solution was replaced every 3 days. After being embedded in paraffin, bone specimens were cut longitudinally into 7-μm sections, which were later incubated at 37°C for 30 min in antigen retrieval solution (0.01 mg/ml proteinase K, 50 mM Tris·HCl, pH 8.0, and 5 mM EDTA). To inhibit background endogenous peroxidase activity, sections were incubated for 1 h with 10% H_2O_2. Nonspecific binding was blocked for 2 h by 4% bovine serum albumin, 10% normal goat serum, and 0.7% Tween-20 in PBS. Thereafter, sections were incubated at 4°C overnight with 1:50 rabbit polyclonal primary antibody against PRLR (catalog no. sc-30225; Santa Cruz Biotechnology, Santa Cruz, CA). After being washed with 0.7% Tween-20 in PBS, sections were incubated for 1 h at room temperature with 1:500 biotinylated goat anti-rabbit IgG (catalog no. 656140; Zymed, South San Francisco, CA) followed by incubation for 1 h with streptavidin-conjugated horseradish peroxidase solution (Zymed) and 3,3′-diaminobenzidine chromogen (Pierce, Rockford, IL). As for the negative control, sections were incubated with 0.7% Tween-20 in PBS in the absence of PRLR primary antibody. Sections were counterstained with hematoxylin and visualized under a light microscope (model BX51TRF; Olympus, Tokyo, Japan).

Measurement of bone calcium and magnesium contents by ion chromatography. A modular ion chromatographic system (Waters, Milford, MA) comprised a model-600 controller, model-600 pump, model-432 conductivity detector, and a cation column containing silica gel with sulfonic acid group (125 × 4 mm inner diameter, 5 μm particle size, model Nucleosil 5SA; Metrohm, Herisau, Switzerland). All components were connected through the Waters SAT/IN module to a Millennium 32 workstation, which performed system control, acquisition, and data analysis. The eluent for simultaneous separation of the divalent cations consisted of 4 mM tartaric acid, 0.5 mM citric acid, and 3 mM ethylenediamine in 5% vol/vol acetone and were degassed for 5 min before use. Eluent flow rates were adjusted at 1.5 ml/min, and the column was equilibrated in eluent for 45 min prior to sample charging. The analytic condition was optimized for isocratic elution using a 100-μl injection loop and total run time of 10 min. Calcium and magnesium were eluted at 5.9 and 7.0 min, respectively. Standard stock solutions were prepared by dissolving appropriate amounts of $CaCl_2$ or $MgCl_2$ in ultrapure Milli-Q water to obtain a final concentration of 1 M and kept at −20°C. Working standard solutions were prepared fresh by diluting the stock solutions to 10, 20, 50, 100, 150, and 200 μM with Milli-Q water (pH ~2.5–3.5 adjusted with 2 M HNO_3) for six-point calibration. The detection limit of both calcium and magnesium at a signal-to-noise ratio of 3:1 appeared to be ~0.02 and ~0.04 μM, respectively. The six-point calibrations for calcium and magnesium showed percent residual standard deviations of 0.9 and 0.5 and correlation coefficients of 0.9989 and 0.9993, respectively. A reproducibility test was performed by injecting standard solutions 10 times on the same day as well as on different days. The relative standard deviations of peak area of calcium and magnesium were varied by less than 0.5% and 3–5%, respectively, during intraday vs. interday tests.

For the analyses of bone calcium and magnesium contents, each bone sample was dissolved in 3 N HCl and diluted 100-fold with distilled water. Thereafter, all samples were filtered through 0.22-μm membranes prior to injection into the column. All samples were analyzed in duplicate and reported as millimoles per gram of dry weight of bone.

DEXA. Bone mineral density (BMD) and bone mineral content (BMC) were determined in the ex vivo whole femora and *L5* vertebrae by DEXA (model Lunar PIXImus2; GE Medical Systems, Madison, WI), operated with software version 2.10, as previously described (8). The system was calibrated daily with a standard material of known BMD and BMC of 0.0690 g/cm^2 and 0.697 g, respectively.

Bone histomorphometry. A tibia was cleaned of adhering tissues and bone marrow. Bone was then dehydrated in 70, 95, and 100% vol/vol ethanol for 3, 3, and 2 days, respectively. Dehydrated bone was embedded in methyl methacrylate resin at 42°C for 48 h. The resin-embedded tibia was cut longitudinally with a microtome equipped with a tungsten carbide blade (model RM2255; Leica, Nussloch, Germany) to obtain 7- and 12-μm-thick sections for the staining and unstaining histomorphometric techniques, respectively (16, 18). For the staining technique, longitudinal sections were mounted on standard microscope slides, deplastinated, dehydrated, and processed for Goldner's trichrome staining (45). The unstained slides were examined for the double lines of calcein labeling (10 mg/kg sc injected at 6-day interval, Sigma). Imaging analysis was performed under a fluorescent/light microscope using the computer-assisted Osteomeasure system (Osteometric, Atlanta, GA), operated with software version 4.1. The region of interest covered secondary spongiosa (the trabecular part of proximal tibia at 1–2 mm distal to the epiphysial plate), which was analyzed to obtain static and dynamic parameters from stained and unstained sections, respectively. Static parameters included trabecular bone volume normalized by tissue volume (BV/TV, %), trabecular number (Tb.N, mm^{-1}), trabecular separation (Tb.Sp, μm), trabecular thickness (Tb.Th, μm), osteoblast surface normalized by bone surface (Ob.S/BS, %), osteoclast surface (Oc.S/BS, %), and eroded surface (ES/BS, %). Dynamic parameters were double labeled surface (dLS/BS, %), mineralizing surface (MS/BS, %), mineral apposition rate (MAR, μm/day), and bone formation rate (BFR/BS, μm^3/μm^2/day). The nomenclature, symbols, and units complied with the report of the American Society for Bone and Mineral Research Nomenclature Committee (31).

For the cortical measurements, midfrontal tibial sections and mid-sagittal vertebral sections were used. Cortical thicknesses of tibiae were averaged from three points, i.e., at 2, 3, and 4 mm distal to the epiphysial plate, whereas those of *L5* vertebrae were averaged from the thickness at one-third and two-thirds of the length of the *L5* vertebral body. Cortical thicknesses were measured with Motic Images Plus 2.0 (Motic Instruments, Richmond, Canada).

Statistical analysis. Results are expressed as means ± SE. Two sets of data were compared with an unpaired Student's *t*-test. One-way analysis of variance with a Newman-Keuls multiple comparison test was used for multiple sets of data. The level of significance for all statistical tests was $P < 0.05$. Data were analyzed with GraphPad Prism 4.0 for Mac OS X (GraphPad Software, San Diego, CA).

RESULTS

Expression of PRLR proteins in bone. Prior to the investigation of the PRL effects on bone, the expression of PRLR proteins in bone was determined by immunohistochemical technique. As shown in Fig. 1, brownish signals of PRLR proteins were observed in flat osteoblasts lining bone trabeculae in the tibiae of nulliparous, pregnant (P21), and lactating (L8) rats. Several hematopoietic cells in bone marrow also showed positive PRLR signals, whereas no signal was observed in osteocytes embedded in bone trabeculae and cortices.

Densitometric analyses of femora and L5 vertebrae of pregnant and lactating rats. At a macroscopic level, bone densitometric analysis using DEXA in femora (a primarily cortical site) and *L5* vertebrae (a primarily trabecular site) demonstrated that BMD was markedly increased in mid- (P14) and late pregnancy (P21) but was decreased in late lactation (L21)

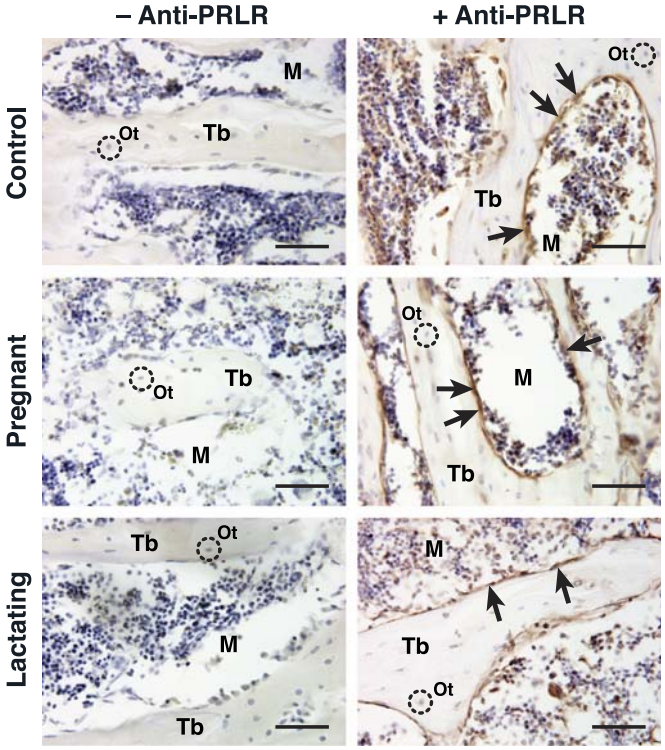

Fig. 1. Immunolocalization of prolactin receptor (PRLR) proteins in the tibiae of control (nulliparous), pregnant (P21), and lactating (L8) rats (n = 3–4 rats per group). Immunostained (+Anti-PRLR) and negative control (−Anti-PRLR) sections were incubated in the presence and absence of anti-PRLR antibody, respectively. Immunoreactive signals were observed in flat osteoblasts (arrows) lining bone trabeculae (Tb) and some leukocytes in bone marrow (M), but not in osteocytes (Ot). Bars, 50 μm.

compared with the age-matched controls (Fig. 2, *A* and *B*). In femora, an increase in BMD was maintained until early lactation (L8; Fig. 2*A*). Fifteen days after weaning, femoral BMD was restored, whereas vertebral BMD remained lower than the control level. Although whole bone BMC was also increased during pregnancy, BMC of L21 lactating rats was comparable to that of age-matched control rats (Fig. 2, *C* and *D*).

Neither exogenous PRL nor Bromo affected femoral and vertebral BMD during pregnancy (Fig. 2, *A* and *B*). On the other hand, Bromo restored femoral BMD but not vertebral BMD in L21 rats (Fig. 2, *A* and *B*). However, PRL administration did not decrease femoral BMD in Bromo-treated L21 rats (Fig. 2*A*). Interestingly, femoral BMDs in L8 and L21 nonsuckling rats were greater than that in age-matched control rats (Fig. 2*A*).

Femoral length, ash weight, and total contents of calcium and magnesium. Femoral length was significantly increased during pregnancy and lactation (Fig. 3*A*). Thereafter, the femoral elongation slowed down, as the femoral length of post-weaning rats was comparable to that of control rats (Fig. 3*A*). Femoral ash weight was increased only in pregnancy, but not in lactation, compared with age-matched control rats (Fig. 3*B*). Neither Bromo nor PRL altered femoral length and ash weight in pregnant rats. However, Bromo completely abolished the lactation-induced increase in femoral length. Exogenous PRL administration partially reversed the Bromo effect on femoral length in L21 rats (Fig. 3*A*).

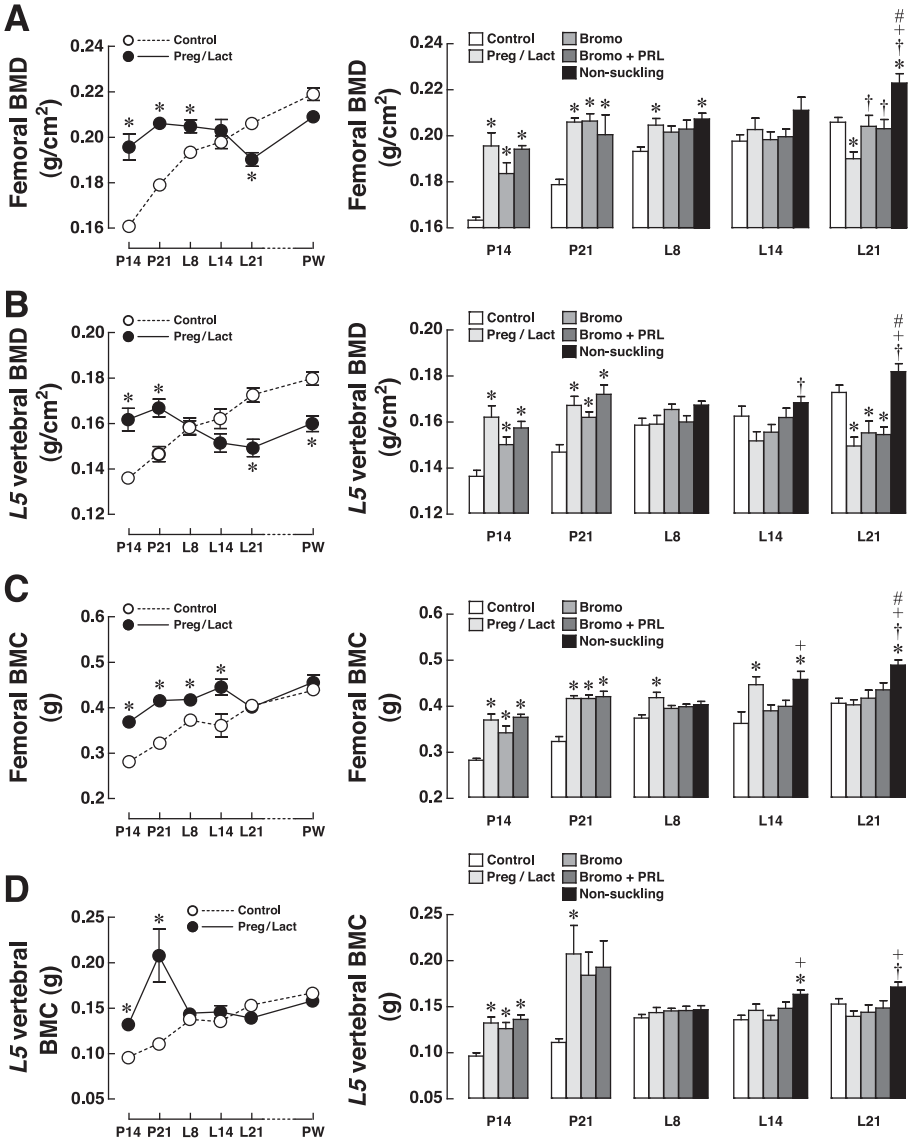

Fig. 2. Bone mineral density (BMD; *A* and *B*) and bone mineral content (BMC; *C* and *D*) of ex vivo femora (primarily cortical sites) and *L5* vertebrae (primarily trabecular sites) of age-matched control, pregnant (P14 and P21), lactating (L8, L14 and L21), and 15-day postweaning (PW) rats, as determined by DEXA. Some pregnant and lactating rats were administered bromocriptine (Bromo) for 7 days (4 $mg \cdot kg^{-1} \cdot day^{-1}$ sc) or Bromo plus PRL sc (Bromo+PRL). PRL doses for pregnant and lactating rats were 0.4 and 0.6 $mg \cdot kg^{-1} \cdot day^{-1}$, respectively. Some rats were permanently separated from their pups after parturition (nonsuckling). All values in line graphs and bar graphs are presented as means ± SE (n = 7–8 rats per each condition). *$P < 0.05$ vs. age-matched control group; †$P < 0.05$ vs. corresponding lactating group; +$P < 0.05$ vs. Bromo group; #$P < 0.05$ vs. Bromo+PRL group.

Since PRL was reported to inhibit in vitro matrix mineralization (39), we further investigated the total calcium and mineral contents normalized by the dry weight of the femora. Normally, bone dry weight includes dry weight of protein matrix and weight of minerals (e.g., calcium, magnesium, and phosphate). Therefore, if the studied conditions do not change the stoichiometry of mineralized bone matrix (i.e., relative quantities of minerals per weight of protein matrix), the total calcium and magnesium contents normalized by the dry weight should be constant. As demonstrated by ion chromatography, these parameters were not altered in pregnant and lactating rats and remained constant after Bromo or Bromo+PRL administration (Fig. 4). In addition, calcium content in bone ash was greater than magnesium content ~40-fold. A constant total calcium content normalized by dry femoral weight was also confirmed by atomic absorption spectrophotometry (Supplemental Fig. S2).

Cortical thicknesses of tibiae and L5 vertebrae. Goldner's trichrome staining of tibial and vertebral sections revealed that the thicknesses of tibial and vertebral cortical shells as well as of trabeculae were markedly increased during pregnancy (Figs. 5*A* and 6, *A* and *B*). The pregnancy-induced increase in cortical thickness was not dependent on PRL (data not shown). In L14 lactating rats, the thickness of tibial cortical shell, but not vertebral cortical shell, remained greater than that in the control groups (Figs. 5*B* and 6, *C* and *D*). In contrast, bone trabeculae in both tibiae and *L5* vertebrae became thinner during lactation (Fig. 5*B*).

Histomorphometry of trabecular microstructure in pregnant and lactating rats. Further investigation by bone histomorphometry in the trabecular portion of tibiae demonstrated that trabecular bone volume and trabecular number were not changed during pregnancy compared with the age-matched controls but were markedly decreased after mid-lactation, which lasted until day 15 postweaning (Fig. 7, *A* and *B*). Trabecular thickness was modestly altered during pregnancy and lactation with a significant increase only at day 15 postweaning (Fig. 7*C*). Trabecular separation was significantly increased after mid-lactation (Fig. 7*D*), consistent with a decrease in trabecular bone volume during the same period.

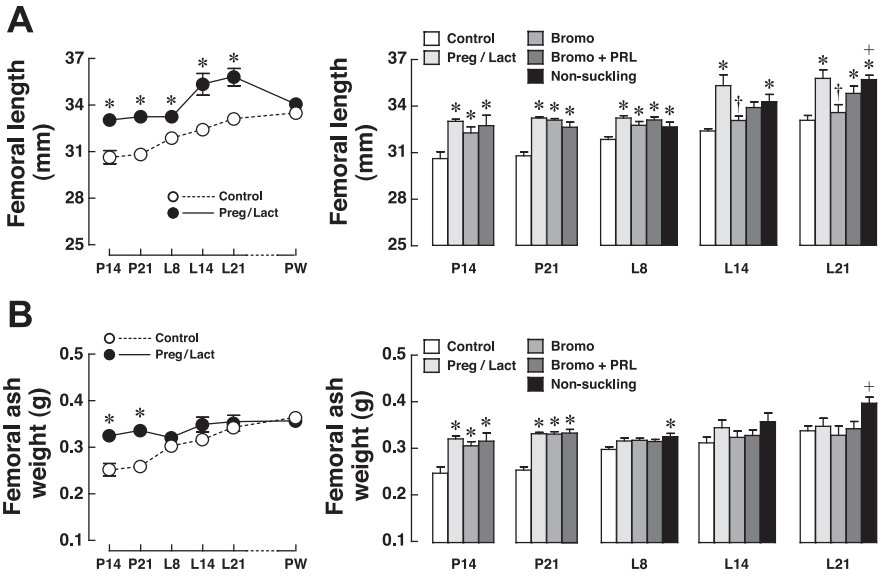

Fig. 3. Length (*A*) and ash weight (*B*) of femora dissected from age-matched control, pregnant (P14 and P21), lactating (L8, L14 and L21), and 15-day postweaning (PW) rats. Ash weight was determined after placing femora in a muffle furnace at 800°C overnight. Some pregnant and lactating rats were administered Bromo for 7 days (4 $mg \cdot kg^{-1} \cdot day^{-1}$ sc) or Bromo+PRL. PRL doses for pregnant and lactating rats were 0.4 and 0.6 $mg \cdot kg^{-1} \cdot day^{-1}$, respectively. Some rats were permanently separated from their pups after parturition (nonsuckling). All values in line graphs and bar graphs are presented as means ± SE ($n = 4–6$ rats per condition). *$P < 0.05$ vs. age-matched control group; †$P < 0.05$ vs. the corresponding lactating group; +$P < 0.05$ vs. Bromo group.

Regarding bone formation-related parameters, although osteoblast surface was decreased during mid-pregnancy (Fig. 8*A*), double labeled surface, mineral apposition rate, and bone formation rate were significantly increased (Fig. 8, *B–D*) compared with the corresponding age-matched control groups. However, these parameters were relatively constant or modestly changed between late pregnancy and mid-lactation but were later drastically increased in late lactation and postweaning (Fig. 8, *A–D*). Mineralizing surface (Supplemental Fig. S3) was consistent with bone formation rate (Fig. 8*D*).

Interestingly, despite having net bone gain during pregnancy, as demonstrated by DEXA, osteoclast surface and eroded surface in tibial trabeculae had already increased from mid-pregnancy and lasted until late lactation (Fig. 9, *A* and *B*). These results suggested that trabecular bone formation and resorption were uncoupled during these reproductive periods, thereby leading to bone gain and bone loss in pregnant and lactating rats, respectively. In other words, "bone modeling" may be present, since bone formation was not proportionally coupled to bone resorption (13). Both osteoclast surface and eroded surface returned to the control values postweaning (Fig. 9, *A* and *B*).

Most histomorphometric parameters, with the exception of osteoblast surface, double labeled surface, and bone formation rate, were not altered in Bromo-treated or Bromo+PRL-treated pregnant rats (Figs. 7–9), suggesting that PRL did not have much influence on trabecular bone changes during pregnancy. On the other hand, during the lactation period, especially in late lactation, changes in several parameters related to both bone formation and resorption, e.g., bone volume, trabecular number, trabecular separation, osteoblast surface, double labeled surface, mineral apposition rate, bone formation rate, osteoclast surface, and eroded surface, were regulated by PRL (Figs. 7–9). Multinucleated or activated osteoclasts were more abundant in Bromo+PRL-treated L21 rats than in Bromo-treated L21 rats (data not shown). However, PRL-induced changes in these parameters showed different times of responses as reflected by nonuniform responses to exogenous

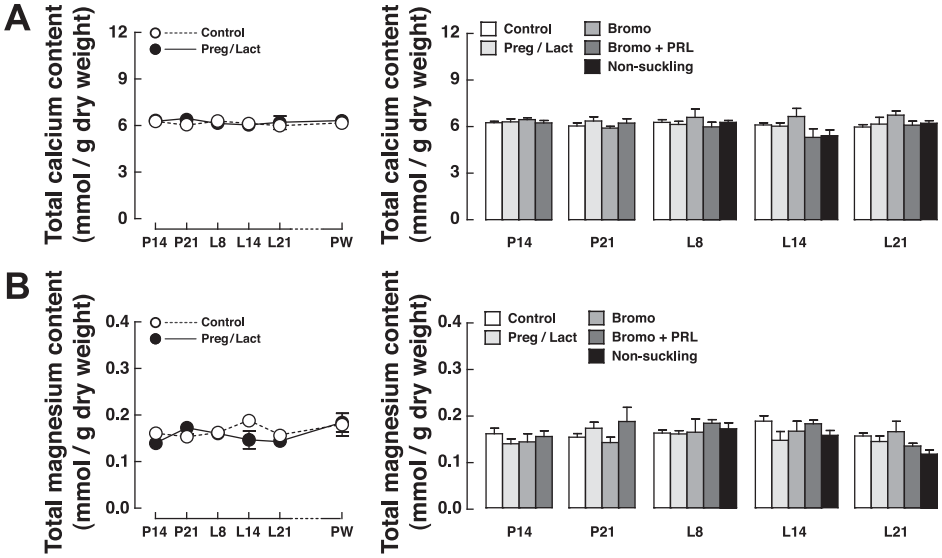

Fig. 4. Total calcium content (*A*) and total magnesium content (*B*) normalized by dry weight of femora obtained from age-matched control, pregnant (P14 and P21), lactating (L8, L14 and L21), and 15-day postweaning (PW) rats, as determined by ion chromatography. Some pregnant and lactating rats were administered Bromo 7 days (4 $mg \cdot kg^{-1} \cdot day^{-1}$ sc) for or Bromo+PRL. PRL doses for pregnant and lactating rats were 0.4 and 0.6 $mg \cdot kg^{-1} \cdot day^{-1}$, respectively. Some rats were permanently separated from their pups after parturition (nonsuckling). All values in line graphs and bar graphs are presented as means ± SE ($n = 4–6$ rats per condition).

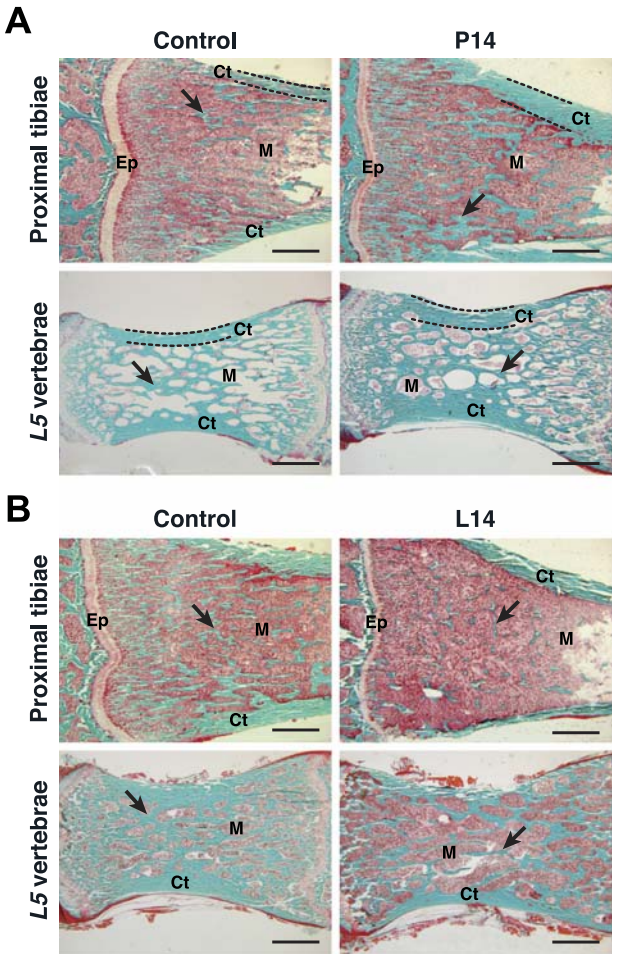

Fig. 5. Goldner's trichrome staining of tibiae (primarily cortical sites) and *L5* vertebrae (primarily trabecular sites) dissected from P14 (*A*) and L14 rats (*B*) and their corresponding age-matched controls (n = 3–4 rats per group). Cortical shell (Ct; bone tissue between dashed lines in *A*), epiphysial plate (Ep), bone trabeculae (arrows), and bone marrow (M) were identified. Mineralized bone matrix, erythrocytes, and cytoplasm were stained green, orange, and red, respectively. Bars, 1,000 μm.

PRL administration (Figs. 7–9). It is noteworthy that trabecular thickness in the rat tibiae was relatively constant from late pregnancy until late lactation, and also not responsive to both Bromo and PRL (Fig. 7*C*).

In nonsuckling rats, which had no hyperprolactinemia and the suckling-induced PRL surge (1, 34), most parameters with the exception of trabecular thickness were not much different from those of the age-matched control rats (Figs. 7–9).

DISCUSSION

How maternal bone adapts during pregnancy and lactation is crucial for growth, development, and calcium metabolism of the offspring. Herein, we provided evidence that bone changes during these periods were complex and time-dependent (pregnancy vs. lactation), and varied with sites of bone (femora/tibiae vs. vertebrae) as well as types of microstructure (cortical shells vs. trabeculae). Specifically, pregnancy predominantly induced femoral and vertebral bone gain in the cortical shells, whereas long-term lactation eventually led to trabecular bone loss. Lactation-induced trabecular bone loss, but not pregnancy-induced cortical bone gain, was found to be regulated by PRL. However, other hormones with elevated plasma levels, such as IGF-I and PTHrP, might also be responsible for bone changes during pregnancy and lactation, respectively (4, 28, 47).

In mid- and late pregnancy, the observed increases in femoral and vertebral BMD were due to an increase in cortical thickness, presumably by enhancing periosteal bone formation (4). Increased femoral bone length (or size), which probably results from pregnancy-enhanced endochondral bone growth (4), may also contribute to the increased femoral BMD in pregnant rats. Since bone size of pregnant rats was larger than that of their age-matched control rats, their whole bone BMC and ash weight were markedly increased during this period. However, the stoichiometry of calcium and magnesium in bone matrix remained unchanged. In contrast to the cortical parts, despite an increase in trabecular thickness in mid-pregnancy, changes in the trabecular microstructure in P14 and P21 rats were modest. Although P14 pregnant rats manifested the enhanced trabecular bone turnover, as indicated by the augmented bone formation and resorption, both processes were still coupled, and no change in trabecular bone volume was observed. These coupled processes in P14 rats could not be explained simply by osteoblast-induced bone formation, since osteoblast surface was indeed decreased in a PRL-dependent manner (Fig. 8*A*). It was hypothesized that surplus minerals supplied by the intestine might accelerate bone calcium acquisition (7, 9), as indicated by the twofold increase in the double labeled surface and mineral apposition rate in P14 rats (Fig. 8, *B* and *C*). On the other hand, uncoupling of trabecular bone formation and resorption, the latter of which being predominant, was evident in late pregnancy and continued throughout lactation. Therefore, the differential changes in cortical and trabecular structures (i.e., net bone gain and loss occurred at

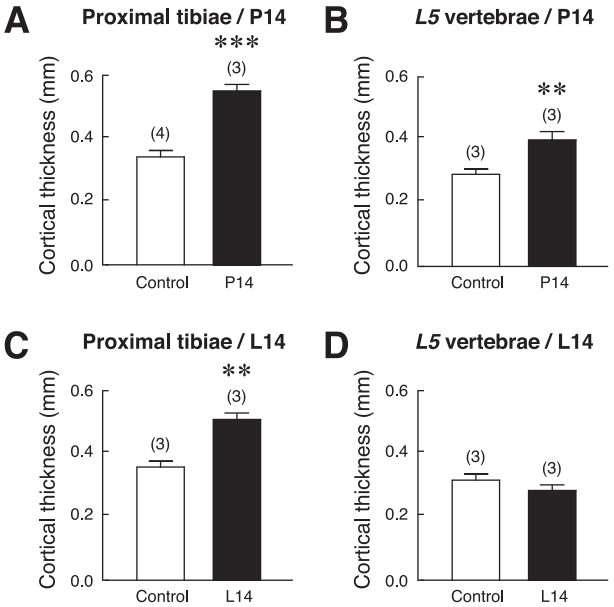

Fig. 6. Average thicknesses of cortical shells in proximal tibiae and *L5* vertebrae of P14 (*A–B*) and L14 (*C–D*) rats. $^{**}P < 0.01$, $^{***}P < 0.001$ vs. its respective control group. Nos. in parentheses represent nos. of experimental animals.

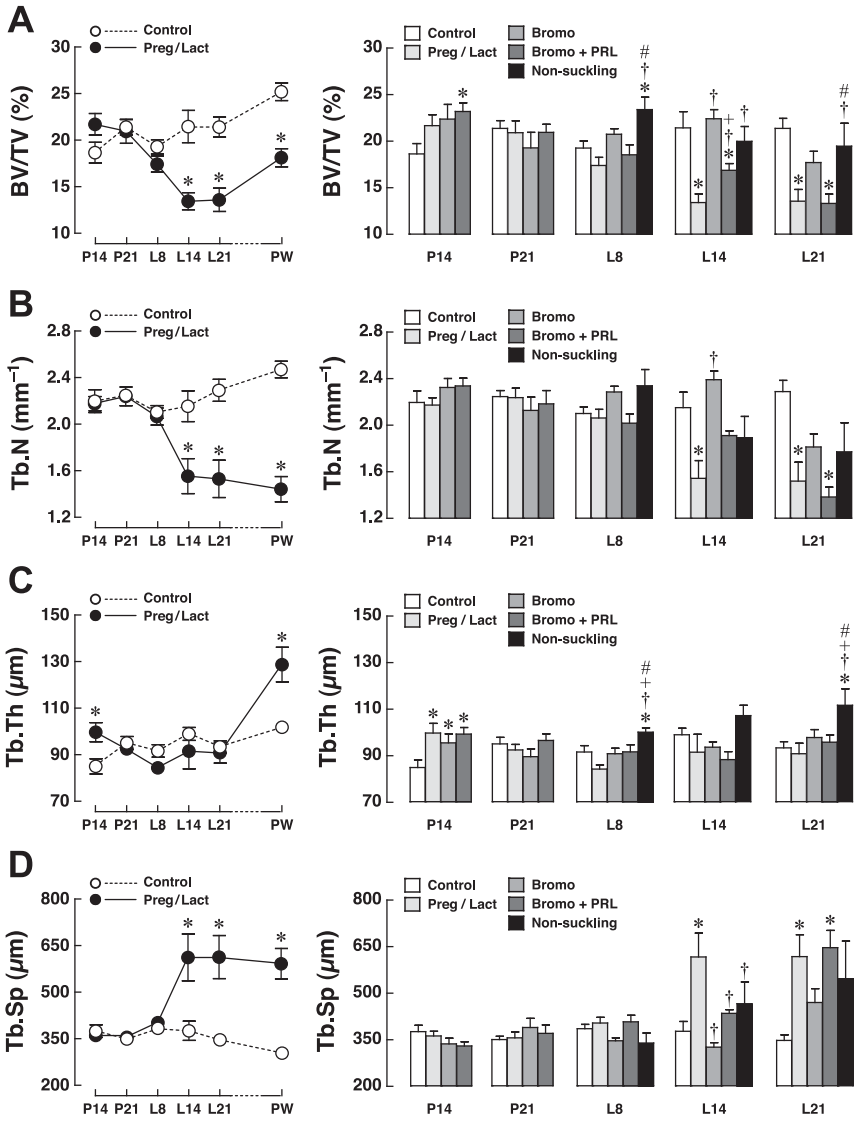

Fig. 7. *A*, trabecular bone volume normalized by tissue volume (BV/TV). *B*, trabecular number (Tb.N); *C*, trabecular thickness (Tb.Th); *D*, trabecular separation (Tb.Sp) of the trabecular portion (secondary spongiosa) of tibiae obtained from age-matched control, pregnant (P14 and P21), lactating (L8, L14 and L21), and 15-day postweaning (PW) rats, as determined by bone histomorphometry. Some pregnant and lactating rats were administered Bromo for 7 days (4 mg·kg^{-1}·day^{-1} sc) or Bromo+PRL. PRL doses for pregnant and lactating rats were 0.4 and 0.6 mg·kg^{-1}·day^{-1}, respectively. Some rats were permanently separated from their pups after parturition (nonsuckling). All values in line graphs and bar graphs are presented as means ± SE (n = 7–8 rats per condition). *$P < 0.05$ vs. age-matched control group; †$P < 0.05$ vs. corresponding lactating group; +$P < 0.05$ vs. Bromo group; #$P < 0.05$ vs. Bromo+PRL group.

different parts of the same bone) indicated a process of bone modeling in this phase of the reproductive cycle (13).

It was postulated that pregnancy-induced bone gain was essential for the preparation of the maternal calcium pool during the last 5 days of pregnancy in rodents and the third trimester in humans for fetal skeletal mineralization and the upcoming lactogenesis (4). In addition, thickening of the cortical shells was important for maintaining bone shape and strength to compensate for the gradual increase in the trabecular separation during lactation (16). Such pregnancy-induced cortical adaptation was certainly under the regulation of hormone(s) other than PRL, such as progesterone and IGF-I (4, 17, 28). PRL might indirectly promote maternal bone gain through stimulation of intestinal calcium absorption to provide more calcium for mineralization (7). However, 1,25$(OH)_2D_3$ and PTHrP might not participate directly in this bone gain, because bone mass was found to be increased in the vitamin D receptor knockout mice (17) and the plasma PTHrP levels were significantly increased in late pregnancy (20), after BMD had already been increased.

During lactation, progressive bone loss was evident, especially in the trabecular portions of both long bones and vertebrae. Since the trabecular surface was much greater than the exposed cortical surface (13), the lactation-induced bone loss occurred mainly in bone trabeculae rather than in cortical shells, thereby leading to a significant decrease in BMD in late lactation. Nevertheless, the endocortical surface of the rat tibiae showed greater erosion during lactation compared with the end of pregnancy (25). Previous investigations in humans also demonstrated that calcium lost during breastfeeding may cause a 10% loss of the total body skeletal mass (22, 37, 41). In rodents nursing around six to eight pups, bone mass could be decreased by ~30% in late lactation (5, 32, 47). Nevertheless, BMC and ash weight were not decreased, because bone size, as indicated by the femoral bone length, in lactating rat was actually larger than that of their age-matched controls. Similar to the pregnant rats, the stoichiometry of calcium and magnesium in bone matrix of lactating rats remained constant (Fig. 4), suggesting that the newly formed osteoid might be rapidly mineralized. It was possible that there was a sufficient amount

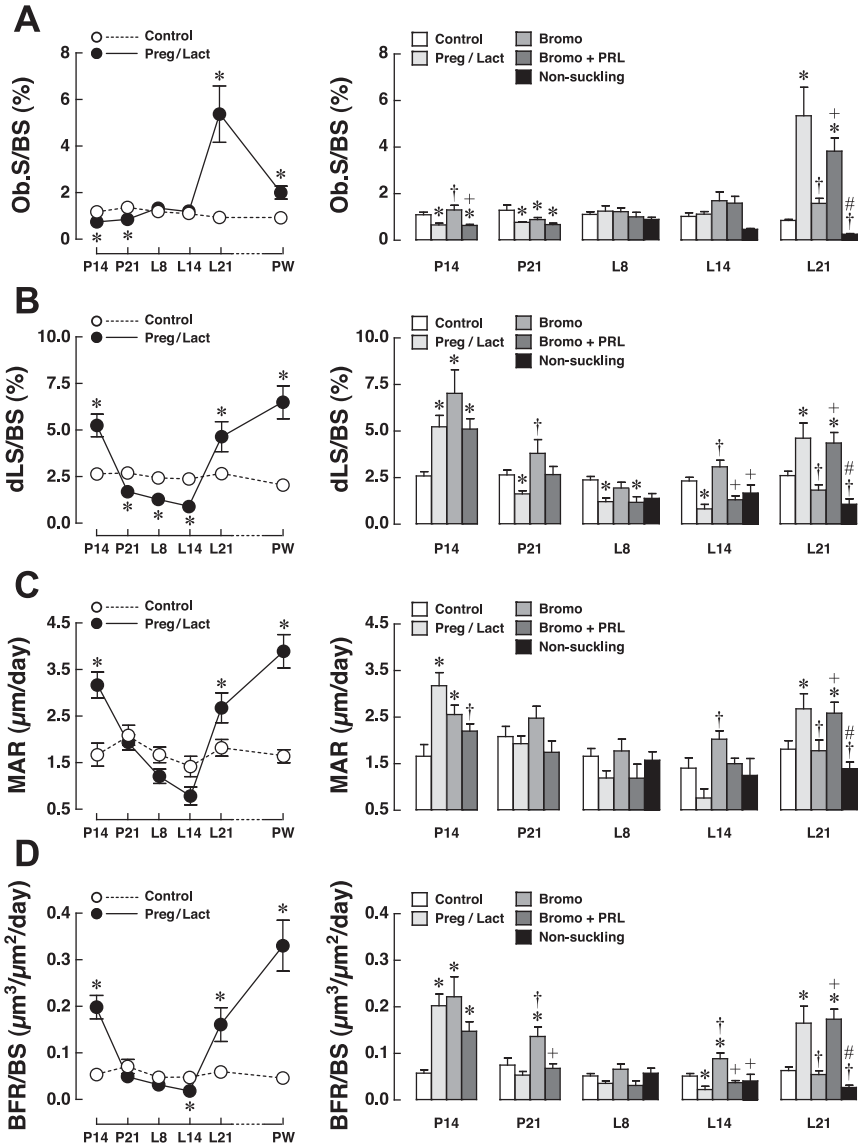

Fig. 8. Trabecular bone formation-related parameters: *A*, osteoblast surface normalized by trabecular bone surface (Ob.S/BS); *B*, double labeled surface (dLS/BS); *C*, mineral apposition rate (MAR); *D*, bone formation rate (BFR/BS) of the secondary spongiosa of tibiae obtained from age-matched control, pregnant (P14 and P21), lactating (L8, L14 and L21), and 15-day postweaning (PW) rats. Some pregnant and lactating rats were administered Bromo for 7 days (4 mg·kg^{-1}·day^{-1} sc) or Bromo+PRL. PRL doses for pregnant and lactating rats were 0.4 and 0.6 mg·kg^{-1}·day^{-1}, respectively. Some rats were permanently separated from their pups after parturition (nonsuckling). Ob.S/BS is a static histomorphometric parameter from the Goldner's trichrome-stained sections; dLS/BS, MAR, and BFR/BS are dynamic histomorphometric parameters from unstained sections. All values in line graphs and bar graphs are presented as means ± SE (n = 6–8 rats per condition). *$P < 0.05$ vs. age-matched control group; †$P < 0.05$ vs. corresponding pregnant or lactating groups; +$P < 0.05$ vs. Bromo group; #$P < 0.05$ vs. Bromo+PRL group.

of mineral supply for mineralization, perhaps from the intestine and kidney (9); otherwise, a decrease in normalized bone calcium content would be apparent as in dietary calcium deficiency with osteomalacia (15, 24, 33, 38).

It was evident that trabecular bone loss in lactating rats was induced by PRL, the plasma levels of which were ~200–300 ng/ml (normal levels ~7–10 ng/ml) and could further elevate up to ~600–800 ng/ml during suckling (1, 6, 7). The presence of PRLR in osteoblasts corroborated a direct effect of PRL on bone metabolism (12, 14, 40). Besides its direct action, PRL may indirectly induce bone resorption by suppressing ovarian estrogen synthesis (48). Furthermore, PRL may be responsible for calcium availability for bone mineralization, as it was the principal stimulator of intestinal calcium absorption in lactating rats (7, 9, 10).

Evidence that supported the PRL actions on bone in this study were based on the use of Bromo, which suppressed PRL release through stimulation of the pituitary D_2 dopaminergic receptors and in turn reduced circulating PRL levels by ~80–90% (3, 7, 35). Since osteoblasts did not express D_2 receptors (43), Bromo should not exert a direct action on this cell type. Although all histomorphometric parameters related to osteoblast functions and bone formation in L21 rats (e.g., osteoblast surface and bone formation rate) were completely inhibited by Bromo and restored by exogenous PRL supplement, changes in some other parameters seemed to be partially PRL dependent (e.g., osteoclast surface in L21 rats). It was possible that other hormones, such as PTHrP from the mammary glands, also contributed to the lactation-induced trabecular bone loss as reported previously (46). On the other hand, the PRL-induced bone changes were not clearly observed at the macroscopic level with DEXA, presumably because the gross changes in femoral BMD required prolonged duration of 2–7 wk of PRL exposure (40, 44).

Furthermore, the results in nonsuckling rats confirmed that the factor(s), either PRL or PTHrP, that induced trabecular bone loss during lactation was related to suckling. Normally, the plasma PRL levels decreased rapidly within 1–2 days after cessation of breastfeeding (26, 34). However, the significant increases in BMD and BMC in nonsuckling rats suggested that

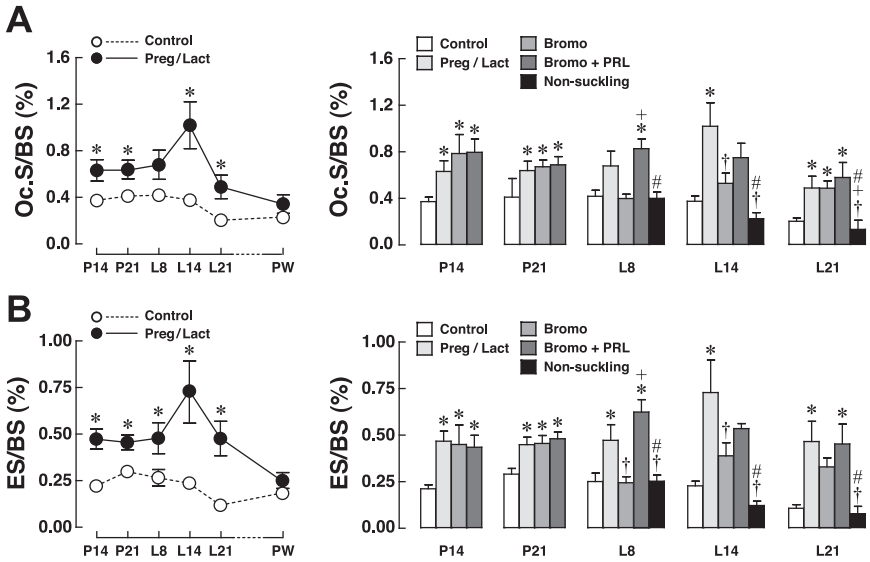

Fig. 9. Trabecular bone resorption-related parameters: osteoclast surface normalized by trabecular bone surface (Oc.S/BS; *A*), and eroded surface (ES/BS; *B*) of the secondary spongiosa of tibiae obtained from age-matched control, pregnant (P14 and P21), lactating (L8, L14 and L21), and 15-day postweaning (PW) rats. Some pregnant and lactating rats were administered Bromo for 7 days (4 $mg \cdot kg^{-1} \cdot day^{-1}$ sc) or Bromo+PRL. PRL doses for pregnant and lactating rats were 0.4 and 0.6 $mg \cdot kg^{-1} \cdot day^{-1}$, respectively. Some rats were permanently separated from their pups after parturition (nonsuckling). Both Oc.S/BS and ES/BS are static histomorphometric parameters from Goldner's trichrome-stained sections. All values in line graphs and bar graphs are presented as means ± SE ($n = 6–8$ rats per condition). $*P < 0.05$ vs. age-matched control group; $\dagger P < 0.05$ vs. corresponding lactating group; $+P < 0.05$ vs. Bromo group; $\#P < 0.05$ vs. Bromo+PRL group.

the absence of suckling pups and normal weaning might differentially affect bone metabolism, because BMD and BMC continued to increase in nonsuckling rats (Fig. 2), although their trabecular histomorphometric parameters showed similar modest changes (Figs. 7–9). It was, therefore, speculated that an endocrine factor that increased cortical bone growth during pregnancy remained active after parturition, perhaps due to the lack of antagonistic signals triggered by suckling.

Previous investigations concerning the direct effect of PRL on osteoblast-induced bone formation at the cellular and molecular levels agreed with the present histomorphometric findings. Specifically, PRL was found to downregulate *Runt*-related transcription factor-2, alkaline phosphatase, and osteocalcin (12, 40). Such direct PRL actions explained the PRL-induced decreases in osteoblast surface in tibial trabeculae of P14 rats and double labeled surface and bone formation rate of L14 rats. Interestingly, in L21 rats there were paradoxical increases in all bone formation-related parameters, which could be prevented by Bromo and restored by exogenous PRL administration (Fig. 8). The exact explanation of this paradox is not known, but it might be related to the PRL-enhanced intestinal calcium absorption (7, 19) and/or the calcitonin-induced renal calcium reabsorption (20), both of which could provide extra calcium for mineralization. Alternatively, extensive bone resorption in late lactation might lead to substantial release of the embedded growth factors, thus in turn stimulating bone formation (13).

Regarding PRL effects on bone resorption, a previous study using human osteoblasts showed that PRL upregulated the expression of receptor activator of nuclear factor-κB ligand (RANKL), while concurrently downregulating the osteoprotegerin (OPG) expression (40), thereby increasing the number of active osteoclasts and their activities. The PRL-induced increase in the RANKL/OPG ratio explained the present findings that osteoclast surface and eroded surface were markedly increased in mid- and late lactation. Besides PRL, mammary gland-derived PTHrP, which could directly stimulate osteoclasts, may also participate in maternal bone resorption, especially when its plasma levels were elevated from midpregnancy to late lactation (20, 46).

After weaning, BMD was restored by increasing trabecular bone formation (Fig. 8) and decreasing bone resorption (Fig. 9). BMD of the primarily cortical sites (e.g., femora) recovered faster than that of the trabecula-rich sites (e.g., *L5* vertebrae). It was apparent that the repair of trabecular microstructure in rats could not be accomplished within 15 days postweaning, but might require up to 20 wk of recovery (4). Similarly, in humans, bone mass could be restored after cessation of breastfeeding, although some mothers might develop the so-called pregnancy- and lactation-induced osteoporosis featuring bone pain, height loss, and fragility fracture (29).

In conclusion, we demonstrated herein that pregnancy increased bone mass predominantly in the cortical shells of both long bones and vertebrae, whereas lactation decreased bone mass predominantly in bone trabeculae. Thus, trabecular structures were an important source of calcium for lactogenesis. Interestingly, bone modeling was discernible during these reproductive periods as a result of increased bone length and uncoupling of bone formation and bone resorption. Although the pregnancy-induced cortical bone gain appeared to be PRL independent, PRL still contributed to maternal bone changes during pregnancy since it could decrease osteoblast surface in P14 rats. On the other hand, suppression of bone formation in mid-lactation and stimulation of bone resorption in mid- and late lactation were clearly PRL dependent and could be explained by the direct PRL actions on osteoblasts (39, 40). The present in vivo data, therefore, provided further information on a dynamic, time-dependent, site-specific adaptation of maternal bone, as well as differential osteoregulatory roles of PRL during pregnancy and lactation.

ACKNOWLEDGMENTS

We thank Jenjira Assapun, Kanogwun Thongchote, and Wasana Saengamnart for excellent technical assistance.

GRANTS

This research was supported by grants from the King Prajadhipok and Queen Rambhai Barni Memorial Foundation, the Faculty of Graduate Studies, Mahidol University, Academic Year 2008 (to P. Suntornsaratoon), the Mahidol University Postdoctoral Fellowship Program (to S. Goswami), and the Thailand Research Fund (RSA5180001 to N. Charoenphandhu).

DISCLOSURES

No conflicts of interest are reported by the authors.

REFERENCES

1. **Arbogast LA, Voogt JL.** Endogenous opioid peptides contribute to suckling-induced prolactin release by suppressing tyrosine hydroxylase activity and messenger ribonucleic acid levels in tuberoinfundibular dopaminergic neurons. *Endocrinology* 139: 2857–2862, 1998.
2. **Binart N, Bachelot A, Bouilly J.** Impact of prolactin receptor isoforms on reproduction. *Trends Endocrinol Metab* 21: 362–368, 2010.
3. **Bonomo IT, Lisboa PC, Passos MC, Alves SB, Reis AM, de Moura EG.** Prolactin inhibition at the end of lactation programs for a central hypothyroidism in adult rat. *J Endocrinol* 198: 331–337, 2008.
4. **Bowman BM, Miller SC.** Skeletal adaptations during mammalian reproduction. *J Musculoskelet Neuronal Interact* 1: 347–355, 2001.
5. **Brommage R, DeLuca HF.** Regulation of bone mineral loss during lactation. *Am J Physiol Endocrinol Metab* 248: E182–E187, 1985.
6. **Charoenphandhu N, Krishnamra N.** Prolactin is an important regulator of intestinal calcium transport. *Can J Physiol Pharmacol* 85: 569–581, 2007.
7. **Charoenphandhu N, Nakkrasae LI, Kraidith K, Teerapornpuntakit J, Thongchote K, Thongon N, Krishnamra N.** Two-step stimulation of intestinal Ca^{2+} absorption during lactation by long-term prolactin exposure and suckling-induced prolactin surge. *Am J Physiol Endocrinol Metab* 297: E609–E619, 2009.
8. **Charoenphandhu N, Tudpor K, Thongchote K, Saengamnart W, Puntheeranurak S, Krishnamra N.** High-calcium diet modulates effects of long-term prolactin exposure on the cortical bone calcium content in ovariectomized rats. *Am J Physiol Endocrinol Metab* 292: E443–E452, 2007.
9. **Charoenphandhu N, Wongdee K, Krishnamra N.** Is prolactin the cardinal calciotropic maternal hormone? *Trends Endocrinol Metab* 2010 Mar 19 [Epub ahead of print] PMID: 20304671.
10. **Charoenphandhu N, Wongdee K, Teerapornpuntakit J, Thongchote K, Krishnamra N.** Transcriptome responses of duodenal epithelial cells to prolactin in pituitary-grafted rats. *Mol Cell Endocrinol* 296: 41–52, 2008.
11. **Clément-Lacroix P, Ormandy C, Lepescheux L, Ammann P, Damotte D, Goffin V, Bouchard B, Amling M, Gaillard-Kelly M, Binart N, Baron R, Kelly PA.** Osteoblasts are a new target for prolactin: analysis of bone formation in prolactin receptor knockout mice. *Endocrinology* 140: 96–105, 1999.
12. **Coss D, Yang L, Kuo CB, Xu X, Luben RA, Walker AM.** Effects of prolactin on osteoblast alkaline phosphatase and bone formation in the developing rat. *Am J Physiol Endocrinol Metab* 279: E1216–E1225, 2000.
13. **Dempster DW.** Anatomy and functions of the adult skeleton. In: *Primer on the Metabolic Bone Diseases and Disorders of Mineral Metabolism*, edited by Favus MJ. Washington, DC: American Society for Bone and Mineral Research, 2006, p. 7–11.
14. **Deng C, Ueda E, Chen KE, Bula C, Norman AW, Luben RA, Walker AM.** Prolactin blocks nuclear translocation of VDR by regulating its interaction with BRCA1 in osteosarcoma cells. *Mol Endocrinol* 23: 226–236, 2009.
15. **Eklou-Kalonji E, Zerath E, Colin C, Lacroix C, Holy X, Denis I, Pointillart A.** Calcium-regulating hormones, bone mineral content, breaking load and trabecular remodeling are altered in growing pigs fed calcium-deficient diets. *J Nutr* 129: 188–193, 1999.
16. **Eriksen EF, Axelrod DW, Melsen F.** *Bone Histomorphometry*. New York: Raven, 1994, p. 33–50.
17. **Fudge NJ, Kovacs CS.** Pregnancy up-regulates intestinal calcium absorption and skeletal mineralization independently of the vitamin D receptor. *Endocrinology* 151: 886–895, 2010.
18. **Iwaniec UT, Wronski TJ, Turner RT.** Histological analysis of bone. *Methods Mol Biol* 447: 325–341, 2008.
19. **Jantarajit W, Thongon N, Pandaranandaka J, Teerapornpuntakit J, Krishnamra N, Charoenphandhu N.** Prolactin-stimulated transepithelial calcium transport in duodenum and Caco-2 monolayer are mediated by the phosphoinositide 3-kinase pathway. *Am J Physiol Endocrinol Metab* 293: E372–E384, 2007.
20. **Kovacs CS.** Calcium and bone metabolism during pregnancy and lactation. *J Mammary Gland Biol Neoplasia* 10: 105–118, 2005.
21. **Kraidith K, Jantarajit W, Teerapornpuntakit J, Nakkrasae LI, Krishnamra N, Charoenphandhu N.** Direct stimulation of the transcellular and paracellular calcium transport in the rat cecum by prolactin. *Pflügers Arch* 458: 993–1005, 2009.
22. **Laskey MA, Prentice A.** Bone mineral changes during and after lactation. *Obstet Gynecol* 94: 608–615, 1999.
23. **Laskey MA, Prentice A, Hanratty LA, Jarjou LM, Dibba B, Beavan SR, Cole TJ.** Bone changes after 3 mo of lactation: influence of calcium intake, breast-milk output, and vitamin D-receptor genotype. *Am J Clin Nutr* 67: 685–692, 1998.
24. **Marie PJ, Pettifor JM, Ross FP, Glorieux FH.** Histological osteomalacia due to dietary calcium deficiency in children. *N Engl J Med* 307: 584–588, 1982.
25. **Miller SC, Bowman BM.** Rapid improvements in cortical bone dynamics and structure after lactation in established breeder rats. *Anat Rec A Discov Mol Cell Evol Biol* 276: 143–149, 2004.
26. **Miller SC, Bowman BM.** Rapid inactivation and apoptosis of osteoclasts in the maternal skeleton during the bone remodeling reversal at the end of lactation. *Anat Rec (Hoboken)* 290: 65–73, 2007.
27. **Naliato EC, Farias ML, Braucks GR, Costa FS, Zylberberg D, Violante AH.** Prevalence of osteopenia in men with prolactinoma. *J Endocrinol Invest* 28: 12–17, 2005.
28. **O'Brien KO, Donangelo CM, Zapata CL, Abrams SA, Spencer EM, King JC.** Bone calcium turnover during pregnancy and lactation in women with low calcium diets is associated with calcium intake and circulating insulin-like growth factor 1 concentrations. *Am J Clin Nutr* 83: 317–323, 2006.
29. **Ofluoglu O, Ofluoglu D.** A case report: pregnancy-induced severe osteoporosis with eight vertebral fractures. *Rheumatol Int* 29: 197–201, 2008.
30. **Pahuja DN, DeLuca HF.** Stimulation of intestinal calcium transport and bone calcium mobilization by prolactin in vitamin D-deficient rats. *Science* 214: 1038–1039, 1981.
31. **Parfitt AM, Drezner MK, Glorieux FH, Kanis JA, Malluche H, Meunier PJ, Ott SM, Recker RR.** Bone histomorphometry: standardization of nomenclature, symbols, and units. Report of the ASBMR Histomorphometry Nomenclature Committee. *J Bone Miner Res* 2: 595–610, 1987.
32. **Peng TC, Garner SC, Kusy RP, Hirsch PF.** Effect of number of suckling pups and dietary calcium on bone mineral content and mechanical properties of femurs of lactating rats. *Bone Miner* 3: 293–304, 1988.
33. **Persson P, Gagnemo-Persson R, Håkanson R.** The effect of high or low dietary calcium on bone and calcium homeostasis in young male rats. *Calcif Tissue Int* 52: 460–464, 1993.
34. **Pi X, Voogt JL.** Effect of suckling on prolactin receptor immunoreactivity in the hypothalamus of the rat. *Neuroendocrinology* 71: 308–317, 2000.
35. **Piyabhan P, Krishnamra N, Limlomwongse L.** Changes in the regulation of calcium metabolism and bone calcium content during growth in the absence of endogenous prolactin and during hyperprolactinemia: a longitudinal study in male and female Wistar rats. *Can J Physiol Pharmacol* 78: 757–765, 2000.
36. **Prentice A.** Calcium in pregnancy and lactation. *Annu Rev Nutr* 20: 249–272, 2000.
37. **Ritchie LD, Fung EB, Halloran BP, Turnlund JR, Van Loan MD, Cann CE, King JC.** A longitudinal study of calcium homeostasis during human pregnancy and lactation and after resumption of menses. *Am J Clin Nutr* 67: 693–701, 1998.
38. **Salgueiro MJ, Torti H, Meseri E, Weill R, Orlandini J, Urriza R, Zubillaga M, Janjetic M, Barrado A, Boccio J.** Dietary zinc effects on zinc, calcium, and magnesium content in bones of growing rats. *Biol Trace Elem Res* 110: 73–78, 2006.
39. **Seriwatanachai D, Krishnamra N, van Leeuwen JP.** Evidence for direct effects of prolactin on human osteoblasts: inhibition of cell growth and mineralization. *J Cell Biochem* 107: 677–685, 2009.
40. **Seriwatanachai D, Thongchote K, Charoenphandhu N, Pandaranandaka J, Tudpor K, Teerapornpuntakit J, Suthiphongchai T, Krishnamra N.** Prolactin directly enhances bone turnover by raising osteoblast-expressed receptor activator of nuclear factor κB ligand/osteoprotegerin ratio. *Bone* 42: 535–546, 2008.
41. **Sowers M.** Pregnancy and lactation as risk factors for subsequent bone loss and osteoporosis. *J Bone Miner Res* 11: 1052–1060, 1996.
42. **Stubbs B.** Antipsychotic-induced hyperprolactinaemia in patients with schizophrenia: considerations in relation to bone mineral density. *J Psychiatr Ment Health Nurs* 16: 838–842, 2009.
43. **Suntornsaratoon P, Wongdee K, Krishnamra N, Charoenphandhu N.** Femoral bone mineral density and bone mineral content in bromocriptine-treated pregnant and lactating rats. *J Physiol Sci* 60: 1–8, 2010.

44. **Thongchote K, Charoenphandhu N, Krishnamra N.** High physiological prolactin induced by pituitary transplantation decreases BMD and BMC in the femoral metaphysis, but not in the diaphysis of adult female rats. *J Physiol Sci* 58: 39–45, 2008.
45. **van't Hof RJ, Clarkin CE, Armour KJ.** Studies of local bone remodeling: the calvarial injection assay. In: *Bone Research Protocols*, edited by Helfrich MH, Ralston SH. Totowa, NJ: Humana, 2003, p. 345–351.
46. **VanHouten JN, Dann P, Stewart AF, Watson CJ, Pollak M, Karaplis AC, Wysolmerski JJ.** Mammary-specific deletion of parathyroid hormone-related protein preserves bone mass during lactation. *J Clin Invest* 112: 1429–1436, 2003.
47. **VanHouten JN, Wysolmerski JJ.** Low estrogen and high parathyroid hormone-related peptide levels contribute to accelerated bone resorption and bone loss in lactating mice. *Endocrinology* 144: 5521–5529, 2003.
48. **Wang C, Chan V.** Divergent effects of prolactin on estrogen and progesterone production by granulosa cells of rat Graafian follicles. *Endocrinology* 110: 1085–1093, 1982.

Opinion

Is prolactin the cardinal calciotropic maternal hormone?

Narattaphol Charoenphandhu[1,2], Kannikar Wongdee[2,3] and Nateetip Krishnamra[1,2]

[1] Department of Physiology, Faculty of Science, Mahidol University, Bangkok 10400, Thailand
[2] Consortium for Calcium and Bone Research (COCAB), Faculty of Science, Mahidol University, Bangkok 10400, Thailand
[3] Faculty of Allied Health Sciences, Burapha University, Chonburi 20131, Thailand

To produce offspring, mothers require a large amount of calcium for fetal growth and milk production. Increased calcium demand leads to enhanced intestinal calcium absorption and stockpiling of bone calcium in pregnancy prior to demineralization in lactation. These coordinated events must be carefully organized by calciotropic hormone(s), but the classical hormones, namely 1,25-dihydroxyvitamin D_3, parathyroid hormone and calcitonin, do not appear to be responsible. Plasma prolactin (PRL) levels are elevated during pregnancy and, in view of the presence of PRL receptors in gut, bone and mammary glands, as well as recent evidence of the stimulatory effects of PRL on intestinal calcium transport, bone resorption and mammary calcium secretion, we postulate that PRL is the cardinal calciotropic hormone during pregnancy and lactation.

Stress on maternal calcium metabolism imposed by pregnancy and lactation

Women lose a huge amount of calcium, ~200–300 mg/day in the third trimester for fetal bone development and ~300–1000 mg/day during breastfeeding [1–3], and three maternal systems, namely intestine, bone and kidney (Figure 1), must work together in a highly coordinated manner under endocrine control to guarantee calcium adequacy for the developing fetus and newborn. Surprisingly, the principal calcium-regulating hormone in pregnancy and lactation remains a controversial issue. Several investigations have shown that neither bone mineral loss nor increased intestinal calcium absorption during these reproductive periods depend on ovarian or adrenal hormones [4]. Moreover, there is no strong correlation between maternal calcium demand and the major calcium-regulating hormones – 1,25-dihydroxyvitamin D_3 [1,25$(OH)_2D_3$], parathyroid hormone (PTH) and calcitonin [3,5,6]. In vitamin D receptor (VDR) knockout mice, expression of the transient receptor potential channel, subfamily V, member 6 (TRPV6), a calcium channel required for transcellular calcium absorption in the small intestine (Box 1), was still upregulated during pregnancy and lactation [7]. A recent study in pregnant VDR knockout mice confirmed that pregnancy stimulates duodenal calcium absorption in a VDR-independent manner [8]. Maternal calcium metabolism must therefore be regulated by some other hormone(s).

Corresponding author: Charoenphandhu, N. (naratt@narattsys.com).

Evidence that supports calciotropic roles of PRL

Plasma levels of PRL, a 23 kDa polypeptide hormone secreted from the anterior pituitary gland, are strikingly elevated during pregnancy (75–100 ng/mL, compared to nonpregnant levels of 7–10 ng/mL) [5], to help maintain functional corpus luteum in pregnancy (for a review on PRL action, see Ref. [9]). To induce lactation, plasma PRL levels are elevated to 200–300 ng/mL, and transiently surge within 15 min of suckling to ~400–800 ng/mL, and these elevated levels last for 60–90 min [10]. Pregnancy and lactation are therefore considered to be physiological hyperprolactinemic states.

Why is PRL a strong candidate for the calcium-regulating hormone during these reproductive periods? In addition to its elevated plasma levels during pregnancy and lactation, PRL has been shown to have proto-osmoregulatory and hypercalcemic roles in fish, and increases branchial and intestinal calcium permeability while preventing excessive demineralization of bone and scale [11,12]. Indeed, on an evolutionary timescale, before PTH first appeared and fully functioned in amphibians, PRL and other PRL-like hormones (e.g. somatolactin) served as the major hypercalcemic hormones in fish [11]. Hypercalcemic activities of PRL are also evident in amphibians, reptiles and birds [11,13]. Although the lower vertebrates such as fishes and amphibians might have different modes of calcium homeostasis than mammals, this suggests a conserved role for PRL in calcium metabolism.

In mammals, PRL receptor (PRLR) expression in intestine, kidney and bone, the major calcium-handling organs, indicates a direct calciotropic action of PRL in these organs [14–16]. In fact, exogenous PRL administration stimulates intestinal calcium absorption in nonpregnant female rats [5] and increases intestinal calcium transport and bone calcium mobilization in vitamin D-deficient rats fed a low calcium diet [6]. PRLR knockout mice also manifest an impairment of bone development [17]. Moreover, in patients with PRL-producing tumors or pathological hyperprolactinemia induced by prolonged uses of antipsychotic drugs (e.g. risperidone and amisulpride, both of which antagonize the PRL-inhibiting factor dopamine), bone resorption is dramatically increased, resulting in low bone mass and overt osteoporosis [18,19].

Two-step stimulation of intestinal calcium absorption by PRL

PRL-stimulated maternal calcium absorption across the intestinal epithelium takes place by a two-step mechanism

1043-2760/$ – see front matter doi:10.1016/j.tem.2010.02.002 Trends in Endocrinology and Metabolism 21 (2010) 395–401

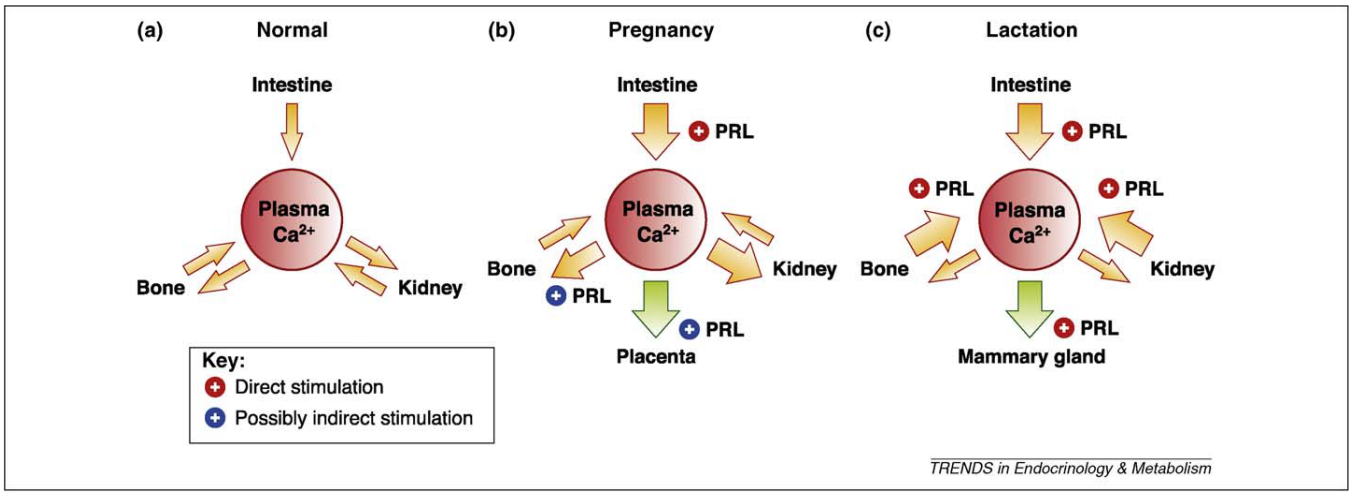

Figure 1. Hypothetical model for maternal total body calcium homeostasis as regulated by PRL. **(a)** Under normal conditions, bone formation and resorption are balanced, and renal calcium excretion is minimal. PRL acts as a coordinator to provide adequate calcium and to mobilize calcium for fetal bone development and milk production. **(b)** During pregnancy, PRL markedly enhances intestinal calcium absorption, that in turn indirectly increases maternal bone calcium accretion and placental calcium transfer [10,27]. If intestinal calcium absorption exceeds the body's requirement plus bone calcium accumulation, excess calcium will be excreted via the kidney, thereby leading to maternal hypercalciuria (also known as absorptive hypercalciuria) [29,33]. **(c)** In late lactation, PRL still enhances the intestinal calcium absorption to supply more calcium for milk production [10]. Adequate milk calcium supply is also achieved by PRL-enhanced renal calcium reabsorption and bone resorption, leading to maternal hypocalciuria and osteopenia, respectively [16,29,37]. Moreover, mammary calcium secretion has been found to be regulated by PRL [47].

(Figure 2) [10], similar to that which occurs in non-mated animals [6,14,20]. Specifically, sustained hyperprolactinemia of 75–100 ng/mL during pregnancy, or 200–300 ng/mL during lactation, induces a long-lasting adaptation in the intestinal absorptive cells to elevate the 'baseline calcium flux' by ~2-fold (Step-1), that is further increased (Step-2) by the transient PRL surge (400–800 ng/mL) ~15–90 min after suckling. Only Step-1 calcium absorption is dependent on *de novo* transcription of genes required for calcium absorption, for example those encoding TRPV6 and calbindin-D_{9k} (Box 1). However, the Step-2 calcium flux is well correlated with milk volume, and it is possible that the PRL surge during suckling serves as a signal to coordinate calcium mobilization from various sources to supply calcium for milk production [10]. Because inhibition of pituitary PRL secretion completely abolishes Step-1 and -2 calcium absorption [10], PRL might serve as a single salient factor for this maternal adaptation.

The duodenum and cecum are highly responsive to PRL [10,20]. Both transcellular and paracellular calcium transport in the duodenum are markedly stimulated by PRL during the reproductive periods [10]. Although the major driving force for paracellular intestinal calcium transport is the calcium concentration gradient, the tight junction acts as a barrier that restricts paracellular ion movement in a charge- and size-selective manner [21]. Paracellular permeability is thus regulated by tight junction proteins including occludin, ZO-1 and claudins [21]. PRL overcomes this barrier by lowering the transepithelial resistance and increasing calcium permeability, in part, by downregulating

Box 1. Redundancy in intestinal calcium transport

Calcium traverses the intestinal epithelium via paracellular and transcellular pathways, with the former being present in most intestinal segments and predominant in the presence of ~2–6 mM luminal calcium as found with a normal diet [50]. In the presence of 10 mM luminal calcium, for example after oral calcium supplementation, the paracellular calcium flux can be ~5 times as high as the transcellular flux [10,14]. However, transcellular calcium transport becomes more significant during low calcium intake or increased calcium demand, for example during pregnancy and lactation [10,24,50]. Nevertheless, the cellular and molecular mechanisms are still controversial and require further investigation.

Transcellular calcium transport in the intestine is a three-step active process, consisting of apical calcium uptake, cytoplasmic calcium translocation and basolateral calcium extrusion. The calcium channel TRPV6 and calbindin-D_{9k} were believed to be responsible for the apical uptake and facilitated diffusion across the cytoplasm, respectively. Thereafter, plasma membrane Ca^{2+}-ATPase-1b ($PMCA_{1b}$) and Na^+/Ca^{2+} exchanger-1 (NCX1) are responsible for ~85% and ~15% of calcium efflux, respectively [51]. Bianco and co-workers reported a 60% decrease in intestinal calcium absorption, growth retardation and low femoral bone mineral density in the TRPV6-null mice [52]. However, more recent investigations showed that TRPV6 knockout, calbindin-D_{9k} knockout, and TRPV6/calbindin-D_{9k} double knockout mice manifested normal serum calcium and $1,25(OH)_2D_3$-dependent active calcium transport [53]. Several alternative or compensatory mechanisms can partially explain these discrepancies. For example, calcium might enter intestinal epithelial cells via other channels, including voltage-dependent calcium channels (Ca_v), and especially when cells are slightly depolarized by apical sodium entry in the presence of high luminal glucose [sodium and glucose enter the cell together via the sodium-dependent glucose transporter (SGLT)-1] [48]. Cytoplasmic calcium translocation might also be accomplished by other calcium-binding proteins such as calmodulin and parvalbumin [25,51], or by vesicular transport or 'tunneling' through the endoplasmic reticulum [51].

It is reasonable to ask the question – why does the gut use so many transport mechanisms and transporters for calcium absorption? Because calcium is essential for many processes in the body and is obtained solely from the diet, such redundancy guarantees that calcium absorption is always sufficient and matches calcium demand. It is also possible that these various mechanisms of calcium absorption are differentially regulated by different hormones or conditions. For example, estrogen, endurance exercise and chronic metabolic acidosis can upregulate TRPV6 expression [7,51,54,55], whereas $Ca_v1.3$ is essential for glucose-stimulated calcium absorption [48].

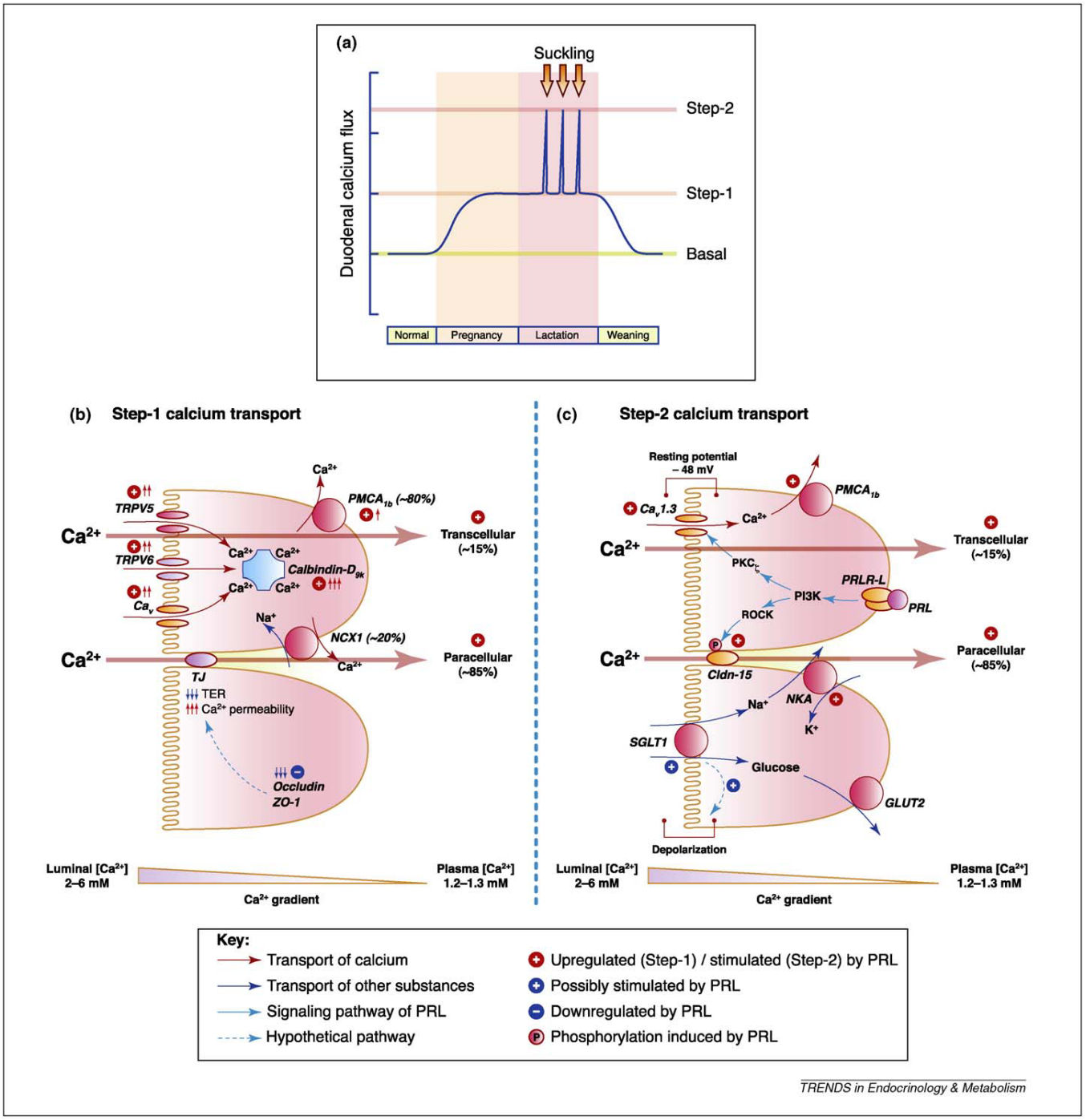

Figure 2. Hypothetical diagram of two-step stimulation of duodenal calcium absorption by PRL and its possible cellular mechanisms [10]. **(a)** Hyperprolactinemia during pregnancy and lactation elevates the 'basal calcium flux' to a new baseline (Step-1), whereas the suckling-induced PRL surge exerts a transient stimulatory effect on the calcium flux, that is further increased to the Step-2 level. This adaptation disappears after weaning. In the presence of a calcium gradient (i.e. luminal calcium > plasma free ionized calcium) and/or solvent drag, the PRL-enhanced paracellular calcium transport is predominant [14,23]. **(b)** The Step-1 calcium flux is achieved by PRL-induced upregulation of genes encoding proteins related to transcellular calcium transport (i.e. TRPV5, TRPV6, Ca_v, calbindin-D_{9k} and $PMCA_{1b}$), and downregulation of genes encoding tight junction (TJ) proteins (i.e. occludin and ZO-1) that are generally essential for the paracellular barrier functions as indicated by a high transepithelial resistance (TER) and restriction of paracellular ion permeability [10]. The degree of up- or downregulation is indicated by the number of small arrows. **(c)** Step-2 calcium transport through the transcellular pathway requires PRL-stimulated apical calcium entry via $Ca_v1.3$, and calcium extrusion via $PMCA_{1b}$, whereas transport through paracellular pathway involves PRL-induced phosphorylation of claudin (Cldn)-15 [10]. PRL signaling is mediated by several proteins, such as long isoform (-L) of PRLR, phosphoinositide 3-kinase (PI3K), Rho-associated kinase (ROCK) and protein kinase C (PKC)-ζ [14,20,22]. Glucose absorption via the sodium-dependent glucose transporter (SGLT)-1 and the glucose transporter (GLUT)-2 is also important for PRL action because sodium entry via SGLT1 can induce depolarization of the apical membrane, thereby activating $Ca_v1.3$ for transcellular calcium transport [48], whereas sodium extrusion via Na^+/K^+-ATPase (NKA) can increase the paracellular hyperosmotic gradient for solvent drag [5,23]. In addition, an increase in paracellular calcium transport induced by solvent drag also results from PRL-stimulated NKA activity [5].

occludin and ZO-1 (Figure 2), thereby leading to Step-1 paracellular calcium transport [10]. Step-2 paracellular calcium transport, on the other hand, is related to the PRL-induced serine phosphorylation of claudin-15 [10]. The downstream PRL signal transduction pathway is not completely understood, but appears to involve phosphoinositide 3-kinase (PI3K)- and Rho-associated kinase (ROCK)-related pathways, and not the classical Janus kinase-2 pathway [10,20,22].

Moreover, calcium also traverses the paracellular space of the proximal small intestine along with osmotic water flow – a process known as solvent drag-induced calcium transport [23]. Solvent drag is induced after sodium entering the cells via sodium-dependent glucose transporter (SGLT)-1, and exiting the cells via Na^+/K^+-ATPase, accumulates in the paracellular space as a standing hyperosmotic gradient (Figure 2) [5,23]. PRL stimulates this solvent drag-induced calcium transport by stimulating Na^+/K^+-ATPase activity [5].

Regarding transcellular calcium transport, PRL-induced upregulation of crucial transporter genes including those encoding TRPV5, TRPV6 and calbindin-D_{9k}, accomplishes Step-1 transcellular calcium transport [7,10,24]. A recent microarray study in duodenal epithelial cells suggested that PRL also upregulated other potential calcium transporters, for example the voltage-dependent L-type calcium channel (Ca_v) and parvalbumin [25], perhaps to ensure adequate intestinal calcium absorption during pregnancy and lactation. However, it remains to be investigated whether PRL directly upregulates these calcium transporter genes, or acts indirectly by stimulating renal and/or local $1,25(OH)_2D_3$ production [24].

In addition, acute PRL exposure directly activates the long isoform of PRLR and its downstream mediators, PI3K and protein kinase C-ζ, thereby leading to Step-2 transcellular calcium transport [10,22]. It appears likely that short isoforms of PRLR do not mediate PRL signaling in intestinal absorptive cells (for a review on PRLRs, see Ref. [9]). PRL-enhanced apical calcium uptake occurs very rapidly, within ~8–10 min after PRL exposure, and requires $Ca_v1.3$ [5,10,22] (Figure 2). We recently demonstrated that TRPV5 and TRPV6 were not involved because double knockdown of TRPV5 and TRPV6 did not abolish PRL-enhanced transcellular calcium transport [26]. Moreover, PRL also stimulates the basolateral calcium extrusion by increasing plasma membrane Ca^{2+}-ATPase-1b ($PMCA_{1b}$) activity [5]. It is noteworthy that the increased numbers of calcium transporter proteins (e.g. TRPV6 and calbindin-D_{9k}) induced by long-term PRL exposure (Step-1) might help to enhance Step-2 transcellular calcium absorption and/or increase the responsiveness of cells to acute PRL exposure during suckling [10].

Enhanced bone turnover and bone calcium release by PRL: friend or foe?

Pregnant mammals, including humans, sheep and rats, exhibit bone calcium accumulation in early and mid-pregnancy [1]. However, there is a slight decrease in maternal bone mineral density due to rapid fetal bone calcium accretion in the third trimester in humans, whereas maternal bone calcium accumulation in rats appears to continue until early lactation [1,27]. Activated osteoclast activity at both trabecular and cortical sites is already evident throughout pregnancy, presumably to prepare the maternal calcium pool for fetal transfer [1,28]. Regulation of maternal bone calcium accumulation is partially PRL-dependent [27,29] and might also be associated with increased plasma levels of progesterone, insulin-like growth factor-I and osteoprotegerin (OPG), the last of which counterbalances osteoclast-mediated bone resorption [1,30]. After delivery, bone resorption is markedly enhanced to release calcium for lactogenesis [3,31]. A ~10–30% reduction in bone mineral density (i.e. osteopenia) and a dramatic decline in bone strength that often accompany lactation sometimes lead to pregnancy and lactation-associated osteoporosis (PLO) featuring back pain, vertebral fracture, and height loss [3,32,33]. Decreased ovarian estrogen and increased mammary production of PTH-related peptide (PTHrP) – a hormone that induces osteoclast formation – can be responsible for maternal osteopenia [33], and PRL might act in concert to fine-tune maternal bone turnover or might even cause PLO.

PRL was previously thought to indirectly enhance bone resorption by suppressing ovarian production of estrogen that normally induces net bone gain [16,18]. However, osteoblasts strongly express PRLR, indicating a direct action of PRL on bone [16,34,35]. At the cellular level, PRL downregulates OPG while concurrently upregulating the receptor activator of nuclear factor-κB ligand (RANKL), a factor generally synthesized and/or released from osteoblasts to increase the number and activity of osteoclasts [16] (Figure 3). Although PRL can also increase osteoblast number *in vivo* [16], fully differentiated or functional osteoblasts could be decreased because PRL downregulates Runx2 (a transcription factor required for osteoblast differentiation), and two important differentiation markers, alkaline phosphatase and osteocalcin [16,34,36]. After weaning, bone mass is restored in both humans and rodents [1,33], coincidently with decreases in osteoblast-derived RANKL [31] and plasma levels of PRL and PTHrP [33]. The long-term effects of lactation-induced osteopenia on subsequent bone health is controversial, ranging from full recovery or minor deficits to a permanent decrease in bone mass [3,31–33,37]. Preexisting low bone mass prior to pregnancy might be a cause of incomplete recovery [38]. However, for the sake of maternal bone health, massive and/or permanent bone loss, if any, should be prevented [39].

Possible regulatory action of PRL on renal calcium handling

Renal calcium excretion is increased during pregnancy, but is decreased during lactation in both humans and rodents [29,33]. Pregnancy-induced hypercalciuria is caused by excess calcium absorption from the intestine (i.e. absorptive hypercalciuria; Figure 1) [33]. Moreover, elevated plasma calcitonin levels in pregnancy could contribute to maternal calciuresis [33].

PRLR expression was reported in renal tubular cells [15], suggesting the kidney as a probable target organ for PRL. As demonstrated by the calcium balance technique,

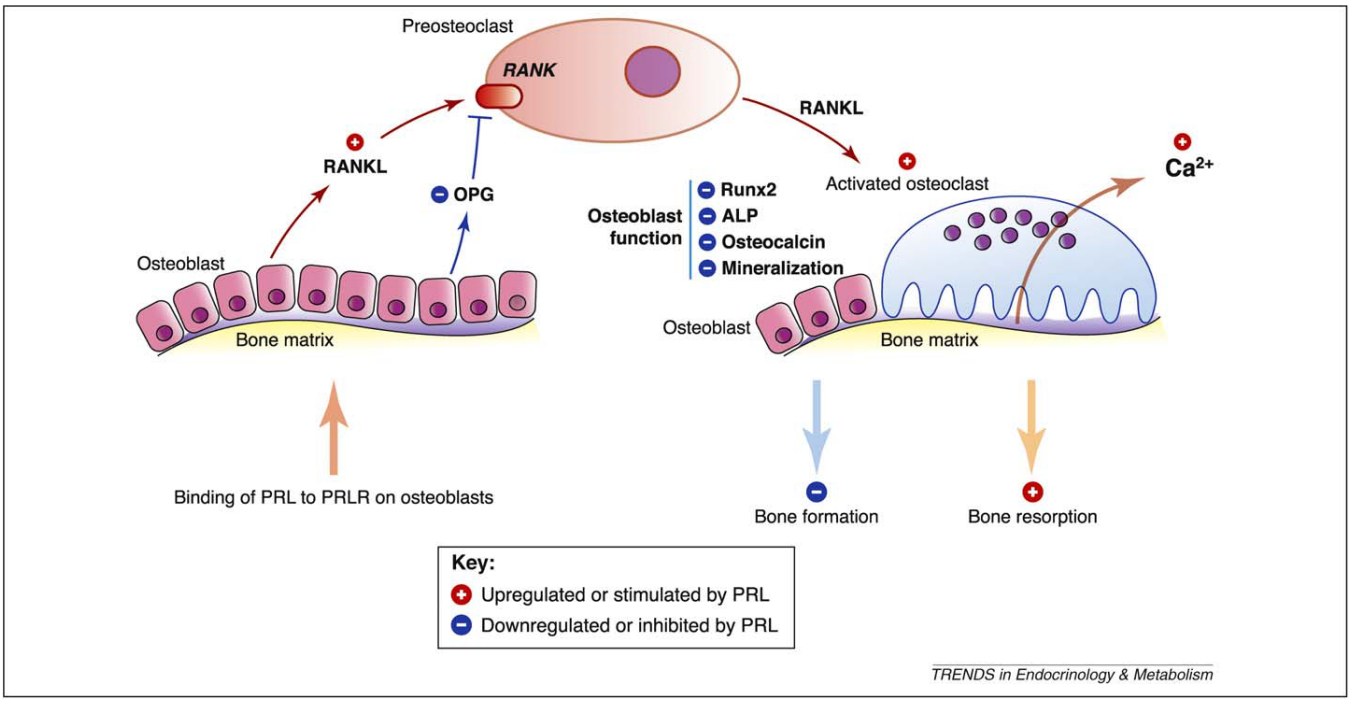

Figure 3. Possible mechanism of PRL-enhanced bone resorption in late lactation. PRL exerts a direct action on bone through osteoblasts because osteoclasts do not express PRLR [34]. Binding of PRL to PRLR on osteoblasts upregulates the expression of the receptor activator of nuclear factor-κB (RANK) ligand (RANKL), and downregulates osteoprotegerin (OPG), a decoy factor that blocks the RANKL–RANK interaction. After binding to its receptor RANK, RANKL induces osteoclastogenesis, activates osteoclasts, and maintains the survival of activated osteoclasts, thereby inducing bone demineralization to release more calcium into the plasma [16]. PRL also suppresses osteoblast functions by decreasing the expression of *Runt*-related transcription factor (Runx)-2, alkaline phosphatase (ALP) and osteocalcin, as well as the osteoblast-induced matrix mineralization [16,34,36]. The net result of PRL action on bone is therefore to stimulate bone resorption and inhibit bone formation.

PRL injection decreased renal calcium excretion in both non-mated and pregnant rats [29,40]. Although it was suggested that exogenous PRL enhanced renal calcium reabsorption [29,40], the role of endogenous PRL released during pregnancy and lactation remains uncertain because inhibition of pituitary PRL release by the dopaminergic agonist bromocriptine did not show a significant increase in renal calcium excretion [29]. Recent investigation showed that combined exposure to PRL and glucocorticoid directly modulates the barrier function of tight junctions in cultured renal epithelial monolayer, possibly by inducing redistribution of tight junction proteins occludin and ZO-1 [41]. Further *in vivo* investigations will be required to confirm a direct action of endogenous PRL on the renal tubular epithelium and on renal calcium handling in lactating animals.

Possible role of PRL in calcium transfer for fetal development and lactogenesis

Placental calcium transfer to the fetus and fetal bone mineralization largely take place in the third trimester in humans and the last five days of pregnancy in rats [42]. Several hormones including PTH and PTHrP are essential for placental calcium transfer in rodents [43]. Although the placenta is responsive to PRL and PRL-like factors [9], the physiological role of PRL in regulating placental calcium transport is currently not known. Nevertheless, it is possible that PRL contributes to calcium transfer across the placenta because it can increase calcium supply to the mother by stimulating intestinal calcium absorption [10].

After parturition, the mammary gland secretes up to 1000 mg/day of milk calcium, the concentration of which varies according to the stage of lactation (~5–8 mM) [1–3,44]. Because milk calcium is the sole calcium source for neonatal bone development and cellular metabolism, milk calcium secretion in mothers on a low calcium diet is maintained by the release of calcium from bone [2,44]. However, the hormone(s) responsible for controlling milk calcium secretion remains elusive.

Generally, transcellular calcium transport from plasma to the acinar lumen of the mammary gland consists of (i) calcium entry at the blood-facing plasma membrane, presumably via canonical transient receptor potential (TRPC) channels, (ii) uptake of cytoplasmic calcium into the Golgi apparatus by secretory pathway Ca^{2+}-ATPase system, and (iii) calcium extrusion via $PMCA_2$ and exocytosis [44,45]. In the Golgi apparatus and exocytotic vesicles, calcium binds to citrate, phosphate, and milk protein casein, the expression of which is enhanced by PRL [44,46]. Administration of exogenous PRL to lactating rats increases milk calcium concentration by ~10% [29]. Recently, PRL was reported to increase the expression of secretory pathway Ca^{2+}-ATPase-2 (SPCA2), and knockdown of SPCA2 abolished PRL-induced calcium uptake into the Golgi apparatus [47]. However, PRL did not alter TRPC channel mRNA expression levels [45]. Although the signaling pathway remains unknown, it is possible that the lactogenic hormone PRL directly regulates milk calcium secretion.

Possible directions for nutraceutical research and maternal health care

Because milk calcium is derived from both diet and bone in as yet unknown proportions, oral calcium supplementation should shift the proportion of milk calcium toward the

Box 2. Outstanding questions

- Does PRL enhance calcium uptake from the plasma into mammary epithelial cells? If so, what are the responsible calcium channels or transporters?
- Is PRL responsible for the maintenance of milk calcium concentration? What is the proportion of milk calcium content derived from diet versus bone?
- What is the exact role of PRL in renal calcium handling? Does PRL directly stimulate calcium reabsorption in the kidney?
- Does PRL directly enhance placental calcium transfer? How does maternal PRL contribute to skeletal development in the fetus?
- Can oral calcium supplementation prior to breastfeeding or PRL surge efficiently prevent maternal bone resorption, or even PLO and postmenopausal osteoporosis later in life, by supplying a larger proportion of calcium from the diet, thus reducing calcium mobilization from bone for milk production?

dietary source [10,39]. However, bone loss in breastfeeding mothers with relatively high calcium intake suggests that calcium supplementation alone is probably not enough to achieve this shift [1,37]. Because Step-2 calcium absorption is triggered by the suckling-induced PRL surge, to maximize the benefit of calcium supplementation we postulate that calcium should be administered orally at an appropriate time (e.g. 30–60 min) prior to breastfeeding in 3–4 divided doses/day (e.g. ~300–400 mg/dose; estimated from the recommended dietary intake of ~1200 mg/day). However, the effectiveness and potential long-term benefits of this regimen in humans remain to be validated.

Furthermore, certain nutrients such as glucose (and perhaps galactose, another substrate of SGLT1) can induce plasma membrane depolarization and increase Na^+/K^+-ATPase activity, thereby leading to $Ca_v1.3$ activation and solvent drag (Figure 2), respectively, both of which are important for PRL-stimulated duodenal calcium absorption [22,23,48]. Moreover, microflora can ferment prebiotics (non-digestible food ingredients) into acidic compounds, that then solubilize insoluble calcium complexes and promote calcium absorption [49], and especially in the cecum where PRL also markedly stimulates both transcellular and paracellular calcium transport [14,20]. It is therefore suggested that nutraceutical scientists might develop a calcium-rich product containing such additional ingredients as a supplement for breastfeeding mothers.

Concluding remarks

Several lines of evidence corroborate that PRL, with elevated plasma levels during mammalian reproductive periods, can be considered to be the cardinal calciotropic hormone that regulates maternal calcium homeostasis. PRL appears not only to provide more 'calcium input' during pregnancy and lactation, but also controls 'calcium output' via milk secretion (Figure 1). In other words, PRL acts as a coordinator to regulate and synchronize the calcium-regulating system to mobilize a sufficient amount of calcium for fetal development and lactogenesis. Calcium adequacy is achieved by PRL-enhanced intestinal calcium absorption, renal calcium reabsorption and bone resorption [6,10,14,27,29]. Although PRL is clearly a calcium regulating hormone, there are several questions that await further investigation (Box 2).

On the basis of findings that PRL stimulates intestinal calcium absorption in a two-step manner, it is suggested that oral calcium supplement for breastfeeding mothers should be given at appropriate times and doses to optimize calcium absorption. The development of a new calcium supplement that is well-absorbed in PRL-responsive intestinal segments including duodenum or cecum [14,20] should provide maximum benefit. Future holistic and integrative approaches in understanding physiological functions of PRL and maternal calcium homeostasis are important for preventing PLO and promoting fetomaternal bone health.

Acknowledgements

This work was supported by the Faculty of Science, Mahidol University, and the Thailand Research Fund.

References

1 Bowman, B.M. and Miller, S.C. (2001) Skeletal adaptations during mammalian reproduction. *J. Musculoskelet. Neuronal Interact.* 1, 347–355
2 Laskey, M.A. *et al.* (1998) Bone changes after 3 mo of lactation: influence of calcium intake, breast-milk output, and vitamin D-receptor genotype. *Am. J. Clin. Nutr.* 67, 685–692
3 Prentice, A. (2000) Calcium in pregnancy and lactation. *Annu. Rev. Nutr.* 20, 249–272
4 Brommage, R. and DeLuca, H.F. (1985) Regulation of bone mineral loss during lactation. *Am. J. Physiol. Endocrinol. Metab.* 248, E182–E187
5 Charoenphandhu, N. and Krishnamra, N. (2007) Prolactin is an important regulator of intestinal calcium transport. *Can. J. Physiol. Pharmacol.* 85, 569–581
6 Pahuja, D.N. and DeLuca, H.F. (1981) Stimulation of intestinal calcium transport and bone calcium mobilization by prolactin in vitamin D-deficient rats. *Science* 214, 1038–1039
7 Van Cromphaut, S.J. *et al.* (2003) Intestinal calcium transporter genes are upregulated by estrogens and the reproductive cycle through vitamin D receptor-independent mechanisms. *J. Bone Miner. Res.* 18, 1725–1736
8 Fudge, N.J. and Kovacs, C.S. (2010) Pregnancy up-regulates intestinal calcium absorption and skeletal mineralization independently of the vitamin D receptor. *Endocrinology* 151, 886–895
9 Soares, M.J. *et al.* (2007) The prolactin family: effectors of pregnancy-dependent adaptations. *Trends Endocrinol. Metab.* 18, 114–121
10 Charoenphandhu, N. *et al.* (2009) Two-step stimulation of intestinal Ca^{2+} absorption during lactation by long-term prolactin exposure and suckling-induced prolactin surge. *Am. J. Physiol. Endocrinol. Metab.* 297, E609–E619
11 Norris, D.O. (2007) Bioregulation of calcium and phosphate homeostasis, In *Vertebrate Endocrinology* (4th edn) (Norris, D.O., ed.), pp. 486–511, Elsevier
12 Takahashi, H. *et al.* (2008) Prolactin inhibits osteoclastic activity in the goldfish scale: a novel direct action of prolactin in teleosts. *Zoolog. Sci.* 25, 739–745
13 Srivastav, A.K. and Yadav, S. (2008) Prolactin effects on ultimobranchial and parathyroid glands in pigeon. *North-West J. Zool.* 4, 300–310
14 Jantarajit, W. *et al.* (2007) Prolactin-stimulated transepithelial calcium transport in duodenum and Caco-2 monolayer are mediated by the phosphoinositide 3-kinase pathway. *Am. J. Physiol. Endocrinol. Metab.* 293, E372–E384
15 Sakai, Y. *et al.* (1999) The prolactin gene is expressed in the mouse kidney. *Kidney Int.* 55, 833–840
16 Seriwatanachai, D. *et al.* (2008) Prolactin directly enhances bone turnover by raising osteoblast-expressed receptor activator of nuclear factor κB ligand/osteoprotegerin ratio. *Bone* 42, 535–546
17 Clément-Lacroix, P. *et al.* (1999) Osteoblasts are a new target for prolactin: analysis of bone formation in prolactin receptor knockout mice. *Endocrinology* 140, 96–105
18 Naliato, E.C. *et al.* (2005) Prevalence of osteopenia in men with prolactinoma. *J. Endocrinol. Invest.* 28, 12–17

19 Stubbs, B. (2009) Antipsychotic-induced hyperprolactinaemia in patients with schizophrenia: considerations in relation to bone mineral density. *J. Psychiatr. Ment. Health Nurs.* 16, 838–842
20 Kraidith, K. *et al.* (2009) Direct stimulation of the transcellular and paracellular calcium transport in the rat cecum by prolactin. *Pflügers Arch.* 458, 993–1005
21 Anderson, J.M. and Van Itallie, C.M. (2009) Physiology and function of the tight junction. *Cold Spring Harb. Perspect. Biol.* (doi:10.1101/cshperspect.a002584)
22 Thongon, N. *et al.* (2009) Enhancement of calcium transport in Caco-2 monolayer through PKC_{ζ}-dependent $Ca_v1.3$-mediated transcellular and rectifying paracellular pathways by prolactin. *Am. J. Physiol. Cell Physiol.* 296, C1373–C1382
23 Tanrattana, C. *et al.* (2004) Prolactin directly stimulated the solvent drag-induced calcium transport in the duodenum of female rats. *Biochim. Biophys. Acta* 1665, 81–91
24 Zhu, Y. *et al.* (1998) Pregnancy and lactation increase vitamin D-dependent intestinal membrane calcium adenosine triphosphatase and calcium binding protein messenger ribonucleic acid expression. *Endocrinology* 139, 3520–3524
25 Charoenphandhu, N. *et al.* (2008) Transcriptome responses of duodenal epithelial cells to prolactin in pituitary-grafted rats. *Mol. Cell Endocrinol.* 296, 41–52
26 Nakkrasae, L.I. *et al.* (2010) Transepithelial calcium transport in prolactin-exposed intestine-like Caco-2 monolayer after combinatorial knockdown of TRPV5, TRPV6 and $Ca_v1.3$. *J. Physiol. Sci.* 60, 9–17
27 Suntornsaratoon, P. *et al.* (2010) Femoral bone mineral density and bone mineral content in bromocriptine-treated pregnant and lactating rats. *J. Physiol. Sci.* 60, 1–8
28 Naylor, K.E. *et al.* (2000) The effect of pregnancy on bone density and bone turnover. *J. Bone Miner. Res.* 15, 129–137
29 Lotinun, S. *et al.* (1998) The study of a physiological significance of prolactin in the regulation of calcium metabolism during pregnancy and lactation in rats. *Can. J. Physiol. Pharmacol.* 76, 218–228
30 Hong, J.S. *et al.* (2005) Maternal plasma osteoprotegerin concentration in normal pregnancy. *Am. J. Obstet. Gynecol.* 193, 1011–1015
31 Ardeshirpour, L. *et al.* (2007) Weaning triggers a decrease in receptor activator of nuclear factor-κB ligand expression, widespread osteoclast apoptosis, and rapid recovery of bone mass after lactation in mice. *Endocrinology* 148, 3875–3886
32 Ofluoglu, O. and Ofluoglu, D. (2008) A case report: pregnancy-induced severe osteoporosis with eight vertebral fractures. *Rheumatol. Int.* 29, 197–201
33 Kovacs, C.S. (2005) Calcium and bone metabolism during pregnancy and lactation. *J. Mammary Gland Biol. Neoplasia* 10, 105–118
34 Coss, D. *et al.* (2000) Effects of prolactin on osteoblast alkaline phosphatase and bone formation in the developing rat. *Am. J. Physiol. Endocrinol. Metab.* 279, E1216–E1225
35 Deng, C. *et al.* (2009) Prolactin blocks nuclear translocation of VDR by regulating its interaction with BRCA1 in osteosarcoma cells. *Mol. Endocrinol.* 23, 226–236
36 Seriwatanachai, D. *et al.* (2009) Evidence for direct effects of prolactin on human osteoblasts: inhibition of cell growth and mineralization. *J. Cell Biochem.* 107, 677–685
37 Chan, S.M. *et al.* (2005) Bone mineral density and calcium metabolism of Hong Kong Chinese postpartum women – a 1-y longitudinal study. *Eur. J. Clin. Nutr.* 59, 868–876
38 Tanriover, M.D. *et al.* (2009) Pregnancy- and lactation-associated osteoporosis with severe vertebral deformities: can strontium ranelate be a new alternative for the treatment? *Spine J.* 9, e20–e24
39 Thomas, M. and Weisman, S.M. (2006) Calcium supplementation during pregnancy and lactation: effects on the mother and the fetus. *Am. J. Obstet. Gynecol.* 194, 937–945
40 Piyabhan, P. *et al.* (2000) Changes in the regulation of calcium metabolism and bone calcium content during growth in the absence of endogenous prolactin and during hyperprolactinemia: a longitudinal study in male and female Wistar rats. *Can. J. Physiol. Pharmacol.* 78, 757–765
41 Peixoto, E.B.M.I. and Collares-Buzato, C.B. (2006) Modulation of the epithelial barrier by dexamethasone and prolactin in cultured Madin–Darby canine kidney (MDCK) cells. *Cell Biol. Int.* 30, 101–113
42 Kovacs, C.S. (2006) Skeletal physiology: fetus and neonate, In *Primer on the Metabolic Bone Diseases and Disorders of Mineral Metabolism* (6th edn) (Favus, M.J., ed.), pp. 50–55, American Society for Bone and Mineral Research
43 Simmonds, C.S. *et al.* (2010) Parathyroid hormone regulates fetal–placental mineral homeostasis. *J. Bone Miner. Res.* doi:10.1359/jbmr.090825. (in press)
44 Neville, M.C. (2005) Calcium secretion into milk. *J. Mammary Gland Biol. Neoplasia* 10, 119–128
45 Anantamongkol, U. *et al.* (2010) Transcriptome analysis of mammary tissues reveals complex patterns of transporter gene expression during pregnancy and lactation. *Cell Biol. Int.* 34, 67–74
46 Stiening, C.M. *et al.* (2008) The effects of endocrine and mechanical stimulation on stage I lactogenesis in bovine mammary epithelial cells. *J. Dairy Sci.* 91, 1053–1066
47 Anantamongkol, U. *et al.* (2007) Regulation of Ca^{2+} mobilization by prolactin in mammary gland cells: possible role of secretory pathway Ca^{2+}-ATPase type 2. *Biochem. Biophys. Res. Commun.* 352, 537–542
48 Mace, O.J. *et al.* (2007) Calcium absorption by $Ca_v1.3$ induces terminal web myosin II phosphorylation and apical GLUT2 insertion in rat intestine. *J. Physiol.* 580, 605–616
49 Tenorio, M.D. *et al.* (2010) Soybean whey enhances mineral balance and caecal fermentation in rats. *Eur. J. Nutr.* doi:10.1007/s00394-009-0060-8. (in press)
50 Wasserman, R.H. (2004) Vitamin D and the dual processes of intestinal calcium absorption. *J. Nutr.* 134, 3137–3139
51 Khanal, R.C. and Nemere, I. (2008) Regulation of intestinal calcium transport. *Annu. Rev. Nutr.* 28, 179–196
52 Bianco, S.D. *et al.* (2007) Marked disturbance of calcium homeostasis in mice with targeted disruption of the Trpv6 calcium channel gene. *J. Bone Miner. Res.* 22, 274–285
53 Benn, B.S. *et al.* (2008) Active intestinal calcium transport in the absence of transient receptor potential vanilloid type 6 and calbindin-D_{9k}. *Endocrinology* 149, 3196–3205
54 Teerapornpuntakit, J. *et al.* (2009) Endurance swimming stimulates transepithelial calcium transport and alters the expression of genes related to calcium absorption in the intestine of rats. *Am. J. Physiol. Endocrinol. Metab.* 296, E775–E786
55 Charoenphandhu, N. *et al.* (2006) Chronic metabolic acidosis stimulated transcellular and solvent drag-induced calcium transport in the duodenum of female rats. *Am. J. Physiol. Gastrointest. Liver Physiol.* 291, G446–G455

Experimental and Molecular Pathology 88 (2010) 305–310

Contents lists available at ScienceDirect

Experimental and Molecular Pathology

journal homepage: www.elsevier.com/locate/yexmp

Claudin expression in the bone-lining cells of female rats exposed to long-standing acidemia

Kannikar Wongdee [a,b,c], Suda Riengrojpitak [b], Nateetip Krishnamra [a,d], Narattaphol Charoenphandhu [a,d,*]

[a] Consortium for Calcium and Bone Research (COCAB), Faculty of Science, Mahidol University, Bangkok, Thailand
[b] Department of Pathobiology, Faculty of Science, Mahidol University, Bangkok, Thailand
[c] Faculty of Allied Health Sciences, Burapha University, Chonburi, Thailand
[d] Department of Physiology, Faculty of Science, Mahidol University, Bangkok, Thailand

ARTICLE INFO

Article history:
Received 13 October 2009
and in revised form 9 December 2009
Available online 24 December 2009

Keywords:
Acidosis
Bone membrane
Claudin
Immunohistochemistry
Osteoblasts
Tight junction

ABSTRACT

Besides enhancing osteoclast-mediated bone resorption, chronic metabolic acidosis (CMA) induces mineral efflux across the epithelial-like bone membrane formed by bone-lining cells (inactive osteoblasts), possibly via the paracellular pathway. However, there was a compensatory mechanism that restricted bone loss in the late phase of CMA, and changes in the expression of claudins, which are tight junction proteins known to regulate epithelial barrier function, were therefore anticipated in bone-lining cells. Herein, primary rat osteoblasts were found to express several transcripts of claudins, i.e., claudin-5, -11, -14, -15 and -16. Their protein expressions in bone-lining cells were demonstrated by immunohistochemistry in decalcified tibial sections. After exposure to CMA induced by oral administration of 1.5% NH_4Cl for 21 days, expression of claudin-14, which normally seals the paracellular space and restricts ion movement, was increased, whereas that of claudin-15 and -16 which form pores for ion transport were decreased. Expressions of claudin-5 and -11 were not changed by CMA. In conclusion, the bone-lining cells of rats exposed to CMA for 21 days upregulated an ion-restrictive claudin (i.e., claudin-14), while downregulating ion-permeable claudins (i.e., claudin-15 and -16). These cellular responses might be parts of a compensatory mechanism accounting for deceleration of bone loss in late CMA.

Introduction

Chronic metabolic acidosis (CMA) is a common acid-base disturbance caused by a reduction in capacity of the kidney to synthesize ammonia and excrete H^+ (e.g., chronic renal failure), continuous loss of HCO_3^- (e.g., distal renal tubular acidosis), or accumulation of acidic substances. A number of studies showed that CMA affects bone metabolism by inducing physicochemical dissolution of bone minerals, suppressing osteoblast-mediated bone formation, and enhancing osteoclast-mediated bone resorption, thereby resulting in massive bone loss, hypercalciuria, nephrocalcinosis and negative calcium balance (Bushinsky and Lechleider, 1987; Dominguez and Raisz, 1979; Kraut et al., 1986; Krieger et al., 1992). However, our recent longitudinal study in rats exposed to CMA for 10 months suggested the existence of an unknown compensatory mechanism that decelerated bone loss and maintained bone mass during CMA (Assapun et al., 2009).

Bone calcium is present in the form of hydroxyapatite crystal, as well as free ions dissolved in the bone extracellular fluid (BECF), which is an intraosseous fluid compartment with different ion compositions from plasma (e.g., high K^+ concentration in BECF) (Green and Kleeman, 1991; Rubinacci et al., 2000). BECF is separated from the plasma by a "functional" epithelial-like bone membrane created by bone-lining cells (inactive osteoblasts), and its ion compositions were reported to be controlled by bone-lining cells (Bushinsky et al., 1989; Parfitt 1989; Soares et al., 1992; Trumbore et al., 1980). In acidosis, calcium is released from BECF by transporting across the bone membrane, presumably via the paracellular pathway (Bushinsky and Frick, 2000; Bushinsky, 2001; Marenzana et al., 2005). Besides calcium, the effluxes of other bone minerals, such as sodium, potassium and phosphate may also help buffer acid during CMA (Bergstrom and Wallace, 1954; Green and Kleeman, 1991).

In normal epithelia, the presence of tight junction is crucial for the fine-tuning of paracellular permeability, the maintenance of epithelial integrity, and the formation of paracellular barrier (Furuse and Tsukita, 2006; Tsukita et al., 2001). Since tight junctions are also present in osteoblasts (Hatakeyama et al., 2008; Prêle et al., 2003; Soares et al., 1992; Weinger and Holtrop, 1974; Wongdee et al., 2008), several investigations have suggested that bone-lining cells might regulate the paracellular ion exchange between the two fluid compartments, i.e., plasma and BECF, in an epithelial-like manner (Bushinsky et al., 1989; Hatakeyama et al., 2008; Rubinacci et al., 2000; Trumbore et al., 1980). However, it was still not known how ions were transported across the tight junction in CMA.

Abbreviations: BECF, bone extracellular fluid; CMA, chronic metabolic acidosis.

* Corresponding author. Department of Physiology, Faculty of Science, Mahidol University, Rama 6 Road, Bangkok 10400, Thailand. Fax: +66 2 354 7154.
E-mail address: naratt@narattsys.com (N. Charoenphandhu).

0014-4800/$ – see front matter © 2009 Elsevier Inc. All rights reserved.
doi:10.1016/j.yexmp.2009.12.005

In general, regulation of tight junction permeability for the paracellular transport of ions and small molecules across normal epithelia requires tight junction proteins of the claudin family, which consists of 24 members. Although claudins are predominantly localized in the tight junction, some claudins (e.g., claudin-3 and -7) can be found in other parts of the plasma membrane (Charoenphandhu et al., 2007; Holmes et al., 2006). Several investigators provided evidence that claudins could be divided into 2 subtypes, i.e., ion-restrictive and ion-permeable claudins (for review Anderson and Van Itallie, 2009). For example, claudin-5, -11 and -14 were demonstrated to seal the paracellular space and restrict paracellular ion movement (Ben-Yosef et al., 2003; Gow et al., 1999; Nitta et al., 2003), while claudin-15 and -16 assembled into a row of channel-like pores for paracellular ion transport (Tsukita et al., 2001; Van Itallie and Anderson, 2006). Interestingly, osteoblasts and bone-lining cells were also reported to express claudins, and their expressions were controlled by various humoral mediators, e.g., insulin-like growth factor I (Hatakeyama et al., 2008; Prêle et al., 2003; Wongdee et al., 2008). Since it was recently shown that long-term exposure to CMA eventually induced a compensatory response to limit bone mineral loss (Assapun et al., 2009), we hypothesized that expression of ion-restrictive claudins may be upregulated, whereas that of ion-permeable claudins were downregulated in the bone-lining cells of rats exposed to long-standing acidemia.

Materials and methods

Animals

Female Sprague–Dawley rats (8-week-old, weighing 180–220 g) were obtained from the National Animal Centre, Salaya, Thailand. They were housed in the laboratory animal husbandry unit under 12:12-h light–dark cycle, and fed regular chows (Perfect Companion, Bangkok, Thailand), and distilled water *ad libitum*. Room temperature was maintained at 20–25 °C, and relative humidity was 50–60%. After acclimatization for 7 days, the rats were randomly divided into two groups, i.e., age-matched control ($n=6$) and CMA groups ($n=4$). In CMA group, rats were provided *ad libitum* for 21 days with water containing 1.5% w/v NH_4Cl (Sigma, St Louis, MO, USA) to induce an acid-loading acidemia. Food and water intake were recorded daily. This study has been approved by the Institutional Animal Care and Use Committee (IACUC) of the Faculty of Science, Mahidol University, Bangkok, Thailand.

Arterial blood gas analysis

Heparinized arterial blood sample (5 mL) was collected from the left ventricle. Blood gas analysis of plasma pH, partial pressure of O_2 and CO_2, and HCO_3^- concentration was performed to confirm the success of CMA induction by using an automated analyzer (model Ultra C; Nova Biomedical, Walthame, MA, USA).

Primary osteoblast culture

Under 50 mg/kg thiopental sodium i.p. anesthesia, tibiae were removed from a 9-week-old rat by sterile surgical technique, as previously described (Charoenphandhu et al., 2008; Wongdee et al., 2008). After the connective tissues and marrow cells were removed, bones were cut into small dice, and cultured in a 25-cm^2 T-flask (Corning, NY, USA) with DMEM supplemented with 15% fetal bovine serum, 100 U/mL penicillin-streptomycin, and 100 μg/mL ascorbate-2-phosphate (Sigma). Cells were incubated at 37 °C with 5% CO_2. Osteoblasts proliferated and migrated from the bone dice into culture medium within 3 days. The medium was changed every 3 days. Six flasks of confluent cells from the same rat were pooled together for total RNA preparation. Five rats ($n=5$) were used in PCR studies.

Total RNA preparation and PCR

The total RNA samples were prepared from primary osteoblasts by using TRIzol reagent (Invitrogen, Carlsbad, CA, USA). Total RNA was then treated with RQ1 RNase-free DNase (Promega, Madison, WI, USA) and subsequently purified by RNeasy mini kit (Qiagen, Valencia, CA, USA) according to the manufacturer's instructions. Purity of the total RNA was determined by the ratio of absorbance readings at 260 and 280 nm, the ratio of which was in the range of 1.8–2.0. One microgram of total RNA was reverse-transcribed with iScript cDNA Synthesis kit (Bio-Rad, Hercules, CA, USA) to cDNA by a Bio-Rad MyCycler. Rat glyceraldehyde-3-phosphate dehydrogenase (GAPDH) served as a control gene to check the consistency of the reverse transcription. Primers used in the PCR studies are shown in Table 1. Conventional PCR was performed with GoTaq Green Master Mix (Promega) and Bio-Rad MyCycler. PCR products were collected at 36 cycles and visualized on 2% agarose gel stained with 1 μg/mL ethidium bromide (Sigma) under UV transilluminator (Alpha Innotech, San Leandro, USA). The important steps, including PCR amplification, cycle optimization and electrophoresis were performed in triplicate.

Bone preparation

As previously described by Wongdee et al. (2008), tibiae from normal and CMA rats were dissected, washed with 0.9% w/v NaCl and fixed at 4 °C overnight in 4% paraformaldehyde in 0.1 M phosphate buffered saline (PBS). Thereafter, they were washed with cold PBS pH 7.4 and decalcified in 20% w/v ethylenediaminetetraacetic acid (EDTA; Sigma) at 4 °C for 3 weeks. Decalcifying solution was replaced every 3 days. The success of decalcification was confirmed by dual-energy X-ray absorptiometry (model Lunar PIXImus2; GE Medical Systems, Madison, WI, USA). Finally, decalcified bones were embedded in paraffin, and cut into 7-μm sections by a microtome.

Immunohistochemistry

After deparaffinization in xylene and graded ethanol, sections were incubated at 37 °C for 30 min in antigen retrieval solution (0.01 mg/mL proteinase K, 50 mM Tris–HCl pH 7.5 and 5 mM EDTA). They were then incubated in 3% H_2O_2 for 1 h to reduce the endogenous peroxidase activity. Non-specific binding was blocked by incubating sections in 4% bovine serum albumin (BSA) in 0.1 M PBS for 2 h. After blocking, sections were incubated overnight at 4 °C with 1:200 anti-claudin-5, -11, -15, -16 (Santa Cruz Biotechnology, CA, USA), or -14 antibodies (Abcam, Cambridge, MA, USA). The sections were later washed with 0.1 M PBS, incubated for 1 h with biotinylated goat anti-rabbit antibody (Zymed, South San Francisco, CA, USA), and finally incubated for 1 h at room temperature with streptavidin-

Table 1
Rattus norvegicus oligonucleotide sequences used in the PCR experiments.

Gene	Accession no.	Primer (forward/reverse)	Product length (bp)
Claudin-5	NM_031701	5′-CGCTTGTGGCACTCTTTGT-3′ 5′-ACTCCCGGACTACGATGTTG-3′	168
Claudin-11	NM_053457	5′-ATTGGCATCATCGTCACAAC-3′ 5′-ATGTCCACCAGGGGCTTG-3′	158
Claudin-14	NM_001013429	5′-CTGTACCTGGGCTTCATC-3′ 5′-CACACATAGTCATTCAACCTG-3′	230
Claudin-15	XM_222085	5′-GCTGTGCCACCGACTCCC-3′ 5′-CAGAGCCCAGTTCATACTTG-3′	330
Claudin-16	NM_131905	5′-ATCTTCTTCAGTACGCTGCC-3′ 5′-CGATGAGTAATACGGTCCC-3′	372
GAPDH	NM_017008	5′-AGTCTACTGGCGTCTTCAC-3′ 5′-TCATATTTCTCGTGGTTCAC-3′	133

GAPDH, glyceraldehyde-3-phosphate dehydrogenase.

conjugated horseradish peroxidase (HRP) solution (Zymed). As for claudin-16, the donkey anti-goat HRP-IgG antibody (Santa Cruz) was used instead of biotinylated antibody/streptavidin-HRP solution. Immunohistochemical reaction was developed with a chromogenic peroxidase substrate 3,3′-diaminobenzidine (DAB; Pierce, Rockford, IL, USA). The negative control sections were obtained by incubating the sections from the control or CMA rats in the absence of primary antibody. Sections were counterstained with hematoxylin and examined under a light microscope (model BX51TRF; Olympus, Tokyo, Japan) and Image-Pro Plus 5 (Media Cybernetics, Bethesda, MD, USA).

Measurement of signal intensity

Densitometric determination of immunohistochemical signals was modified from the method of Lehr et al. (1999). Selection of DAB-positive signals (brownish color) was performed with Adobe Photoshop 9 (Adobe System, San Jose, CA, USA) by filtering the specific color shade (in red-green-blue [RGB] mode) and color intensity in the regions of interest (ROI). The RGB color range was red = 142, green = 103 and blue = 65, and the fuzziness value was adjusted to 75%. All pixels with DAB-positive color on the ROI were automatically highlighted by the software. Pixel counting was performed by the Histogram command, which showed the numbers of the total and DAB-positive pixels in the ROI. Relative signal intensity was normalized to the negative control signals (i.e., signals from the negative control sections). The relative signal intensity was calculated as followed,

$$\text{Relative intensity} = (\text{Positive pixels}/\text{Total pixels})_{\text{Age-matched control or CMA}} / (\text{Positive pixels}/\text{Total pixels})_{\text{Negative control}}$$

Statistical analysis

The results are expressed as means ± SE. Comparisons between CMA and control groups were determined by unpaired Student's *t*-test. The level of significance for all statistical tests was $p<0.05$. Data were analyzed by GraphPad Prism 5.0 for Windows (GraphPad Software, San Diego, CA, USA).

Results

CMA was induced by continuous acid-loading with 1.5% NH_4Cl given in drinking water for 21 days. Plasma pH of CMA rats was significantly lower than that of control rats, i.e., 7.27 ± 0.02 ($n=4$) vs. 7.37 ± 0.04 ($n=6$, $p<0.05$), respectively, with a decrease in plasma HCO_3^- concentration. Daily water intake was not less than 60 mL/day, suggesting that consumption of NH_4Cl-containing water in CMA rats was sufficient to induce sustained acidemia throughout the experimental period. The present blood gas profile represented a normal metabolic response to CMA, consistent with that reported previously by Charoenphandhu et al. (2007).

Prior to immunohistochemical localization of claudins, PCR experiments were performed to demonstrate that primary osteoblasts derived from the tibiae of adult female rats expressed claudins. As shown in Fig. 1, primary rat osteoblasts strongly expressed claudin-5, -11, -14, -15 and -16 transcripts. Immunohistochemical analysis in tibial sections also confirmed that claudin-5, -11, -14, -15 and -16 proteins were expressed in the bone-lining cells (inactive or flat osteoblasts), but not in osteocytes or marrow cells (Figs. 2A–J). Morphology and localization of the present bone-lining cells were consistent with those described previously (Weinger and Holtrop, 1974). After exposure to long-standing acidemia, bone-lining cells upregulated claudin-14 expression by 1.62-fold, while downregulating expression of claudin-15 and -16 by 2.87- and 6.15-fold, respectively (Figs. 2 and 3). However, the expressions of claudin-5 and -11 were not changed by CMA (Figs. 2 and 3).

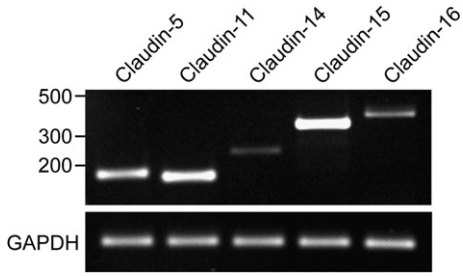

Fig. 1. Representative electrophoretic bands of claudin-5, -11, -14, -15 and -16 in primary rat osteoblasts ($n=5$). Expression of GAPDH, a housekeeping gene, is presented along with the studied genes. Numbers on the left indicate the base pairs of PCR products.

Discussion

During CMA, a number of compensatory responses are initiated to alleviate acidemia and negative calcium balance, e.g., increased intestinal calcium and phosphate absorption, and enhanced renal H^+ excretion and HCO_3^- reabsorption (Rose and Post, 2001). Bone also participates in the neutralization of H^+ by liberating calcium and other minerals, e.g., sodium, potassium, carbonate and phosphate, from BECF across bone membrane into the plasma (Bergstrom and Wallace, 1954; Bushinsky et al., 2003; Green and Kleeman, 1991; Rose and Post, 2001), leading to reduced bone mineral content. This compartmentalization (i.e., BECF and plasma) is achieved by a layer of bone-lining cells (Parfitt 1989; Soares et al., 1992). In addition, CMA also induced more calcium efflux from bone by enhancing the osteoclast-mediated bone resorption (Assapun et al., 2009). However, recent evidence showed that prolonged exposure to CMA appeared to induce a compensatory response in bone to restrict bone loss (Assapun et al., 2009). Specifically, a marked decrease in bone mass was observed only in the early phase of CMA. Thereafter, the rate of bone loss was gradually decreased (Assapun et al., 2009). Nevertheless, the exact mechanism responsible for this observation was unknown. It has been suggested that calcium efflux from BECF to plasma occurred through the paracellular pathway (Marenzana et al., 2005), perhaps across the tight junction formed by osteoblasts and bone-lining cells (Soares et al., 1992; Weinger and Holtrop, 1974). Since the paracellular ion transport in normal epithelia could be regulated and restricted by certain tight junction proteins of the claudin family (Anderson and Van Itallie, 2009), the CMA-induced changes in claudin expression in bone-lining cells might be a part of the adaptive response of bone to minimize mineral loss. Indeed, the possibility of the CMA-induced upregulation of claudin expression in epithelial cells is not totally without suggestive evidence. Recently, 21-day CMA was found to increase the expression of claudin-2, -3, -6, -8, -11, -12, -14, -19 and -22 in the duodenal epithelial cells, which presumably contributed to the CMA-induced increase in the intestinal calcium absorption (Charoenphandhu et al., 2006 and 2007).

In the present study, we found that expression of claudin-14 was upregulated, while that of claudin-15 and -16 was downregulated in the bone-lining cells. The expression patterns of claudins generally vary among different epithelia or epithelial-like structure, i.e., they are the "fingerprint" of the epithelia. Most claudins increase the tightness of tight junction and create a barrier to restrict the paracellular ion transport (e.g., claudin-5, -11 and -14), whereas some claudins possess the ion-permeable property (e.g., claudin-15 and -16), which were essential in the formation of paracellular pores to facilitate ion movement (Tsukita et al., 2001; Anderson and Van Itallie, 2009).

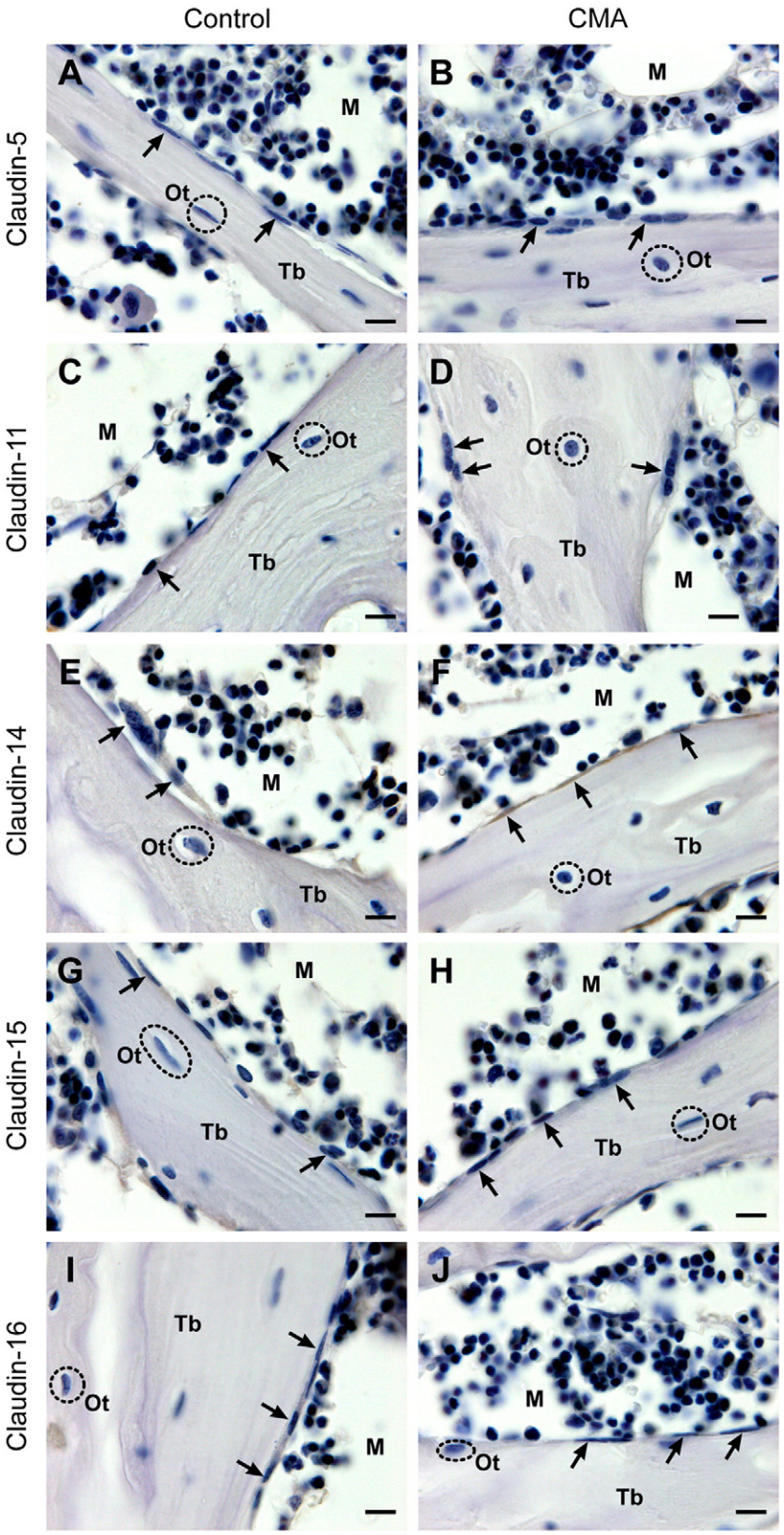

Fig. 2. (A–J) Immunohistochemical localization of claudin-5, -11, -14, -15 and -16 in paraffin-embedded decalcified tibial sections from control and CMA rats. The positive signals of claudins were seen in bone-lining cells (inactive osteoblasts; arrows), which covered bone trabeculae (Tb). No signal was detected in osteocytes (Ot) or bone marrow (M). Bars, 10 μm.

For instance, claudin-5 is expressed in endothelial cells for the maintenance of blood-brain barrier to protect the brain from circulating neurotoxic substances (Nitta et al., 2003). Similarly, claudin-11 is expressed in sertoli cells in the testis and forms the blood-testis barrier to prevent autoimmune responses against differentiated germ cells (Furuse and Tsukita, 2006). Nevertheless,

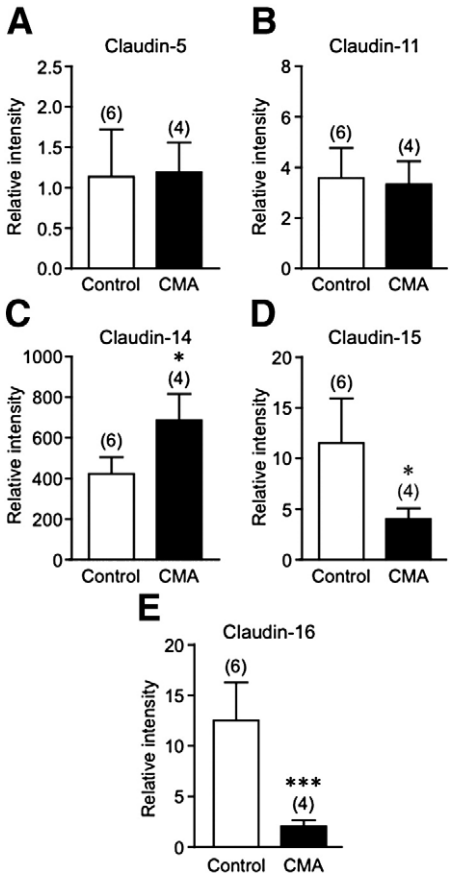

Fig. 3. (A–E) Relative signal intensity (arbitrary unit) of the expression of claudin-5, -11, -14, -15, and -16 in paraffin-embedded decalcified tibial sections from control and CMA rats. The intensities of the negative control sections were normalized to 1. Numbers in parentheses represent the number of animals in each group. *$p<0.05$, and ***$p<0.001$ compared with its respective control group.

expressions of claudin-5 and -11 in bone-lining cells were not changed by CMA.

Similar to claudin-5 and -11, claudin-14 also shows an ion-restrictive property. Under normal conditions, claudin-14 is expressed in several epithelia, e.g., the outer hair cells of the inner ear and intestinal epithelium of rodents (Ben-Yosef et al., 2003; Holmes et al., 2006; Charoenphandhu et al., 2007). In humans, mutations of claudin-14 may lead to deafness because its presence is essential for the maintenance of proper ion compositions of the endolymph and perilymph for sound transduction (Ben-Yosef et al., 2003). Overexpression of claudin-14 in Madin–Darby canine kidney-II monolayer led to an increase in the transepithelial resistance and a decrease in the paracellular cation permeability (Ben-Yosef et al., 2003). It was thus possible that upregulation of claudin-14 in bone-lining cells may enhance barrier function of the bone membrane to restrict mineral efflux from bone.

In contrast to claudin-14, claudin-15 and -16 have ion-permeable property, and can form the paracellular pores for cation transport (Van Itallie et al., 2003). Claudin-15 knockout mice manifested an enlargement of the proximal small intestine by ~2-fold with a decrease in the transepithelial ionic conductance (Tamura et al., 2008). Knockdown of claudin-15 also reduced cation permeability in the intestine-like Caco-2 monolayer (Charoenphandhu et al., 2009). Similarly, claudin-16 is involved in the regulation of the paracellular cation transport, especially calcium and magnesium reabsorption in the thick ascending limb of the loop of Henle (Simon et al., 1999). A strong evidence for the significance of claudin-16 is from its mutation that leads to a lethal inherited disease called familial hypomagnesemia with hypercalciuria and nephrocalcinosis. Since claudin-15 and -16 normally enhance the paracellular cation transport, downregulation of both claudins in the present study suggested that mineral efflux across the bone membrane was reduced.

In conclusion, the bone-lining cells responded to CMA by upregulating claudin-14 and downregulating claudin-15 and -16, which could partially explain the previous *in vivo* findings that, in prolonged exposure to CMA, further bone loss was prevented, and bone mineral content was maintained at a subnormal level thereafter (Assapun et al., 2009). However, future investigation is required to demonstrate the molecular mechanisms of the CMA-induced changes in claudin expression in bone-lining cells in relation with changes in the rate of mineral efflux across the bone membrane in CMA rats.

Conflict of interest statement
The authors declare no conflict of interest.

Acknowledgments

We thank Kukiat Tudpor and Jirawan Thongbunchoo for the excellent technical assistance. This research was supported by grants from the Strategic Consortia for Capacity Building of University Faculties and Staff, Commission on Higher Education, Thailand (to K.W.), and the Thailand Research Fund (to N.C. and N.K.).

References

Anderson, J.M., Van Itallie, C.M., 2009. Physiology and function of the tight junction. Cold Spring Harb. Perspect. Biol. 1 doi:10.1101/cshperspect.a002584.
Assapun, J., Charoenphandhu, N., Krishnamra, N., 2009. Early acceleration phase and late stationary phase of remodeling imbalance in long bones of male rats exposed to long-standing acidemia: a 10-month longitudinal study using bone histomorphometry. Calcif. Tissue Int. 85, 1–9.
Ben-Yosef, T., Belyantseva, I.A., Saunders, T.L., Hughes, E.D., Kawamoto, K., Van Itallie, C.M., Beyer, L.A., Halsey, K., Gardner, D.J., Wilcox, E.R., Rasmussen, J., Anderson, J.M., Dolan, D.F., Forge, A., Raphael, Y., Camper, S.A., Friedman, T.B., 2003. Claudin 14 knockout mice, a model for autosomal recessive deafness *DFNB29*, are deaf due to cochlear hair cell degeneration. Hum. Mol. Genet. 12, 2049–2061.
Bergstrom, W.H., Wallace, W.M., 1954. Bone as sodium and potassium reservoir. J. Clin. Invest. 33, 867–873.
Bushinsky, D.A., 2001. Acid–base imbalance and the skeleton. Eur. J. Nutr. 40, 238–244.
Bushinsky, D.A., Lechleider, R.J., 1987. Mechanism of proton-induced bone calcium release: calcium carbonate dissolution. Am. J. Physiol. Renal Physiol. 253, F998–F1005.
Bushinsky, D.A., Frick, K.K., 2000. The effects of acid on bone. Curr. Opin. Nephrol. Hypertens. 9, 369–379.
Bushinsky, D.A., Chabala, J.M., Levi-Setti, R., 1989. Ion microprobe analysis of mouse calvariae *in vitro*: evidence for a "bone membrane". Am. J. Physiol. Endocrinol. Metab. 256, E152–E158.
Bushinsky, D.A., Smith, S.B., Gavrilov, K.L., Gavrilov, L.F., Li, J., Levi-Setti, R., 2003. Chronic acidosis-induced alteration in bone bicarbonate and phosphate. Am. J. Physiol. Renal Physiol. 285, F532–F539.
Charoenphandhu, N., Tudpor, K., Pulsook, N., Krishnamra, N., 2006. Chronic metabolic acidosis stimulated transcellular and solvent drag-induced calcium transport in the duodenum of female rats. Am. J. Physiol. Gastrointest. Liver Physiol. 291, G446–G455.
Charoenphandhu, N., Wongdee, K., Tudpor, K., Pandaranandaka, J., Krishnamra, N., 2007. Chronic metabolic acidosis upregulated claudin mRNA expression in the duodenal enterocytes of female rats. Life Sci. 80, 1729–1737.
Charoenphandhu, N., Teerapornpuntakit, J., Methawasin, M., Wongdee, K., Thongchote, K., Krishnamra, N., 2008. Prolactin decreases expression of Runx2, osteoprotegerin, and RANKL in primary osteoblasts derived from tibiae of adult female rats. Can. J. Physiol. Pharmacol. 86, 240–248.
Charoenphandhu, N., Nakkrasae, L., Kraidith, K., Teerapornpuntakit, J., Thongchote, K., Thongon, N., Krishnamra, N., 2009. Two-step stimulation of intestinal Ca^{2+} absorption during lactation by long-term prolactin exposure and suckling-induced prolactin surge. Am. J. Physiol. Endocrinol. Metab. 297, E609–E619.
Dominguez, J.H., Raisz, L.G., 1979. Effects of changing hydrogen ion, carbonic acid, and bicarbonate concentrations on bone resorption *in vitro*. Calcif. Tissue Int. 29, 7–13.
Furuse, M., Tsukita, S., 2006. Claudins in occluding junctions of humans and flies. Trends Cell Biol. 16, 181–188.
Gow, A., Southwood, C.M., Li, J.S., Pariali, M., Riordan, G.P., Brodie, S.E., Danias, J., Bronstein, J.M., Kachar, B., Lazzarini, R.A., 1999. CNS myelin and sertoli cell tight junction strands are absent in *Osp/claudin-11* null mice. Cell 99, 649–659.
Green, J., Kleeman, C.R., 1991. Role of bone in regulation of systemic acid–base balance. Kidney Int. 39, 9–26.
Hatakeyama, N., Kojima, T., Iba, K., Murata, M., Thi, M.M., Spray, D.C., Osanai, M., Chiba, H., Ishiai, S., Yamashita, T., Sawada, N., 2008. IGF-I regulates tight-junction protein

claudin-1 during differentiation of osteoblast-like MC3T3-E1 cells via a MAP-kinase pathway. Cell Tissue Res. 334, 243–254.
Holmes, J.L., Van Itallie, C.M., Rasmussen, J.E., Anderson, J.M., 2006. Claudin profiling in the mouse during postnatal intestinal development and along the gastrointestinal tract reveals complex expression patterns. Gene Expr. Patterns 6, 581–588.
Kraut, J.A., Mishler, D.R., Singer, F.R., Goodman, W.G., 1986. The effects of metabolic acidosis on bone formation and bone resorption in the rat. Kidney Int. 30, 694–700.
Krieger, N.S., Sessler, N.E., Bushinsky, D.A., 1992. Acidosis inhibits osteoblastic and stimulates osteoclastic activity *in vitro*. Am. J. Physiol. Renal Physiol. 262, F442–F448.
Lehr, H.A., van der Loos, C.M., Teeling, P., Gown, A.M., 1999. Complete chromogen separation and analysis in double immunohistochemical stains using Photoshop-based image analysis. J. Histochem. Cytochem. 47, 119–126.
Marenzana, M., Shipley, A.M., Squitiero, P., Kunkel, J.G., Rubinacci, A., 2005. Bone as an ion exchange organ: evidence for instantaneous cell-dependent calcium efflux from bone not due to resorption. Bone 37, 545–554.
Nitta, T., Hata, M., Gotoh, S., Seo, Y., Sasaki, H., Hashimoto, N., Furuse, M., Tsukita, S., 2003. Size-selective loosening of the blood–brain barrier in claudin-5-deficient mice. J. Cell Biol. 161, 653–660.
Parfitt, A.M., 1989. Plasma calcium control at quiescent bone surfaces: a new approach to the homeostatic function of bone lining cells. Bone 10, 87–88.
Prêle, C.M., Horton, M.A., Caterina, P., Stenbeck, G., 2003. Identification of the molecular mechanisms contributing to polarized trafficking in osteoblasts. Exp. Cell Res. 282, 24–34.
Rose, B.D., Post, T.W., 2001. Metabolic acidosis, In: Rose, B.D., Post, T.W. (Eds.), Clinical physiology of acid-base and electrolyte disorders, 5th ed. McGraw-Hill, Singapore, pp. 578–646.
Rubinacci, A., Benelli, F.D., Borgo, E., Villa, I., 2000. Bone as an ion exchange system: evidence for a pump-leak mechanism devoted to the maintenance of high bone K^+. Am. J. Physiol. Endocrinol. Metab. 278, E15–E24.
Simon, D.B., Lu, Y., Choate, K.A., Velazquez, H., Al-Sabban, E., Praga, M., Casari, G., Bettinelli, A., Colussi, G., Rodriguez-Soriano, J., McCredie, D., Milford, D., Sanjad, S., Lifton, R.P., 1999. Paracellin-1, a renal tight junction protein required for paracellular Mg^{2+} resorption. Science 285, 103–106.
Soares, A.M., Arana-Chavez, V.E., Reid, A.R., Katchburian, E., 1992. Lanthanum tracer and freeze-fracture studies suggest that compartmentalisation of early bone matrix may be related to initial mineralisation. J. Anat. 181, 345–356.
Tamura, A., Kitano, Y., Hata, M., Katsuno, T., Moriwaki, K., Sasaki, H., Hayashi, H., Suzuki, Y., Noda, T., Furuse, M., Tsukita, S., Tsukita, S., 2008. Megaintestine in claudin-15-deficient mice. Gastroenterology 134, 523–534.
Trumbore, D.C., Heideger, W.J., Beach, K.W., 1980. Electrical potential difference across bone membrane. Calcif. Tissue Int. 32, 159–168.
Tsukita, S., Furuse, M., Itoh, M., 2001. Multifunctional strands in tight junctions. Nat. Rev. Mol. Cell Biol. 2, 285–293.
Van Itallie, C.M., Anderson, J.M., 2006. Claudins and epithelial paracellular transport. Annu. Rev. Physiol. 68, 403–429.
Van Itallie, C.M., Fanning, A.S., Anderson, J.M., 2003. Reversal of charge selectivity in cation or anion-selective epithelial lines by expression of different claudins. Am. J. Physiol. Renal Physiol. 285, F1078–F1084.
Weinger, J.M., Holtrop, M.E., 1974. An ultrastructural study of bone cells: the occurrence of microtubules, microfilaments and tight junctions. Calcif. Tissue Res. 14, 15–29.
Wongdee, K., Pandaranandaka, J., Teerapornpuntakit, J., Tudpor, K., Thongbunchoo, J., Thongon, N., Jantarajit, W., Krishnamra, N., Charoenphandhu, N., 2008. Osteoblasts express claudins and tight junction-associated proteins. Histochem. Cell Biol. 130, 79–90.

J Physiol Sci (2010) 60:9–17
DOI 10.1007/s12576-009-0068-0

ORIGINAL PAPER

Transepithelial calcium transport in prolactin-exposed intestine-like Caco-2 monolayer after combinatorial knockdown of TRPV5, TRPV6 and $Ca_v1.3$

La-iad Nakkrasae · Narongrit Thongon · Jirawan Thongbunchoo · Nateetip Krishnamra · Narattaphol Charoenphandhu

Received: 13 August 2009 / Accepted: 7 October 2009 / Published online: 3 November 2009

Abstract The milk-producing hormone prolactin (PRL) increases the transcellular intestinal calcium absorption by enhancing apical calcium uptake through voltage-dependent L-type calcium channel (Ca_v) 1.3. However, the redundancy of apical calcium channels raised the possibility that $Ca_v1.3$ may operate with other channels, especially transient receptor potential vanilloid family calcium channels (TRPV) 5 or 6, in an interdependent manner. Herein, TRPV5 knockdown (KD), TRPV5/TRPV6, TRPV5/$Ca_v1.3$, and TRPV6/$Ca_v1.3$ double KD, and TRPV5/TRPV6/$Ca_v1.3$ triple KD Caco-2 monolayers were generated by transfecting cells with small interfering RNAs (siRNA). siRNAs downregulated only the target mRNAs, and did not induce compensatory upregulation of the remaining channels. After exposure to 600 ng/mL PRL, the transcellular calcium transport was increased by ~2-fold in scrambled siRNA-treated, TRPV5 KD and TRPV5/TRPV6 KD monolayers, but not in TRPV5/$Ca_v1.3$, TRPV6/$Ca_v1.3$ and TRPV5/TRPV6/$Ca_v1.3$ KD monolayers. The results suggested that $Ca_v1.3$ was the sole apical channel responsible for the PRL-stimulated transcellular calcium transport in intestine-like Caco-2 monolayer.

Keywords Calcium absorption · Small interfering RNA (siRNA) · Transcellular transport · Triple knockdown · Voltage-dependent calcium channel (Ca_v)

L. Nakkrasae · N. Thongon · J. Thongbunchoo · N. Krishnamra · N. Charoenphandhu
Consortium for Calcium and Bone Research (COCAB), Faculty of Science, Mahidol University, Bangkok, Thailand

L. Nakkrasae
Department of Biology, Faculty of Science, Khon Kaen University, Khon Kaen, Thailand

N. Thongon
Department of Medical Science, Faculty of Science, Burapha University, Chonburi, Thailand

N. Krishnamra · N. Charoenphandhu (✉)
Department of Physiology, Faculty of Science, Mahidol University, Rama VI Road, Bangkok 10400, Thailand
e-mail: naratt@narattsys.com

Introduction

Prolactin (PRL) has been shown to be a calcium-regulating hormone since it could stimulate transcellular calcium absorption in intestinal epithelium of rats as well as in intestine-like Caco-2 monolayers [1–4]. Transcellular calcium transport is crucial during high calcium demand, such as pregnancy, lactation, or inadequate calcium intake [5]. It is a three-step process consisting of (1) apical calcium entry via transient receptor potential vanilloid Ca^{2+} channels (TRPV) 5, TRPV6 and voltage-dependent L-type calcium channel (Ca_v) 1.3, (2) cytoplasmic diffusion in a calbindin-D_{9k}-bound form, and (3) basolateral extrusion via plasma membrane Ca^{2+}-ATPase (PMCA) and Na^+/Ca^{2+} exchanger (NCX) [6–9]. In general, $Ca_v1.3$ mediates intestinal calcium absorption under certain conditions, e.g., in the presence of depolarization state induced by glucose absorption [7, 8].

Recently, PRL was found to rapidly enhance transcellular calcium absorption in a non-genomic manner via $Ca_v1.3$, but not TRPV6 [9]. Pituitary-grafted rats with hyperprolactinemia also exhibited upregulation of L-type calcium channels [10]. However, the redundancy of apical calcium channels raised the possibility that the PRL-stimulated transcellular calcium transport may still require the presence of TRPV5 and/or TRPV6. Alternatively, one channel may be upregulated to compensate for the absence of the others. For example, TRPV5 knockout mice with

hypercalciuria responded to negative calcium balance by upregulating TRPV6 expression in the small intestine to increase calcium absorption [11]. Indeed, it was not known whether calcium entry through TRPV5 contributed to the PRL-stimulated calcium flux in the intestine. Since TRPV5 and TRPV6, known to share 75% homology at the amino acid level and exhibit a similar ion permeation sequence for divalent cations ($Ca^{2+} > Sr^{2+} \approx Ba^{2+} > Mn^{2+}$), were co-expressed in the intestinal epithelial cells [12, 13], it was necessary to investigate the participation of TRPV5 in the PRL-stimulated calcium transport. Furthermore, whether $Ca_v1.3$ is the sole calcium channel required for PRL action was still not known.

Therefore, the objectives of the present study were (1) to examine the involvement of TRPV5 in the PRL-stimulated calcium absorption in intestinal epithelial monolayer, (2) to investigate whether an absence of one calcium channel led to upregulation of the others, and (3) to provide evidence that $Ca_v1.3$ was the sole calcium channel which mediated the PRL-stimulated calcium transport. Human colorectal adenocarcinoma cell line, Caco-2 cells, were used in the present study as they are easy to manipulate genetically. Despite being derived from the colon and having relatively low basal calcium flux compared to the small intestine [14], confluent Caco-2 monolayer has been widely used in the studies of drugs or hormones that enhance calcium absorption since it possesses characteristics of the small intestine, including the presence of the brush border, expression of sucrase-isomaltase enzymes, and expression of the transcellular calcium transporters [15–17]. Moreover, Caco-2 monolayer also expresses functional PRL receptors and responds well to PRL by increasing transcellular calcium flux by ~2-fold, similar to that observed in the rat duodenum [14].

Materials and methods

Cell culture

Caco-2 cells (ATCC No. HTB-37) were grown in Dulbecco's modified Eagle medium (DMEM; Sigma, St. Louis, MO, USA) supplemented with 15% fetal bovine serum (FBS; Gibco, Grand Island, NY, USA), 1% L-glutamine (Gibco), 1% non-essential amino acid (Sigma), 100 U/mL penicillin/streptomycin (Sigma), and 0.25 μL/mL amphotericin B (Sigma). Cells were later propagated in 25-cm^2 T-flask (Corning, NY, USA) under a humidified atmosphere containing 5% CO_2 at 37°C, and subcultured as described in the ATCC protocol. Confluent Caco-2 monolayers were prepared by seeding cells (5.0×10^5 cells/cm^2) on a polyester Snapwell with 12 mm diameter and 0.4 μm pore size (Corning). Culture medium was changed daily after 48 h of seeding.

Small interfering RNA transfection

Small interfering RNA oligonucleotides targeted for human TRPV5, TRPV6, and $Ca_v1.3$ as well as scrambled sequences were designed by siRNA Target Designer (version 1.51; Promega, Madison, WI, USA), as shown in Table 1. All oligonucleotides were synthesized by T7 RiboMax Express RNAi System (Promega) according to the manufacturer's instruction. At day 12 after seeding of Caco-2 cells on a Snapwell, in vitro transfection was performed with 10 μg/mL polyethyleneimine (PEI) and 1 μmol/mL siRNA molecules to generate TRPV5 knockdown (KD), TRPV5/TRPV6, TRPV5/$Ca_v1.3$, TRPV6/$Ca_v1.3$ double KD, and TRPV5/TRPV6/$Ca_v1.3$ triple KD monolayers. At day 14 (i.e., 48 h after transfection), the Snapwell was mounted in an Ussing chamber with an exposed surface area of 1.13 cm^2 to measure the electrical parameters and calcium fluxes, as previously described [18]. Efficiency of siRNA was evaluated by quantitative real-time PCR (qRT-PCR). Recent investigations showed that conventional siRNA KD successfully abolished the functions of TRPV5 and TRPV6 channels, as determined by patch-clamp technique [19, 20]. This KD protocol was approved by the Institutional Biosafety Committee of the Mahidol University.

Quantitative real-time PCR and sequencing

Expression levels of TRPV5, TRPV6 and $Ca_v1.3$ were quantified by a real-time PCR (model MiniOpticon; Bio-Rad) as described previously [9]. Glyceraldehyde-3-phosphate dehydrogenase (GAPDH), a housekeeping gene, served as a control for normalization. Sense and antisense primers used for qRT-PCR are presented in Table 2. PCR reaction was performed with iQ SYBR Green SuperMix (Bio-Rad). Relative expression of TRPV5, TRPV6 or $Ca_v1.3$ over GAPDH was calculated from the threshold

Table 1 siRNA oligonucleotides used in KD study

Targets	siRNA oligonucleotides
TRPV5 siRNA	5′-GGCACUUGAAUCUUGGACU-3′
	5′-AAAGUCCAAGAUUCAAGUGCC-3′
TRPV6 siRNA	5′-GGGAAACACAGUGUUACAC-3′
	5′-GTGUAACACUGUGUUUCCC-3′
$Ca_v1.3$ siRNA	5′-GAGCACCUUUGACAAUUUC-3′
	5′-AAGAAAUUGUCAAAGGTGCUC-3′
Scramble siRNA	5′-GGCGCAAUAAAGCAAGACC-3′
	5′-AAGGUCUUGCUUUAUUGCCC-3′

TRPV5/6 Transient receptor potential vanilloid family Ca^{2+} channels 5/6, *$Ca_v1.3$* voltage-dependent L-type Ca^{2+} channel 1.3

Table 2 *Homo sapiens* oligonucleotide sequences used in the qRT-PCR experiments

Name	Accession no.	Primer (forward/reverse)	Product length (bp)
TRPV5	NM_019841	5′–CACTGTTATTGATGCACCTGC–3′	120
		5′–CCATCATGGCGATGAACA–3′	
TRPV6	AF365928	5′–TCTGACTGCGTGTTCTCAC–3′	144
		5′–ACATTCCTTGGCGTTCAT–3′	
$Ca_v1.3$	NM_000720	5′–TGATCCAAGTGGAGCAGTCA–3′	113
		5′–GTGTGAAAGTCCGGTAGGAGA–3′	
GAPDH	NM_002046	5′–CTGGTAAAGTGGATATTGTTG–3′	359
		5′–GAGGCTGTTGTCATACTTCTC–3′	

TRPV5/6 Transient receptor potential vanilloid family Ca^{2+} channels 5/6, *$Ca_v1.3$* voltage-dependent L-type Ca^{2+} channel 1.3, *GAPDH* glyceraldehyde-3-phosphate dehydrogenase

cycle (C_t) values by using $2^{\Delta Ct}$ method. Besides melting curve analysis, PCR products were also visualized on 1.5% agarose gel stained with 1.0 μg/mL ethidium bromide. After electrophoresis, PCR bands were extracted by HiYield Gel/PCR DNA Extraction kit (Real Biotech Corporation, Taipei, Taiwan), and were sequenced by ABI Prism 3100 Genetic Analyzer (Applied Biosystems, Foster City, CA, USA). qRT-PCR experiments were performed in triplicate.

Bathing solution for Ussing chamber technique

The bathing solution for Ussing chamber experiments contained (in mmol/L) 118 NaCl, 4.7 KCl, 1.1 $MgCl_2$, 1.25 $CaCl_2$, 23 $NaHCO_3$, 12 D-glucose and 2 mannitol (all purchased from Sigma). The solution was continuously gassed with humidified 5% CO_2 in 95% O_2, maintained at 37°C, pH 7.4, and had an osmolality of 290–293 mmol/kg water. Distilled water used in the present work had a resistance higher than 18.3 MΩ cm and a free ionized calcium concentration of <2.5 nmol/L.

Measurement of electrical parameters

Three electrical parameters, i.e., potential (voltage) difference (PD), short-circuit current (I_{sc}), and transepithelial resistance (TER), were determined as described previously [14]. In brief, a pair of Ag/AgCl electrodes connected to agar bridges (3.0 mol/L KCl per 4% agar) was located near each surface of the mounted Snapwell for measurement of PD. The other ends of the PD-sensing electrodes were connected to a pre-amplifier (model EVC-4000; World Precision Instruments, Sarasota, FL, USA). Another pair of Ag/AgCl electrodes connected in series to the EVC-4000 current-generating unit was placed at the end of each hemichamber to supply I_{sc}, which is external current to nullify PD. TER was calculated from Ohm's equation. Fluid resistance was automatically subtracted by the EVC-4000 system.

Calcium flux measurement

Calcium fluxes were determined by the method of Thongon et al. [9]. In brief, after a 20-min incubation in the Ussing chamber, the bathing solution was changed with a fresh one. The solution on one side contained ^{45}Ca (initial specific activity of 5 mCi/mL, final specific activity of ~450–500 mCi/mol; Amersham, Buckinghamshire, UK). Unidirectional flux of calcium ($J_{H\rightarrow C}$, nmol h^{-1} cm^{-2}) from the hot side (H) to the cold side (C) was calculated with Eqs. 1 and 2.

$$J_{H\rightarrow C} = R_{H\rightarrow C}/(S_H \times A) \quad (1)$$

$$S_H = C_H/C_T \quad (2)$$

where $R_{H\rightarrow C}$ is the rate of tracer appearance in the cold side (cpm/h), S_H the specific activity in the hot side (cpm/nmol), A the surface area of Snapwell (cm^2), C_H is a radioactivity in the hot side (cpm), and C_T is the total calcium in the hot side (nmol). ^{45}Ca radioactivity in counts per minute (cpm) was analyzed by liquid scintillation spectrophotometer (model Tri-Carb 3100; Packard, Meriden, CT, USA). Total calcium concentration in the hot side was determined by atomic absorption spectrophotometer (model SpectrAA-300; Varian Techtron, Springvale, Australia). In the absence of transepithelial calcium gradient, i.e., bathing solution in both hemichambers contained equal calcium concentration of 1.25 mmol/L, the measured calcium fluxes represented the transcellular active calcium transport [9, 14]. In some experiments, Caco-2 monolayer was exposed on the basolateral side to 600 ng/mL recombinant human PRL (rhPRL; purity >97%; catalog no. 682-PL; R&D Systems, Minneapolis, MN, USA), which is the maximal effective concentration reported by Jantarajit et al. [14].

Statistic analysis

Unless otherwise specified, results are expressed as mean ± SE. Multiple sets of data were compared by one-way analysis of variance (ANOVA) with Dunnett's

multiple comparison test. The level of significance for all statistical tests was $P < 0.05$. Data were analyzed by GraphPad Prism (version 4.0 for Mac OS X; GraphPad Software, San Diego, CA, USA).

Results

Expression of TRPV5, TRPV6 and $Ca_v1.3$ in TRPV5 KD monolayer

Since it was not known whether TRPV5 mediated the PRL-stimulated transcellular calcium transport, we generated TRPV5 KD monolayers to demonstrate the significance of TRPV5 for such PRL action. After being treated with PEI, scrambled siRNA, or TRPV5 siRNA, Caco-2 cells exhibited a stable expression of GAPDH (Fig. 1a), indicating that GAPDH could be used as a control transcript. mRNA expression of TRPV5, but not TRPV6 or $Ca_v1.3$, markedly decreased in TRPV5 KD cells by ~17-fold (Fig. 1b–e). The results suggested that TRPV5 siRNA was effective in suppressing TRPV5 expression without causing compensatory upregulation of TRPV6 and $Ca_v1.3$.

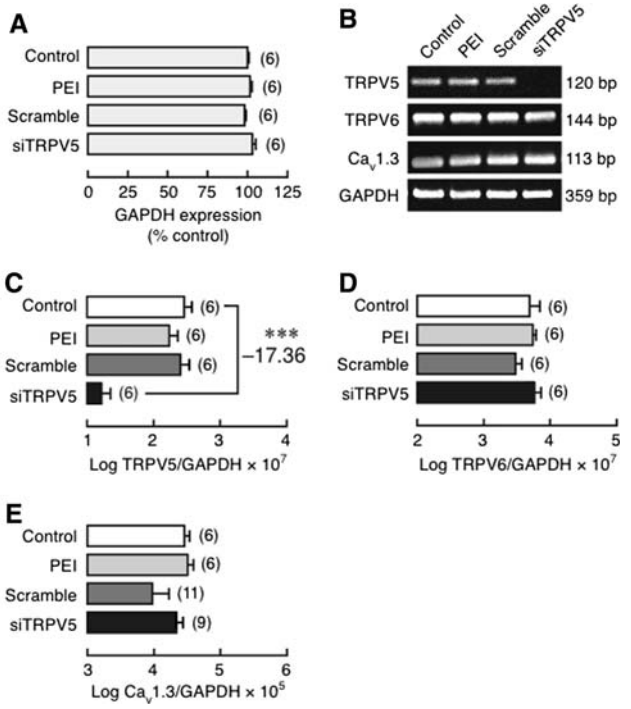

Fig. 1 **a** Expression of glyceraldehyde-3-phosphate dehydrogenase (*GAPDH*) mRNA in the control, PEI-treated, scrambled siRNA (*Scramble*)-transfected and TRPV5 siRNA (*siTRPV5*)-transfected Caco-2 monolayers. GAPDH expression of the control group was adjusted to 100%, while those of other groups were relative to the control group. **b** Representative electrophoretic bands of TRPV5, TRPV6 and $Ca_v1.3$ expression in the control, PEI, Scramble and siTRPV5 groups. **c–e** Expression of TRPV5, TRPV6 and $Ca_v1.3$ in TRPV5 KD Caco-2 monolayer as demonstrated by qRT-PCR. Expression levels were normalized by GAPDH expression. Values are presented as log mean ± SE. ***$P < 0.001$ compared with the control group. Value of fold difference was also presented along with the *statistical symbol*. *Numbers* in *parentheses* represent the number of independent experiments. Each experiment was performed in triplicate

PRL-enhanced calcium transport in TRPV5 KD monolayer

After being exposed to 600 ng/mL rhPRL, both control and TRPV5 KD monolayers manifested an approximately twofold increase in the transcellular calcium transport (Fig. 2). The basal calcium transport was not affected by transfecting agent PEI, scrambled siRNA, or TRPV5 siRNA. The results, therefore, suggested that TRPV5 may not be required for the PRL-enhanced transcellular calcium transport.

Expression of TRPV5, TRPV6 and $Ca_v1.3$ in Caco-2 monolayers after combinatorial KD

To exclude the possibility that, in response to PRL, the remaining two channels were upregulated to compensate for the absence of the other channels after single KD of TRPV5, TRPV6, or $Ca_v1.3$, we generated Caco-2 monolayers with double KD of TRPV5/TRPV6, TRPV5/$Ca_v1.3$, or TRPV6/$Ca_v1.3$, or triple KD of TRPV5/TRPV6/$Ca_v1.3$. We first demonstrated that, in a control monolayer, exposure to 600 ng/mL rhPRL for 60 min did not alter TRPV5, TRPV6, and $Ca_v1.3$ expression (Fig. 3a). Moreover, GAPDH expression was stable in both double and triple

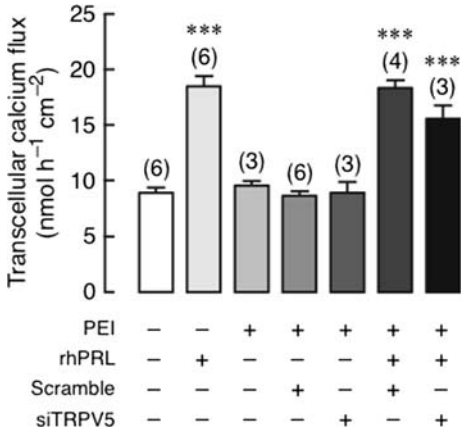

Fig. 2 Transcellular calcium transport in Caco-2 monolayer transfected with TRPV5 siRNA (*siTRPV5*) with or without 600 ng/mL rhPRL exposure. Scrambled siRNA was used as a negative control. Monolayer was bathed on both sides with 1.25 mmol/L calcium-containing solution. ***$P < 0.001$ compared with the control group. *Numbers* in *parentheses* represent the number of independent experiments

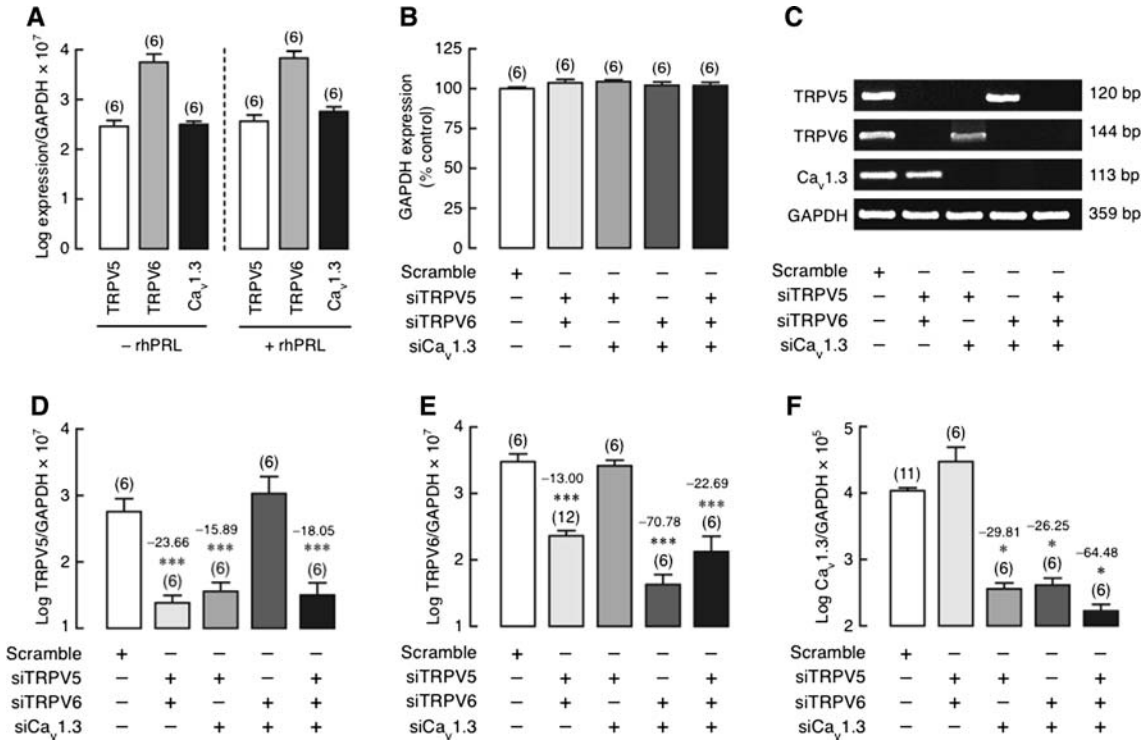

Fig. 3 **a** Expression of TRPV5, TRPV6, and $Ca_v1.3$ mRNA in Caco-2 monolayer directly exposed for 60 min to 600 ng/mL rhPRL. **b** GAPDH expression in TRPV5/TRPV6, TRPV5/$Ca_v1.3$, TRPV6/$Ca_v1.3$ double KD, and TRPV5/TRPV6/$Ca_v1.3$ triple KD monolayers. GAPDH expression in scrambled siRNA-treated group was adjusted to 100%. **c** Representative electrophoretic bands of TRPV5, TRPV6, and $Ca_v1.3$ mRNA expression in double and triple KD monolayers. **d**–**f** Expression of TRPV5, TRPV6, and $Ca_v1.3$ mRNA in double and triple KD Caco-2 monolayers as demonstrated by qRT-PCR. Expression levels were normalized by GAPDH expression. Data are presented as log mean ± SE. $*P < 0.05$, $***P < 0.001$ compared with the scrambled siRNA-treated group. Values of fold differences were also presented along with the *statistical symbols*. *Numbers* in *parentheses* represent the number of independent experiments. Each experiment was performed in triplicate. siTRPV5, siTRPV6, and si$Ca_v1.3$ mean siRNAs against TRPV5, TRPV6, and $Ca_v1.3$ mRNA, respectively

KD monolayers (Fig. 3b). TRPV5 mRNA expressions in TRPV5/TRPV6, TRPV5/$Ca_v1.3$, and triple KD monolayers were decreased by ~24-, ~16-, and ~18-fold, respectively, whereas no significant change was found in TRPV6/$Ca_v1.3$ KD monolayer (Fig. 3c, d). Similarly, TRPV6 and $Ca_v1.3$ mRNA expressions were downregulated only in the presence of their target siRNA molecules (Fig. 3c, e, f). These findings indicated that there was no compensatory expression of the remaining channel when mRNAs of the two channels were disrupted. In other words, the lack of expression of one channel could not be rescued by expression of the others.

PRL-enhanced calcium transport in Caco-2 monolayers after combinatorial KD of TRPV5, TRPV6 and $Ca_v1.3$

In TRPV5/TRPV6 double KD monolayer, 600 ng/mL rhPRL was able to stimulate the transcellular calcium transport, similar to that observed in the control and PEI-treated monolayers (Fig. 4). However, in TRPV5/$Ca_v1.3$, TRPV6/$Ca_v1.3$ double KD, and triple KD monolayers, the PRL-stimulated transcellular calcium transport was completely abolished (Fig. 4). Such combinatorial KD had no effect on the basal calcium transport, PD, I_{sc}, or the PRL-induced decrease in TER (Figs. 4, 5), the latter of which indirectly represented an increase in the paracellular permeability by PRL [9, 18, 21]. The results corroborated that $Ca_v1.3$ was the sole calcium channels required for the PRL-stimulated transcellular calcium transport across the intestinal epithelium.

Discussion

A significant amount of maternal calcium (~200–400 mg/day) is lost during pregnancy and lactation for fetal growth and milk production, thus resulting in severe negative calcium balance and osteopenia [22]. In lactation, PRL is not only an important hormone for lactogenesis but also for the regulation of overall calcium metabolism in pregnancy and lactation, in part, by stimulating renal calcium reabsorption and transcellular calcium absorption in the small

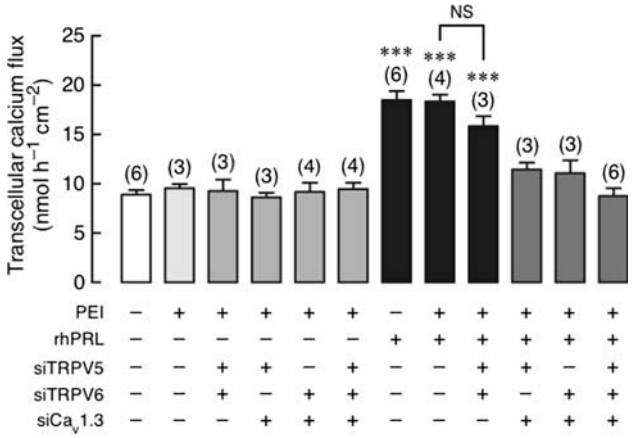

Fig. 4 Transcellular calcium transport in TRPV5/TRPV6, TRPV5/$Ca_v1.3$, TRPV6/$Ca_v1.3$ double KD, and TRPV5/TRPV6/$Ca_v1.3$ triple KD monolayers directly exposed to 600 ng/mL rhPRL. PEI was a transfecting agent. Monolayer was bathed on both sides with 1.25 mmol/L calcium-containing solution. ***$P < 0.001$ compared with the scrambled siRNA-treated group (negative control). *Numbers* in *parentheses* represent the number of independent Snapwells. siTRPV5, siTRPV6, and siCa$_v$1.3 mean siRNAs against TRPV5, TRPV6, and $Ca_v1.3$ mRNA, respectively. *NS* Not significant

intestine, thereby ameliorating stress on calcium metabolism [2, 5]. Previous investigations in duodenal epithelial cells showed that PRL enhanced the transcellular calcium transport by increasing the apical (brush-border) calcium uptake [23]. The present study further demonstrated that $Ca_v1.3$ was the sole apical calcium channel for the PRL-stimulated transcellular calcium transport in Caco-2 monolayer, which is an accepted model for calcium absorption study [9, 15].

Three calcium channels, namely TRPV5, TRPV6, and $Ca_v1.3$, were co-expressed on the apical membrane of duodenal, jejunal, and colonic epithelial cells [24, 25]. For the past decade, TRPV6 has been postulated to be the principal calcium channel for apical calcium entry in the small intestine, whereas TRPV5, with its expression being much lower than that of TRPV6 in both duodenum [26] and Caco-2 cells (Fig. 3a), was thought to play a minor role. However, physiological significance of TRPV6 became doubtful when TRPV6 null mice were found to be normocalcemic and responded to $1,25(OH)_2D_3$ by increasing transcellular calcium transport, similar to that observed in the wild-type mice [27, 28]. Moreover, Morgan and co-workers [8] suggested that TRPV5 and TRPV6 could not have been involved in the glucose-stimulated calcium absorption since both channels normally operated at negative membrane potentials below −90 mV (hyperpolarization), whereas postprandial glucose-rich luminal condition usually led to cell depolarization. Therefore, in the presence of luminal glucose, $Ca_v1.3$ must have been responsible for the intestinal calcium absorption [7, 8].

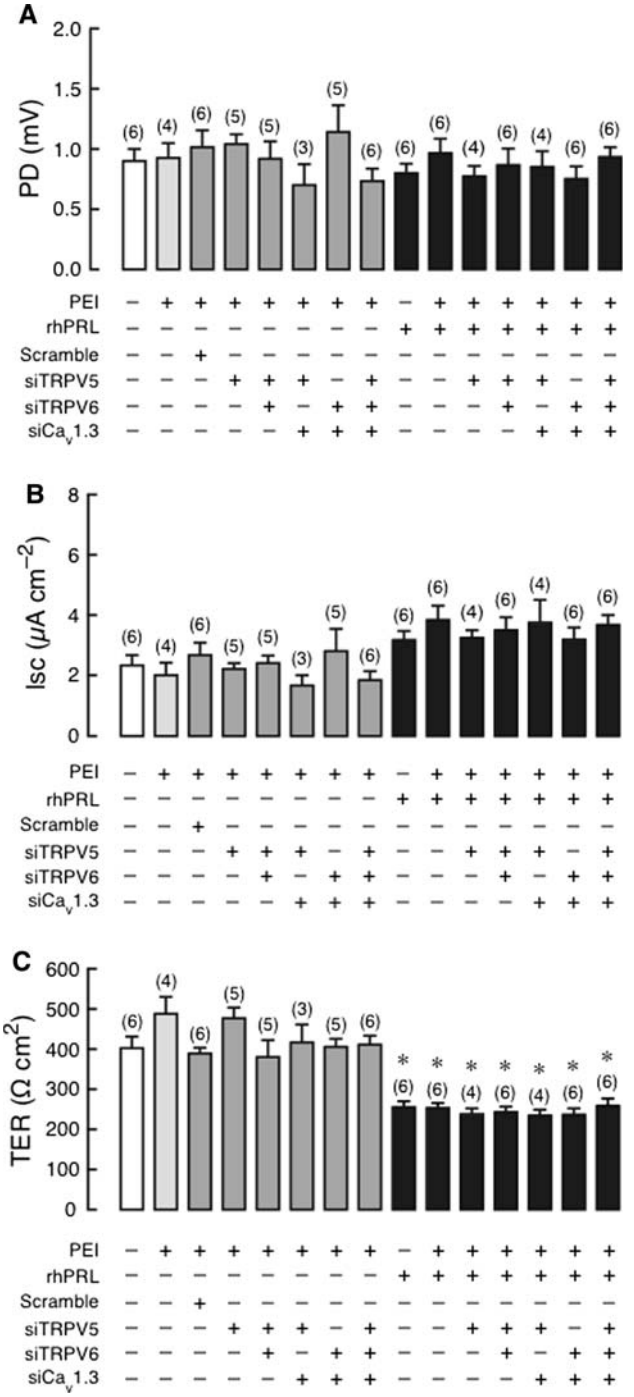

Fig. 5 **a** Transepithelial potential difference (*PD*), **b** short-circuit current (I_{sc}), and **c** transepithelial resistance (*TER*) in TRPV5 KD, TRPV5/TRPV6, TRPV5/$Ca_v1.3$, TRPV6/$Ca_v1.3$ double KD, and TRPV5/TRPV6/$Ca_v1.3$ triple KD monolayers directly exposed to 600 ng/mL rhPRL. PEI was a transfecting agent. The apical side had negative voltage with respect to the basolateral side. *$P < 0.05$ compared with the scrambled siRNA-treated group. *Numbers* in *parentheses* represent the number of independent Snapwells. siTRPV5, siTRPV6, and siCa$_v$1.3 mean siRNAs against TRPV5, TRPV6, and $Ca_v1.3$ mRNA, respectively. The absence of changes in PRL actions in KD monolayers indicated that these calcium channels were not required for the PRL-induced increase in paracellular permeability

Nevertheless, intestinal TRPV5 and TRPV6 could be important for the enhancement of transcellular calcium transport in certain stimulating conditions, such as chronic metabolic acidosis, and long-term exposure to estrogen or $1,25(OH)_2D_3$ [26, 29–31]. Indeed, TRPV6 expression was markedly upregulated after $1,25(OH)_2D_3$ administration to vitamin D-deficient mice [32]. A number of hormones or local factors, such as parathyroid hormone, arginine vasopressin, prostaglandin E_2, and calcitonin, were also found to activate TRPV5 and/or TRPV6 by raising intracellular cAMP or cGMP levels [33]. It is possible that TRPV5, TRPV6, and $Ca_v1.3$ may differentially respond to various stimuli or extracellular environments. In other words, these channels have their own unique properties and can function independently of each other. Such a hypothesis was confirmed by the present findings that neither TRPV5 nor $Ca_v1.3$ was upregulated when TRPV6 expression was suppressed by siRNA. Nevertheless, other alternative mechanisms for apical calcium entry might exist, since TRPV5/TRPV6/$Ca_v1.3$ triple KD Caco-2 monolayer still exhibited transcellular calcium flux with a magnitude comparable to that of normal monolayer. Possible alternative pathways included the vesicular transport and voltage-dependent T-type calcium channels, the latter of which was reported to mediate the testosterone-stimulated calcium transport in renal tubular epithelium [34]. Alternatively, since siRNA-induced calcium channel KD did not totally suppress mRNA expression of target calcium channels (Fig. 3d–f), it was possible that a small number of calcium channels were sufficient to allow calcium entry under a non-stimulated condition. Feedback regulation of calcium influx could also explain the unaltered basal calcium transport after triple KD, which should lead to a decrease in the intracellular calcium concentration (Ca_i). Low Ca_i has been postulated to promote activities of TRPV5 and TRPV6 channels [35, 36], thereby leading to an increase in calcium influx.

Our previous investigation provided evidence that stimulatory effect of PRL on transepithelial calcium transport was abolished by $Ca_v1.3$ KD or L-type calcium channel blockers, nifedipine and verapamil, in the apical solution, but not in the basolateral solution [9]. $Ca_v1.3$ thus appeared to be responsible for apical calcium entry in PRL-exposed intestinal epithelium [9], but participation of TRPV5 and compensatory TRPV6 upregulation after $Ca_v1.3$ KD were still possible and were not excluded experimentally. Herein, we further elucidated that only $Ca_v1.3$ was involved in the PRL-stimulated transcellular calcium transport across the intestinal epithelium. Interdependent or interactive functions of TRPV5, TRPV6, and $Ca_v1.3$ in the presence of PRL could also be ruled out because enhanced transcellular calcium transport was still observed in TRPV5/TRPV6 double KD Caco-2 monolayer.

Molecular mechanism by which PRL stimulates intestinal calcium absorption is poorly understood. Recent studies in duodenal epithelium and Caco-2 monolayer substantiated pivotal roles of phosphoinositide 3-kinase (PI3K) and protein kinase C (PKC), especially PKC_ζ isozyme, in the intracellular PRL signaling [14]. Panspecific PKC inhibitor (GF109203X) was shown to diminish the PRL-accelerated apical calcium uptake [9]. Although $Ca_v1.3$ could be phosphorylated by several PKC isozymes, e.g., $PKC_{\beta II}$ [7], it is not known whether PRL-activated PKC directly phosphorylated $Ca_v1.3$. Since Na^+ and glucose uptake through sodium-dependent glucose transporter 1 (SGLT1) at the apical membrane is coupled with $Ca_v1.3$ opening, which requires cell depolarization induced by SGLT1-mediated Na^+ entry [8, 37], it is also possible that PRL indirectly activates $Ca_v1.3$ by acting through SGLT1, known to be expressed in Caco-2 cells [38].

Besides the transcellular calcium transport, PRL could also stimulate calcium transport across the paracellular route [5]. The observed decrease in TER by PRL in the present study confirmed an increase in paracellular permeability, which could facilitate the paracellular calcium transport [9, 18, 21]. Due to its non-saturable passive nature, paracellular calcium transport could become substantial after ingestion of calcium-rich meals, or in the presence of a transepithelial calcium gradient [6]. Moreover, the presence of PRL-induced decrease in TER in TRPV5/TRPV6/$Ca_v1.3$ KD monolayer suggested that the PRL-enhanced paracellular permeability did not involve the functions of these three calcium channels, although perijunctional cytoskeletal rearrangement, an initial step to increase paracellular permeability, may be controlled, in part, by apical calcium entry [37, 39].

In conclusion, we used siRNA-based combinatorial KD technique to elucidate that the apical calcium entry step in the PRL-stimulated transcellular calcium transport in the intestine-like Caco-2 monolayer occurred solely via $Ca_v1.3$. Although intestinal epithelial cells expressed several calcium channels, i.e., TRPV5, TRPV6, and $Ca_v1.3$, there was no redundancy in their functions, at least during PRL exposure, since the PRL-stimulated calcium transport was totally diminished after $Ca_v1.3$ siRNA transfection. The present results, therefore, provided corroborative evidence for better understanding of the cellular mechanism of PRL in intestinal epithelial cells, and could explain the mechanism by which PRL stimulated intestinal calcium absorption in pregnant and lactating animals.

Acknowledgments This research was supported by grants from the Mahidol University Postdoctoral Fellowship Program (to L. Nakkrasae), the Faculty of Science, Mahidol University (SCY52-02 and SCR52-01 to N. Charoenphandhu), the Commission on Higher Education, and the Thailand Research Fund (RSA5180001 to N. Charoenphandhu, and RTA5080008 to N. Krishnamra).

Conflict of interest statement The authors declare no conflict of interest.

References

1. Boass A, Lovdal JA, Toverud SU (1992) Pregnancy- and lactation-induced changes in active intestinal calcium transport in rats. Am J Physiol Gastrointest Liver Physiol 263:G127–G134
2. Charoenphandhu N, Nakkrasae LI, Kraidith K, Teerapornpuntakit J, Thongchote K, Thongon N, Krishnamra N (2009) Two-step stimulation of intestinal Ca^{2+} absorption during lactation by long-term prolactin exposure and suckling-induced prolactin surge. Am J Physiol Endocrinol Metab 297:E609–E619
3. Krishnamra N, Taweerathitam P (1995) Acute effect of prolactin on active calcium absorption in rats. Can J Physiol Pharmacol 73:1185–1189
4. Krishnamra N, Wirunrattanakij Y, Limlomwongse L (1998) Acute effects of prolactin on passive calcium absorption in the small intestine by in vivo perfusion technique. Can J Physiol Pharmacol 76:161–168
5. Charoenphandhu N, Krishnamra N (2007) Prolactin is an important regulator of intestinal calcium transport. Can J Physiol Pharmacol 85:569–581
6. Hoenderop JG, Nilius B, Bindels RJ (2005) Calcium absorption across epithelia. Physiol Rev 85:373–422
7. Morgan EL, Mace OJ, Affleck J, Kellett GL (2007) Apical GLUT2 and $Ca_v1.3$: regulation of rat intestinal glucose and calcium absorption. J Physiol 580:593–604
8. Morgan EL, Mace OJ, Helliwell PA, Affleck J, Kellett GL (2003) A role for $Ca_v1.3$ in rat intestinal calcium absorption. Biochem Biophys Res Commun 312:487–493
9. Thongon N, Nakkrasae LI, Thongbunchoo J, Krishnamra N, Charoenphandhu N (2009) Enhancement of calcium transport in Caco-2 monolayer through PKC_ζ-dependent $Ca_v1.3$-mediated transcellular and rectifying paracellular pathways by prolactin. Am J Physiol Cell Physiol 296:C1373–C1382
10. Charoenphandhu N, Wongdee K, Teerapornpuntakit J, Thongchote K, Krishnamra N (2008) Transcriptome responses of duodenal epithelial cells to prolactin in pituitary-grafted rats. Mol Cell Endocrinol 296:41–52
11. Hoenderop JG, van Leeuwen JP, van der Eerden BC, Kersten FF, van der Kemp AW, Merillat AM, Waarsing JH, Rossier BC, Vallon V, Hummler E, Bindels RJ (2003) Renal Ca^{2+} wasting, hyperabsorption, and reduced bone thickness in mice lacking TRPV5. J Clin Invest 112:1906–1914
12. Hoenderop JG, Hartog A, Stuiver M, Doucet A, Willems PH, Bindels RJ (2000) Localization of the epithelial Ca^{2+} channel in rabbit kidney and intestine. J Am Soc Nephrol 11:1171–1178
13. Zhuang L, Peng JB, Tou L, Takanaga H, Adam RM, Hediger MA, Freeman MR (2002) Calcium-selective ion channel, CaT1, is apically localized in gastrointestinal tract epithelia and is aberrantly expressed in human malignancies. Lab Invest 82:1755–1764
14. Jantarajit W, Thongon N, Pandaranandaka J, Teerapornpuntakit J, Krishnamra N, Charoenphandhu N (2007) Prolactin-stimulated transepithelial calcium transport in duodenum and Caco-2 monolayer are mediated by the phosphoinositide 3-kinase pathway. Am J Physiol Endocrinol Metab 293:E372–E384
15. Nakane M, Ma J, Rose AE, Osinski MA, Wu-Wong JR (2007) Differential effects of vitamin D analogs on calcium transport. J Steroid Biochem Mol Biol 103:84–89
16. Yee S (1997) In vitro permeability across Caco-2 cells (colonic) can predict in vivo (small intestinal) absorption in man—fact or myth. Pharm Res 14:763–766
17. Zweibaum A, Triadou N, Kedinger M, Augeron C, Robine-Leon S, Pinto M, Rousset M, Haffen K (1983) Sucrase-isomaltase: a marker of foetal and malignant epithelial cells of the human colon. Int J Cancer 32:407–412
18. Thongon N, Nakkrasae LI, Thongbunchoo J, Krishnamra N, Charoenphandhu N (2008) Prolactin stimulates transepithelial calcium transport and modulates paracellular permselectivity in Caco-2 monolayer: mediation by PKC and ROCK pathways. Am J Physiol Cell Physiol 294:C1158–C1168
19. Irnaten M, Blanchard-Gutton N, Harvey BJ (2008) Rapid effects of 17β-estradiol on epithelial TRPV6 Ca^{2+} channel in human T84 colonic cells. Cell Calcium 44:441–452
20. Irnaten M, Blanchard-Gutton N, Praetorius J, Harvey BJ (2009) Rapid effects of 17β-estradiol on TRPV5 epithelial Ca^{2+} channels in rat renal cells. Steroids 74:642–649
21. Greger R (1996) Epithelial transport. In: Greger R, Windhorst U (eds) Comprehensive human physiology: from cellular mechanisms to integration, 1st edn. Springer, Berlin, pp 1217–1232
22. Prentice A (2000) Calcium in pregnancy and lactation. Annu Rev Nutr 20:249–272
23. Charoenphandhu N, Limlomwongse L, Krishnamra N (2006) Prolactin directly enhanced Na^+/K^+- and Ca^{2+}-ATPase activities in the duodenum of female rats. Can J Physiol Pharmacol 84:555–563
24. Hoenderop JG, Vennekens R, Muller D, Prenen J, Droogmans G, Bindels RJ, Nilius B (2001) Function and expression of the epithelial Ca^{2+} channel family: comparison of mammalian ECaC1 and 2. J Physiol 537:747–761
25. Peng JB, Chen XZ, Berger UV, Weremowicz S, Morton CC, Vassilev PM, Brown EM, Hediger MA (2000) Human calcium transport protein CaT1. Biochem Biophys Res Commun 278:326–332
26. Van Cromphaut SJ, Dewerchin M, Hoenderop JG, Stockmans I, Van Herck E, Kato S, Bindels RJ, Collen D, Carmeliet P, Bouillon R, Carmeliet G (2001) Duodenal calcium absorption in vitamin D receptor-knockout mice: functional and molecular aspects. Proc Natl Acad Sci USA 98:13324–13329
27. Benn BS, Ajibade D, Porta A, Dhawan P, Hediger M, Peng JB, Jiang Y, Oh GT, Jeung EB, Lieben L, Bouillon R, Carmeliet G, Christakos S (2008) Active intestinal calcium transport in the absence of transient receptor potential vanilloid type 6 and calbindin-D_{9k}. Endocrinology 149:3196–3205
28. Kutuzova GD, Sundersingh F, Vaughan J, Tadi BP, Ansay SE, Christakos S, DeLuca HF (2008) TRPV6 is not required for 1α, 25-dihydroxyvitamin D_3-induced intestinal calcium absorption in vivo. Proc Natl Acad Sci USA 105:19655–19659
29. Charoenphandhu N, Tudpor K, Pulsook N, Krishnamra N (2006) Chronic metabolic acidosis stimulated transcellular and solvent drag-induced calcium transport in the duodenum of female rats. Am J Physiol Gastrointest Liver Physiol 291: G446–G455
30. Van Abel M, Hoenderop JG, Dardenne O, St Arnaud R, Van Os CH, Van Leeuwen HJ, Bindels RJ (2002) 1,25-dihydroxyvitamin D_3-independent stimulatory effect of estrogen on the expression of ECaC1 in the kidney. J Am Soc Nephrol 13:2102–2109
31. Weber K, Erben RG, Rump A, Adamski J (2001) Gene structure and regulation of the murine epithelial calcium channels ECaC1 and 2. Biochem Biophys Res Commun 289:1287–1294
32. Song Y, Peng X, Porta A, Takanaga H, Peng JB, Hediger MA, Fleet JC, Christakos S (2003) Calcium transporter 1 and epithelial calcium channel messenger ribonucleic acid are differentially regulated by 1,25 dihydroxyvitamin D_3 in the intestine and kidney of mice. Endocrinology 144:3885–3894
33. den Dekker E, Hoenderop JG, Nilius B, Bindels RJ (2003) The epithelial calcium channels, TRPV5 and TRPV6: from identification towards regulation. Cell Calcium 33:497–507

34. Couchourel D, Leclerc M, Filep J, Brunette MG (2004) Testosterone enhances calcium reabsorption by the kidney. Mol Cell Endocrinol 222:71–81
35. Lambers TT, Mahieu F, Oancea E, Hoofd L, de Lange F, Mensenkamp AR, Voets T, Nilius B, Clapham DE, Hoenderop JG, Bindels RJ (2006) Calbindin-D_{28K} dynamically controls TRPV5-mediated Ca^{2+} transport. EMBO J 25:2978–2988
36. Niemeyer BA, Bergs C, Wissenbach U, Flockerzi V, Trost C (2001) Competitive regulation of CaT-like-mediated Ca^{2+} entry by protein kinase C and calmodulin. Proc Natl Acad Sci USA 98:3600–3605
37. Mace OJ, Morgan EL, Affleck JA, Lister N, Kellett GL (2007) Calcium absorption by $Ca_v1.3$ induces terminal web myosin II phosphorylation and apical GLUT2 insertion in rat intestine. J Physiol 580:605–616
38. Mahraoui L, Rodolosse A, Barbat A, Dussaulx E, Zweibaum A, Rousset M, Brot-Laroche E (1994) Presence and differential expression of SGLT1, GLUT1, GLUT2, GLUT3 and GLUT5 hexose-transporter mRNAs in Caco-2 cell clones in relation to cell growth and glucose consumption. Biochem J 298(Pt 3): 629–633
39. Pérez M, Barber A, Ponz F (1997) Modulation of intestinal paracellular permeability by intracellular mediators and cytoskeleton. Can J Physiol Pharmacol 75:287–292

CELL BIOCHEMISTRY AND FUNCTION
Cell Biochem Funct 2010; **28**: 45–51.
Published online 13 October 2009 in Wiley InterScience
(www.interscience.wiley.com) **DOI**: 10.1002/cbf.1617

Changes in the mRNA expression of osteoblast-related genes in response to β_3-adrenergic agonist in UMR106 cells†

Amporn Nuntapornsak[1‡], Kannikar Wongdee[2,3‡], Jirawan Thongbunchoo[2], Nateetip Krishnamra[1,2] and Narattaphol Charoenphandhu[1,2*]

[1]*Department of Physiology, Faculty of Science, Mahidol University, Bangkok, Thailand*
[2]*Consortium for Calcium and Bone Research (COCAB), Faculty of Science, Mahidol University, Bangkok, Thailand*
[3]*Department of Medical Science, Faculty of Science, Burapha University, Chonburi, Thailand*

Activation of adrenergic receptors (AR) was demonstrated to result in either bone gain or bone loss depending on the activated AR subtypes and concentrations of agonists used. While β_2-AR agonist was extensively investigated as an osteopenic agent, effects of β_3-AR activation on osteoblasts were still elusive. Rat osteoblast-like UMR106 cells were herein found to express several AR subtypes, including β_3-AR. After exposure to a low-dose β_3-AR agonist BRL37344 (10 nmol L^{-1}), UMR106 cells downregulated the mRNA expression of transcription factors Runx2 and Dlx5, which are important for initiation of osteoblast differentiation. Low-dose BRL37344 also decreased the expression ratio of receptor activator of nuclear factor κB ligand (RANKL) over osteoprotegerin (OPG), suggesting the protective effect of β_3-AR agonist against bone resorption. Alkaline phosphatase expression was markedly decreased, whereas expressions of osteocalcin and osteopontin were increased by 100 nmol L^{-1} BRL37344, indicating that β_3-AR activation could accelerate the transition of matrix maturation stage to mineralization stage. In conclusion, β_3-AR activation in rat osteoblasts induced alteration in the expression of osteoblast-related transcription factor genes as well as genes required for bone formation and resorption. The present results also suggest that, besides β_2-AR, β_3-AR is another AR subtype responsible for the sympathetic nervous system-induced bone remodeling. Copyright © 2009 John Wiley & Sons, Ltd.

KEY WORDS — adrenergic receptor; alkaline phosphatase; bone remodeling; osteocalcin; osteoprotegerin; real-time PCR

INTRODUCTION

Besides humoral control, bone is regulated by an autonomic neural control via nerve fibers expressing catecholamine-synthesizing enzyme tyrosine hydroxylase and neuropeptide Y.[1] The sympathetic nervous system (SNS) has recently been demonstrated to play an important role in bone metabolism, in part, by suppressing osteoblast-induced bone formation and stimulating osteoclast differentiation and multinuclearity, thereby leading to bone loss.[2–6] Several studies indicated that β_2-adrenergic receptor (AR) in osteoblasts was responsible for SNS-induced bone loss through the upregulation of receptor activator of nuclear factor κB ligand (RANKL), a key osteoblast-derived mediator for osteoclastogenesis, and the downregulation of soluble decoy receptor osteoprotegerin (OPG), which could neutralize RANKL action.[2,7] Thus, chronic administration of a low-dose non-selective β-AR antagonist propranolol (0.1 mg kg^{-1}) could lead to significant bone gain. On the other hand, β_1-AR may mediate bone formation because administration of high-dose propranolol (20 mg kg^{-1}), which was believed to inhibit β_1-AR, did not increase bone mass.[8] Moreover, activation of α_1-AR in osteoblasts was reported to enhance osteoblast proliferation as well as the expression of RANKL and OPG.[7,9] It seemed that osteoblasts differentially responded to different AR subtype activation and concentrations of agonists or antagonists.[7–9]

In addition to β_2-AR and α_1-AR, β_3-adrenergic signaling may have a role in the bone remodeling process,[10] such as modulation of osteoblast differentiation, although the direct effect of β_3-AR on osteoblasts was not known. β_3-AR transcripts are primarily expressed in adipocytes, heart, skeletal muscles, the enteric nervous system, smooth muscle of the gastrointestinal tract and in the urogenital system.[11–14] It was reported that β_3-AR transcripts were not expressed in human osteoblasts and human osteosarcoma MG-63 cells as demonstrated by conventional RT-PCR.[7] However, β_3-AR transcripts were recently demonstrated in primary mouse osteoblasts by quantitative real-time PCR (qRT-PCR),[2] It was, therefore, possible that β_3-AR was expressed in a species-specific manner. Since activation of β_3-AR could accelerate the differentiation process in several cell types, such as adipocytes,[15] changes in the expression of osteoblast-related transcription factor genes, e.g., zinc finger

* Correspondence to: N. Charoenphandhu, M.D., Ph.D., Faculty of Science, Department of Physiology, Mahidol University, Rama VI Road, Bangkok 10400, Thailand. Tel & Fax: +66-2-354-7154.
E-mail: naratt@narattsys.com
†The authors declare no conflict of interest.
‡A.N. and K.W. contributed equally to this study.

Received 1 July 2009
Revised 22 August 2009
Accepted 27 August 2009

transcription factor AJ18, *runt*-related transcription factor (Runx) 2, osterix and distal-less homeobox (Dlx) 5, and genes related to osteoblast differentiation, e.g., RANKL, OPG, alkaline phosphatase, osteocalcin, and osteopontin were anticipated.

The objectives of the present study were (i) to investigate β_3-AR expression in rat osteoblast-like UMR106 cells and rat primary osteoblasts as well as distribution of β_3-AR in rat tissues, and (ii) to demonstrate the direct effects of β_3-AR stimulation on the expression of transcription factors, RANKL/OPG ratio, and genes associated with osteoblast differentiation.

MATERIALS AND METHODS

Animals

Female Sprague-Dawley rats (8-week-old, weighing 180–200 g) were obtained from the National Animal Centre, Thailand. They were housed in hanging stainless steel cages under 12:12-h light-dark cycle, and fed regular chow (Perfect Companion, Bangkok, Thailand). Room temperature was maintained at 20–25°C and relative humidity was 50–60%. This study has been approved by the Institutional Animal Care and Use Committee (IACUC) of the Faculty of Science, Mahidol University, Bangkok, Thailand.

Cell culture

Rat osteoblast-like UMR106 cells (American Type Culture Collection [ATCC] No. CRL-1661) were cultured in 100-mm petri dish with Dulbecco's modified Eagle's medium (DMEM) (Sigma, St. Louis, MO, USA) supplemented with 10% fetal bovine serum (FBS) (PAA, Pasching, Austria), and 100 U ml^{-1} penicillin-streptomycin (Gibco, Grand Island, NY, USA). Cells were incubated at 37°C with 5% CO_2 and subcultured according to the ATCC's protocol.

Primary osteoblast culture

Under 50 mg kg^{-1} thiopental sodium i.p. anesthesia, tibiae, and femora were removed from a rat by sterile surgical technique, as previously described.[16,17] After removing the connective tissues and marrow cells, bones were cut into small dice, and cultured in a 25-cm^2 T-flask (Corning, NY, USA) with DMEM supplemented with 15% FBS, 100 U ml^{-1} penicillin-streptomycin, and 100 μg ml^{-1} ascorbate-2-phosphate (Sigma). Cells were incubated at 37°C with 5% CO_2. Osteoblasts proliferated and migrated from the bone dice into culture medium within 3 days. The medium was changed every 3 days. Confluent cells from the same rat in six flasks were pooled together for total RNA preparation.

Cell proliferation assay

UMR106 cells were incubated in 96-well culture plate (3000 cells/well). After incubation with β_3-AR agonist for 48 h, cell proliferation was determined by 5-bromo-2′-deoxy-uridine (BrdU) labeling and detection kit III (catalog no. 11444611001, Roche, Mannheim, Germany) according to the manufacturer's instruction. The absorbance of each well was determined at 405 nm with a reference wavelength of 490 nm by a microplate reader (model 1420, Wallac, Turku, Finland). Experiments were performed in triplicate.

Total RNA preparation

The total RNA samples were prepared from UMR106 cells, primary osteoblasts, omental fat, whole brain, mucosal scrapings from duodenum and jejunum, liver, kidney, lung, and heart by using TRIzol reagent (Invitrogen, Carlsbad, CA, USA). They were then treated with RQ1 RNase-free DNase (Promega, Madison, WI, USA) and subsequently purified by RNeasy mini kit (Qiagen, Valencia, CA, USA) according to the manufacturer's instructions. Purity of the total RNA was determined by the ratio of absorbance readings at 260 and 280 nm, the ratio of which was in the range of 1.8–2.0. One microgram of total RNA was reverse-transcribed with iScript cDNA Synthesis kit (Bio-Rad, Hercules, CA, USA) to cDNA by a Bio-Rad MyCycler. Rat glyceraldehyde-3-phosphate dehydrogenase (GAPDH) served as a control gene to check the consistency of the reverse transcription.

Quantitative real-time PCR (qRT-PCR) and sequencing

Primers used in the present study are shown in Table 1. qRT-PCR and melting curve analyses were performed by Bio-Rad MiniOpticon with iQ SYBR Green SuperMix (Bio-Rad) as previously described.[16,17] Conventional PCR was performed with GoTaq Green Master Mix (Promega) and Bio-Rad MyCycler. PCR products were visualized on 2% agarose gel stained with 1 μg ml^{-1} ethidium bromide (Sigma) under UV transilluminator (Alpha Innotech, San Leandro, USA). After electrophoresis, all PCR products were extracted by HiYield Gel/PCR DNA Extraction kit (Real Biotech Corporation, Taipei, Taiwan), and were sequenced by ABI Prism 3100 Genetic Analyzer (Applied Biosystems, Foster City, CA, USA). PCR experiments were performed in triplicate.

Experimental protocol

UMR106 cells, primary osteoblasts, omental fat, whole brain, duodenal, and jejunal epithelial cells, liver, kidney, lung, and heart were first investigated for β_3-AR expression by using conventional RT-PCR. Other AR subtypes, including α_1, α_2, β_1, and β_2, were also studied in UMR106 cells. In some experiments, confluent UMR106 cells were incubated with normal medium (control, 0 nmol L^{-1} BRL37344) or medium containing various concentrations of 10, 100, and 1000 nmol L^{-1} BRL37344 (Sigma), a selective β_3-AR agonist, for 48 h prior to determination of osteoblast gene expression. Since it was reported that the half maximal effective concentrations (EC50) of BRL37344 for lipolysis in rat adipose tissues and relaxation of the rat distal colon were between 3.3–27.5 nmol L^{-1},[18] the lowest BRL37344 concentration used in the present study should fall within this range, i.e., 10 nmol L^{-1}. Expressions of AJ18, Runx2, osterix,

DOI: 10.1002/cbf

Table 1. *Rattus norvegicus* oligonucleotide sequences used in the PCR experiments

Gene	Accession no.	Primer (forward/reverse)	Product length (bp)
Adrenergic receptor (AR) genes			
α_{1b}-AR	NM_016991	5′–ATGAATCCCGATCTGGACAC–3′ 5′–CACGATGGCAAAGAGGATG–3′	183
α_{1d}-AR	NM_024483	5′–CGGGCCTTACTGTTTACACTG–3′ 5′–GGACAGTTTGCACAGTCTGAAC–3′	164
α_{2a}-AR	NM_012739	5′–TGCTCATGCTGTTCACCGT–3′ 5′–ACCAGTAGCCCATAACCTCGT–3′	174
α_{2b}-AR	NM_138505	5′–AGCAGTGGGACAACTTGGAA–3′ 5′–TGCAGATGGCTCTGAAGCA–3′	155
α_{2c}-AR	NM_138506	5′–TGGTGGGTTTCCTCATCGT–3′ 5′–GAAAAGGGCATGACCAGTGT–3′	154
β_1-AR	NM_012701	5′–CATCGTGCTGCTCATCGTA–3′ 5′–CACAGAAGAAGGAGCCGTACT–3′	194
β_2-AR	NM_012492	5′–AGCCACCTACGGTCTCTGAAT–3′ 5′–AAGTCGCTGTCATTCCCGT–3′	150
β_3-AR	NM_013108	5′–CCACCACCACCCTGCTTATTA–3′ 5′–TGGGAACACAGAACCTGGAGA–3′	145
Osteoblast-related genes			
AJ18	AF321874	5′–GTCCCTGGTATGTATCAC–3′ 5′–GAAGACTTTGGCTAAAAC–3′	133
Dlx5	NM_012943	5′–CTCTCTAGGACTGACGCAAAC–3′ 5′–GAGTTACACGCCATAGGGTC–3′	135
Osterix	AY177399	5′–GCCTACTTACCCGTCTGA–3′ 5′–CTCCAGTTGCCCACTATT–3′	139
Runx2	XM_001066909	5′–TAACGGTCTTCACAAATCCTC–3′ 5′–GGCGGTCAGAGAACAAACTA–3′	135
Alkaline phosphatase	NM_013059	5′–GCAGGATCGGAACGTCAAT–3′ 5′–ATGAGTTGGTAAGGCAGGGTC–3′	144
Osteocalcin	J04500	5′–CACAGGGAGGTGTGTGAG–3′ 5′–TGTGCCGTCCATACTTTC–3′	203
Osteopontin	NM_012881	5′–TTCACTGCCAGCACACAA–3′ 5′–TTTGACCTCAGTCCGTAAGC–3′	101
OPG	NM_012870	5′–ATTGGCTGAGTGTTCTGGT–3′ 5′–CTGGTCTCTGTTTTGATGC–3′	140
RANKL	NM_057149	5′–TCGCTCTGTTCCTGTACT–3′ 5′–AGTGCTTCTGTGTCTTCG–3′	145
Housekeeping gene			
GAPDH	NM_017008	5′–AGTCTACTGGCGTCTTCAC–3′ 5′–TCATATTTCTCGTGGTTCAC–3′	133

Dlx5, RANKL, OPG, alkaline phosphatase, osteocalcin, osteopontin were determined by qRT-PCR. The effect of β_3-agonist on cell proliferation was determined by BrdU cell proliferation assay.

Statistical analysis

The results are expressed as means ± SE or log means ± SE. Statistical analysis was performed by Mann–Whitney nonparametric test. The level of significance was $p < 0.05$. Data were analyzed by GraphPad Prism 5 (GraphPad Software, San Diego, CA, USA).

RESULTS

Expression of β_3-AR transcripts in UMR106 cells and rat tissues

As shown in Figure 1A, UMR106 cells strongly expressed several osteoblast differentiation markers, including AJ18, Runx2, osterix and Dlx5, indicating that UMR106 cells used in the present study were differentiated osteoblasts as reported previously.[16,17] These cells also expressed a number of AR subtypes, i.e., α_{1b}, α_{1d}, α_{2a}, α_{2b}, α_{2c}, β_1, β_2, and β_3 (Figure 1B). Expression of β_2-AR, which has

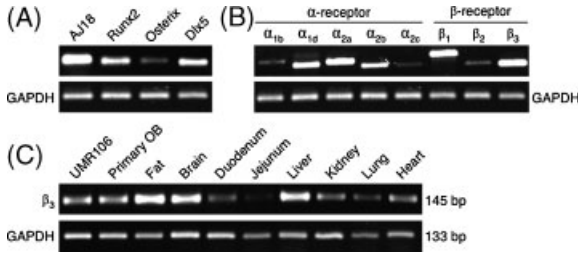

Figure 1. (A) Representative electrophoretic bands of osteoblast-related transcription factors AJ18, Runx2, osterix and Dlx5 in osteoblast-like UMR106 cells ($n = 5$). (B) Expression profile of adrenergic receptor (AR) subtypes in UMR106 cells ($n = 5$). (C) β_3-AR expression in UMR106 cells, primary osteoblasts (OB) and various tissues of normal rats, i.e., omental fat, brain, duodenal, and jejunal epithelial cells, liver, kidney, lung, and heart ($n = 5$ each). Expression of GAPDH, a housekeeping gene, was presented along with the studied genes. All PCR products were collected at 36 cycles

DOI: 10.1002/cbf

been thought to be the principal AR in osteoblasts, was much weaker than that of β_3-AR. Intense β_3-AR expression in UMR106 cells suggested that, in addition to β_2-AR,[2,7] β_3-AR mediated adrenergic signaling to modulate osteoblast functions. Moreover, β_3-AR was also found in primary rat osteoblasts as well as in adipose tissue, brain, duodenal, and jejunal epithelial cells, liver, kidney, lung, and heart (Figure 1C). Sequencing of PCR products confirmed the specificity of PCR reaction.

Effect of β_3-AR agonist on RANKL/OPG ratio

Since activation of SNS could alter bone remodeling, perhaps by changing the ratio of RANKL/OPG expression,[7] mRNA expressions of RANKL and OPG were determined in this study. Herein, we first demonstrated that 10–1000 nmol L^{-1} BRL37344, a selective β_3-AR agonist, did not affect GAPDH mRNA expression (data not shown) or cell proliferation (Figure 2). Expressions of all studied genes were thus normalized by GAPDH expression. Low-dose BRL37344 (10 nmol L^{-1}) significantly downregulated RANKL mRNA expression (Figure 3A) by 58%, without effect on OPG expression (Figure 3B), thereby leading to a decrease in RANKL/OPG ratio by 47% (Figure 3C). On the other hand, high-dose BRL37344 (1000 nmol L^{-1}) downregulated OPG expression (Figure 3B) by 31%, but had no effect on RANKL expression or RANKL/OPG ratio. A decrease in RANKL/OPG ratio by low-dose BRL37344 suggested a β_3-AR activation-induced suppression of bone resorption. Such BRL37344 actions were observed after 48 h, but not 24 h of incubation (data not shown).

Effects of β_3-AR agonist on osteoblast-related transcription factor expression

Four transcription factors, namely AJ18, Runx2, osterix and Dlx5 (Figures 1A and 4), are important for the initial step of osteoblast differentiation.[19,20] After 48 h exposure to low-dose BRL37344 (10 nmol L^{-1}), expressions of Runx2 (Figure 4B) and Dlx5 (Figure 4D), but not AJ18 (Figure 4A) and osterix (Figure 4C), were markedly decreased by 69% and 82%, respectively. In contrast, moderate-dose BRL37344 (100 nmol L^{-1}) significantly upregulated expressions of AJ18 (Figure 4A), osterix (Figure 4C) and Dlx5 (Figure 4D) by 6.26-, 5.96- and 2.11-fold, respectively. Although high-dose BRL37344 (1000 nmol L^{-1}) was without effect on the expression of AJ18, Runx2 and osterix, it could induce a 50% decrease in Dlx5 expression (Figure 4D). The results indicated that β_3-AR agonist modulated expression of these transcription factors in a complex dose-dependent manner.

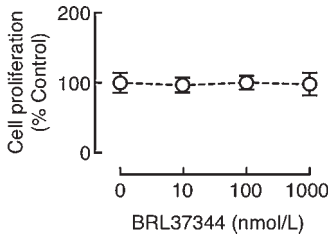

Figure 2. Proliferation of UMR106 cells after exposure for 48 h to 10, 100, and 1000 nmol L^{-1} BRL37344 ($n = 5$ per group). Cell proliferation was determined by 5-bromo-2′-deoxy-uridine (BrdU) labeling assay

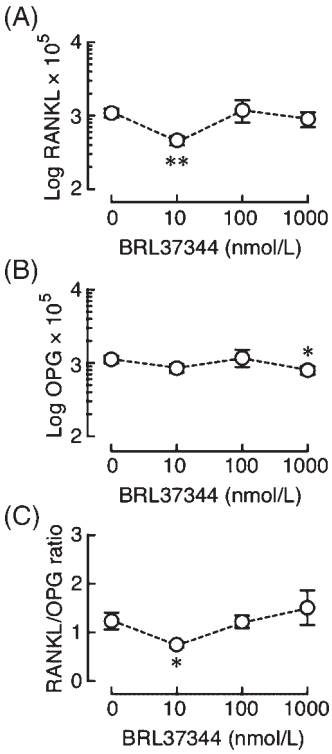

Figure 3. Expression of (A) RANKL, (B) OPG, and (C) RANKL/OPG ratio in UMR106 cells incubated for 48 h with 10, 100, and 1000 nmol L^{-1} BRL37344 ($n = 5$ per group). Expression of each studied gene was normalized by GAPDH mRNA expression. * $p < 0.05$, ** $p < 0.01$ compared with the control group (0 nmol L^{-1} BRL37344)

Effects of β_3-AR agonist on the mRNA expression of alkaline phosphatase, osteocalcin, and osteopontin

Under normal conditions, alkaline phosphatase is markedly expressed during the matrix maturation stage (early differentiation), while osteocalcin and osteopontin are expressed at the matrix mineralization stage (late differentiation).[21,22] After 48 h exposure to 10, 100, or 1000 nmol L^{-1} BRL37344, alkaline phosphatase expression was downregulated by 69%, 75% and 89%, respectively, in a dose-response manner (Figure 4E). However, 10 or 100 nmol L^{-1} BRL37344 upregulated osteocalcin expression by 65% and 311%, respectively (Figure 4F), while only 100 nmol L^{-1} BRL37344 induced a ~10-fold increase in osteopontin expression (Figure 4G). These results suggested that β_3-AR activation in rat osteoblasts might shift the differentiation stage from matrix maturation phase toward the matrix mineralization phase.

DOI: 10.1002/cbf

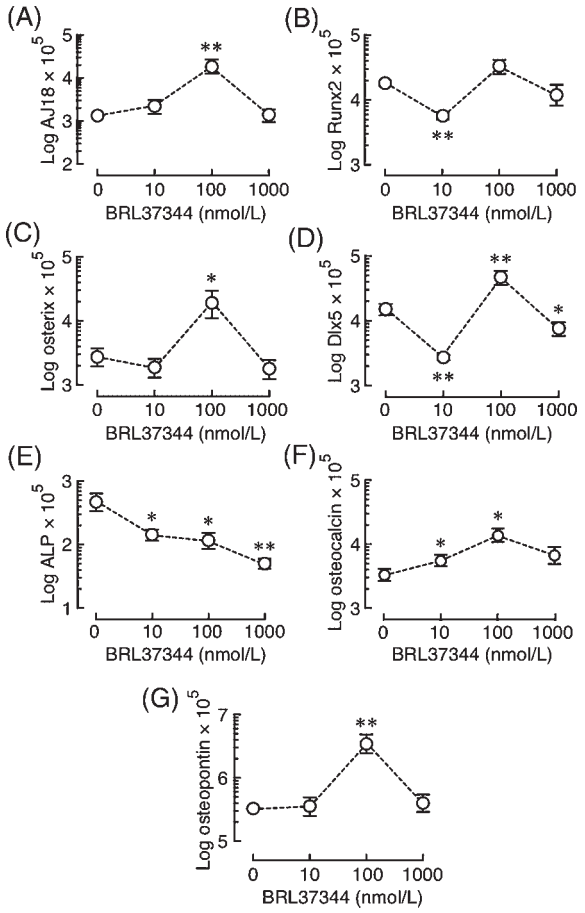

Figure 4. Expression of (A) AJ18, (B) Runx2, (C) osterix, (D) Dlx5, (E) alkaline phosphatase (ALP), (F) osteocalcin, and (G) osteopontin in UMR106 cells incubated for 48 h with 10, 100, and 1000 nmol L^{-1} BRL37344 ($n = 5$ per group). Expression of each studied gene was normalized by GAPDH mRNA expression. * $p < 0.05$, ** $p < 0.01$ compared with the control group (0 nmol L^{-1} BRL37344)

DISCUSSION

β-adrenergic system has recently been postulated to be a part of the SNS-mediated bone turnover.[2,10,23] β-AR is classified into three subtypes, namely β_1-AR, β_2-AR, and β_3-AR. β_2-AR appears to be upstream in the adrenergic signaling controlling bone remodeling.[2,7,23–25] However, the SNS-mediated bone turnover was also regulated through other AR subtypes, such as α_1-AR.[7,9] Herein, we provided further evidence that activation of β_3-AR could modulate expression of several genes related to osteoblast functions and bone remodeling in osteoblast-like UMR106 cells.

β_3-AR is a member of G-protein-coupled receptor family and is expressed in adipocytes, heart, skeletal muscles, bone marrow mesenchymal stem cells, enteric nervous system, smooth muscle of the gastrointestinal tract, and urogenital system.[11–14,25] By using conventional PCR, β_3-AR mRNA was found to be constitutively expressed in both UMR106 cells and rat primary osteoblasts, consistent with the previous report in mouse primary osteoblasts.[2] However, β_3-AR transcripts were not detected by conventional PCR in some human osteoblast-like cell lines, e.g., TE-85, SaOS-2, MG-63, and OHS-4.[26] It was possible that β_3-AR was expressed in human osteoblasts but at a relatively low level, which was not detected by the conventional PCR. Alternatively, β_3-AR expression may be restricted only to rodents.

Expressions of several osteoblast-related genes were altered by β_3-AR agonist. Alkaline phosphatase expression was downregulated in BRL37344-exposed osteoblasts. Although alkaline phosphatase is a generic marker of differentiated osteoblasts, its expression depends on the stage of osteoblast differentiation.[22] Osteoblast development generally proceeds through three distinct molecular events, i.e., cell proliferation, matrix maturation (early differentiation), and mineralization (late differentiation),[22,27,28] each of which requires different sets of stimulatory factors. Factors that enhance development in one stage may be inhibitory in the others. For example, fibroblast growth factor-8 which strongly stimulated osteoblast proliferation, was found to suppress osteoblast differentiation.[29] Normally, a decline in cell proliferation is accompanied by an increase in alkaline phosphatase, a marker of matrix maturation phase. In the last stage, mineralization was indicated by increases in osteocalcin and osteopontin expression.[21,22] Therefore, downregulation of alkaline phosphatase with upregulation of osteocalcin and osteopontin by 10–100 nmol L^{-1} BRL37344 suggested that β_3-AR activation accelerated the phase transition from matrix maturation to the mineralization stage of osteoblast differentiation.

Osteoblast differentiation was generally regulated by several osteoblast-specific transcription factors.[19,20] In the present study, β_3-AR activation altered the expressions of Runx2, Dlx5, AJ18, and osterix, all of which are important for commitment of osteoblast lineage.[19] Runx2 induces proliferation of the mesenchymal stem cells,[30,31] and initiates differentiation of those cells to pre-osteoblasts (early differentiation stage),[19,28] but it was also reported to inhibit the late differentiation stage.[30] Dlx5 is a bone-inducing transcription factor that acts as a transcriptional activator of Runx2 expression. Thus, a decrease in Runx2 expression (Figure 4B), which may have resulted from a low-dose β_3-AR agonist-induced downregulation of Dlx5 (Figure 4D), would lead to suppression of osteoblast differentiation. In contrast, both Dlx5 and AJ18 were upregulated by higher concentration of β_3-AR agonist (100 nmol L^{-1}). Since Runx2 expression can be suppressed by AJ18,[19,20] concurrent upregulation of AJ18 and Dlx5 resulted in no change in Runx2 expression. In addition, expression of osterix which induced osteoblast differentiation but inhibited proliferation,[32,33] was also upregulated by a moderate dose of β_3-AR agonist. Taken together, we speculated that β_3-AR activation triggered the transition of proliferating pre-osteoblasts to the early differentiation stage, and accelerated differentiation of immature osteoblasts into mature osteoblasts. The absence of change in osteoblast proliferation (Figure 2) agreed with our

DOI: 10.1002/cbf

hypothesis that β_3-AR activation predominantly affected osteoblast differentiation, and not proliferation.

Regarding bone remodeling regulators RANKL and OPG,[34] in contrast to β_2-AR which has been known to increase RANKL/OPG ratio,[2,7] β_3-AR activation by low-dose BRL37344 decreased the expression ratio of RANKL/OPG. Thus, β_3-AR activation may help prevent bone resorption and slow down bone turnover. However, it was not known as to why the high-dose β_3-AR agonist did not alter the RANKL/OPG ratio, but the results suggested that osteoblast responses to the β_3-AR agonist may be biphasic. Bonnet *et al*.[8] investigated the dose-dependent effects of β-blocker propranolol on trabecular and cortical bone of ovariectomized rats and found that, at low doses, propranolol exhibited a protective effect on trabecular and cortical bones, but such effect disappeared at higher doses. Hence, the biphasic action of AR agonists and antagonists may not be uncommon; however, the underlying mechanism remains to be investigated.

In conclusion, the present investigation provided evidence that rat osteoblast-like UMR106 cells and primary rat osteoblasts, known to be target cells of the SNS, strongly expressed β_3-AR. β_3-AR activation was likely to direct proliferating pre-osteoblasts toward the differentiation process since the β_3-AR agonist induced downregulation of Runx2, which was important for proliferation of osteoblast progenitors,[30,31] and upregulation of several osteoblast differentiation markers, e.g., osterix, osteocalcin, and osteopontin.[19,21,22] Furthermore, the low-dose β_3-AR agonist may have a protective effect against bone resorption as indicated by a decrease in the RANKL/OPG expression ratio. Although this study was performed at the transcriptional level, the findings suggested the significance of the β_3-AR system in the regulation of osteoblast function and bone remodeling. However, further investigations are required to demonstrate the molecular mechanisms of β_3-AR in osteoblasts as well as the effects of β_3-AR activation on bone metabolism *in vivo*.

ACKNOWLEDGEMENTS

The authors thank Dr. Jantarima Pandaranandaka for helpful discussion, and Kanogwun Thongchote for excellent technical assistance. This research was supported by grants from the Faculty of Science, Mahidol University (SCR52-01 to N. Charoenphandhu), the Commission on Higher Education, and the Thailand Research Fund (RTA5080008 to N. Krishnamra).

REFERENCES

1. Serre CM, Farlay D, Delmas PD, Chenu C. Evidence for a dense and intimate innervation of the bone tissue, including glutamate-containing fibers. *Bone* 1999; **25**: 623–629.
2. Aitken SJ, Landao-Bassonga E, Ralston SH, Idris AI. β_2-Adrenoreceptor ligands regulate osteoclast differentiation *in vitro* by direct and indirect mechanisms. *Arch Biochem Biophys* 2009; **482**: 96–103.
3. Elefteriou F. Regulation of bone remodeling by the central and peripheral nervous system. *Arch Biochem Biophys* 2008; **473**: 231–236.
4. Pierroz DD, Bouxsein ML, Rizzoli R, Ferrari SL. Combined treatment with a β-blocker and intermittent PTH improves bone mass and microarchitecture in ovariectomized mice. *Bone* 2006; **39**: 260–267.
5. Takeuchi T, Tsuboi T, Arai M, Togari A. Adrenergic stimulation of osteoclastogenesis mediated by expression of osteoclast differentiation factor in MC3T3-E1 osteoblast-like cells. *Biochem Pharmacol* 2001; **61**: 579–586.
6. Yirmiya R, Goshen I, Bajayo A, *et al*. Depression induces bone loss through stimulation of the sympathetic nervous system. *Proc Natl Acad Sci USA* 2006; **103**: 16876–16881.
7. Huang HH, Brennan TC, Muir MM, Mason RS. Functional α_1- and β_2-adrenergic receptors in human osteoblasts. *J Cell Physiol* 2009; **220**: 267–275.
8. Bonnet N, Laroche N, Vico L, Dolleans E, Benhamou CL, Courteix D. Dose effects of propranolol on cancellous and cortical bone in ovariectomized adult rats. *J Pharmacol Exp Ther* 2006; **318**: 1118–1127.
9. Nishiura T, Abe K. α_1-Adrenergic receptor stimulation induces the expression of receptor activator of nuclear factor κB ligand gene via protein kinase C and extracellular signal-regulated kinase pathways in MC3T3-E1 osteoblast-like cells. *Arch Oral Biol* 2007; **52**: 778–785.
10. Bouxsein ML, Devlin MJ, Glatt V, Dhillon H, Pierroz DD, Ferrari SL. Mice lacking β-adrenergic receptors have increased bone mass but are not protected from deleterious skeletal effects of ovariectomy. *Endocrinology* 2009; **150**: 144–152.
11. Berkowitz DE, Nardone NA, Smiley RM, *et al*. Distribution of β_3-adrenoceptor mRNA in human tissues. *Eur J Pharmacol* 1995; **289**: 223–228.
12. Cellek S, Thangiah R, Bassil AK, *et al*. Demonstration of functional neuronal β_3-adrenoceptors within the enteric nervous system. *Gastroenterology* 2007; **133**: 175–183.
13. Chamberlain PD, Jennings KH, Paul F, *et al*. The tissue distribution of the human β_3-adrenoceptor studied using a monoclonal antibody: direct evidence of the β_3-adrenoceptor in human adipose tissue, atrium and skeletal muscle. *Int J Obes Relat Metab Disord* 1999; **23**: 1057–1065.
14. Roberts SJ, Papaioannou M, Evans BA, Summers RJ. Functional and molecular evidence for β_1-, β_2- and β_3-adrenoceptors in human colon. *Br J Pharmacol* 1997; **120**: 1527–1535.
15. Dallner OS, Chernogubova E, Brolinson KA, Bengtsson T. β_3-adrenergic receptors stimulate glucose uptake in brown adipocytes by two mechanisms independently of glucose transporter 4 translocation. *Endocrinology* 2006; **147**: 5730–5739.
16. Charoenphandhu N, Teerapornpuntakit J, Methawasin M, Wongdee K, Thongchote K, Krishnamra N. Prolactin decreases expression of Runx2, osteoprotegerin, and RANKL in primary osteoblasts derived from tibiae of adult female rats. *Can J Physiol Pharmacol* 2008; **86**: 240–248.
17. Wongdee K, Pandaranandaka J, Teerapornpuntakit J, *et al*. Osteoblasts express claudins and tight junction associated proteins. *Histochem Cell Biol* 2008; **130**: 79–90.
18. Oriowo MA, Chapman H, Kirkham DM, Sennitt MV, Ruffolo RR Jr, Cawthorne MA. The selectivity *in vitro* of the stereoisomers of the β_3-adrenoceptor agonist BRL 37344. *J Pharmacol Exp Ther* 1996; **277**: 22–27.
19. Komori T. Regulation of osteoblast differentiation by transcription factors. *J Cell Biochem* 2006; **99**: 1233–1239.
20. Lee MH, Kim YJ, Yoon WJ, *et al*. Dlx5 specifically regulates Runx2 type II expression by binding to homeodomain-response elements in the *Runx2* distal promoter. *J Biol Chem* 2005; **280**: 35579–35587.
21. Jung C, Ou YC, Yeung F, Frierson HF Jr, Kao C. Osteocalcin is incompletely spliced in non-osseous tissues. *Gene* 2001; **271**: 143–150.
22. Owen TA, Aronow M, Shalhoub V, *et al*. Progressive development of the rat osteoblast phenotype in vitro: reciprocal relationships in expression of genes associated with osteoblast proliferation and differentiation during formation of the bone extracellular matrix. *J Cell Physiol* 1990; **143**: 420–430.
23. Bonnet N, Pierroz DD, Ferrari SL. Adrenergic control of bone remodeling and its implications for the treatment of osteoporosis. *J Musculoskelet Neuronal Interact* 2008; **8**: 94–104.

DOI: 10.1002/cbf

24. Bonnet N, Benhamou CL, Malaval L, *et al*. Low dose β-blocker prevents ovariectomy-induced bone loss in rats without affecting heart functions. *J Cell Physiol* 2008; **217**: 819–827.
25. Takahata Y, Takarada T, Iemata M, *et al*. Functional expression of β_2 adrenergic receptors responsible for protection against oxidative stress through promotion of glutathione synthesis after Nrf2 upregulation in undifferentiated mesenchymal C3H10T1/2 stem cells. *J Cell Physiol* 2009; **218**: 268–275.
26. Kellenberger S, Muller K, Richener H, Bilbe G. Formoterol and isoproterenol induce c-*fos* gene expression in osteoblast-like cells by activating β_2-adrenergic receptors. *Bone* 1998; **22**: 471–478.
27. Datta HK, Ng WF, Walker JA, Tuck SP, Varanasi SS. The cell biology of bone metabolism. *J Clin Pathol* 2008; **61**: 577–587.
28. Ducy P, Schinke T, Karsenty G. The osteoblast: a sophisticated fibroblast under central surveillance. *Science* 2000; **289**: 1501–1504.
29. Lin JM, Callon KE, Lin JS, *et al*. Actions of fibroblast growth factor-8 in bone cells in vitro. *Am J Physiol Endocrinol Metab* 2009; **297**: E142–E150.
30. Liu W, Toyosawa S, Furuichi T, *et al*. Overexpression of Cbfa1 in osteoblasts inhibits osteoblast maturation and causes osteopenia with multiple fractures. *J Cell Biol* 2001; **155**: 157–166.
31. Schroeder TM, Jensen ED, Westendorf JJ. Runx2: a master organizer of gene transcription in developing and maturing osteoblasts. *Birth Defects Res C Embryo Today* 2005; **75**: 213–225.
32. Cao Y, Zhou Z, de Crombrugghe B, *et al*. Osterix, a transcription factor for osteoblast differentiation, mediates antitumor activity in murine osteosarcoma. *Cancer Res* 2005; **65**: 1124–1128.
33. Nakashima K, Zhou X, Kunkel G, *et al*. The novel zinc finger-containing transcription factor osterix is required for osteoblast differentiation and bone formation. *Cell* 2002; **108**: 17–29.
34. Fazzalari NL, Kuliwaba JS, Atkins GJ, Forwood MR, Findlay DM. The ratio of messenger RNA levels of receptor activator of nuclear factor κB ligand to osteoprotegerin correlates with bone remodeling indices in normal human cancellous bone but not in osteoarthritis. *J Bone Miner Res* 2001; **16**: 1015–1027.

DOI: 10.1002/cbf

J Physiol Sci (2010) 60:1–8
DOI 10.1007/s12576-009-0059-1

ORIGINAL PAPER

Femoral bone mineral density and bone mineral content in bromocriptine-treated pregnant and lactating rats

Panan Suntornsaratoon · Kannikar Wongdee · Nateetip Krishnamra · Narattaphol Charoenphandhu

Received: 13 February 2009 / Accepted: 6 August 2009 / Published online: 17 September 2009

Abstract Since hyperprolactinemia was found to induce osteopenia in the metaphysis of long bone in non-mated female rats, pregnant and lactating rats with sustainedly high plasma prolactin (PRL) levels might also exhibit some changes in their long bones. We performed a longitudinal study in pregnant, lactating and post-weaning rats, using dual-energy X-ray absorptiometry to demonstrate site-specific changes (i.e., metaphysis vs. diaphysis) in femoral bone mineral density (BMD) and content (BMC). The results showed that femoral metaphyseal BMD and BMC were higher when compared to their age-matched controls during pregnancy, before decreasing in late lactation and post-weaning. On the other hand, femoral diaphyseal BMC increased during pregnancy, early lactating and mid-lactating periods without change during late lactation and post-weaning. After 7 days of bromocriptine administration which inhibited endogenous PRL secretion, the lactation-induced increases in BMC during early and mid-lactating periods were abolished. Moreover, a decrease in metaphyseal BMD during late lactation was restored to the control levels by bromocriptine. However, bromocriptine did not antagonize the pregnancy-induced increases in BMD and BMC. It could be concluded that the effect of PRL on bone was variable during the reproductive periods. While having no effect on femoral BMD and BMC during pregnancy, PRL was responsible for bone gain in early and mid-lactating periods, but induced bone loss during late lactating period.

Keywords Bone density · Dual-energy X-ray absorptiometry (DXA) · Femur · Lactation · Pregnancy

P. Suntornsaratoon · N. Krishnamra · N. Charoenphandhu (✉)
Department of Physiology, Faculty of Science,
Mahidol University, Rama VI Road,
Bangkok 10400, Thailand
e-mail: naratt@narattsys.com

K. Wongdee
Department of Medical Science, Faculty of Science,
Burapha University, Chonburi 20131, Thailand

P. Suntornsaratoon · K. Wongdee · N. Krishnamra · N. Charoenphandhu
Consortium for Calcium and Bone Research (COCAB),
Faculty of Science, Mahidol University, Rama VI Road,
Bangkok 10400, Thailand

Introduction

Previous investigations in non-mated female rats demonstrated that short-term exposure to high plasma prolactin (PRL) levels induced by 4 weeks of anterior pituitary transplantation (AP) led to net bone gain, while prolonged PRL exposure longer than 4 weeks gradually led to net bone loss [1, 2]. Such hyperprolactinemic effects appeared to be observed primarily at the trabecular sites, e.g., vertebrae and sternum, but not the cortical sites, e.g., tibiae and femora [3, 4]. However, by using dual-energy X-ray absorptiometric (DXA) analysis on specific regions of rat femur, we found that prolactin could decrease bone mineral density (BMD) and content (BMC) of the femoral metaphysis, which was predominantly trabecular bone, but not diaphysis which was predominantly cortical bone [5]. Thus, it was possible that elevated plasma PRL levels during pregnancy (~75–100 ng/mL) and lactation (~200–300 ng/mL), i.e., physiological hyperprolactinemia, could alter BMD and BMC of the long bone.

Reports on site-specific changes in BMD and BMC (metaphysis vs. diaphysis) of long bone during pregnancy and lactation in rats were controversial. Zeni and co-workers

[6] reported that in situ BMDs of the proximal and distal tibiae were not changed on the first day postpartum, but were decreased at the end of lactation. Similarly, single-photon absorptiometric analysis revealed greater lactation-induced bone loss in the femoral metaphysis than in the diaphysis [7]. However, densitometric changes at mid-pregnancy and mid-lactation, which have high rates of maternal calcium loss, were presently not known. Nishiwaki and co-workers [8] demonstrated decreases in BMDs in the distal femur, lumbar spine and caudal spine (i.e., trabecular sites) at week 2–3 of lactation, but changes in cortical BMDs were not studied. Thus, a complete longitudinal densitometric study was first performed to demonstrate changes in site-specific femoral BMD and BMC during these reproductive periods.

To investigate the effects of endogenous PRL on BMD and BMC during pregnancy and lactation, an inhibitor of pituitary PRL secretion, bromocriptine, was administered to the animals. Bromocriptine is a dopaminergic D2 receptor agonist which mimics the hypothalamic PRL-inhibitory factor dopamine, thereby suppressing PRL release from the pituitary lactotrophs [9, 10]. Since osteoblasts were found to directly respond to several monoamines, e.g., serotonergic and adrenergic agonists [11], expression of D2 receptors, which have two isoforms known as long and short isoforms, was also determined to exclude possible direct actions of bromocriptine on osteoblasts.

Materials and methods

Animals

Non-mated (nulliparous) and pregnant (primiparous) Sprague–Dawley rats (8-week-old, weighing 210–220 g), were obtained from the Animal Centre of Thailand, Salaya, Thailand. They were placed in hanging stainless steel cages, fed standard chow containing 1% w/w calcium and 4,000 IU/kg vitamin D (Perfect Companion, Bangkok, Thailand), and distilled water ad libitum under 12:12 h light:dark cycle. Room temperature was controlled at 23–25°C, and the relative humidity was about 50–60%. Body weight and food intake were recorded daily. After delivery, the litter size was adjusted to eight pups per dam. Animals were cared for in accordance with the "Guiding Principles for the Care and Use of Animals in the Field of Physiological Sciences". This study has been approved by the Institutional Animal Care and Use Committee (IACUC) of the Faculty of Science, Mahidol University.

Experimental design

Rats were divided into 6 groups, i.e., 14-day pregnancy (P14; mid-pregnancy), 21-day pregnancy (P21; late pregnancy), 8-day lactation (L8; early lactation), 14-day lactation (L14; mid-lactation), 21-day lactation (L21; late lactation), and 15-day post-weaning (PW), with ages of 10, 11, 12, 13, 14, and 16 weeks, respectively. In some experiments, prior to the removal of femora, pregnant and lactating rats were administered for 7 days with 4 mg/kg per day bromocriptine s.c., which have been known to diminish plasma PRL in pregnant and lactating rats [1, 9]. Thus, each group consisted of vehicle-treated mated (pregnant or lactating) rats, bromocriptine-treated mated rats, and vehicle-treated age-matched non-mated control rats. Bromocriptine (Sigma, St. Louis, MO, USA) was first dissolved in a mixture (vehicle) of tartaric acid, absolute ethanol, and normal saline, as described previously [12]. After the rats were killed, BMD and BMC of proximal metaphysis, distal metaphysis (trabecular sites), and diaphysis (cortical site) of the femur were determined.

Primary osteoblast culture

As described previously [13], tibiae were dissected from a 9-week-old non-mated female rat by sterile surgical technique. After removing the connective tissues and marrow cells, the bones were cut into small dice, and incubated on a shaker (60 cycles/min) for 2 h at 37°C in a 25-cm^2 T-flask (Corning, NY, USA) containing DMEM supplemented with 100 U/mL penicillin/streptomycin and 2 mg/mL collagenase (all purchased from Sigma). Thereafter, bone dice were washed with DMEM, and then cultured in DMEM supplemented with 15% FBS, 100 U/mL penicillin/streptomycin, 100 μg/mL ascorbate-2-phosphate, and 0.5 mM sodium pyruvate (Sigma) at 37°C with 5% CO_2. Osteoblasts proliferated and migrated from bone dice into the media within 3 days. Media were changed daily until day 20 for expression study. Rat osteoblast-like UMR-106 cells [American Type Culture Collection (ATCC) no. CRL-1661] were cultured as described by the ATCC's instruction.

Polymerase chain reaction (PCR) and sequencing

Total RNA was prepared from primary rat osteoblasts, UMR-106 cells, pituitary glands, gastrocnemius muscle (negative control), and brain (positive control) using TRIzol reagent (Invitrogen, Carlsbad, CA, USA), and purified with RNeasy Mini kit (Qiagen, Valencia, CA, USA). 1 μg of the total RNA was reverse-transcribed with oligo-dT_{20} primer and iScript kit (Bio-Rad, Hercules, CA, USA). Glyceraldehyde-3-phosphate dehydrogenase (GAPDH), a housekeeping gene, served as a control gene to check the consistency of reverse transcription. Conventional PCR was performed for 36 cycles with the GoTaq Green Master Mix (Promega, Madison, WI, USA) and Bio-rad

MyCycler. Oligonucleotide sequences used as primers were 5′-CAGTCGAGCTTTCAGAGCCAA-3′ and 5′-TCC ATTCTCCGCCTGTTCA-3′ for long isoform of rat D2 receptor (amplicon 129 bp), 5′-TATGGCTTGAAGAG CCGTG-3′ and 5′-TGTCTGCCTTCCCTTCTGA-3′ for short isoform of rat D2 receptor (amplicon 134 bp), and 5′-AGTCTACTGGCGTCTTCAC-3′ and 5′-TCATATTTC TCGTGGTTCAC-3′ for GAPDH (amplicon 133 bp). PCR products were visualized on a 1.5% agarose gel stained with 1.0 μg/mL ethidium bromide under a UV transilluminator (Alpha Innotech, San Leandro, CA, USA). After electrophoresis, PCR products were purified by the HiYield Gel/PCR DNA Extraction kit (Real Biotech Corporation, Taipei, Taiwan), and were sequenced by the ABI Prism 3100 Genetic Analyzer (Applied Biosystems, Foster City, CA, USA).

BMD and BMC measurements

Site-specific BMD and BMC were determined by the modified methods of Binkley et al. [14] and Thongchote et al. [5]. Femora of pregnant and lactating rats were removed and cleaned of adhesive tissue. Femoral BMD and BMC were assessed by a dual-energy X-ray absorptiometer (model Lunar PIXImus2; GE Medical Systems, Madison, WI, USA), operated with software version 2.10. The dual-energy supply was 80/35 kVp at 500 μA. The regions of interest (ROI) for femoral metaphysis included the proximal and distal 8 mm of the femur, whereas the ROI of femoral diaphysis included the middle part of the femur between its 8-mm ends. The machine was calibrated daily using a phantom provided by the manufacturer. The interassay coefficient of variation was less than 0.3%.

Statistical analysis

Results are expressed as mean ± SE. Two-group and multiple comparisons were performed by Student's *t* test and one-way ANOVA with Newman–Keuls post-test, respectively. The level of significance for all statistical tests was $P < 0.05$. Data were analyzed by GraphPad Prism 4.0 for Mac OS X (GraphPad Software, San Diego, CA, USA).

Results

Prior to investigating the effects of PRL on site-specific BMD and BMC of femora of pregnant and lactating rats, expression of dopaminergic D2 receptor was determined. As shown in Fig. 1, long isoform D2 receptor expression was observed only in pituitary gland and brain (positive control), but not in primary rat osteoblasts, osteoblast-like UMR-106 cells, or gastrocnemius muscle (negative control). Short isoform of D2 receptor mRNAs were not expressed in osteoblasts. Thus, the results indicated that bromocriptine had no direct action on osteoblasts.

Densitometric analysis in non-mated control rats showed that femoral BMD and BMC of both trabecular sites (proximal and distal metaphyses) and cortical site (diaphysis) increased with age (Figs. 2, 3). When compared to non-mated control, BMD of proximal femoral metaphysis in the P14, P21, and L8 groups were significantly higher, while that of the L21 and PW groups were lower (Fig. 2a). BMC of the proximal metaphysis was also higher during pregnancy (P14 and P21), early lactation (L8), and mid-lactation (L14), without any difference from control thereafter (Fig. 2b). Similarly, BMD of distal femoral metaphysis in the P14 and P21 groups were markedly elevated when compared to non-mated control, and became lower in the L21 and PW groups (Fig. 2c). BMC of distal femoral metaphysis was higher in the P14, P21, and L14 groups, and later became lower in the PW group (Fig. 2d). Neither BMD nor BMC of distal metaphysis in the L8 group was different from the control values. As for the cortical site, when compared to control, significantly higher BMD was found in the P14, P21, and L14 groups (Fig. 3a), while higher diaphyseal BMC was found in the P14, P21, L8, and L14 groups (Fig. 3b).

To demonstrate the effects of PRL on femoral BMD and BMC in pregnant and lactating rats, bromocriptine was administered for 7 days prior to removal of the femora. As shown in Fig. 4, suppression of PRL secretion had no effect on the pregnancy-induced increases in BMD and BMC in the P14 and P21 groups. On the other hand, during lactation, an absence of PRL abolished increases in metaphyseal and diaphyseal BMC, but not BMD, in the L8 and L14 groups (Fig. 5a–d). In the L21 group, absence of PRL secretion also prevented a decrease in BMD and restored it to the control levels (Fig. 5e), without effect on BMC (Fig. 5f).

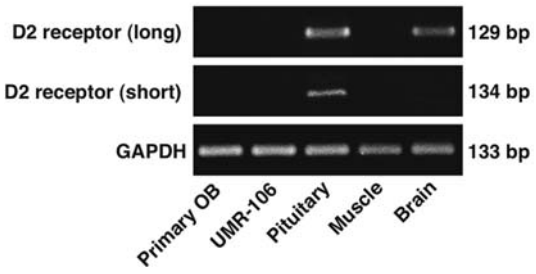

Fig. 1 Expression of long and short isoforms of subtype 2 dopamine (*D2*) receptor mRNAs in primary rat osteoblasts (*OB*), osteoblast-like UMR-106 cells, and pituitary gland. Gastrocnemius muscle and brain were used as negative and positive controls, respectively. Glyceraldehyde-3-phosphate dehydrogenase (*GAPDH*) is a housekeeping gene. This result was a representative of three independent repeats

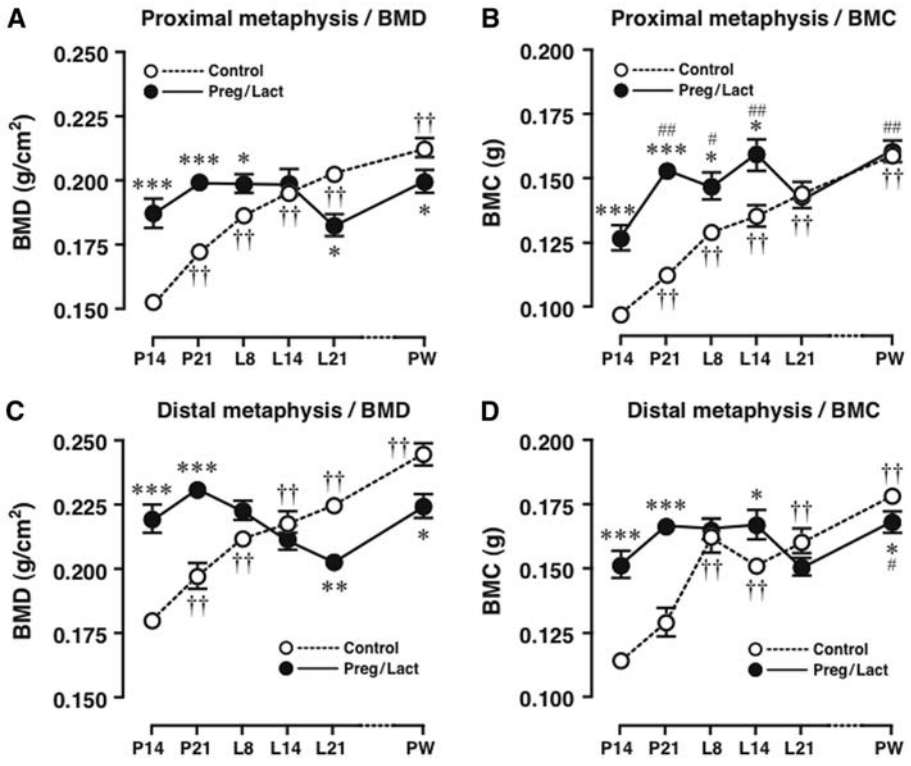

Fig. 2 BMD and BMC of **a–b** proximal and **c–d** distal femoral metaphyses in mated (pregnant, lactating, and post-weaning) and non-mated age-matched control rats ($n = 7$–9 per group). $^{*}P < 0.05$, $^{**}P < 0.01$, $^{***}P < 0.001$ compared with its respective age-matched control group. $^{\dagger\dagger}P < 0.01$ compared with age-matched control of P14 group. $^{\#}P < 0.05$, $^{\#\#}P < 0.01$ compared with the P14 group. *P14* and *P21* designate 14- and 21-day pregnant rats, while *L8*, *L14*, and *L21* designate 8-, 14-, and 21-day lactating rats, respectively. *PW* indicates 15-day post-weaning rats

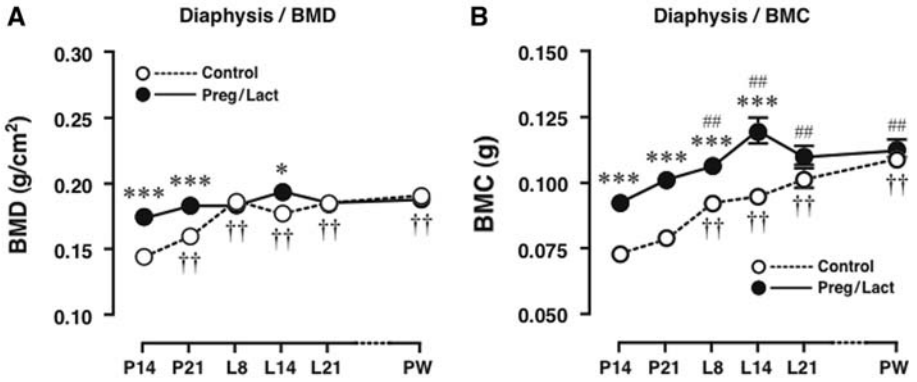

Fig. 3 **a** BMD and **b** BMC of femoral diaphyses in mated (pregnant, lactating, and post-weaning) and non-mated age-matched control rats ($n = 7$–9 per group). $^{*}P < 0.05$, $^{***}P < 0.001$ compared with its respective age-matched control group. $^{\dagger\dagger}P < 0.01$ compared with age-matched control of P14 group. $^{\#\#}P < 0.01$ compared with P14 group. *P14* and *P21* designate 14- and 21-day pregnant rats, while *L8*, *L14*, and *L21* designate 8-, 14-, and 21-day lactating rats, respectively. *PW* indicates 15-day post-weaning rats

Discussion

Little is currently known regarding the effects of hyperprolactinemia during pregnancy and lactation on the long bone. In the present study, we demonstrated that BMD and BMC of both trabecular and cortical parts of the rat femur were significantly increased during pregnancy until mid-lactation (L14). During late lactation (L21) and 15-day post-weaning, BMD of trabecular bone, but not cortical bone, was decreased. Furthermore, effects of PRL on bone during these reproductive periods were evaluated by administration of a selective D2 receptor agonist bromocriptine. The results suggested that PRL secreted from the pituitary gland was responsible for BMD and BMC changes during lactation, but not pregnancy. Daily administration of 4 mg/kg per day bromocriptine for 7 days was recently shown to decrease serum PRL of L7 rats by greater than 50% [15]. Moreover, in L7 rats with suckling, a single dose of bromocriptine injection markedly decrease serum PRL level from ~430 to ~100 ng/mL [15]. Since direct effect of bromocriptine on bone has never been reported, and osteoblasts did not express D2 receptor (Fig. 1), the bromocriptine effects observed in the present study

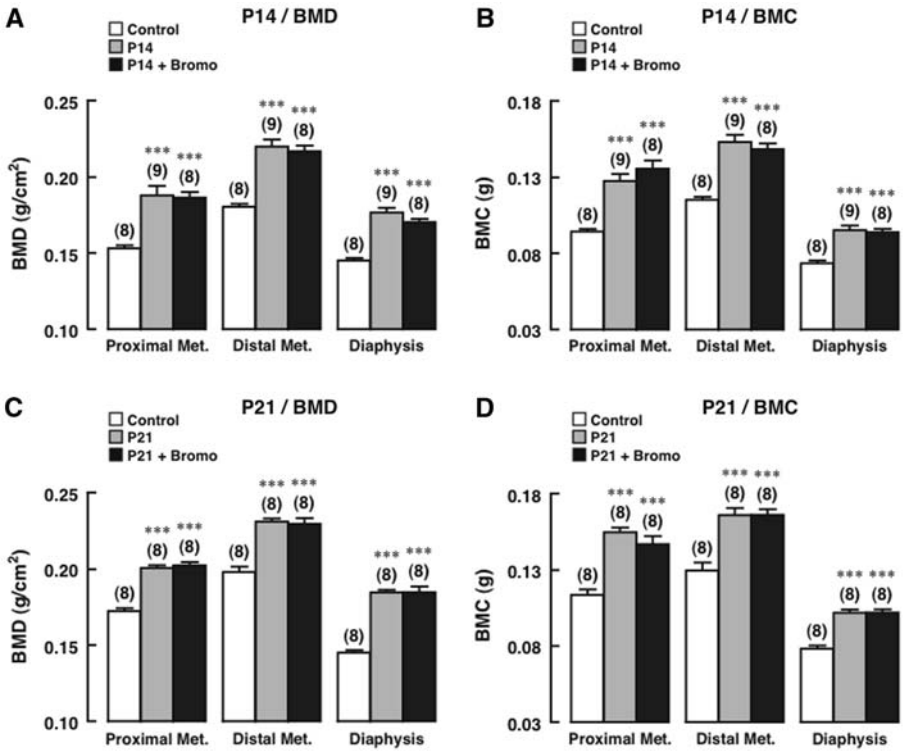

Fig. 4 BMD and BMC of proximal and distal femoral metaphyses (*Met.*) and femoral diaphyses in **a**,**b** 14-day pregnant rats (*P14*), and **c**,**d** 21-day pregnant rats (*P21*) treated with bromocriptine (*Bromo*). ***$P < 0.001$ compared with vehicle-treated age-matched control group. *Numbers in parentheses* represent the number of animals in each group

should occur through suppression of pituitary PRL release.

In general, fetal development during pregnancy leads to a massive drain on maternal calcium pool [16]. In humans, ~200–300 mg/day calcium was lost during the second and third trimester to maintain bone calcium accretion in the fetus [17]. However, changes in bone density during pregnancy remained controversial. Several investigators showed that there was no change in BMD in either pregnant women or rats [6, 16, 18]. In contrast, Gonen and coworkers [19] reported increased BMD of lumbar vertebrae, femur and tibia in pregnant rats, whereas others reported pregnancy-induced osteoporosis in humans [20, 21]. Such controversy could partly be due to the fact that an in situ densitometric measurement in living subjects is not sensitive enough to detect a slight change in bone density. Herein, by using ex vivo densitometric measurement, BMD and BMC of pregnant rats were found to increase at both femoral metaphysis and diaphysis. Despite the lack of evidence for the underlying mechanism, we speculated that the enhanced intestinal calcium absorption, in part, due to elevated serum PRL, placental lactogen and/or $1,25(OH)_2D_3$ levels, was responsible for supplying calcium both for fetuses, and for maternal trabecular and cortical bone calcium accretion [15, 22, 23], thereby leading to increases in ash weight, calcium content, and cross-sectional area of femur [1, 24]. Changes in the size and cross-sectional area of femur without proportional change in the total calcium content partially explained why BMC changes occurred in an absence of BMD change. Increased bone calcium content during pregnancy, as indicated by BMC (Figs. 2, 3), may also provide a reserved calcium pool for later use in milk production.

During lactation, an increase in BMC persisted until mid-lactation, presumably due to the lactation-induced increase in intestinal calcium absorption and renal calcium reabsorption [15, 16, 25]. PRL surge during suckling (~400–650 ng/mL) may further contribute to the elevated BMC, since short-term hyperprolactinemia of 2–4 weeks could increase bone calcium content in the rat femur, and further augment calcium absorption in the small intestine [1, 15, 26]. Besides metaphysis, PRL also had a positive effect on the femoral diaphysis of L8 and L14 rats, despite having no effect on the cortical sites in non-mated rats [4]. Although diaphyseal bone gain could be due to periosteal or endosteal bone formation, little is known regarding the direct effect of PRL on both processes in early lactation. We speculated that PRL did affect cortical bone but only in rats fed high-calcium diet [4], and perhaps in rats with enhanced intestinal calcium absorption. Bone histomorphometric study in hyperprolactinemic rats as well as in early lactating rats should reveal the effect of PRL on endosteal and periosteal calcium accretion.

When breastfeeding was prolonged, ongoing calcium loss in milk production eventually culminated in osteopenia in late lactation (L21), which was still detected at day 15 post-weaning. In exclusively breastfeeding women, calcium loss during this period can be as high as

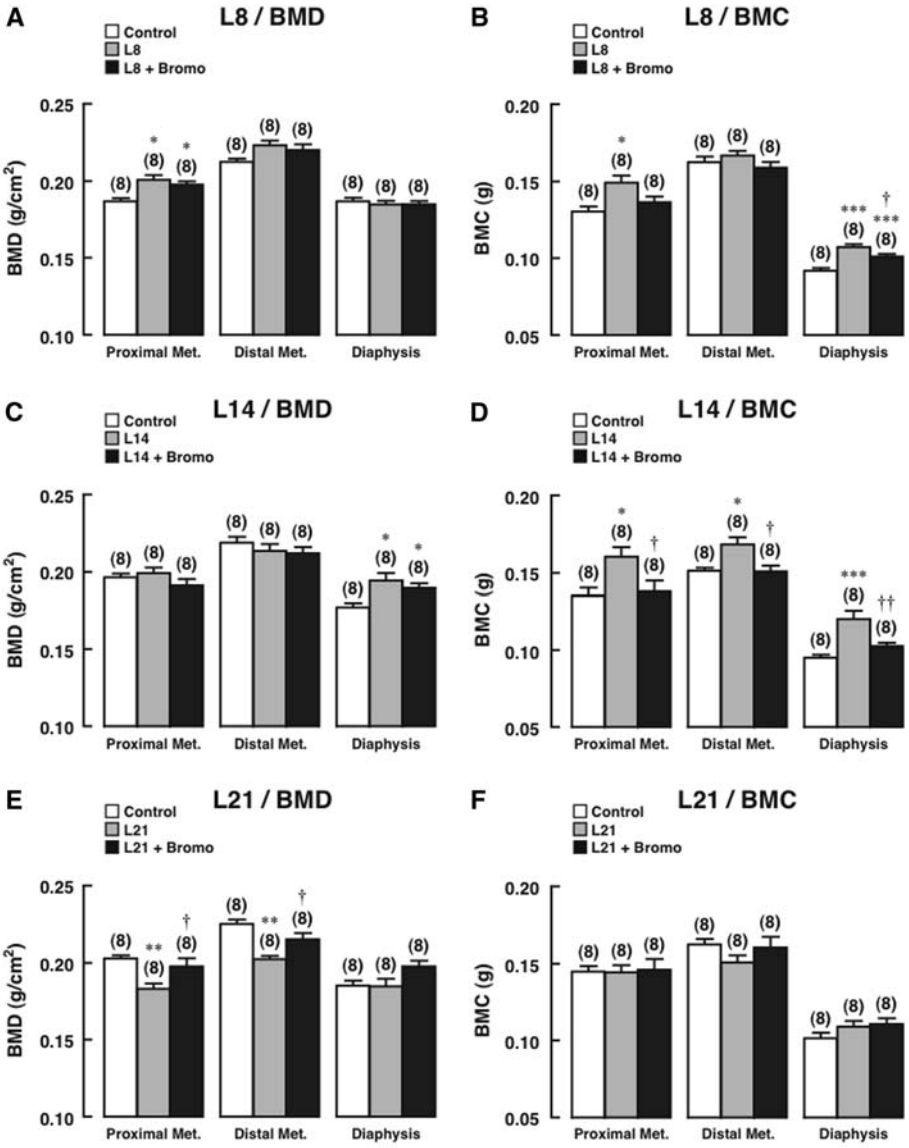

Fig. 5 BMD and BMC of proximal and distal femoral metaphyses (*Met.*) and femoral diaphyses in **a**,**b** 8-day lactating rats (*L8*), **c**,**d** 14-day lactating rats (*L14*), and **e**,**f** 21-day lactating rats (*L21*) treated with bromocriptine (*Bromo*). $^{*}P < 0.05$, $^{**}P < 0.01$, $^{***}P < 0.001$ compared with vehicle-treated age-matched control group. $^{\dagger}P < 0.05$, $^{\dagger\dagger}P < 0.01$ compared with its respective vehicle-treated lactating group. *Numbers in parentheses* represent the number of animals in each group

400 mg/day [17], while lactating rats lose 20–30% of their skeletal mass over 21 days of lactation [27, 28]. Interestingly, the observed bone loss only at trabecular site (metaphysis) was similar to that previously reported in rat vertebrae and distal femur [8]. Predominant bone loss in metaphyses may be due to the fact that the trabecular sites have more surface areas for bone resorption than the cortical sites. Several weeks after weaning, bone mass appeared to be completely restored to the normal level [16], presumably due to an increase in osteoclast apoptosis and decreased expression of osteoblast-derived bone resorption mediator, receptor activator of nuclear factor κB ligand (RANKL) [29].

A number of hormones act in concert to regulate bone resorption process during lactation. For example, parathyroid hormone-related protein (PTHrP) produced by the mammary gland is able to stimulate bone resorption and mobilize bone calcium for lactogenesis, whereas calcitonin helps to limit bone loss during lactation [16, 30]. In the present study, a decrease in metaphyseal BMD during late lactation was likely to be due to a lactogenic hormone PRL. Although PRL could induce a net bone gain in young growing rats or after short-term exposure in adults, chronic hyperprolactinemia longer than 5 weeks may lead to progressive trabecular osteopenia [2]. In non-mated female rats, chronic hyperprolactinemia markedly decreased trabecular bone volume and trabecular number, while enhancing bone turnover [2].

Since high plasma PRL levels suppressed ovarian estrogen synthesis [31–33], hyperprolactinemia-induced osteopenia was previously thought to be due to estrogen depletion. However, the presence of PRL receptors in primary rat osteoblasts and osteoblast-like MG-63 cells indicated direct PRL action on bone [2, 13]. At the

molecular level, PRL upregulated RANKL and downregulated osteoprotegerin (OPG) in osteoblasts, thereby enhancing osteoclastogenesis and osteoclast-mediated bone resorption [2]. PRL also suppressed alkaline phosphatase activity and osteocalcin expression, both of which were important for the osteoblast-mediated bone formation [2]. Although the aforementioned mechanism is able to explain metaphyseal bone loss in rat femur during late lactation, the molecular mechanism by which PRL increased bone mass during early and mid-lactation is currently unknown. In addition to the PRL-enhanced intestinal calcium absorption to supply more calcium for bone formation [23], it was possible that, during these reproductive periods, PRL may upregulate OPG rather than RANKL in osteoblasts of lactating rats, similar to that observed in human fetal osteoblasts [34], thus in turn reducing osteoclast proliferation.

In conclusion, from pregnancy to mid-lactation, BMD and BMC of both femoral metaphysis and diaphysis were increased. On the other hand, net bone loss was observed only in the femoral metaphysis during late lactation and day 15 post-weaning. Such bone changes during lactation, but not pregnancy, were found to be under the regulation of PRL. Interestingly, in contrast to non-mated rats in which PRL predominantly affected trabecular sites [3, 4], PRL induced net bone gain in both trabecular and cortical parts of femur of L8 and L14 rats, presumably to expand the calcium storage pool. Therefore, the present findings, together with the facts that PRL is able to stimulate intestinal calcium absorption and renal calcium reabsorption [1, 15, 23], suggested that PRL orchestrated total body calcium metabolism during lactation to guarantee an adequate calcium supply for milk production.

Acknowledgments We thank Kanogwun Thongchote, Jarinthorn Teerapornpuntakit, and Jirawan Thongbunchoo for the excellent technical assistance. This work was supported by the Thailand Research Fund (RSA5180001 to N. Charoenphandhu), the Faculty of Science, Mahidol University (SCR52-01 to N. Charoenphandhu), and the Faculty of Graduate Studies, Mahidol University, Academic Year 2008 (to P. Suntornsaratoon).

Conflict of interest statement The authors declare no conflicts of interest.

References

1. Piyabhan P, Krishnamra N, Limlomwongse L (2000) Changes in the regulation of calcium metabolism and bone calcium content during growth in the absence of endogenous prolactin and during hyperprolactinemia: a longitudinal study in male and female Wistar rats. Can J Physiol Pharmacol 78:757–765
2. Seriwatanachai D, Thongchote K, Charoenphandhu N, Pandaranandaka J, Tudpor K, Teerapornpuntakit J, Suthiphongchai T, Krishnamra N (2008) Prolactin directly enhances bone turnover by raising osteoblast-expressed receptor activator of nuclear factor κB ligand/osteoprotegerin ratio. Bone 42:535–546
3. Puntheeranurak S, Charoenphandhu N, Krishnamra N (2006) Enhanced trabecular-bone calcium deposition in female rats with a high physiological dose of prolactin diminishes after ovariectomy. Can J Physiol Pharmacol 84:993–1002
4. Charoenphandhu N, Tudpor K, Thongchote K, Saengamnart W, Puntheeranurak S, Krishnamra N (2007) High-calcium diet modulates effects of long-term prolactin exposure on the cortical bone calcium content in ovariectomized rats. Am J Physiol Endocrinol Metab 292:E443–E452
5. Thongchote K, Charoenphandhu N, Krishnamra N (2008) High physiological prolactin induced by pituitary transplantation decreases BMD and BMC in the femoral metaphysis, but not in the diaphysis of adult female rats. J Physiol Sci 58:39–45
6. Zeni SN, Di Gregorio S, Mautalen C (1999) Bone mass changes during pregnancy and lactation in the rat. Bone 25:681–685
7. Hagaman JR, Sanchez TV, Myers RC (1985) The effect of lactation on the mineral distribution profile of the rat femur by single photon absorptiometry. Bone 6:301–305
8. Nishiwaki M, Yasumizu T, Hoshi K, Ushijima H (1999) Effect of pregnancy, lactation and weaning on bone mineral density in rats as determined by dual-energy X-ray absorptiometry. Endocr J 46:711–716
9. Bonomo IT, Lisboa PC, Passos MC, Alves SB, Reis AM, de Moura EG (2008) Prolactin inhibition at the end of lactation programs for a central hypothyroidism in adult rat. J Endocrinol 198:331–337
10. Pi X, Voogt JL (2001) Mechanisms for suckling-induced changes in expression of prolactin receptor in the hypothalamus of the lactating rat. Brain Res 891:197–205
11. Elefteriou F (2008) Regulation of bone remodeling by the central and peripheral nervous system. Arch Biochem Biophys 473:231–236
12. Lux VA, Ramirez MI, Libertun C (1988) Natural and artificially induced ovulatory models related to lactation in the rat: role of prolactin. Proc Soc Exp Biol Med 188:301–307
13. Charoenphandhu N, Teerapornpuntakit J, Methawasin M, Wongdee K, Thongchote K, Krishnamra N (2008) Prolactin decreases expression of Runx2, osteoprotegerin, and RANKL in primary osteoblasts derived from tibiae of adult female rats. Can J Physiol Pharmacol 86:240–248
14. Binkley N, Dahl DB, Engelke J, Kawahara-Baccus T, Krueger D, Colman RJ (2003) Bone loss detection in rats using a mouse densitometer. J Bone Miner Res 18:370–375
15. Charoenphandhu N, Nakkrasae LI, Kraidith K, Teerapornpuntakit J, Thongchote K, Thongon N, Krishnamra N (2009) Two-step stimulation of intestinal Ca^{2+} absorption during lactation by long-term prolactin exposure and suckling-induced prolactin surge. Am J Physiol Endocrinol Metab 297:E609–E619
16. Kovacs CS, Kronenberg HM (2006) Skeletal physiology: pregnancy and lactation. In: Favus MJ (ed) Primer on the metabolic bone diseases and disorders of mineral metabolism, 6th edn. American Society for Bone and Mineral Research, Washington, DC, pp 63–68
17. Prentice A (2000) Calcium in pregnancy and lactation. Annu Rev Nutr 20:249–272
18. Ritchie LD, Fung EB, Halloran BP, Turnlund JR, Van Loan MD, Cann CE, King JC (1998) A longitudinal study of calcium homeostasis during human pregnancy and lactation and after resumption of menses. Am J Clin Nutr 67:693–701
19. Gonen E, Sahin I, Ozbek M, Kovalak E, Yologlu S, Ates Y (2005) Effects of pregnancy and lactation on bone mineral density, and their relation to the serum calcium, phosphorus, calcitonin and parathyroid hormone levels in rats. J Endocrinol Invest 28:322–326

20. Dunne F, Walters B, Marshall T, Heath DA (1993) Pregnancy associated osteoporosis. Clin Endocrinol 39:487–490
21. Smith R, Athanasou NA, Ostlere SJ, Vipond SE (1995) Pregnancy-associated osteoporosis. QJM 88:865–878
22. Fleet JC (2006) Molecular regulation of calcium metabolism. In: Weaver CM, Heaney RP (eds) Calcium in human health, 1st edn. Humana Press, New Jersey, pp 163–189
23. Jantarajit W, Thongon N, Pandaranandaka J, Teerapornpuntakit J, Krishnamra N, Charoenphandhu N (2007) Prolactin-stimulated transepithelial calcium transport in duodenum and Caco-2 monolayer are mediated by the phosphoinositide 3-kinase pathway. Am J Physiol Endocrinol Metab 293:E372–E384
24. Miller SC, Shupe JG, Redd EH, Miller MA, Omura TH (1986) Changes in bone mineral and bone formation rates during pregnancy and lactation in rats. Bone 7:283–287
25. Boass A, Lovdal JA, Toverud SU (1992) Pregnancy- and lactation-induced changes in active intestinal calcium transport in rat. Am J Physiol 263:G127–G134
26. Tudpor K, Charoenphandhu N, Saengamnart W, Krishnamra N (2005) Long-term prolactin exposure differentially stimulated the transcellular and solvent drag-induced calcium transport in the duodenum of ovariectomized rats. Exp Biol Med 230:836–844
27. Brommage R, DeLuca HF (1985) Regulation of bone mineral loss during lactation. Am J Physiol 248:E182–E187
28. Peng TC, Garner SC, Kusy RP, Hirsch PF (1988) Effect of number of suckling pups and dietary calcium on bone mineral content and mechanical properties of femurs of lactating rats. Bone Miner 3:293–304
29. Ardeshirpour L, Dann P, Adams DJ, Nelson T, VanHouten J, Horowitz MC, Wysolmerski JJ (2007) Weaning triggers a decrease in receptor activator of nuclear factor-κB ligand expression, widespread osteoclast apoptosis, and rapid recovery of bone mass after lactation in mice. Endocrinology 148:3875–3886
30. Woodrow JP, Sharpe CJ, Fudge NJ, Hoff AO, Gagel RF, Kovacs CS (2006) Calcitonin plays a critical role in regulating skeletal mineral metabolism during lactation. Endocrinology 147:4010–4021
31. Naliato EC, Farias ML, Braucks GR, Costa FS, Zylberberg D, Violante AH (2005) Prevalence of osteopenia in men with prolactinoma. J Endocrinol Invest 28:12–17
32. Schlechte JA (1995) Clinical impact of hyperprolactinaemia. Baillières Clin Endocrinol Metab 9:359–366
33. Wang C, Chan V (1982) Divergent effects of prolactin on estrogen and progesterone production by granulosa cells of rat Graafian follicles. Endocrinology 110:1085–1093
34. Seriwatanachai D, Charoenphandhu N, Suthiphongchai T, Krishnamra N (2008) Prolactin decreases the expression ratio of receptor activator of nuclear factor κB ligand/osteoprotegerin in human fetal osteoblast cells. Cell Biol Int 32:1126–1135

Two-step stimulation of intestinal Ca^{2+} absorption during lactation by long-term prolactin exposure and suckling-induced prolactin surge

Narattaphol Charoenphandhu, La-iad Nakkrasae, Kamonshanok Kraidith, Jarinthorn Teerapornpuntakit, Kanogwun Thongchote, Narongrit Thongon and Nateetip Krishnamra

Am J Physiol Endocrinol Metab 297:E609-E619, 2009. First published 30 June 2009; doi:10.1152/ajpendo.00347.2009

Am J Physiol Endocrinol Metab 297: E609–E619, 2009.
First published June 30, 2009; doi:10.1152/ajpendo.00347.2009.

Two-step stimulation of intestinal Ca^{2+} absorption during lactation by long-term prolactin exposure and suckling-induced prolactin surge

Narattaphol Charoenphandhu,[1,2] La-iad Nakkrasae,[1] Kamonshanok Kraidith,[2] Jarinthorn Teerapornpuntakit,[2] Kanogwun Thongchote,[2] Narongrit Thongon,[1,3] and Nateetip Krishnamra[1,2]

[1]*Consortium for Calcium and Bone Research;* [2]*Department of Physiology, Faculty of Science, Mahidol University, Bangkok; and* [3]*Department of Medical Science, Faculty of Science, Burapha University, Chonburi, Thailand*

Submitted 27 May 2009; accepted in final form 26 June 2009

Charoenphandhu N, Nakkrasae L, Kraidith K, Teerapornpuntakit J, Thongchote K, Thongon N, Krishnamra N. Two-step stimulation of intestinal Ca^{2+} absorption during lactation by long-term prolactin exposure and suckling-induced prolactin surge. *Am J Physiol Endocrinol Metab* 297: E609–E619, 2009. First published June 30, 2009; doi:10.1152/ajpendo.00347.2009.—During pregnancy and lactation, the enhanced intestinal Ca^{2+} absorption serves to provide Ca^{2+} for fetal development and lactogenesis; however, the responsible hormone and its mechanisms remain elusive. We elucidated herein that prolactin (PRL) markedly stimulated the transcellular and paracellular Ca^{2+} transport in the duodenum of pregnant and lactating rats as well as in Caco-2 monolayer in a two-step manner. Specifically, a long-term exposure to PRL in pregnancy and lactation induced an adaptation in duodenal cells at genomic levels by upregulating the expression of genes related to transcellular transport, e.g., TRPV5/6 and calbindin-D_{9k}, and the paracellular transport, e.g., claudin-3, thereby raising Ca^{2+} absorption rate to a new "baseline" (Step 1). During suckling, PRL surge further increased Ca^{2+} absorption to a higher level (Step 2) in a nongenomic manner to match Ca^{2+} loss in milk. PRL-enhanced apical Ca^{2+} uptake was responsible for the increased transcellular transport, whereas PRL-enhanced paracellular transport required claudin-15, which regulated epithelial cation selectivity and paracellular Ca^{2+} movement. Such nongenomic PRL actions were mediated by phosphoinositide 3-kinase, protein kinase C, and RhoA-associated coiled-coil-forming kinase pathways. In conclusion, two-step stimulation of intestinal Ca^{2+} absorption resulted from long-term PRL exposure, which upregulated Ca^{2+} transporter genes to elevate the transport baseline, and the suckling-induced transient PRL surge, which further increased Ca^{2+} transport to the maximal capacity. The present findings also suggested that Ca^{2+} supplementation at 15–30 min prior to breastfeeding may best benefit the lactating mother, since more Ca^{2+} could be absorbed as a result of the suckling-induced PRL surge.

calcium transport; lactating rats; pituitary transplantation; pregnancy; small interfering RNA

A TREMENDOUS AMOUNT of maternal Ca^{2+} (>200 mg/day) is lost during pregnancy and lactation for fetal growth and milk production, thereby leading to severe negative Ca^{2+} balance and progressive osteopenia in mothers (12, 29). Therefore, adequate oral Ca^{2+} intake is of critical importance for the maintenance of fetomaternal bone health (29, 30). How intestinal Ca^{2+} absorption is regulated during these reproductive periods is still elusive, but it is known to be $1,25(OH)_2D_3$ independent (16, 26). Our previous investigations in nulliparous rats and Caco-2 monolayer indicated that the lactogenic hormone prolactin (PRL) markedly enhanced the transepithelial Ca^{2+} transport through signaling pathways involving phosphoinositide 3-kinase (PI3K) as well as two serine/threonine kinases, namely protein kinase C (PKC) and RhoA-associated coiled-coil-forming kinase (ROCK) (20, 34, 35). Despite the markedly elevated plasma PRL levels during pregnancy (75–100 ng/ml), lactation (200–300 ng/ml), and suckling (400–650 ng/ml), i.e., >10 times the normal levels (7–10 ng/ml), physiological significances of the PRL-enhanced intestinal Ca^{2+} absorption in pregnancy and lactation have never been elucidated.

Generally, Ca^{2+} traverses the intestinal epithelium via transcellular and paracellular pathways (14). Transcellular active Ca^{2+} transport is a three-step metabolically energized process consisting of apical Ca^{2+} entry via the transient receptor potential vanilloid family Ca^{2+} channels (TRPV) 5/6 and L-type voltage-dependent Ca^{2+} channels (Ca_v), cytoplasmic Ca^{2+} translocation in a calbindin-D_{9k}-bound form, and basolateral Ca^{2+} extrusion via plasma membrane Ca^{2+}-ATPase ($PMCA_{1b}$) (18, 35). In contrast, the paracellular passive Ca^{2+} transport, which is dependent on the transepithelial Ca^{2+} gradient, does not occur when both sides of the epithelium contain equal Ca^{2+} concentration (14, 35) but may increase with a decrease in transepithelial resistance. Paracellular ion movement is normally regulated by the size- and charge-selective properties of the tight junction, which contains several charge-selective claudin proteins arranged in arrays of channel-like barriers (38). A number of claudins, such as claudin-2, -3, -8, -10, -12, and -15, were found to be cation selective (1, 15, 39, 40). Several mediators, e.g., PKA, PKC, PI3K, and ROCK, can modulate paracellular permselectivity in part via claudin phosphorylation (2, 11, 19, 31, 34).

Although PRL was reported to stimulate both transcellular and paracellular Ca^{2+} transport in ex vivo duodenal tissues (7), there was a disparity among results obtained from different models of PRL exposure. In the 4-wk anterior pituitary (AP)-grafted rats with sustained plasma PRL of 90–100 ng/ml comparable with the levels attained during pregnancy, the marked increase in duodenal Ca^{2+} transport was long lasting and was observed in PRL-free solution (36). In contrast, ex vivo duodenal tissue exhibited an abrupt increase in Ca^{2+} transport only when directly exposed to a much higher PRL concentration (>400 ng/ml) comparable with the levels of suckling-induced PRL surge (20). It is thus hypothesized that a modest hyperprolactinemia during pregnancy and lactation leads to a long-lasting adaptation in the intestinal absorptive cells to enhance Ca^{2+} absorption, whereas PRL surge after

Address for reprint requests and other correspondence: N. Charoenphandhu, Dept. of Physiology, Faculty of Science, Mahidol University, Rama VI Road, Bangkok 10400, Thailand (e-mail: naratt@narattsys.com).

intermittent suckling rapidly but transiently induces a further increase in Ca^{2+} absorption.

Therefore, the objectives of the present study were *1*) to elucidate the physiological significance of PRL in the regulation of intestinal Ca^{2+} absorption during pregnancy, lactation, and suckling and *2*) to demonstrate possible mechanisms and signaling pathways of the PRL-enhanced intestinal Ca^{2+} transport. Duodenum was used in this study because it is the efficient site for both transcellular and paracellular Ca^{2+} transport (18). In some experiments, human colorectal adenocarcinoma Caco-2 monolayer, a standard model for Ca^{2+} absorption study, was used since it can be genetically manipulated and has functional properties similar to the small intestinal cells (6, 44, 45).

MATERIALS AND METHODS

Animals. Pregnant and age-matched nulliparous Sprague-Dawley rats were obtained from the National Laboratory Animal Centre (Nakhon Pathom, Thailand). They were housed in the husbandry unit for ≥7 days prior to the experiments and were fed standard pellets and distilled water ad libitum. After delivery, the litter size was adjusted to 8 pups/dam. On the experimental day, pups were separated from the dam (−suckling) for 2 h before Ca^{2+} flux study. As for the suckling group (+suckling), pups were returned to the dam after 2-h separation, and suckling was allowed for 30 min before Ca^{2+} flux study. Milk volume was calculated from the weight of pups before and after suckling and milk density of 1.61 g/ml. In some experiments, dams were injected daily with bromocriptine and/or PRL subcutaneously (purified from ovine pituitary gland, catalog no. L6520; Sigma) for 7 days or given single injections 1 h prior to the experiment. This study was approved by the Animal Care and Use Committee of the Faculty of Science, Mahidol University.

Cell culture. Caco-2 cells (American Type Culture Collection no. HTB-37) were grown in Dulbecco's modified Eagle medium (Sigma) supplemented with 15% fetal bovine serum, 1% L-glutamine, 1% nonessential amino acid, 100 U/ml penicillin-streptomycin, and 0.25 μl/ml amphotericin B. Confluent Caco-2 monolayers were prepared by seeding cells (5×10^5 cells/cm^2) on polyester Snapwell with 12-mm diameter and 0.4-μm pore size (Corning). Culture medium was changed daily after 48 h of seeding. Monolayers were incubated at 37°C for 14 days in a humidified atmosphere containing 5% CO_2. To investigate PRL effects on Ca^{2+} transport, Caco-2 monolayer was exposed to 600 ng/ml recombinant human PRL (rhPRL; purity >97%, catalog no. 682-PL; R & D Systems), the most effective concentration reported by Jantarajit et al. (20).

Small interfering RNA transfection. Small interfering RNA (siRNA) oligonucleotides targeted for long isoform of human PRL receptor (PRLR-L; 5′-GGGCUAUAGCAUGGUGACCUU-3′ and 5′-GGUCACCAUGCUAUAGCCCUU-3′) and claudin-15 (5′-GCAAAUACGGCAGAAACGCUU-3′ and 5′-UUCGUUUAUGCCGUCUUUGCG-3′) were designed by siRNA Target Designer 1.51 and synthesized by T7 RiboMax Express RNAi System (Promega). Scramble siRNA (5′-GGCGCAAUAAAGCAAGACC-3′ and 5′-GGUCUUGCUUUAUUGCGCC-3′), which had no homology to any other genes, was used as a negative control. As described previously (35), Caco-2 cells were first plated on Snapwell at 5×10^5 cells/cm^2. On *day 12* after seeding, in vitro transfection was performed with 10 μg/ml polyethyleneimine (PEI) and 1 μmol/ml siRNA. On *day 14* (i.e., 48 h after transfection), siRNA-treated monolayers were used for the experiments. Efficiency of siRNA was evaluated by quantitative real-time PCR (qRT-PCR). The knockdown protocol was approved by the Institutional Biosafety Committee of Mahidol University.

AP transplantation. As described previously (10), two 10-wk-old donor rats were decapitated to collect the pituitary glands, which were immediately transplanted under the renal capsule of a recipient rat (i.e., 2 glands/rat). Sham operation consisted of exposure of the left kidney and a gentle touch of the renal fascia with forceps. Visual examination of the well-vascularized hypophyseal graft and immunohistochemical staining for PRL production were performed at the end

Table 1. *Oligonucleotide sequences used in PCR study*

Gene (Accession No.)	Primer	Product Length, bp
	Homo sapiens	
PRLR-S (AF416619)		145
Forward	5′-GGTGACCCCTTGATGTTG-3′	
Reverse	5′-TTCTGGTATATGCTCTTCAGC-3′	
PRLR-L (NM_000949)		100
Forward	5′-ACTTGCCTCTTTCTCCAG-3′	
Reverse	5′-TCCCTCAAGAATACTAAGCAG-3′	
Claudin-2 (NM_020384)		102
Forward	5′-CTCTTCAGGCGTAATGGA-3′	
Reverse	5′-CTTGGTGCTATGGTCTTTC-3′	
Claudin-3 (NM_001306)		121
Forward	5′-CTGCTCTGCTGCTCGTGT-3′	
Reverse	5′-TAGTCCTTGCGGTCGTAGC-3′	
Claudin-8 (NM_199328)		97
Forward	5′-TGGTGCTGATTGTTGGAGGAG-3′	
Reverse	5′-GTTGTGCGATGGGAAGGTATC-3′	
Claudin-10 (NM_182848)		179
Forward	5′-CTCTGGTGTCTGGTGTCG-3′	
Reverse	5′-GATAGTAAAATGCGGTCGG-3′	
Claudin-12 (NM_012129)		174
Forward	5′-GCCCATATACAATCTCTTAG-3′	
Reverse	5′-GTAAAGCCATACCTTACTTC-3′	
Claudin-15 (NM_014343)		90
Forward	5′-AAGTGGAGACGGACCTGAGC-3′	
Reverse	5′-GCGGCTAAGGAGGGTTGT-3′	
GAPDH (NM_002046)		359
Forward	5′-CTGGTAAAGTGGATATTGTTG-3′	
Reverse	5′-GAGGCTGTTGTCATACTTCTC-3′	
	Rattus norvegicus	
PRLR-S (NM_012630)		120
Forward	5′-TTCTACCACCATCGCAAC-3′	
Reverse	5′-CTGATCTCGTTTGTCATTGAG-3′	
PRLR-L (NM_001034111)		107
Forward	5′-TCAAGCAACCGCAGACTC-3′	
Reverse	5′-CAGTTTAGCCAATCGTTCCA-3′	
PRL (NM_012629)		171
Forward	5′-CAAACCTTCTGTTCTGCC-3′	
Reverse	5′-CACGATCTTGGACATACTG-3′	
TRPV5 (NM_053787)		163
Forward	5′-CTTACGGGTTGAACACCACCA-3′	
Reverse	5′-TTGCAGAACCACAGAGCCTCTA-3′	
TRPV6 (NM_053686)		80
Forward	5′-ATCCGCCGCTATGCAC-3′	
Reverse	5′-AGTTTTTCTGGTCACTGTTTTTGG-3′	
Calbindin-D_{9k} (X_16635)		174
Forward	5′-CCCGAAGAAATGAAGAGCATTTT-3′	
Reverse	5′-TTCTCCATCACCGTTCTTATCCA-3′	
$PMCA_{1b}$ (NM_053311)		109
Forward	5′-CGCCATCTTCTGCACAATT-3′	
Reverse	5′-CAGCCATTGTTCTATTGAAAGTTC-3′	
ZO-1 (XM_218747)		270
Forward	5′-GTATCCGATTGTTGTGTTCC-3′	
Reverse	5′-TCACTTGTAGCACCATCCGC-3′	
Occludin (NM_031329)		188
Forward	5′-CACGTTCGACCAATGC-3′	
Reverse	5′-CCCGTTCCATAGGCTC-3′	
Claudin-3 (NM_031700)		246
Forward	5′-GCACCCACCAAGATCCTCTA-3′	
Reverse	5′-AGGCTGTCTGTCCTCTTCCA-3′	
Claudin-15 (XM_222085)		330
Forward	5′-GCTGTGCCACCGACTCCC-3′	
Reverse	5′-CAGAGCCCAGTTCATACTTG-3′	
GAPDH (NM_017008)		133
Forward	5′-AGTCTACTGGCGTCTTCAC-3′	
Reverse	5′-TCATATTTCTCGTGGTTCAC-3′	

PRLR-S and -L, short and long isoforms, respectively, of prolactin receptor; PRL, prolactin; TRPV5 and -6, transient receptor potential vanilloid family Ca^{2+} channels 5 and 6, respectively; $PMCA_{1b}$, plasma membrane Ca^{2+}-ATPase isoform 1b.

of the experiments to confirm successful AP transplantation (10). At 4 wk after transplantation, plasma PRL levels are known to increase to 90–100 ng/ml (28).

Surgery and tissue collection. A median laparotomy was performed under 50 mg/kg ip pentobarbitone sodium (Abbott) anesthesia. Duodenal segment was removed and cut longitudinally to expose the mucosa. Duodenal segment was then mounted in a modified Ussing chamber to measure Ca^{2+} fluxes, as described previously (20). The tissue was incubated for 20 min in the chamber before the 60-min experiment. For mRNA and protein expression studies, epithelial cells were collected by scraping the mucosal surface with an ice-cold glass slide (10). Arterial blood (5 ml) was also collected by cardiac puncture.

Determination of serum PRL. Serum PRL concentrations were determined by rat PRL enzyme immunoassay kit (catalog no. A05101; SPI Bio, Massy Cedex, France) according to the manufacturer's instruction. The sensitivity of the assay was 0.4 ng/ml, and the intra- and interassay coefficients of variation were 10 and 15%, respectively.

RNA isolation, PCR, and sequencing. By using TRIzol reagent (Invitrogen), total RNA was prepared according to the method of Charoenphandhu et al. (10). One microgram of total RNA was reverse-transcribed with oligo$(dT)_{20}$ primer and iScript kit (Bio-Rad). Glyceraldehyde-3-phosphate dehydrogenase (GAPDH), a housekeeping gene, served as a control gene to check the consistency of reverse transcription. Primers are presented in Table 1 (9, 20, 34). Amplification reaction using conventional thermal cycler was performed with GoTaq Green Master Mix (Promega), whereas qRT-PCR using real-time PCR (model MiniOpticon; Bio-Rad) was performed with iQ SYBR Green SuperMix (Bio-Rad) according to the manufacturers' instructions. Relative expression was calculated from the threshold cycle (C_T) values by using the $2^{-\Delta\Delta C_T}$ method, and twofold change was considered significant (10). PCR products were also visualized on a 1.5% agarose gel stained with 1.0 μg/ml ethidium bromide under a UV transilluminator (Alpha Innotech). After electrophoresis, PCR products were extracted by HiYield Gel/PCR DNA Extraction kit (Real Biotech, Taipei, Taiwan) and were sequenced by ABI Prism 3100 Genetic Analyzer (Applied Biosystems). qRT-PCR experiments were performed in triplicate.

Immunoprecipitation. Cell lysate was sonicated and incubated at 4°C for 20 min. Thereafter, lysate was incubated for 2 h at 4°C on a rocking platform with 1:1,000 rabbit polyclonal antibodies against claudin-2, -3, -8, -10, -12, or -15 (Santa Cruz Biotechnology). The mixture was then incubated at 4°C for 2 h with EZview Red protein-A affinity gel (Sigma). Beads were washed three times and resuspended in 50 μl of buffer containing 20% glycerol, 10% SDS, 1% bromophenol blue, 4% 2-mercaptoethanol, and 0.5 mol/l Tris·HCl, pH 6.8. Eluted proteins were subjected to Western blot analysis.

Western blot analysis. As described previously (20), 100-μg proteins were separated by SDS-PAGE and transferred to a nitrocellulose membrane (Amersham) by electroblotting. Membranes were blocked at 25°C for 4 h with 5% nonfat milk and were probed overnight at 4°C with 1:1,000 rabbit polyclonal antibodies (Santa Cruz Biotechnology) raised against the conserved extracellular domain of PRLR, claudins, or phosphorylated amino acid residues (i.e., phosphorylated serine, thyrosine, and threonine). Membranes were also reprobed with 1:5,000 anti-β-actin monoclonal or 1:1,000 anti-claudin polyclonal antibodies (Santa Cruz Biotechnology). After 2-h incubation at 25°C with 1:2,000 secondary antibodies (Santa Cruz Biotechnology), blots were visualized by enhanced chemiluminescence kit (Amersham).

Confocal laser-scanning microscopy. Caco-2 cells were plated on coverslips in six-well culture plates (10^5 cells/cm^2) and maintained for 12 days. On *day 12*, cells were transfected with claudin-15 siRNA. After 48-h incubation, the monolayer was fixed with 100% ethanol for 20 min at −20°C. After blocking nonspecific bindings, cells were then incubated overnight at 4°C with 1:20 rabbit anti-occludin or claudin-15 polyclonal antibodies (Santa Cruz Biotechnology). They were later rinsed with phosphate-buffered saline (PBS) with Tween-20, pH 7.4, prior to 3-h incubation with 1:300 Alexa fluor 488-conjugated secondary antibody (Molecular Probes) at room temperature. For negative controls, cells were incubated with 3% bovine serum albumin in PBS instead of specific antibody. Images were captured with a FV1000 confocal laser-scanning microscope (Olympus).

Bathing solution for Ussing chamber study. The bathing solution, continuously gassed with humidified 5% CO_2 in 95% O_2, contained (in mmol/l) 118 NaCl, 4.7 KCl, 1.1 $MgCl_2$, 1.25 $CaCl_2$, 23 $NaHCO_3$,

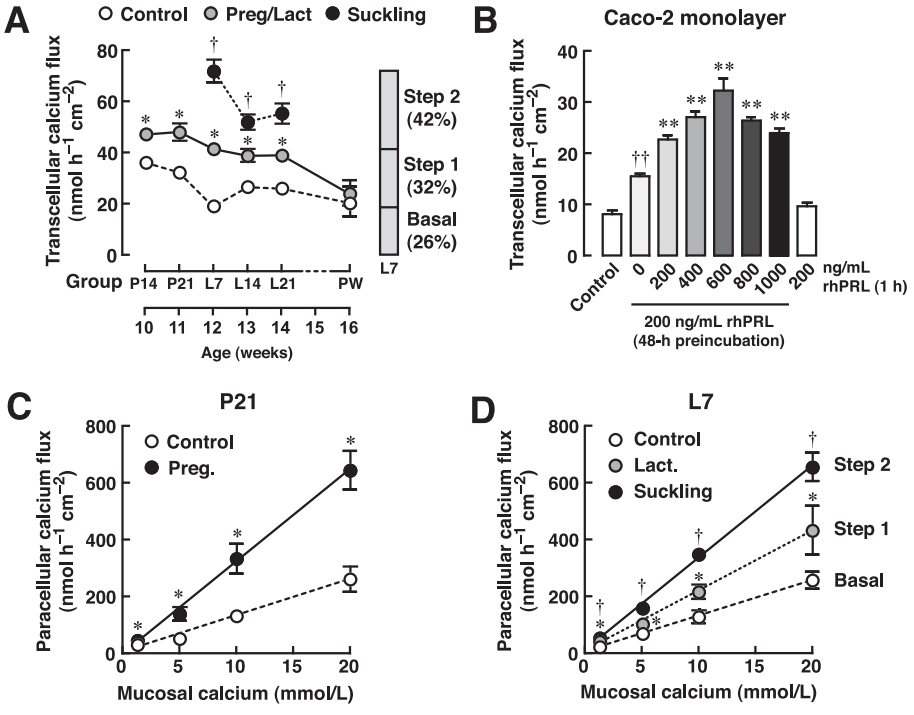

Fig. 1. *A*: transcellular Ca^{2+} transport in the duodenum of pregnant/lactating, suckling, and age-matched control rats (n = 5–9). Ca^{2+} flux was studied at midpregnancy (P14), late pregnancy (P21), early lactation (L7), midlactation (L14), late lactation (L21), and 15-day postweaning (PW). Two-step stimulation of the transcellular Ca^{2+} transport and the %contribution in L7 rats are depicted. $^*P < 0.05$ compared with control group; †$P < 0.05$ compared with corresponding lactating group. *B*: transcellular Ca^{2+} transport in 200 ng/ml recombinant human prolactin (rhPRL)-preincubated Caco-2 monolayer after acute exposure (1 h) to 200–1,000 ng/ml rhPRL (n = 3–6). Preincubation with 200 ng/ml rhPRL for 48 h was to represent long-term PRL effects in lactation, whereas acute PRL exposure was to mimic PRL surge during suckling. ††$P < 0.01$ compared with control group; $^{**}P < 0.01$ compared with preincubated group without acute PRL treatment. *C* and *D*: paracellular Ca^{2+} transport in the duodenum of P21, L7, and L7 + suckling rats (n = 5–6/each Ca^{2+} concentration). Ca^{2+} flux was measured in the presence of transepithelial Ca^{2+} gradient (i.e., various mucosal Ca^{2+} concentrations). Two-step stimulation was demonstrated during lactation. $^*P < 0.05$ compared with control group; †$P <$ 0.05 compared with corresponding lactating group.

12 D-glucose, and 2 mannitol (Sigma). The solution was maintained at 37°C, pH 7.4, and had an osmolality of 290–295 mmol/kg H_2O. In some experiments, PRL or inhibitors of gene transcription [RNA polymerase II inhibitor; 50 μmol/l 5,6-dichloro-1-β-D-ribobenzimidazole (DRB); Calbiochem], protein synthesis [70 μmol/l cycloheximide (CCH); Sigma], PI3K (75 μmol/l LY294002; Tocris), PKC (panspecific inhibitor; 1 μmol/l GF109203X; AG Scientific), or ROCK (1 μmol/l Y27632; Calbiochem) were added in the bathing solution.

Electrical measurement. Potential difference (PD), short-circuit current (Isc), and transepithelial resistance (TER) were determined as previously described (20). Briefly, a pair of Ag/AgCl electrodes connected to agar bridges (3.0 mol/l KCl per 4 g% agar) was located near each surface of the mounted tissue or Snapwell for measurement of PD. The other ends of the PD-sensing electrodes were connected to a preamplifier (model EVC-4000; World Precision Instruments) and finally to PowerLab 4/30 (AD Instruments). Another pair of Ag/AgCl electrodes was placed at the end of each hemichamber to supply Isc, which was also measured by a PowerLab 4/30 connected in series to EVC-4000 current-generating unit. TER and conductance were calculated by Ohm's equation.

Calcium flux measurement. Ca^{2+} flux was determined by the method of Charoenphandhu et al. (9). Briefly, after 20-min incubation, Ussing chamber was filled with fresh bathing solution. One side was $^{45}CaCl_2$-containing bathing solution (initial amount of 5 mCi/ml, final specific activity of ~450–500 mCi/mol; Amersham). ^{45}Ca radioactivity was analyzed by a liquid scintillation spectrophotometer (model Tri-Carb 3100; Packard Instruments). Total Ca^{2+} concentration of the bathing solution was analyzed by an atomic absorption spectrophotometer (model SpectrAA-300; Varian Techtron, Springvale, Australia). Ca^{2+} fluxes in the absence of Ca^{2+} concentration gradient (i.e., bathing solution in both hemichambers contained equal Ca^{2+} concentration) represented the active Ca^{2+} transport. The Ca^{2+} gradient-dependent paracellular passive fluxes were measured by determining Ca^{2+} fluxes in the presence of varying apical Ca^{2+} concentrations (9).

Permeability measurement. Permeability of sodium (P_{Na}) and chloride (P_{Cl}), which were indicative of charge selectivity, were measured by the dilution potential technique (34). In brief, duodenal epithelium or Caco-2 monolayer was equilibrated for 20 min in normal bathing solution containing 145 mmol/l NaCl before the apical solution was substituted with 72.5 mmol/l NaCl. Osmolality was maintained by an

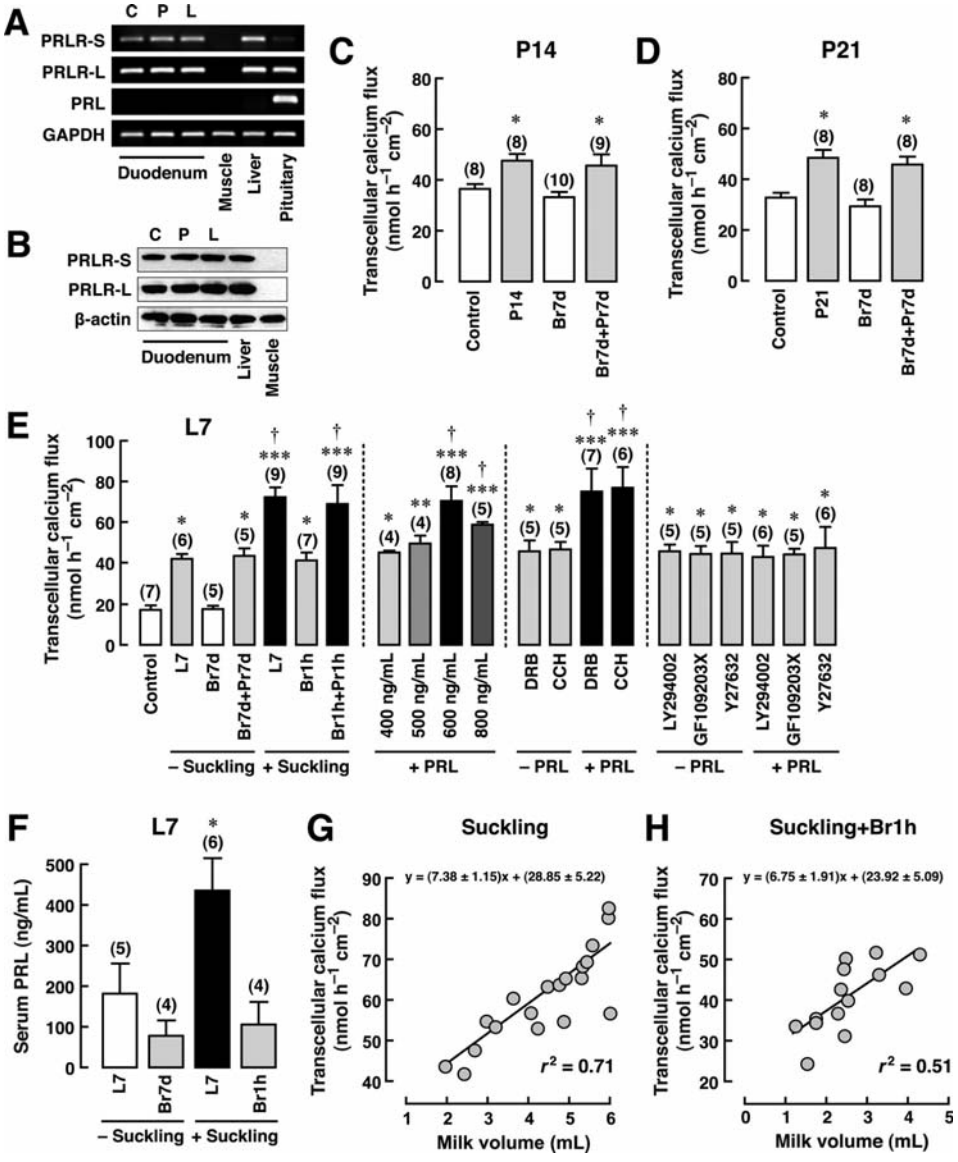

Fig. 2. Representative images of mRNA (n = 3; *A*) and protein expression (n = 3; *B*) of short (PRLR-S) and long (PRLR-L) isoforms of PRL receptors (PRLR) and PRL (mRNA only) in the duodenum of nonmated control (C), pregnant (P), and lactating (L) rats. GAPDH was a housekeeping gene for PCR study, whereas β-actin was a housekeeping gene for Western blot analysis. Liver and muscle served as positive and negative controls, respectively, for PRLR expression. Pituitary gland was a positive control for PRL expression. *C* and *D*: transcellular Ca^{2+} transport in P14 and P21 rats administered with bromocriptine (Br7d) with or without PRL supplementation (Pr7d) for 7 days. *$P < 0.05$ compared with control group. Numbers of animals are shown in parentheses. *E*: transcellular Ca^{2+} transport in L7 rats with (+suckling) or without suckling (−suckling). Bromocriptine injection 1 h (Br1h) prior to Ca^{2+} flux study was to abolish the suckling-induced PRL surge, which was mimicked by concurrent PRL supplementation (Pr1h). In some experiments, duodenal tissues of L7 rats (−suckling) were acutely exposed to 400–800 ng/ml PRL in the bathing solution, which resembled acute exposure during PRL surge. To demonstrate PRL-signaling pathways, PRL and inhibitors of gene transcription [50 μmol/l 5,6-dichloro-1-β-D-ribobenzimidazole (DRB)], protein biosynthesis [70 μmol/l cycloheximide (CCH)], phosphoinositide 3-kinase (PI3K; 75 μmol/l LY-294002), PKC (1 μmol/l GF-109203X), or RhoA-associated coiled-coil-forming kinase (ROCK; 1 μmol/l Y-27632) were added in the solution. *$P < 0.05$, **$P < 0.01$, and ***$P < 0.001$ compared with nonmated control group (Basal Ca^{2+} flux). †$P < 0.05$ compared with L7 −suckling (Step 1 Ca^{2+} flux). *F*: serum PRL levels in L7 rats. PRL surge was determined at 30 min postsuckling. *$P < 0.05$ compared with L7 −suckling group. *G* and *H*: correlation between Ca^{2+} fluxes and milk volume in suckling rats. Data were pooled from L7, L14, and L21 rats with (total animals = 14) or without (total animals = 19) Br1h administration.

equivalent amount of mannitol. Changes in the PD before and after fluid replacement (i.e., dilution potential) were recorded every 10 s until stable. P_{Na}/P_{Cl} was calculated from the dilution potential by using the Goldman-Hodgkin-Katz equation, whereas P_{Na} and P_{Cl} were calculated from the transepithelial conductance and P_{Na}/P_{Cl} by using Kimizuka-Koketsu equations (34). Permeability of Ca^{2+} (P_{Ca}) was calculated from the paracellular Ca^{2+} flux and the difference between apical and basolateral Ca^{2+} concentrations, as described previously (34).

^{45}Ca uptake study. Caco-2 cells were seeded on Snapwells for 12 days. On *day 12*, in vitro transfection was performed with 10 μg/ml PEI and 1 nmol/ml claudin-15 siRNA. Control cells were treated only with PEI. After 48-h incubation, the monolayer was exposed to 600 ng/ml rhPRL for 1 h and then bathed on the apical side with bathing solution containing 16,000 counts·min^{-1}·100 μl^{-1} $^{45}CaCl_2$ for 2 min before harvesting. ^{45}Ca radioactivity was analyzed by liquid scintillation spectrophotometer.

Statistical analysis. Results are expressed as means ± SE. Two sets of data were compared using the unpaired Student *t*-test. One-way analysis of variance with Dunnett's multiple comparison test was used for multiple sets of data. Linear regression with slope analysis was performed for correlation study. The level of significance was $P < 0.05$. Data were analyzed by GraphPad Prism 4.0 (GraphPad Software, San Diego, CA).

RESULTS

Two-step stimulation of duodenal Ca^{2+} absorption during pregnancy and lactation. Transepithelial Ca^{2+} transport was investigated in primiparous rats at different reproductive phases, i.e., midpregnancy (*day 14*; P14), late pregnancy (*day 21*; P21), early lactation (*day 7*; L7), midlactation (*day 14*; L14), late lactation (*day 21*; L21), and 15-day postweaning (PW), as well as in their age-matched nulliparous controls. Lactating rats were separated from pups for 2 h prior to Ca^{2+} flux study. As demonstrated by Ussing chamber technique (Fig. 1*A*), the transcellular Ca^{2+} transport was increased significantly in pregnancy and lactation, but not PW, to a new "baseline" level (Step 1). Thirty-minute suckling further increased the transcellular Ca^{2+} transport to a new level above the elevated baseline (Step 2). In L7 rats, Step 1 and Step 2 Ca^{2+} fluxes contributed ~32 and ~42%, respectively, to the total transcellular Ca^{2+} flux (Fig. 1*A*). Similarly, Caco-2 monolayer preincubated with 200 ng/ml rhPRL (dissolved in culture medium) for 48 h to represent long-term PRL exposure later exhibited 90% increase in the transcellular Ca^{2+} transport, although bathing solution in Ussing chamber contained no rhPRL (Fig. 1*B*). Acute exposure of preincubated Caco-2 monolayer to 200–1,000 ng/ml rhPRL (dissolved in bathing solution) further enhanced the transcellular Ca^{2+} transport in a dose-response manner. However, without 48-h preincubation, 200 ng/ml rhPRL in bathing solution was unable to stimulate Ca^{2+} transport (Fig. 1*B*).

The paracellular Ca^{2+} transport was also enhanced in P21 rats (Fig. 1*C*). Furthermore, consistent with the transcellular

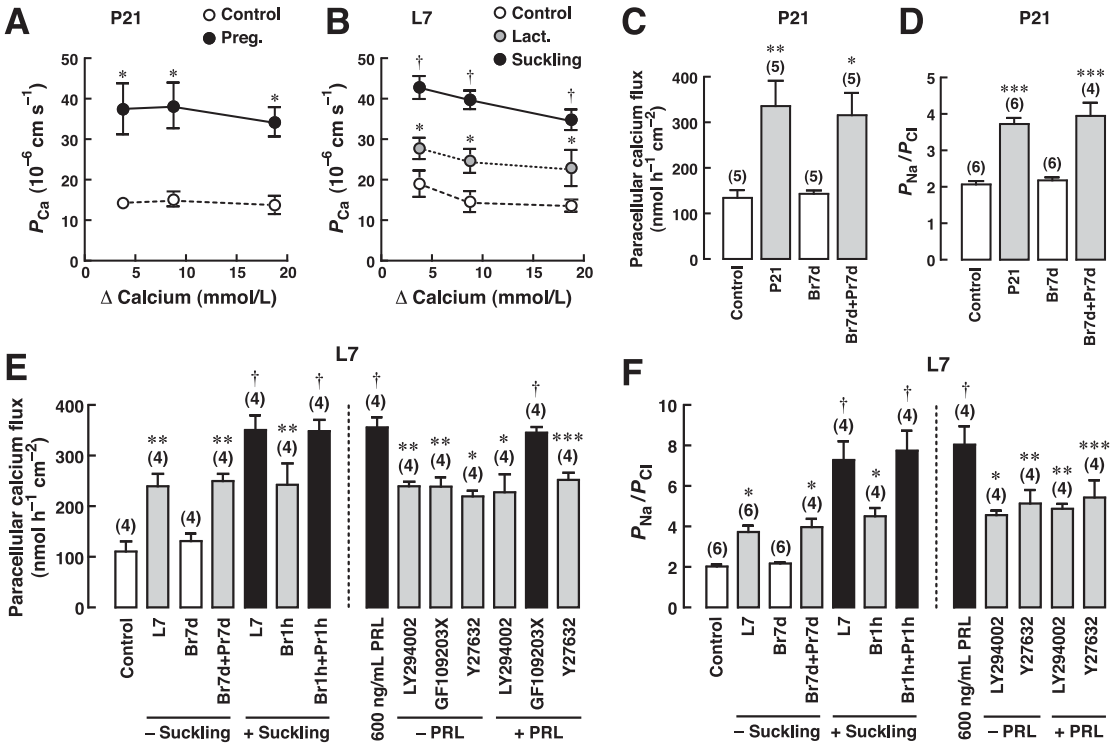

Fig. 3. *A* and *B*: permeability of Ca^{2+} (P_{Ca}) in the duodenum of pregnant, lactating, and suckling rats (n = 5–6/each Ca^{2+} concentration) plotted against Ca^{2+} concentration differences between apical and basolateral compartments (Δcalcium). *C*: paracellular Ca^{2+} fluxes measured in the presence of 10 mmol/l apical Ca^{2+} in the duodenum of P21 rats. *D*: permeability of sodium/chloride (P_{Na}/P_{Cl}) as an indicator of charge selectivity in the duodenum of P21 rats. *E* and *F*: paracellular duodenal Ca^{2+} transport and P_{Na}/P_{Cl} in L7 rats with or without suckling. In some experiments, L7 rats were administered with Br7d or Br1h to suppress chronic PRL secretion and suckling-induced PRL surge, respectively. PRL signalings were investigated by exposing 600 ng/ml PRL-treated L7 duodenal tissues to various inhibitors. $*P < 0.05$, $**P < 0.01$, and $***P < 0.001$ compared with control group (Basal). $\dagger P < 0.05$ compared with L7 −suckling (Step 1). Numbers in parentheses represent the number of rats.

transport, the two-step stimulation of the paracellular Ca^{2+} transport was similarly observed in L7 rats (Fig. 1*D*).

PRL as a regulator of transcellular Ca^{2+} transport during pregnancy and lactation. To find out whether PRL was the key regulator of the two-step increase in Ca^{2+} transport in lactating animals, the presence of PRLR was first investigated in the duodenal epithelial cells of P21, L7, and control rats. By using conventional PCR (Fig. 2*A*) and Western blot analysis (Fig. 2*B*), short (PRLR-S) and long (PRLR-L) isoforms of PRLR were identified, confirming the duodenum as a target of PRL. Figure 2*A* also shows that duodenal cells did not express endogenous PRL; i.e., the observed PRL effects were due to circulating PRL.

In P14 and P21 rats, 7-day administration of 4 $mg \cdot kg^{-1} \cdot day^{-1}$ sc bromocriptine (Br7d), an inhibitor of pituitary PRL secretion, completely abolished the pregnancy-enhanced transcellular Ca^{2+} transport (Step 1), whereas exogenous PRL supplementation [0.6 $mg \cdot kg^{-1} \cdot day^{-1}$ sc for 7 days (Pr7d)] totally reversed the bromocriptine effects (Fig. 2, *C* and *D*). Inhibition of Step 1 Ca^{2+} transport by Br7d was also observed in L7 (Fig. 2*E*), L14, and L21 rats (data not shown). Interestingly, in L7 rats with suckling, a single dose of 4 mg/kg bromocriptine administered 1 h before suckling (Br1h) completely abolished PRL surge (Fig. 2*F*) as well as the Step 2 transcellular Ca^{2+} transport (Fig. 2*E*), which was restored by a single dose of PRL [0.6 mg/kg sc (Pr1h)]. In addition, there was a strong correlation between the volume of milk ingested by pups and Ca^{2+} absorption during suckling (Fig. 2*G*). Such correlation became less significant after Br1h administration (Fig. 2*H*), suggesting that PRL surge may be the signal to match Ca^{2+} absorption with Ca^{2+} loss in milk.

The enhanced Ca^{2+} transport by the suckling-induced PRL surge could be mimicked in vitro by incubating an ex vivo duodenal tissue from L7 rats in bathing solution containing 600 and 800 but not 400 and 500 ng/ml PRL (Fig. 2*E*). The acute stimulatory effect of 600 ng/ml PRL was not abolished by inhibitors of gene transcription (50 μmol/l DRB) or protein biosynthesis (70 μmol/l cycloheximide) (Fig. 2*E*) but was completely abolished by inhibitors of PI3K (75 μmol/l LY-294002), PKC (1 μmol/l GF-109203X), and ROCK (1 μmol/l Y-27632). The present findings suggested that the acute stimulatory effect of PRL surge on the transcellular Ca^{2+} transport (Step 2) in lactating rats was mediated by nongenomic signaling pathways involving PI3K, PKC, and ROCK.

PRL as a regulator of paracellular Ca^{2+} transport during pregnancy and lactation. In addition to transcellular Ca^{2+} transport, pregnancy and lactation increased paracellular Ca^{2+} permeability (P_{Ca}; Fig. 3, *A* and *B*), whereas it decreased the TER (Supplemental Fig. S1, *A* and *B*; Supplemental Material for this article is available at the *AJP-Endocrinology and Metabolism* web site) of the duodenal epithelium. Suckling further increased P_{Ca} above the baseline level in lactation (Fig. 3*B*). The findings that decreases in TER that accompanied the increased Ca^{2+} transport were abolished by Br7d and then restored by Pr7d (Supplemental Fig. S1, *A* and *B*) strongly suggested that PRL was responsible for these responses. Further studies in P21 rats demonstrated that long-term PRL exposure markedly stimulated the gradient-dependent paracellular passive Ca^{2+} flux (Fig. 3*C*) in part by increasing the cation selectivity of the paracellular space, as indicated by the permeability ratio of sodium/chloride (P_{Na}/P_{Cl}) (Fig. 3*D*). The PRL-induced increase in P_{Na}/P_{Cl} in pregnancy resulted from an increase in P_{Na}, without a change in P_{Cl} (Supplemental Fig. S1, *C* and *D*).

Long-term PRL exposure during lactation also stimulated the paracellular Ca^{2+} transport (Fig. 3*E*) and increased P_{Na}/P_{Cl} (Fig. 3*F*) by raising P_{Na} (Supplemental Fig. S1*E*), without affecting P_{Cl} (Supplemental Fig. S1*F*). Suckling-induced PRL surge further increased the paracellular Ca^{2+} flux, P_{Na}/P_{Cl}, and P_{Na} above the baseline levels in lactation. Acute effects of direct exposure to 600 ng/ml PRL, which mimicked the suckling-induced PRL surge, were totally diminished by inhibitors of PI3K and ROCK, but not by PKC inhibitor (Fig. 3, *E* and *F*, and Supplemental Fig. S1, *E* and *F*). These findings corroborated that the acute effects of PRL surge on the paracellular Ca^{2+} transport (Step 2) and charge selectivity in lactating rats were mediated by nongenomic PI3K and ROCK pathways.

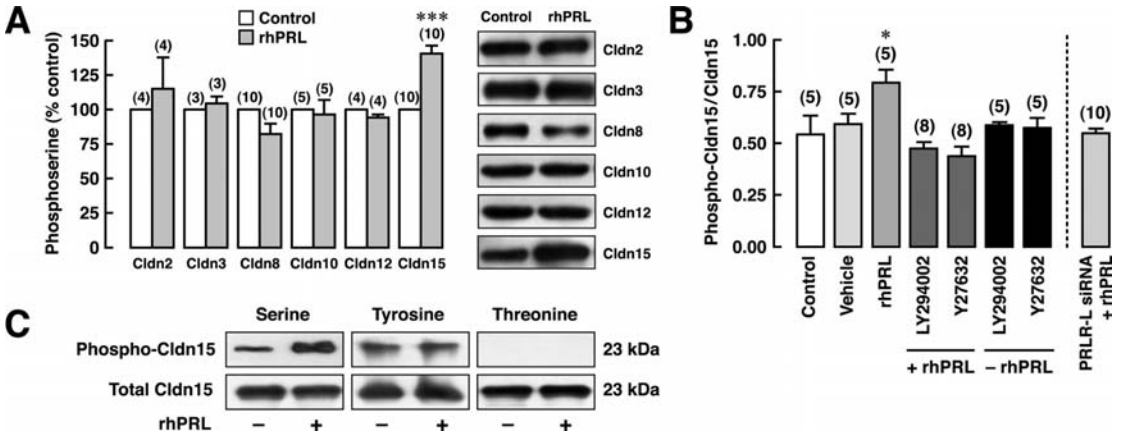

Fig. 4. *A*: phosphorylated claudin (Cldn)-2, -3, -8, -10, -12, and -15 at serine residues in 600 ng/ml rhPRL-treated Caco-2 monolayers, as demonstrated by immunoprecipitation. Representative electrophoretic images were also depicted. ***$P < 0.001$ compared with its respective control. Numbers in parentheses represent the number of independent monolayers. *B*: serine-phosphorylated Cldn-15 levels normalized with total claudin-15 in 600 ng/ml rhPRL-treated native and PRLR-L knockdown Caco-2 monolayers. In some experiments, 75 μmol/l LY-294002 or 1 μmol/l Y-27632 was added in the medium to demonstrate PRL-signaling pathways. *$P < 0.05$ compared with control group. *C*: representative bands of phosphorylated Cldn-15 at serine and tyrosine residues in rhPRL-treated Caco-2 monolayers ($n = 5$), as demonstrated by immunoprecipitation. Cldn-15 did not exhibit threonine phosphorylation.

Claudin-15 was essential for the PRL-stimulated paracellular Ca^{2+} transport. Since PRL augmented the paracellular Ca^{2+} transport by altering the charge selectivity of duodenal epithelium, it was possible that PRL may have changed the properties of certain charge-selective proteins of the claudin family. Generally, alterations of claudin functions are regulated by phosphorylation (11, 19). Therefore, we determined the amount of phosphorylated claudins in 600 ng/ml rhPRL-exposed Caco-2 monolayer by immunoprecipitation technique. The results showed that PRL induced serine phosphorylation of claudin-15 but not claudin-2, -3, -8, -10, or -12 (Fig. 4*A*). Serine phosphorylation of claudin-15 was prevented by PI3K and ROCK inhibitors as well as PRLR-L knockdown using siRNA (Fig. 4*B*). PRL was without effect on tyrosine or threonine phosphorylation of claudin-15 (Fig. 4*C*). PRLR-L siRNA did not interfere with PRLR-S or claudin-15 expression (Fig. 5*A*).

To verify the involvement of claudin-15 in the PRL-stimulated paracellular Ca^{2+} transport, Caco-2 monolayer was subjected to claudin-15 siRNA transfection. Claudin-15 knockdown markedly reduced mRNA expression, protein expression, and membrane localization of claudin-15 (Fig. 5, *B–F*), as demonstrated by qRT-PCR, Western blot analysis, and confocal laser-scanning microscopic techniques, respectively. Claudin-15 siRNA did not alter the expression of claudin-2, -3, -8, -10, -12, or occludin (Fig. 5, *C–F*). Scrambled siRNA and transfecting agent (10 μg/ml PEI) had no effect on claudin-15 expression (Fig. 5*B*). Ussing chamber study of normal Caco-2 monolayer showed that 600 ng/ml rhPRL markedly increased the paracellular Ca^{2+} transport (Fig. 6*A*) and P_{Ca} (Fig. 6*B*), whereas it decreased TER (Fig. 6*C*), similar to what was observed in the duodenum of lactating rats. This PRL-enhanced paracellular Ca^{2+} transport could be explained by a large increase in cation selectivity (P_{Na}/P_{Cl} and P_{Na}) and a slight decrease in P_{Cl} (Fig. 6*D* and Supplemental Fig. S2, *A* and *B*). Moreover, PRL effects on the paracellular Ca^{2+} flux, P_{Ca}, TER, P_{Na}/P_{Cl}, and P_{Na} were diminished after claudin-15 knockdown (Fig. 6, *A–D*, and Supplemental Fig. S2*A*). Since

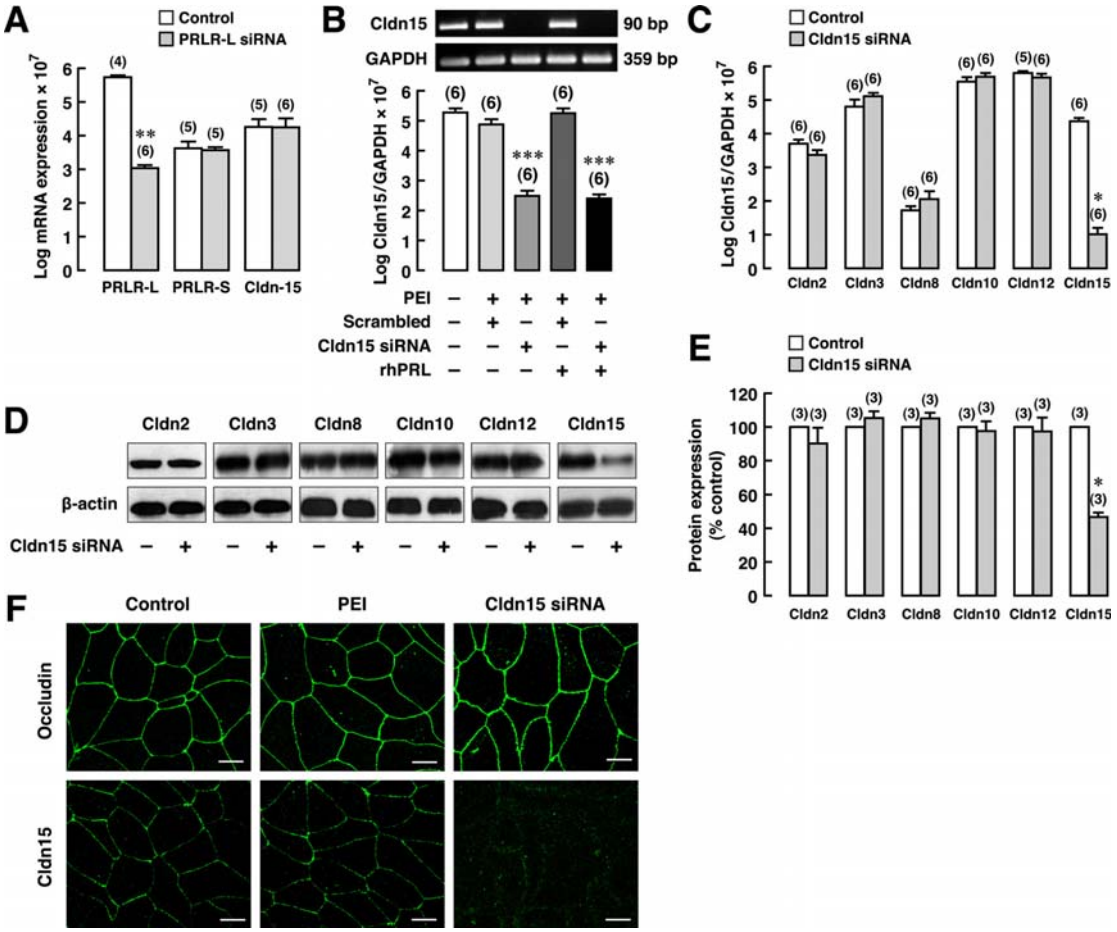

Fig. 5. *A*: expression of PRLR-L, PRLR-S, and Cldn-15 in PRLR-L knockdown Caco-2 cells, as demonstrated by quantitative real-time PCR (qRT-PCR). $^{**}P < 0.01$, small interfering RNA (siRNA) vs. control [polyethyleneimine (PEI) treated]. Numbers in parentheses represent the number of independent samples. *B*: Cldn-15 expression normalized by GAPDH expression in Cldn-15 siRNA-treated Caco-2 monolayers. Some monolayers were also exposed to 600 ng/ml rhPRL for 1 h before qRT-PCR study. Representative electrophoretic bands of Cldn-15 from conventional PCR were also illustrated along with those of GAPDH (36 cycles). $^{***}P < 0.001$ compared with control (open bar). *C–E*: mRNA and protein expression of Cldn-2, -3, -8, -10, -12, and -15, as demonstrated by qRT-PCR and Western blot analysis, respectively, in Cldn-15 siRNA-treated Caco-2 monolayers. Cldn protein expression was normalized by β-actin expression. $^{*}P < 0.05$ compared with corresponding control. *F*: localization of tight junction protein occludin and Cldn-15 in control (no treatment), PEI-treated, and Cldn-15 siRNA-treated Caco-2 monolayers, as demonstrated by confocal laser-scanning microscopic technique. Cldn-15 fluorescent signals were detected on the lateral membrane of control and PEI-treated monolayers but not in Cldn-15 siRNA-treated monolayer. Cldn-15 knockdown had no effect on occludin localization. Scale bars, 10 μm.

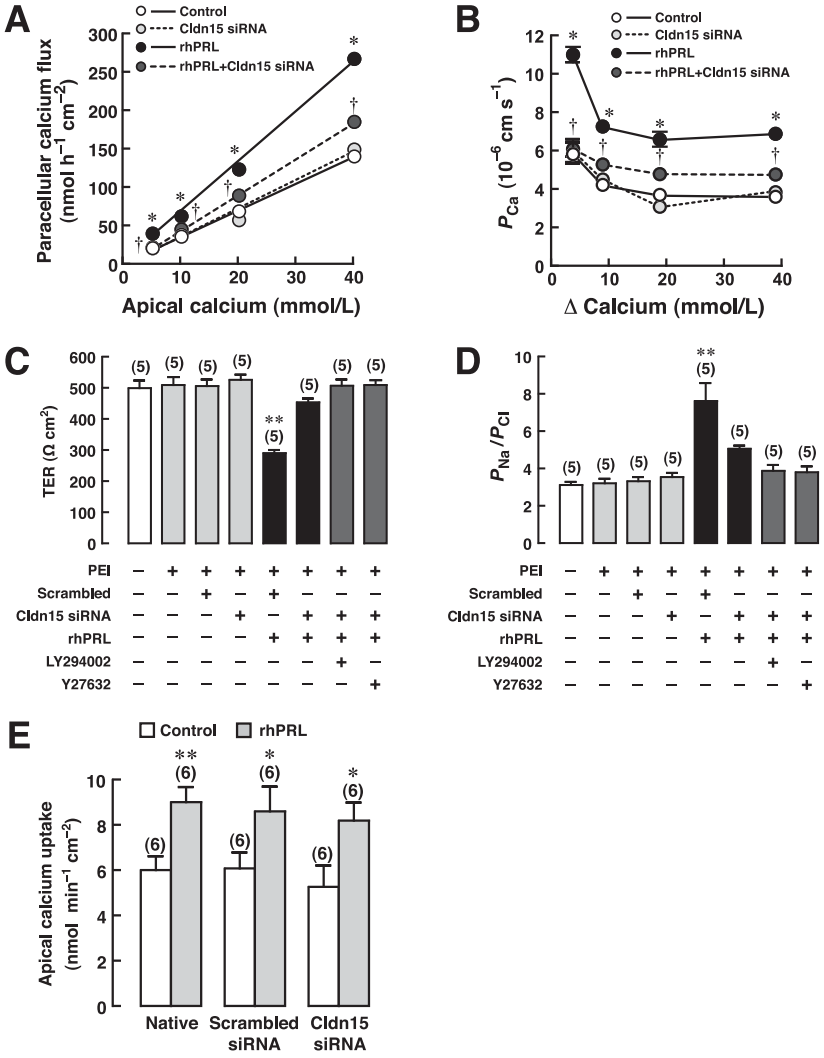

Fig. 6. *A* and *B*: paracellular Ca^{2+} transport and P_{Ca} in native and Cldn-15 knockdown Caco-2 monolayers directly exposed to 600 ng/ml rhPRL (n = 5/each Ca^{2+} concentration). *$P < 0.05$ rhPRL vs. control; †$P < 0.05$, rhPRL vs. rhPRL + Cldn-15 siRNA. *C* and *D*: transepithelial resistance (TER) and P_{Na}/P_{Cl} of native and Cldn-15 knockdown Caco-2 monolayers directly exposed to rhPRL or rhPRL plus inhibitors. **$P < 0.01$, rhPRL vs. control (open bar). *E*: ^{45}Ca uptake at 2 min in native (PEI-treated) and Cldn-15 knockdown Caco-2 monolayers directly exposed to rhPRL. *$P <$ 0.05 and **$P < 0.01$ compared with its respective control group. Numbers in parentheses represent the number of independent experiments.

PI3K and ROCK inhibitors did not further increase TER (Fig. 6*C*) or further decrease P_{Na}/P_{Cl} and P_{Na} (Fig. 6*D* and Supplemental Fig. S2*A*), the cation-selective claudin-15 might be a target of both mediators.

PRL stimulated apical Ca^{2+} uptake. To determine the effect of PRL on Ca^{2+} entry, which is the first step of the transcellular Ca^{2+} transport, ^{45}Ca uptake study was performed in Caco-2 monolayer. Two minutes after ^{45}Ca-containing medium was added to the apical compartment, the PRL-stimulated Ca^{2+} uptake of comparable rates was observed in both native and claudin-15 knockdown Caco-2 monolayers (Fig. 6*E*), suggesting that acute PRL exposure stimulated the transcellular Ca^{2+} transport by enhancing apical Ca^{2+} uptake.

Long-term PRL exposure altered the expression of genes related to Ca^{2+} transport and permselectivity. Besides nongenomic actions induced by transient PRL surge during suckling, chronic PRL exposure during pregnancy and lactation may induce long-lasting adaptations to enhance Ca^{2+} absorption, e.g., upregulation of certain Ca^{2+} transporter genes. Thus, the Step 1 Ca^{2+} transport was completely diminished by Br7d but not by Br1h (Fig. 2*E*). This hypothesis was confirmed by using nulliparous rats transplanted with two extra AP glands under the renal fascia. In the absence of hypothalamic inhibition, the AP grafts continuously released PRL but not other AP hormones that, in contrast, required hypothalamic stimulation. The AP-grafted rats were hyperprolactinemic with reported plasma PRL levels of ~90–100 ng/ml, comparable with the levels attained during pregnancy (28). PRL synthesis in AP grafts was confirmed by immunohistochemistry (Fig. 7, *A* and *B*).

Four weeks after AP transplantation, hyperprolactinemia led to upregulation of several genes involved in Ca^{2+} transport, i.e., TRPV5, TRPV6, calbindin-D_{9k}, and claudin-3 (9, 18), whereas the tight junction genes ZO-1 and occludin were downregulated (Fig. 7*C*).

DISCUSSION

The question of what factor enhances the intestinal Ca^{2+} absorption to mitigate negative Ca^{2+} balance and optimize fetomaternal Ca^{2+} homeostasis in pregnancy and lactation has remained enigmatic for decades. In humans, mothers lose ~200–300 and ~300–400 mg of Ca^{2+} each day during pregnancy and lactation, respectively, thereby leading to an ~10% decrease in total bone mass (29). Rodents with a litter of 8–10 pups may lose up to 20% of their skeletal mass in milk

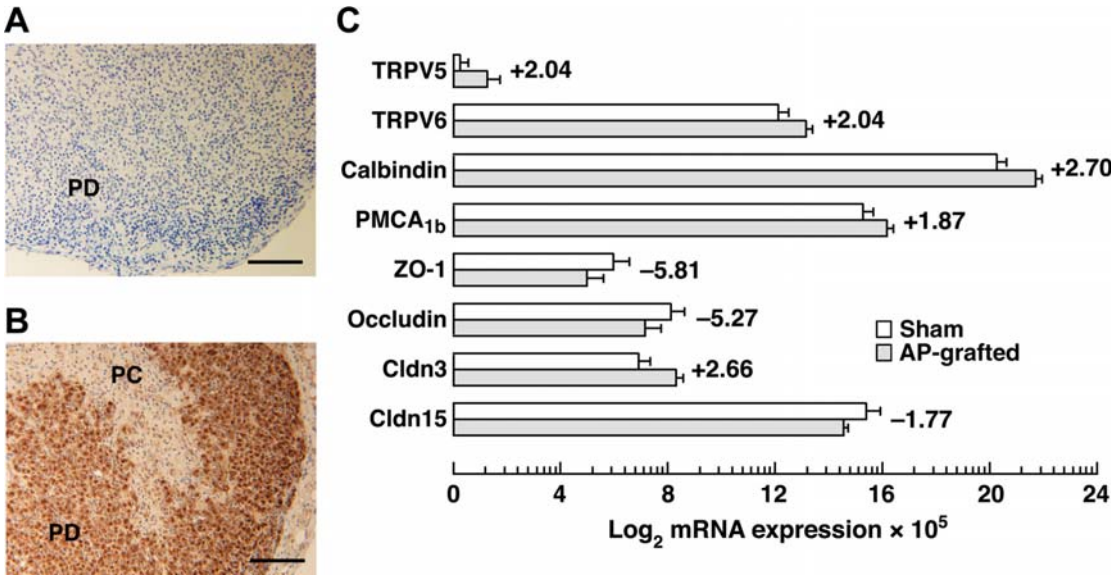

Fig. 7. Representative photomicrographic images of a pituitary graft dissected from a 4-wk anterior pituitary (AP) rat (n = 10). *A*: control image for PRL immunohistochemical analysis; i.e., the 4-μm paraffin-embedded section was incubated with secondary antibody in the absence of anti-PRL primary antibody. Active signs of microvascular endothelial damage and lymphoid proliferation were not seen, suggesting no graft rejection and allograft vasculopathy. *B*: immunohistochemical staining of an implanted pituitary gland with anti-PRL antibody. The pars distalis (PD) is strongly labeled with brownish products of peroxidase, whereas the perirenal connective tissues (PC) do not show PRL immunoreactivity. Scale bars, 100 μm. *C*: expression of genes related to Ca^{2+} transport and paracellular permeability in duodenal epithelial cells of 4-wk hyperprolactinemic AP-grafted rats (n = 7–10) vs. age-matched sham rats (n = 7–10), as demonstrated by qRT-PCR ($\log_2$ means ± SE × 10^5). Fold change value of each gene is presented on its respective columns. + and −, upregulation and downregulation, respectively. TRPV5 and -6, transient receptor potential vanilloid family Ca^{2+} channels 5 and 6, respectively; $PMCA_{1b}$, plasma$_{1b}$ Ca^{2+} ATPase isoform 1b.

production (27). With such high Ca^{2+} loss, it is surprising that intestinal Ca^{2+} absorption during pregnancy and lactation is $1,25(OH)_2D_3$ independent and does not correlate with the levels of other Ca^{2+}-regulating hormones, namely parathyroid hormone (PTH), PTH-related peptide, calcitonin, and estrogen (14, 29). Herein, we elucidated for the first time that PRL is a novel Ca^{2+}-regulating hormone that induces a two-step stimulation of Ca^{2+} absorption during pregnancy, lactation, and suckling. Therefore, PRL is essentially a regulator of Ca^{2+} balance by controlling both input (i.e., provision of Ca^{2+}) and output (i.e., lactogenesis) of Ca^{2+} in these reproductive phases.

Long-term PRL exposure over a period of several days led to an adaptive elevation of the basal intestinal Ca^{2+} transport to a new baseline (Step 1). This adaptation occurred at genomic levels through alteration of gene expression and was abolished by Br7d but not Br1h. In suckling rats (+suckling), Br1h could only decrease Step 2 Ca^{2+} transport to Step 1 level without further decreasing Step 1 Ca^{2+} transport (Fig. 2*E*). van Cromphaut et al. (37) previously showed that upregulation of TRPV6, calbindin-D_{9k}, and $PMCA_{1b}$ could account for the enhanced transcellular Ca^{2+} absorption in the duodenum of pregnant and lactating mice. Similarly, the present findings showed PRL-induced upregulation of TRPV5, TRPV6, and calbindin-D_{9k} in the duodenal cells of AP-grafted rats, which was consistent with an earlier report of a 25% upregulation of duodenal calbindin-D_{9k} by 9-day administration of PRL (5). Moreover, our previous genome-wide study in the rat duodenum by microarray indicated the PRL-induced increases in the expression of other Ca^{2+} transporter genes, namely Ca_v and parvalbumin, which may also contribute to the enhanced transcellular Ca^{2+} absorption (4, 10). Upregulation of these Ca^{2+} transporter genes, i.e., TRPV5, TRPV6, and Ca_v for apical Ca^{2+} uptake or calbindin-D_{9k} and parvalbumin for cytoplasmic diffusion, stressed the importance of adequate Ca^{2+} supply for fetal development and lactogenesis. Such redundancy also explains why TRPV6/calbindin-D_{9k} double-knockout mice were normocalcemic and still exhibited transcellular active Ca^{2+} absorption (3).

The Step 1 enhancement of the paracellular Ca^{2+} absorption appeared to involve the PRL-induced downregulation of occludin and ZO-1, both of which are important for the tight junction assembly, size-selective paracellular permeability, and maintenance of transepithelial resistance (13, 41). A decrease in transepithelial resistance after long-term PRL exposure in P21 and L7 rats (Supplemental Fig. S1, *A* and *B*) suggested possible enlargement of paracellular pores for passage of small solutes. In addition to the size selectivity, long-term PRL exposure also altered the charge selectivity of the paracellular barriers to favor cations over anions (i.e., an increase in P_{Na}/P_{Cl}; Fig. 3, *D* and *F*), which was consistent with the PRL-induced upregulation of cation-selective tight junction gene claudin-3. Previous investigations provided evidence that duodenal claudin-3 expression was $1,25(OH)_2D_3$ dependent (23), and its upregulation was associated with conditions of increased intestinal Ca^{2+} absorption, e.g., chronic metabolic acidosis (9). Although PRL augmented both transcellular and paracellular components of Step 1 Ca^{2+} absorption, the latter may be of greater physiological significance since, under normal luminal Ca^{2+} concentration of ~2–6 mmol/l (42), the paracellular Ca^{2+} flux was about three times greater than the transcellular flux (i.e., ~150 vs. ~50 $nmol \cdot h^{-1} \cdot cm^{-2}$). Nevertheless, transcellular active Ca^{2+} transport may become significant in low dietary Ca^{2+} intake condition.

The present results (Fig. 2), together with previous findings by Tudpor et al. (36), suggested that chronic PRL effects on the intestinal Ca^{2+} absorption (Step 1) were seen at plasma PRL concentrations ~100–200 ng/ml, as in pregnancy and lactation. In contrast, the acute stimulatory effect on Ca^{2+} absorption required ~400 ng/ml PRL, as attained during the suckling-induced PRL surge (Fig. 2*F*). This acute effect, which was superimposed on chronic PRL action, was responsible for the Step 2 transcellular and paracellular Ca^{2+} transport and could also be mimicked in vitro in Caco-2 monolayer (Fig. 1*B*) and in 600–800 ng/ml PRL-exposed duodenum of L7 rats (Fig. 2*E*). Moreover, the significant correlation between the suckling-enhanced transcellular Ca^{2+} flux and milk volume was suggestive of the orchestrating role of PRL in matching Ca^{2+} absorption to Ca^{2+} loss in milk.

Regarding the mechanisms of acute PRL action, it has been reported that PRL stimulated PMCA activity in purified basolateral membrane of the rat duodenum, thereby enhancing Ca^{2+} extrusion (8). Moreover, consistent with the previous report (35), the Step 2 transcellular Ca^{2+} transport also resulted from the PRL-enhanced apical Ca^{2+} entry, particularly via $Ca_v1.3$. However, further in vivo investigation is required to confirm that the mechanisms by which PRL enhanced apical Ca^{2+} entry in the Step 1 and Step 2 transcellular Ca^{2+} transport were different, i.e., TRPV5/6 for Step 1 and $Ca_v1.3$ for Step 2. On the other hand, the Step 2 paracellular Ca^{2+} transport was likely to be dependent on phosphorylation of certain charge-selective claudins. Ikari et al. (19) revealed that serine phosphorylation of the kidney-specific claudin-16 by protein kinase A was crucial for Mg^{2+} reabsorption in the thick ascending limb of the loop of Henle. Although a number of claudins, e.g., claudin-3, -8, and -10, were cation selective (1, 39, 40), and some, e.g., claudin-2 and -12, were required for the $1,25(OH)_2D_3$-stimulated Ca^{2+} absorption (15), only claudin-15 was essential for the PRL-induced increases in the paracellular Ca^{2+} transport, cation selectivity, and Ca^{2+} permeability as well as the decrease in transepithelial resistance (Fig. 6, *A–D*). Since claudin-15 possesses several negatively charged amino acids on the first extracellular loop for cation permeability (39), it was not surprising to find that P_{Na}, but not P_{Cl}, was markedly increased by PRL. The significance of claudin-15 was demonstrated recently in claudin-15-knockout mice that exhibited a decrease in the paracellular ion permeability and enlargement of the small intestine (33). Since claudin-15 mRNA was not upregulated in the long-term PRL-exposed duodenal epithelial cells, claudin-15 may be important only for the Step 2 paracellular Ca^{2+} transport or nongenomic PRL action. Alternatively, long-term exposure to PRL may increase protein expression and/or activity of claudin-15 without an increase in claudin-15 mRNA expression.

Since we found previously that PRLR-L knockdown diminished the transcellular Ca^{2+} transport in Caco-2 monolayer (34), and PRLR-L knockdown in this study completely abolished the PRL-induced claudin-15 phosphorylation, it was likely that the PRL-enhanced Ca^{2+} absorption was mediated by PRLR-L despite the fact that both PRLR-L and -S were expressed in duodenal epithelial cells of pregnant and lactating rats and in Caco-2 monolayer. This was consistent with the PRL-induced increases in lactogenesis and electrolyte transport in mammary epithelial cells (25). Although PRL actions in Step 1 Ca^{2+} absorption involved de novo gene transcription and those in Step 2 were, in contrast, nongenomic, their signal transduction should be quite similar since the signals presumably originated from the same receptor isoform. Step 2 transcellular Ca^{2+} absorption was mediated by PI3K, PKC, and ROCK, whereas claudin-15 phosphorylation and paracellular Ca^{2+} transport were dependent only on PI3K and ROCK, similar to that in the duodenum of nulliparous rat (20). However, PI3K, PKC, and ROCK are closely associated since both PKC and ROCK are downstream from PI3K (17). The ROCK-related pathway of PRL signaling was also reported in endothelial cells (24), whereas the PKC pathway mediated PRL actions in adrenocortical cells (21) and cholangiocytes (32). In the small intestine, PKC activation is known to be important for both apical Ca^{2+} entry and basolateral Ca^{2+} extrusion (22), presumably via phosphorylation of TRPV6 and PMCA, respectively. Interestingly, PRL signaling in the small intestine was independent of Janus kinase 2, an important mediator of PRL in mammary epithelial cells (43).

In conclusion, we elucidated the complexity of PRL-induced stimulation of intestinal Ca^{2+} absorption in pregnancy and lactation and demonstrated a two-step stimulation in suckling. Long-term PRL exposure led to adaptations of intestinal cells at genomic levels to upregulate several Ca^{2+} transport genes, thereby raising the "baseline" Ca^{2+} absorption (Step 1). During suckling, transient PRL surge further increased Ca^{2+} absorption (Step 2) within 30 min to the maximal capacity, which apparently matched Ca^{2+} loss in milk. The PRL-stimulated Step 2 Ca^{2+} transport occurred via both transcellular and paracellular pathways in a PI3K/PKC/ROCK-dependent manner in part by increasing apical Ca^{2+} uptake and claudin-15 phosphorylation, respectively. Thus, the present findings provide significant fundamental knowledge for physiological, nutraceutical, and medical scientists to gain more insight into Ca^{2+} homeostasis in the reproductive periods and for further development of Ca^{2+}-fortified diet to help alleviate negative Ca^{2+} balance. The finding that suckling-induced PRL surge considerably increases the efficiency of intestinal Ca^{2+} absorption may provide direction for health policy. For example, Ca^{2+} supplementation at 15–30 min prior to breastfeeding may best benefit fetal and maternal Ca^{2+} metabolism while reducing the incidence of pregnancy-induced osteoporosis.

ACKNOWLEDGMENTS

We thank Dr. Kannikar Wongdee and Jirawan Thongbunchoo for excellent technical assistance.

GRANTS

This research was supported by grants from the Mahidol University Postdoctoral Fellowship Program (to L. Nakkrasae), the Faculty of Science, Mahidol University (SCY52-02 and SCR52-01 to N. Charoenphandhu), the Royal Golden Jubilee Ph.D Program (PHD/0042/2551 to J. Teerapornpuntakit), and the Thailand Research Fund (RSA5180001 to N. Charoenphandhu).

REFERENCES

1. **Angelow S, Kim KJ, Yu AS.** Claudin-8 modulates paracellular permeability to acidic and basic ions in MDCK II cells. *J Physiol* 571: 15–26, 2006.
2. **Banan A, Zhang LJ, Shaikh M, Fields JZ, Choudhary S, Forsyth CB, Farhadi A, Keshavarzian A.** theta Isoform of protein kinase C alters barrier function in intestinal epithelium through modulation of distinct claudin isotypes: a novel mechanism for regulation of permeability. *J Pharmacol Exp Ther* 313: 962–982, 2005.

3. **Benn BS, Ajibade D, Porta A, Dhawan P, Hediger M, Peng JB, Jiang Y, Oh GT, Jeung EB, Lieben L, Bouillon R, Carmeliet G, Christakos S.** Active intestinal calcium transport in the absence of transient receptor potential vanilloid type 6 and calbindin-D_{9k}. *Endocrinology* 149: 3196–3205, 2008.
4. **Bindels RJ, Timmermans JA, Hartog A, Coers W, van Os CH.** Calbindin-D_{9k} and parvalbumin are exclusively located along basolateral membranes in rat distal nephron. *J Am Soc Nephrol* 2: 1122–1129, 1991.
5. **Bruns ME, Vollmer SS, Bruns DE, Overpeck JG.** Human growth hormone increases intestinal vitamin D-dependent calcium-binding protein in hypophysectomized rats. *Endocrinology* 113: 1387–1392, 1983.
6. **Carr G, Haslam IS, Simmons NL.** Voltage dependence of transepithelial guanidine permeation across Caco-2 epithelia allows determination of the paracellular flux component. *Pharm Res* 23: 540–548, 2006.
7. **Charoenphandhu N, Krishnamra N.** Prolactin is an important regulator of intestinal calcium transport. *Can J Physiol Pharmacol* 85: 569–581, 2007.
8. **Charoenphandhu N, Limlomwongse L, Krishnamra N.** Prolactin directly enhanced Na^+/K^+- and Ca^{2+}-ATPase activities in the duodenum of female rats. *Can J Physiol Pharmacol* 84: 555–563, 2006.
9. **Charoenphandhu N, Tudpor K, Pulsook N, Krishnamra N.** Chronic metabolic acidosis stimulated transcellular and solvent drag-induced calcium transport in the duodenum of female rats. *Am J Physiol Gastrointest Liver Physiol* 291: G446–G455, 2006.
10. **Charoenphandhu N, Wongdee K, Teerapornpuntakit J, Thongchote K, Krishnamra N.** Transcriptome responses of duodenal epithelial cells to prolactin in pituitary-grafted rats. *Mol Cell Endocrinol* 296: 41–52, 2008.
11. **D'Souza T, Indig FE, Morin PJ.** Phosphorylation of claudin-4 by PKC_ϵ regulates tight junction barrier function in ovarian cancer cells. *Exp Cell Res* 313: 3364–3375, 2007.
12. **Dunne F, Walters B, Marshall T, Heath DA.** Pregnancy associated osteoporosis. *Clin Endocrinol (Oxf)* 39: 487–490, 1993.
13. **Fischer S, Wobben M, Marti HH, Renz D, Schaper W.** Hypoxia-induced hyperpermeability in brain microvessel endothelial cells involves VEGF-mediated changes in the expression of zonula occludens-1. *Microvasc Res* 63: 70–80, 2002.
14. **Fleet JC.** Molecular regulation of calcium metabolism. In: *Calcium in Human Health*, edited by Weaver CM and Heaney RP. Totowa, NJ: Humana, 2006, p. 163–189.
15. **Fujita H, Sugimoto K, Inatomi S, Maeda T, Osanai M, Uchiyama Y, Yamamoto Y, Wada T, Kojima T, Yokozaki H, Yamashita T, Kato S, Sawada N, Chiba H.** Tight junction proteins claudin-2 and -12 are critical for vitamin D-dependent Ca^{2+} absorption between enterocytes. *Mol Biol Cell* 19: 1912–1921, 2008.
16. **Halloran BP, DeLuca HF.** Calcium transport in small intestine during pregnancy and lactation. *Am J Physiol Endocrinol Metab* 239: E64–E68, 1980.
17. **Hirsch E, Costa C, Ciraolo E.** Phosphoinositide 3-kinases as a common platform for multi-hormone signaling. *J Endocrinol* 194: 243–256, 2007.
18. **Hoenderop JG, Nilius B, Bindels RJ.** Calcium absorption across epithelia. *Physiol Rev* 85: 373–422, 2005.
19. **Ikari A, Ito M, Okude C, Sawada H, Harada H, Degawa M, Sakai H, Takahashi T, Sugatani J, Miwa M.** Claudin-16 is directly phosphorylated by protein kinase A independently of a vasodilator-stimulated phosphoprotein-mediated pathway. *J Cell Physiol* 214: 221–229, 2008.
20. **Jantarajit W, Thongon N, Pandaranandaka J, Teerapornpuntakit J, Krishnamra N, Charoenphandhu N.** Prolactin-stimulated transepithelial calcium transport in duodenum and Caco-2 monolayer are mediated by the phosphoinositide 3-kinase pathway. *Am J Physiol Endocrinol Metab* 293: E372–E384, 2007.
21. **Kaminska B, Ciereszko RE, Opalka M, Dusza L.** Prolactin signaling in porcine adrenocortical cells: involvement of protein kinases. *Domest Anim Endocrinol* 23: 475–491, 2002.
22. **Khanal RC, Nemere I.** Endocrine regulation of calcium transport in epithelia. *Clin Exp Pharmacol Physiol* 35: 1277–1287, 2008.
23. **Kutuzova GD, DeLuca HF.** Gene expression profiles in rat intestine identify pathways for 1,25-dihydroxyvitamin D_3 stimulated calcium absorption and clarify its immunomodulatory properties. *Arch Biochem Biophys* 432: 152–166, 2004.
24. **Lee SH, Kunz J, Lin SH, Yu-Lee LY.** 16-kDa prolactin inhibits endothelial cell migration by down-regulating the Ras-Tiam1-Rac1-Pak1 signaling pathway. *Cancer Res* 67: 11045–11053, 2007.
25. **Neville MC, Morton J.** Physiology and endocrine changes underlying human lactogenesis II. *J Nutr* 131: 3005S–3008S, 2001.
26. **Pahuja DN, DeLuca HF.** Stimulation of intestinal calcium transport and bone calcium mobilization by prolactin in vitamin D-deficient rats. *Science* 214: 1038–1039, 1981.
27. **Peng TC, Garner SC, Kusy RP, Hirsch PF.** Effect of number of suckling pups and dietary calcium on bone mineral content and mechanical properties of femurs of lactating rats. *Bone Miner* 3: 293–304, 1988.
28. **Piyabhan P, Krishnamra N, Limlomwongse L.** Changes in the regulation of calcium metabolism and bone calcium content during growth in the absence of endogenous prolactin and during hyperprolactinemia: a longitudinal study in male and female Wistar rats. *Can J Physiol Pharmacol* 78: 757–765, 2000.
29. **Prentice A.** Calcium in pregnancy and lactation. *Annu Rev Nutr* 20: 249–272, 2000.
30. **Sabour H, Hossein-Nezhad A, Maghbooli Z, Madani F, Mir E, Larijani B.** Relationship between pregnancy outcomes and maternal vitamin D and calcium intake: A cross-sectional study. *Gynecol Endocrinol* 22: 585–589, 2006.
31. **Stamatovic SM, Dimitrijevic OB, Keep RF, Andjelkovic AV.** Protein kinase C_α-RhoA cross-talk in CCL2-induced alterations in brain endothelial permeability. *J Biol Chem* 281: 8379–8388, 2006.
32. **Taffetani S, Glaser S, Francis H, DeMorrow S, Ueno Y, Alvaro D, Marucci L, Marzioni M, Fava G, Venter J, Vaculin S, Vaculin B, Lam IP, Lee VH, Gaudio E, Carpino G, Benedetti A, Alpini G.** Prolactin stimulates the proliferation of normal female cholangiocytes by differential regulation of Ca^{2+}-dependent PKC isoforms. *BMC Physiol* 7: 6, 2007.
33. **Tamura A, Kitano Y, Hata M, Katsuno T, Moriwaki K, Sasaki H, Hayashi H, Suzuki Y, Noda T, Furuse M, Tsukita S.** Megaintestine in claudin-15-deficient mice. *Gastroenterology* 134: 523–534, 2008.
34. **Thongon N, Nakkrasae LI, Thongbunchoo J, Krishnamra N, Charoenphandhu N.** Prolactin stimulates transepithelial calcium transport and modulates paracellular permselectivity in Caco-2 monolayer: mediation by PKC and ROCK pathways. *Am J Physiol Cell Physiol* 294: C1158–C1168, 2008.
35. **Thongon N, Nakkrasae LI, Thongbunchoo J, Krishnamra N, Charoenphandhu N.** Enhancement of calcium transport in Caco-2 monolayer through PKCζ-dependent $Ca_v1.3$-mediated transcellular and rectifying paracellular pathways by prolactin. *Am J Physiol Cell Physiol* 296: C1373–C1382, 2009.
36. **Tudpor K, Charoenphandhu N, Saengamnart W, Krishnamra N.** Long-term prolactin exposure differentially stimulated the transcellular and solvent drag-induced calcium transport in the duodenum of ovariectomized rats. *Exp Biol Med (Maywood)* 230: 836–844, 2005.
37. **van Cromphaut SJ, Rummens K, Stockmans I, van Herck E, Dijcks FA, Ederveen AG, Carmeliet P, Verhaeghe J, Bouillon R, Carmeliet G.** Intestinal calcium transporter genes are upregulated by estrogens and the reproductive cycle through vitamin D receptor-independent mechanisms. *J Bone Miner Res* 18: 1725–1736, 2003.
38. **Van Itallie CM, Anderson JM.** Claudins and epithelial paracellular transport. *Annu Rev Physiol* 68: 403–429, 2006.
39. **Van Itallie CM, Fanning AS, Anderson JM.** Reversal of charge selectivity in cation or anion-selective epithelial lines by expression of different claudins. *Am J Physiol Renal Physiol* 285: F1078–F1084, 2003.
40. **Van Itallie CM, Rogan S, Yu A, Vidal LS, Holmes J, Anderson JM.** Two splice variants of claudin-10 in the kidney create paracellular pores with different ion selectivities. *Am J Physiol Renal Physiol* 291: F1288–F1299, 2006.
41. **Wang W, Dentler WL, Borchardt RT.** VEGF increases BMEC monolayer permeability by affecting occludin expression and tight junction assembly. *Am J Physiol Heart Circ Physiol* 280: H434–H440, 2001.
42. **Wasserman RH.** Vitamin D and the dual processes of intestinal calcium absorption. *J Nutr* 134: 3137–3139, 2004.
43. **Xie J, LeBaron MJ, Nevalainen MT, Rui H.** Role of tyrosine kinase Jak2 in prolactin-induced differentiation and growth of mammary epithelial cells. *J Biol Chem* 277: 14020–14030, 2002.
44. **Yee S.** In vitro permeability across Caco-2 cells (colonic) can predict in vivo (small intestinal) absorption in man—fact or myth. *Pharm Res* 14: 763–766, 1997.
45. **Zweibaum A, Triadou N, Kedinger M, Augeron C, Robine-Leon S, Pinto M, Rousset M, Haffen K.** Sucrase-isomaltase: a marker of foetal and malignant epithelial cells of the human colon. *Int J Cancer* 32: 407–412, 1983.

Pflugers Arch - Eur J Physiol (2009) 458:993–1005
DOI 10.1007/s00424-009-0679-6

TRANSPORT PHYSIOLOGY

Direct stimulation of the transcellular and paracellular calcium transport in the rat cecum by prolactin

Kamonshanok Kraidith · Walailuk Jantarajit · Jarinthorn Teerapornpuntakit · La-iad Nakkrasae · Nateetip Krishnamra · Narattaphol Charoenphandhu

Received: 12 January 2009 / Revised: 5 April 2009 / Accepted: 28 April 2009 / Published online: 17 May 2009

Abstract Prolactin (PRL) is reported to stimulate calcium absorption in the rat's small intestine. However, little is known regarding its effects on the cecum, a part of the large intestine with the highest rate of intestinal calcium transport. We demonstrated herein by quantitative real-time polymerase chain reaction and Western blot analysis that the cecum could be a target organ of PRL since cecal epithelial cells strongly expressed PRL receptors. In Ussing chamber experiments, PRL enhanced the transcellular cecal calcium absorption in a biphasic dose–response manner. PRL also increased the paracellular calcium permeability and passive calcium transport in the cecum, which could be explained by the PRL-induced decrease in transepithelial resistance and increase in cation selectivity of the cecal epithelium. PRL actions in the cecum were abolished by inhibitors of phosphoinositide 3-kinase (PI3K), protein kinase C (PKC), and RhoA-associated coiled-coil forming kinase (ROCK), but not inhibitors of gene transcription and protein biosynthesis. In conclusion, PRL directly enhanced the transcellular and paracellular calcium transport in the rat cecum through the nongenomic signaling pathways involving PI3K, PKC, and ROCK.

Keywords Calcium absorption · Dilution potential · Paracellular transport · Prolactin receptor · Transcellular transport · Ussing chamber

Introduction

During pregnancy and lactation, prolactin (PRL) serves as a calcium-regulating hormone which markedly stimulates intestinal calcium absorption to help alleviate negative calcium balance due to massive calcium loss for fetal growth and milk production [5]. The PRL-enhanced calcium absorption has been intensively investigated in the small intestine [6, 25], especially in the duodenum, where the transcellular active calcium transport is prominent [11, 29]. However, the effects of PRL on the large intestine as well as its mechanisms were largely unknown.

It is widely known that, in monogastric herbivores, rats and humans, the cecum is for absorption of fluids and salts and is the site for luminal microfloral production of short-chain fatty acids, folate, and vitamin K [16, 32, 33]. Studies on the intestinal calcium absorption demonstrated that, besides the duodenum, the proximal part of the large intestine, particularly the cecum, is another important site for the transcellular active calcium transport [40]. Moreover, experiments in rats showed that when compared to other intestinal segments, cecum has the highest rate of calcium transport [28, 39]. Under normal conditions, it was suggested that the cecal epithelium absorbs a significant amount of free calcium which is released during microbial fermentation of the cecal contents through production of short-chain fatty acids and other acidic molecules, such as lactic acid, butyric acid, and

Electronic supplementary material The online version of this article (doi:10.1007/s00424-009-0679-6) contains supplementary material, which is available to authorized users.

K. Kraidith · N. Krishnamra · N. Charoenphandhu (✉)
Department of Physiology, Faculty of Science,
Mahidol University,
Rama VI Road,
Bangkok 10400, Thailand
e-mail: naratt@narattsys.com

W. Jantarajit · J. Teerapornpuntakit · L.-i. Nakkrasae · N. Krishnamra · N. Charoenphandhu
Consortium for Calcium and Bone Research (COCAB),
Faculty of Science, Mahidol University,
Bangkok, Thailand

succinic acid, as well as calcium released from the degradation of dietary fiber [10, 36]. Accumulation of free calcium in the cecal lumen may also be enough to increase the paracellular passive calcium transport [28]. Since PRL plays an important role in supplying additional calcium to the body, we postulated that it may increase the cecal calcium absorption via both transcellular and paracellular routes as seen in the small intestine [5].

Generally, the transcellular calcium transport is a three-step metabolically energized process, consisting of the apical uptake via the transient receptor potential vanilloid family calcium channel 5 and 6 (TRPV5/6) and L-type calcium channel $Ca_v1.3$, cytoplasmic translocation in a calbindin-D_{9k}-bound form, and the basolateral extrusion via the plasma membrane Ca^{2+}-ATPase 1b ($PMCA_{1b}$) and Na^+/Ca^{2+} exchanger 1 (NCX1) [20, 30, 49]. In contrast, the paracellular passive calcium transport is dependent on the transepithelial calcium gradient and is absent when both sides of the epithelium have equal calcium concentration [29]. Paracellular calcium movement is regulated by the tight junction, which contains several charge-selective proteins, particularly claudin-2, claudin-3, and claudin-12, arranged in the arrays of channel-like paracellular pores [14, 30]. Besides, the integrity of the tight junction is regulated by tight junction proteins, such as zonula occludens-1 (ZO-1) and occludin [50].

It is apparent that the paracellular calcium transport is predominant in the small intestine [10, 29]. However, when calcium demand is markedly increased, such as during pregnancy and lactation, contribution from the transcellular transport component to the total calcium absorption becomes more significant, in part, as a result of the stimulatory action of PRL [3, 5]. Recently, we demonstrated in the duodenum and Caco-2 monolayer that PRL enhanced both transcellular active and paracellular passive calcium transport through the phosphoinositide 3-kinase (PI3K), protein kinase C (PKC), and RhoA-associated coiled-coil forming kinase (ROCK) pathways [25, 48, 49]. However, PRL signaling in the large intestine, including the cecum, had never been investigated.

Therefore, the objectives of the present study were (a) to demonstrate that the cecum was a target organ of PRL, (b) to investigate the effects of PRL on the cecal calcium transport, and (c) to investigate the mechanisms of the PRL-enhanced calcium absorption in the cecum.

Materials and methods

Animals

Female Sprague–Dawley rats (8 weeks old, weighing 180–200 g) were obtained from the National Laboratory Animal Centre, Thailand. They were placed in hanging stainless steel cages, fed with standard pellets containing 1% wt/wt calcium and 100 IU vitamin D per 100 g of diet (Perfect Companion, Bangkok, Thailand), and provided with distilled water ad libitum under 12:12 h light/dark cycle. The room had temperature of 20–25°C, humidity of 50–60%, and average illuminance of 150–200 lux in the daytime. Body weight and food intake were recorded daily. This study has been approved by the Institutional Animal Care and Use Committee of the Faculty of Science, Mahidol University, Bangkok, Thailand.

Tissue preparation

After 7-day acclimatization, the rat was anesthetized by administering 50 mg/kg sodium pentobarbitone i.p. (Abbott, North Chicago, IL, USA). Thereafter, median laparotomy was performed. Duodenum (10 cm), proximal and distal jejunum (10 cm each), ileum (8 cm), cecum (4 cm), and proximal and distal colon (8 cm each) were removed and cut longitudinally to expose the mucosa. In the calcium transport experiments, the muscularis proper was stripped off before the tissue was mounted in a modified Ussing chamber as described previously [25]. The tissue was incubated for 20 min in the chamber before the 60-min experiment was carried out. As for the mRNA and protein expression studies, epithelial cells were collected by scraping the mucosal surface with an ice-cold glass slide [8].

Total RNA preparation and cDNA synthesis

Total RNA was extracted from mucosal scrapings by using TRIzol reagent (Invitrogen, Carlsbad, CA, USA) and purified with RNeasy Mini kit (Qiagen, Valencia, CA, USA). Purity and integrity of RNA were determined by 260/280 nm absorbance and denaturing agarose gel electrophoresis, respectively [8]. One microgram of the total RNA was then reverse-transcribed to cDNA with the oligo-dT_{20} primer and the iScript kit (Bio-Rad, Hercules, CA, USA). Glyceraldehyde-3-phosphate dehydrogenase (GAPDH), a housekeeping gene, served as a control gene to check the consistency of the reverse transcription.

Quantitative real-time PCR and sequencing

Primers used in this study were shown in Table 1. Quantitative real-time polymerase chain reaction (qRT-PCR) and melting curve analysis were performed by the Bio-rad MiniOpticon with the iQ SYBR Green SuperMix (Bio-rad) as previously described [8]. Relative expression of PRL receptor (PRLR) over GAPDH was calculated from the threshold cycle (C_t) values by using $2^{\Delta C_t}$ method. The

Table 1 *Rattus norvegicus* oligonucleotide sequences used in qRT-PCR experiments

Name	Accession no.	Primer (forward/reverse)	Product length (bp)
Prolactin receptors			
PRLR-S	NM_012630	5′-TTCTACCACCATCGCAAC-3′ 5′-CTGATCTCGTTTGTCATTGAG-3′	120
PRLR-L	NM_001034111	5′-TCAAGCAACCGCAGACTC-3′ 5′-CAGTTTAGCCAATCGTTCCA-3′	107
Transcellular genes			
TRPV5	NM_053787	5′-CTTACGGGTTGAACACCACCA-3′ 5′-TTGCAGAACCACAGAGCCTCTA-3′	163
TRPV6	NM_053686	5′-ATCCGCCGCTATGCAC-3′ 5′-AGTTTTTCTGGTCACTGTTTTTGG-3′	80
$Ca_v1.3$	NM_017298	5′-TCAGCGTCAGTGTGTGGAATA-3′ 5′-CGAAAGGCGAGGAGTTCAC-3′	110
Calbindin-D_{9k}	X_16635	5′-CCCGAAGAAATGAAGAGCATTTT-3′ 5′-TTCTCCATCACCGTTCTTATCCA-3′	174
$PMCA_{1b}$	NM_053311	5′-CGCCATCTTCTGCACAATT-3′ 5′-CAGCCATTGTTCTATTGAAAGTTC-3′	109
NCX1	NM_019268	5′-GTTGTGTTCGCTTGGGTTGC-3′ 5′-CGTGGGAGTTGACTACTTTC-3′	163
Paracellular genes			
Claudin-2	NM_001106846	5′-GCTGCTGAGGGTAGAATGA-3′ 5′-GCTCGCTTGATAAGTGTCC-3′	107
Claudin-3	NM_031700	5′-GCACCCACCAAGATCCTCTA-3′ 5′-AGGCTGTCTGTCCTCTTCCA-3′	246
Claudin-12	XM_001067932	5′-CCTTCAAGTCTTCGGTGCC-3′ 5′-CAGGAGGATGGGAGTACAG-3′	312
ZO-1	XM_218747	5′-GTATCCGATTGTTGTGTTCC-3′ 5′-TCACTTGTAGCACCATCCGC-3′	270
Occludin	NM_031329	5′-CACGTTCGACCAATGC-3′ 5′-CCCGTTCCATAGGCTC-3′	188
Housekeeping gene			
GAPDH	NM_017008	5′-AGTCTACTGGCGTCTTCAC-3′ 5′-TCATATTTCTCGTGGTTCAC-3′	133

PRLR-S short isoform of prolactin receptor, *PRLR-L* long isoform of prolactin receptor, *TRPV5* transient receptor potential vanilloid family Ca^{2+} channel 5, *TRPV6* transient receptor potential vanilloid family Ca^{2+} channel 6, *$Ca_v1.3$* voltage-dependent L-type Ca^{2+} channel 1.3, *$PMCA_{1b}$* plasma membrane Ca^{2+}-ATPase isoform 1b, *NCX1* Na^+/Ca^{2+} exchanger 1, *ZO-1* zonula occludens-1, *GAPDH* glyceraldehyde-3-phosphate dehydrogenase

PCR products were also visualized on a 1.5% agarose gel stained with 1.0 μg/mL ethidium bromide under a UV transilluminator (Alpha Innotech, San Leandro, CA, USA). After electrophoresis, all PCR products were purified from a gel by the HiYield Gel/PCR DNA Extraction kit (Real Biotech Corporation, Taipei, Taiwan) and sequenced by the ABI Prism 3100 Genetic Analyzer (Applied Biosystems, Foster City, CA, USA).

Western blot analysis

As previously described [25], scraped mucosal cells were lysed in lysis buffer (0.5 mmol/L Tris pH 7.5, 1.5 mol/L NaCl, 10% NP-40, 5% DOC, 10 mmol/L Na ethylenediaminetetraacetic acid, 1 mmol/L phenylmethylsulfonyl fluoride, 1 μg/mL leupeptin, 1 μg/mL aprotinin, 1 μg/mL pepstatin A; all purchased from Sigma, St. Louis, MO, USA). Lysates were sonicated at 4°C and centrifuged at 20,000×*g* for 10 min. One hundred micrograms proteins were separated by sodium dodecyl sulfate polyacrylamide gel electrophoresis and transferred to a nitrocellulose membrane (Amersham, Buckinghamshire, UK) by electroblotting. Membranes were blocked at 25°C for 4 h with 5% nonfat milk and were probed overnight at 4°C with 1:500 rabbit antirat PRLR polyclonal antibodies (catalog no. sc-30225; Santa Cruz Biotechnology, Santa Cruz, CA, USA) raised against the conserved extracellular domain. Membranes were later reprobed with 1:5,000 mouse antirat β-actin monoclonal antibodies (catalog no. sc-47778; Santa Cruz). After 2-h incubation at 25°C with 1:20,000 goat antirabbit (catalog no. sc-2004) or antimouse (catalog no. sc-2005) secondary antibodies (Santa Cruz), blots were visualized by enhanced chemiluminescence kit (Amersham).

Bathing solution for Ussing chamber study

The bathing solution continuously gassed with humidified 5% CO_2 in 95% O_2, contained (in mmol/L) 118 NaCl, 4.7 KCl, 1.1 $MgCl_2$, 1.25 $CaCl_2$, 23 $NaHCO_3$, 12 D-glucose, and 2 mannitol (all purchased from Sigma). The solution